Cover Page

Universiteit Leiden

Leiden University
Repository

The handle http://hdl.handle.net/1887/54937 holds various files of this Leiden University dissertation.

Author: Dam, A.D. van
Title: INFLAMED FAT: immune modulation of adipose tissue and lipid metabolism
Issue Date: 2017-10-19

INFLAMED FAT

IMMUNE MODULATION OF ADIPOSE TISSUE

AND LIPID METABOLISM

Andrea van Dam

INFLAMED FAT

IMMUNE MODULATION OF ADIPOSE TISSUE
AND LIPID METABOLISM

Andrea van Dam

INFLAMED FAT

IMMUNE MODULATION OF ADIPOSE TISSUE
AND LIPID METABOLISM

PROEFSCHRIFT

Ter verkrijging van
de graad van Doctor aan de Universiteit Leiden,
op gezag van Rector Magnificus prof. Mr. C.J.J.M. Stolker,
volgens besluit van het College voor Promoties
te verdedigen op donderdag 19 oktober 2017
klokke 16.15 uur

door

Andrea Dingena van Dam
Geboren te Cabanatuan City
in 1988

Promotor   Prof. dr. P.C.N. Rensen

Copromotor   Dr. M.R. Boon

Leden promotiecommissie
    Prof. dr. M. Yazdanbakhsh
    Prof. dr. E. Lutgens (AMC, Amsterdam)
    Prof. dr. M.P.J. de Winther (AMC, Amsterdam)
    Prof. dr. F. Karpe (OCDEM, University of Oxford, Oxford)

TABLE OF CONTENTS

Chapter 1

General introduction and outline

OBESITY, ETHNICITY AND RISK OF METABOLIC DISORDERS

According to the World Health Organization, the worldwide prevalence of obesity, defined as a body mass index (BMI) > 30 kg/m^2, has nearly doubled since 1980 and at least 2.8 million people die each year as a result of obesity. This number is expected to further increase over the next decade. Obesity has a great impact on public health as it leads to disorders such as type 2 diabetes and cardiovascular disease (1, 2). It has become evident that besides BMI, ethnicity determines the risk of developing both type 2 diabetes (3-5) and cardiovascular disease (6-9). South Asians, who originate from the Indian subcontinent and compose 20% of the world population, have a higher risk of developing these pathologies compared to white Caucasians. Despite the presence of predisposing classical risk factors such as central obesity, insulin resistance and dyslipidemia in this population (10, 11), the high prevalence of type 2 diabetes and cardiovascular disease in South Asians cannot be explained by these factors alone (9, 12). This suggests that other, non-classical, risk factors underlie their increased susceptibility (13).

LIPID METABOLISM

Obesity develops as a result of a long-term positive energy balance and storage of lipids in several tissues. The most abundant lipid types in our diet are triglycerides and cholesterol. Triglycerides are the storage form of the main source of energy for the body, *i.e.* fatty acids. Fatty acids are burnt by the heart and muscle to generate adenosine triphosphate (ATP), a molecule that carries energy in the form of a covalent bond holding a phosphate group. ATP is required for many cellular and metabolic processes such as muscle contraction (14). Brown adipose tissue (BAT) uses fatty acids to generate heat rather than ATP (15) (**Fig. 1**). When intake of energy exceeds the body's needs, fatty acids are stored as triglycerides in white adipose tissue (WAT), a process that also uses glucose to generate the glycerol backbone to which fatty acids are esterified (16). For humans, cholesterol does not provide energy, but is an essential component of cell membranes and a precursor for synthesis of steroid hormones, vitamin D, and bile acids. Interestingly, cholesterol from the host is also used by certain bacteria such as *Mycobacterium bovis* as energy source when they colonize a host (17, 18).

Lipids are hydrophobic and thus insoluble in blood, for which they are transported in lipoprotein particles. Lipoprotein particles exist of a lipid-rich core containing triglycerides and cholesteryl esters, the storage forms of fatty acids and cholesterol, respectively, surrounded by an amphipathic monolayer of phospholipids and unesterified cholesterol in which specific proteins (*i.e.* apolipoproteins) are embedded. Upon a meal, dietary triglycerides and cholesterol are taken up by intestinal cells, which assemble the lipids into triglyceride-rich lipoproteins carrying apolipoprotein B (apoB) named chylomicrons, that subsequently travel via the lymph to the blood. From the blood, they can provide tissues

with fatty acids. The liver secretes triglyceride-rich lipoprotein particles, named very-low density lipoproteins (VLDL), into the blood to supply tissues for their energy demand as well, which is crucial especially during times of fasting. Chylomicrons and VLDL deliver fatty acids mainly to heart, muscle and adipose tissues as these tissues express lipoprotein lipase (LPL), an enzyme essential for lipolysis of triglycerides within these lipoproteins. Subsequent uptake of the disengaged fatty acids is mediated by expression of cell surface receptors such as CD36. During lipolysis, the triglyceride-rich lipoproteins become enriched with apolipoprotein E (ApoE). ApoE binds the low density lipoprotein receptor (LDLR) or LDL-related protein (LRP) on the liver, ensuring hepatic clearance of the remnant particles (14, 19).

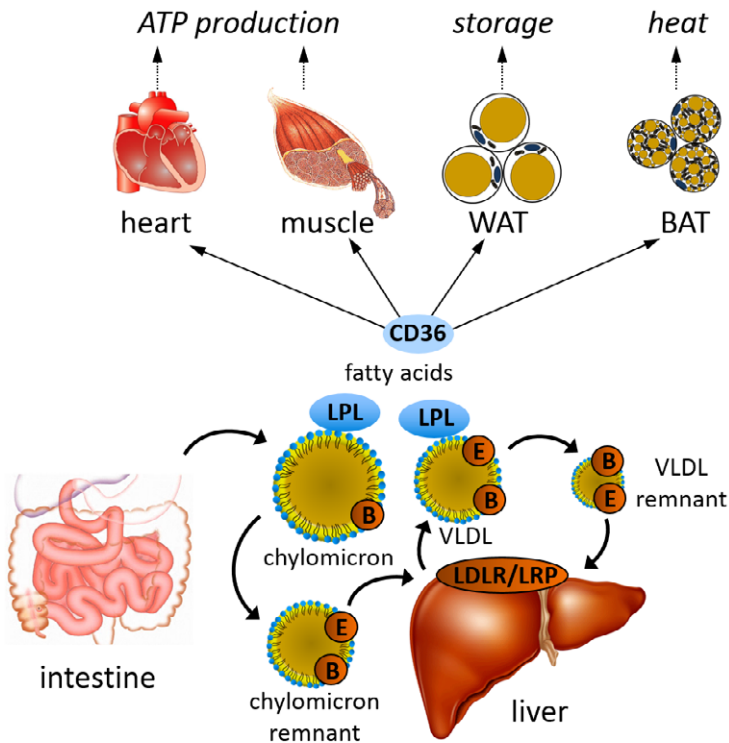**Figure 1. Schematic representation of triglyceride-rich lipoprotein metabolism.** *See text for explanation. ATP, adenosine triphosphate; B, apolipoprotein B; BAT, brown adipose tissue; E, apolipoprotein E; LDLR, low density lipoprotein receptor; LPL, lipoprotein lipase; LRP, low density lipoprotein-related protein; TRL, triglyceride-rich lipoprotein; VLDL, very low density lipoprotein; WAT, white adipose tissue.*

ADIPOSE TISSUE TYPES

Adipose tissue is the main site for energy storage during obesity. WAT is the most abundant adipose tissue type, found throughout the body in different subcutaneous and visceral depots (20). WAT is a major participant in energy regulation of the body, not only by storing excess ingested glucose and fatty acids in the form of triglycerides in the adipocytes but also by releasing fatty acids as a result of intracellular lipolysis to meet the energy needs of other organs. In addition, WAT is an endocrine organ. It responds to hormonal signals and signals from the nervous system and it expresses and releases endocrine factors including leptin, adiponectin, cytokines, chemokines and components of the complement system. This endocrine function of WAT influences essential metabolic processes, including lipid and glucose homeostasis (21). The spherical adipocytes within WAT characteristically contain a single large lipid droplet and a few mitochondria that are dispersed in a thin surrounding layer of cytoplasm.

Another type of adipose tissue is BAT. This tissue is found in the neck, above the clavicles and around the spine in humans (22-24). In contrast to WAT, which stores energy, BAT combusts fatty acids to generate heat and maintain body temperature, a process that is defined as non-shivering thermogenesis. Hence brown adipocytes, that are smaller than white adipocytes, contain many mitochondria and typically hold multiple small lipid droplets (20). Thermogenesis is induced by catecholamine signaling. Catecholamines signal via all types of adrenergic receptors including β1, β2, β3, α1 and α2, although not all of these have stimulatory effects on thermogenesis. Expression of the stimulatory β3-adrenergic receptor on brown adipocytes is likely the most specific and relevant for heat production (25). Apart from adrenergic receptor expression, thermogenesis is dependent on intracellular lipolysis and the presence of uncoupling protein 1 (UCP1). Intracellular lipolysis of triglycerides yields fatty acids, which are used as substrates for heat production and can directly activate UCP1. UCP1 resides in the inner mitochondrial membrane and, upon activation, facilitates proton leak, which disturbs the proton gradient that is generated by oxidative phosphorylation resulting from fatty acid oxidation. This "uncouples" electron transport from synthesis of ATP and leads to production of heat (25, 26). From rodent studies, it is known that besides classical brown adipocytes with high UCP1 expression, brown-like cells with very low basal but highly inducible UCP1 expression exist. These cells usually reside in WAT and are called beige adipocytes, and considerable evidence suggests that human BAT is mainly composed of beige adipocytes (27-29).

In addition to adipocytes, adipose tissue is composed of pre-adipocytes, endothelial cells, fibroblasts, nerve tissue and immune cells. This contributes to the complexity and metabolic and endocrine functions of adipose tissue. Adipose tissue not only responds to hormonal and neural signaling, it also expresses and secretes a range of factors named adipokines. These factors include cytokines, chemokines and complement components (21). The secretion of adipokines accounts for the role of adipose tissue in systemic signaling pathways, such as regulation of energy balance and inflammation (30, 31). Differences exist in the complexity and endocrine functions of adipose tissue depots. For example, BAT is

more densely vascularized and innervated than WAT (20) whereas the transcript levels of inflammatory genes in BAT are generally lower than in WAT (32, 33).

WHITE ADIPOSE TISSUE INFLAMMATION IN OBESITY

Increased storage of lipids in WAT during obesity leads to hypertrophy of adipocytes, hypoxia, and eventually cell death, causing adipose tissue dysfunction and fibrosis. Dysfunctional and dying adipocytes change the local microenvironment by leakage of fatty acids and other products. The altered microenvironment causes release of adipokines (*e.g.* IL-6, TNF, CCL2) and recruitment of inflammatory cells by WAT (31, 34).

In WAT of lean mice, 10-15% of the cells are macrophages, whereas WAT of obese mice contains 45-60% macrophages (35). Resident macrophages in lean WAT have a predominant anti-inflammatory or M2 phenotype. In obesity, inflammatory monocytes are recruited to WAT, where they differentiate, acquire a pro-inflammatory or M1 phenotype and form the majority of macrophages (35, 36). Other myeloid cells that play a role in WAT include neutrophils and eosinophils. Neutrophils are very short-lived cells that infiltrate the WAT within 3 days after exposure to a high-fat diet (37, 38). The amount of eosinophils is inversely correlated with adiposity, and depletion of eosinophils in mice results in obesity and insulin resistance (39).

The repertoire of immune cells found in WAT also comprises lymphoid cells. More specifically, 10% of the stromal vascular fraction of lean WAT consists of T cells. During obesity, the total amount of T cells, CD8^{+} cytotoxic T cells and CD4^{+} effector T cells in WAT increase, whereas CD4^{+} Tregs decrease (40). Furthermore, pro-inflammatory Th1 T cells increase while more anti-inflammatory Th2 T cells decrease, altogether resulting in increased inflammation in obese WAT (39, 41-43). The chronic low-grade inflammation in obese WAT includes the recruitment of B cells, natural killer cells and mast cells (44, 45). Overall, a variety of immune cells infiltrate WAT during obesity, inducing a switch from a homeostatic anti-inflammatory environment to a state of chronic low-grade inflammation.

Due to the extensive communication between adipocytes and immune cells, chronic inflammation as occurs in obesity disturbs insulin signalling in the tissue (34, 46) thereby contributing to development of type 2 diabetes as will be further described below.

IMMUNE MODULATION OF BROWN AND BEIGE ADIPOSE TISSUE

In contrast to the well-established presence of different immune cell types in WAT, the presence and role of the immune system in the development, function and activity of BAT is still largely unknown. Interestingly, many factors that modulate energy expenditure, the hallmark of BAT activity, affect inflammation too, all in all suggesting that the immune

system is involved in BAT function. These factors include environmental temperature (47, 48), the biological clock (49, 50), hormones (51, 52) and food intake (53).

Macrophages, the most abundant immune cells in WAT, are present in BAT as demonstrated by flow cytometry and qPCR (54). Evaluation of gene networks in BAT shows that immune cell trafficking is upregulated upon high-fat diet feeding (55). Furthermore, like WAT, BAT secretes adipokines (*e.g.* IL-6). Although the transcript levels of pro-inflammatory cytokines in BAT are lower compared to WAT, augmented expression of pro-inflammatory cytokines has been found in obese compared to lean BAT. These pro-inflammatory factors are thought to diminish BAT function (30).

The limited research that has been done into the role of immune cells in BAT may suggest that macrophages play a role in non-shivering thermogenesis. Cold exposure increases M2 macrophages in both WAT and BAT, which release the catecholamine noradrenaline that in turn activates BAT and induces browning of WAT (54, 56). Eosinophils indirectly contribute to thermogenesis by promoting activation of M2 macrophages within adipose tissue (56, 57). Besides macrophages, type 2 innate lymphoid cells are important mediators of beiging of WAT (58). So, although knowledge about the role of immune cells in BAT and beiging WAT lags behind, inflammation is probably an important player in brown adipocyte function as well.

INFLAMMATION SIGNIFICANTLY CONTRIBUTES TO TYPE 2 DIABETES AND CARDIOVASCULAR DISEASE

A key mechanism by which inflammation leads to insulin resistance is inhibition of insulin signaling pathways in several metabolic tissues (59). After a meal, insulin is released by the pancreas and acts on its target tissues including muscle, liver and adipose tissues. Stimulation of the insulin receptor induces the uptake of glucose by these tissues (60, 61). The inflammatory cytokines TNF and IL-6, and the acute phase protein C-reactive protein (CRP) can directly inhibit the insulin pathway and thereby induce insulin resistance (62-64). Moreover, inflammation activates a number of intracellular serine/threonine kinases such as c-Jun N-terminal kinases (JNKs) and IκB kinase (IKK) which inhibit insulin signaling. Inhibition of insulin signaling leads to peripheral insulin resistance and subsequent hyperglycemia, which can result in development of type 2 diabetes (59). On top of that, since insulin normally reduces VLDL production, decreased insulin sensitivity in the liver leads to enhanced production of VLDL and thereby to hyperlipidemia (65).

Atherosclerosis is the pathology underlying cardiovascular disease, and the main risk factor for the development of atherosclerosis is hypercholesterolemia. Atherosclerosis development is initiated by retention of low-density lipoproteins (LDL) and very-low-density lipoprotein (VLDL) remnant particles in the vessel wall. In response, the vessel wall releases oxidative and pro-inflammatory factors that modify these particles, for example by oxidation, resulting in oxidized LDL (oxLDL) (66, 67). LDL is also modified by hydrolyzing enzymes that are present in the lesions (68, 69). Immune cells, mainly monocytes, are
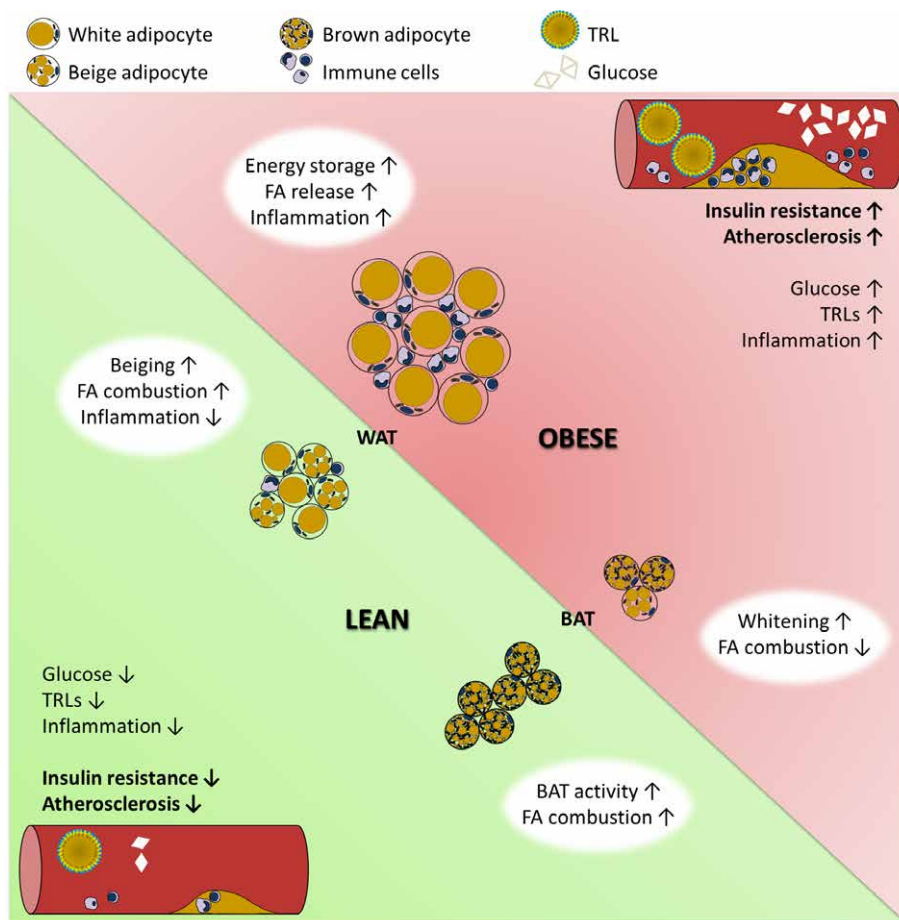
Figure 2. The proposed role of white and brown adipose tissue in the development of insulin resistance and atherosclerosis during obesity. *In obesity, both energy storage and fatty acid release are enhanced in white adipose tissue (WAT). Immune cells infiltrate the WAT, causing systemic inflammation. Brown adipose tissue (BAT) displays a whitened phenotype in obesity, resulting in decreased combustion of fatty acids. Therapeutic strategies to reduce insulin resistance and atherosclerosis should on the one hand focus on activation of brown adipocytes and beiging of white adipocytes to reduce circulating triglyceride-rich lipoproteins, and on the other hand on reducing adipose tissue and systemic inflammation. BAT, brown adipose tissue; FA, fatty acid; TRL, triglyceride-rich lipoprotein; WAT, white adipose tissue.*

recruited from the circulation upon the expression of chemoattractants like tumor necrosis factor (TNF) (70) and monocyte chemoattractant protein-1 (MCP-1) in the lesions (71). Locally produced factors, such as monocyte-colony stimulating factor (M-CSF) (72), promote the differentiation of monocytes into macrophages. Macrophages scavenge the accumulating and modified lipoproteins thereby developing into foam cells. Foam cells augment the inflammatory response, resulting in additional recruitment of immune cells

into the atherosclerotic plaque (66, 67). Ultimately, plaques can rupture and/or occlude the vessel, leading to a cardiovascular event in *e.g.* the heart (myocardial infarction) or brain (stroke) (71). In many cell types that are involved in buildup of the atherosclerotic plaque, intracellular inflammatory pathways (*e.g.* JNK and IKK) and transcription factors (*e.g.* nuclear factor κ-light-chain-enhancer of activated B cells; NFκB) control the expression of adhesion molecules and inflammatory chemokines and cytokines. Besides local inflammation in the vasculature, other peripheral sources of inflammation can augment the development of atherosclerosis, including chronic infection (73, 74) and obese liver and WAT (75).

Taken together, inflammation is an important factor in the development of both type 2 diabetes and cardiovascular disease. Together with therapeutic interventions that activate BAT or induce browning, resulting in enhanced nutrient combustion, strategies that reduce inflammation may help to mitigate these pathologies (**Fig. 2**).

OUTLINE OF THIS THESIS

As is evident from this chapter (**chapter 1**) of this thesis, inflammation plays an important role in the development of insulin resistance and atherosclerosis by disturbing both WAT and BAT, and targeting inflammation may thus hold therapeutic potential. Although widely used compounds to treat type 2 diabetes and cardiovascular disease, such as respectively metformin and statins, have pleiotropic anti-inflammatory effects (76-78), no strategies currently exist that primarily target inflammation in the treatment of these disorders. A better understanding of the interaction between inflammatory pathways in metabolic tissues and metabolic derangements is a prerequisite for the development of novel compounds that dampen inflammation to treat individuals with these pathologies.

The research described in this thesis was performed to address three key objectives: 1) gain more insight into the role of the immune system in obesity, insulin resistance, dyslipidemia and atherosclerosis, 2) study inflammation in a human population with a particularly high risk to develop type 2 diabetes and cardiovascular disease, and 3) study the therapeutic potential of reducing inflammation by pharmacological strategies on obesity and glucose and lipid metabolism in pre-clinical models, with emphasis on BAT and WAT.

To address the first key objective, we studied the effect of a potent inflammatory trigger on lipid metabolism and atherosclerosis. Bacille-Calmette-Guérin (BCG), prepared from attenuated live *Mycobacterium bovis*, is the only licensed and widely used vaccine against tuberculosis and modulates atherosclerosis development via immunomodulatory mechanisms. However, previous studies are conflicting with regards to whether BCG protects against or enhances atherosclerosis and did not take into account the effect of BCG on metabolism of cholesterol, the main driver of atherosclerosis. The aim of **chapter 2** therefore was to elucidate the effect of BCG on cholesterol metabolism and atherosclerosis development. In the next chapter, we switched our focus from immune modulation of lipid metabolism and atherosclerosis to glucose metabolism and type

2 diabetes. During the development of obesity, B cells accumulate in WAT and produce pathogenic IgG antibodies, which contribute to the development of glucose intolerance. IgG antibodies signal by binding to Fcγ receptors (FcγR) and by activating the complement system. In **chapter 3**, the purpose was to investigate whether activation of FcγR and/or complement pathway mediate the development of glucose intolerance in WAT.

To meet our second key objective, we performed a human study in which we compared Dutch South Asians and Dutch white Caucasians. These ethnic groups were selected because of the strikingly elevated risk of developing type 2 diabetes that South Asians have when compared to white Caucasians. Even though their increased risk of type 2 diabetes is well-established and inflammation is known to contribute to the development of this disease, inflammatory pathways in South Asians have not been extensively studied previously. The intent in **chapter 4** was therefore to investigate the inflammatory state of blood and metabolic tissues in Dutch South Asians compared to Dutch white Caucasians.

In the final part of this thesis, studies are described that focus on the treatment of metabolic inflammation and disease by targeting BAT and WAT (key objective 3). Salsalate is an anti-inflammatory drug that improves glucose intolerance and dyslipidemia in type 2 diabetic patients, but the mechanisms behind these effects are unclear. The research in **chapter 5** was designed to unravel these mechanisms. We assessed the effects of salsalate on lipid metabolism and adipose tissue inflammation *in vivo*, and investigated the molecular pathways mediating direct effects of salsalate on brown adipocytes *in vitro*. We then aspired to assess the therapeutic potential of targeting GPR120, a fatty acid receptor that mediates anti-inflammatory and insulin-sensitizing effects. Interestingly, cold exposure markedly increases the expression of GPR120 in BAT and WAT. These immunomodulatory and fat-related properties of GPR120 prompted us to investigate the effects of GPR120 deficiency and treatment with a GPR120 agonist on obesity and lipid metabolism in **chapter 6**.

Finally, the results from these studies and their implications for the development of therapeutic strategies are discussed in **chapter 7**.

REFERENCES

1. Berrington de Gonzalez A, Hartge P, Cerhan JR, Flint AJ, Hannan L, MacInnis RJ, Moore SC, Tobias GS, Anton-Culver H, Freeman LB, Beeson WL, Clipp SL, English DR, Folsom AR, Freedman DM, Giles G, Hakansson N, Henderson KD, Hoffman-Bolton J, Hoppin JA, Koenig KL, Lee I-M, Linet MS, Park Y, Pocobelli G, Schatzkin A, Sesso HD, Weiderpass E, Willcox BJ, Wolk A, Zeleniuch-Jacquotte A, Willett WC, Thun MJ: Body-Mass Index and Mortality among 1.46 Million White Adults. New England Journal of Medicine 2010;363:2211-2219

2. Knight JA: Diseases and disorders associated with excess body weight. Annals of clinical and laboratory science 2011;41:107-121

3. Whiting DR, Guariguata L, Weil C, Shaw J: IDF diabetes atlas: global estimates of the prevalence of diabetes for 2011 and 2030. Diabetes research and clinical practice 2011;94:311-321

4. Bindraban NR, van Valkengoed IG, Mairuhu G, Holleman F, Hoekstra JB, Michels BP, Koopmans RP, Stronks K: Prevalence of diabetes mellitus and the performance of a risk score among Hindustani Surinamese, African Surinamese and ethnic Dutch: a cross-sectional population-based study. BMC public health 2008;8:271

5. Chiu M, Austin PC, Manuel DG, Shah BR, Tu JV: Deriving ethnic-specific BMI cutoff points for assessing diabetes risk. Diabetes care 2011;34:1741-1748

6. Joshi P, Islam S, Pais P, Reddy S, Dorairaj P, Kazmi K, Pandey MR, Haque S, Mendis S, Rangarajan S, Yusuf S: Risk factors for early myocardial infarction in South Asians compared with individuals in other countries. Jama 2007;297:286-294

7. Balarajan R: Ethnic differences in mortality from ischaemic heart disease and cerebrovascular disease in England and Wales. BMJ (Clinical research ed) 1991;302:560-564

8. Chaturvedi N, Fuller JH: Ethnic differences in mortality from cardiovascular disease in the UK: do they persist in people with diabetes? Journal of epidemiology and community health 1996;50:137-139

9. Anand SS, Yusuf S, Vuksan V, Devanesen S, Teo KK, Montague PA, Kelemen L, Yi C, Lonn E, Gerstein H, Hegele RA, McQueen M: Differences in risk factors, atherosclerosis, and cardiovascular disease between ethnic groups in Canada: the Study of Health Assessment and Risk in Ethnic groups (SHARE). Lancet (London, England) 2000;356:279-284

10. McKeigue PM, Shah B, Marmot MG: Relation of central obesity and insulin resistance with high diabetes prevalence and cardiovascular risk in South Asians. Lancet (London, England) 1991;337:382-386

11. Raji A, Gerhard-Herman MD, Warren M, Silverman SG, Raptopoulos V, Mantzoros CS, Simonson DC: Insulin resistance and vascular dysfunction in nondiabetic Asian Indians. The Journal of clinical endocrinology and metabolism 2004;89:3965-3972

12. Forouhi NG, Sattar N, Tillin T, McKeigue PM, Chaturvedi N: Do known risk factors explain the higher coronary heart disease mortality in South Asian compared with European men? Prospective follow-up of the Southall and Brent studies, UK. Diabetologia 2006;49:2580-2588

13. Boon MR, Bakker LE, van der Linden RA, van Ouwerkerk AF, de Goeje PL, Counotte J, Jazet IM, Rensen PC: High prevalence of cardiovascular disease in South Asians: Central role for brown adipose tissue? Critical reviews in clinical laboratory sciences 2015;52:150-157

14. Williams KJ: Molecular processes that handle -- and mishandle -- dietary lipids. The Journal of clinical investigation 2008;118:3247-3259

1

15. Khedoe PP, Hoeke G, Kooijman S, Dijk W, Buijs JT, Kersten S, Havekes LM, Hiemstra PS, Berbée JF, Boon MR, Rensen PC: Brown adipose tissue takes up plasma triglycerides mostly after lipolysis. Journal of lipid research 2015;56:51-59

16. Tchernof A, Despres JP: Pathophysiology of human visceral obesity: an update. Physiological reviews 2013;93:359-404

17. Pandey AK, Sassetti CM: Mycobacterial persistence requires the utilization of host cholesterol. Proceedings of the National Academy of Sciences of the United States of America 2008;105:4376-4380

18. Wipperman MF, Sampson NS, Thomas ST: Pathogen roid rage: cholesterol utilization by Mycobacterium tuberculosis. Critical reviews in biochemistry and molecular biology 2014;49:269-293

19. Klop B, Elte JW, Cabezas MC: Dyslipidemia in obesity: mechanisms and potential targets. Nutrients 2013;5:1218-1240

20. Cinti S: The adipose organ. Prostaglandins, leukotrienes, and essential fatty acids. Prostaglandins Leukot Essent Fatty Acids 2005;73:9-15

21. Kershaw EE, Flier JS: Adipose tissue as an endocrine organ. The Journal of clinical endocrinology and metabolism 2004;89:2548-2556

22. Cypess AM, Lehman S, Williams G, Tal I, Rodman D, Goldfine AB, Kuo FC, Palmer EL, Tseng YH, Doria A, Kolodny GM, Kahn CR: Identification and importance of brown adipose tissue in adult humans. The New England journal of medicine 2009;360:1509-1517

23. Virtanen KA, Lidell ME, Orava J, Heglind M, Westergren R, Niemi T, Taittonen M, Laine J, Savisto NJ, Enerback S, Nuutila P: Functional brown adipose tissue in healthy adults. The New England journal of medicine 2009;360:1518-1525

24. van Marken Lichtenbelt WD, Vanhommerig JW, Smulders NM, Drossaerts JM, Kemerink GJ, Bouvy ND, Schrauwen P, Teule GJ: Cold-activated brown adipose tissue in healthy men. The New England journal of medicine 2009;360:1500-1508

25. Cannon B, Nedergaard J: Brown adipose tissue: function and physiological significance. Physiological reviews 2004;84:277-359

26. Fedorenko A, Lishko PV, Kirichok Y: Mechanism of fatty-acid-dependent UCP1 uncoupling in brown fat mitochondria. Cell 2012;151:400-413

27. Wu J, Bostrom P, Sparks LM, Ye L, Choi JH, Giang AH, Khandekar M, Virtanen KA, Nuutila P, Schaart G, Huang K, Tu H, van Marken Lichtenbelt WD, Hoeks J, Enerback S, Schrauwen P, Spiegelman BM: Beige adipocytes are a distinct type of thermogenic fat cell in mouse and human. Cell 2012;150:366-376

28. Xue R, Lynes MD, Dreyfuss JM, Shamsi F, Schulz TJ, Zhang H, Huang TL, Townsend KL, Li Y, Takahashi H, Weiner LS, White AP, Lynes MS, Rubin LL, Goodyear LJ, Cypess AM, Tseng YH: Clonal analyses and gene profiling identify genetic biomarkers of the thermogenic potential of human brown and white preadipocytes. Nature medicine 2015;21:760-768

29. Shinoda K, Luijten IH, Hasegawa Y, Hong H, Sonne SB, Kim M, Xue R, Chondronikola M, Cypess AM, Tseng YH, Nedergaard J, Sidossis LS, Kajimura S: Genetic and functional characterization of clonally derived adult human brown adipocytes. Nature medicine 2015;21:389-394

30. Villarroya F, Cereijo R, Villarroya J, Giralt M: Brown adipose tissue as a secretory organ. Nature reviews Endocrinology 2017;13:26-35

31. Ouchi N, Parker JL, Lugus JJ, Walsh K: Adipokines in inflammation and metabolic disease. Nature Reviews Immunology 2011;11:85-97

32. Roberts-Toler C, O'Neill BT, Cypess AM: Diet-induced obesity causes insulin resistance in

mouse brown adipose tissue. Obesity (Silver Spring, Md) 2015;23:1765-1770

33. Ortega MT, Xie L, Mora S, Chapes SK: Evaluation of macrophage plasticity in brown and white adipose tissue. Cellular immunology 2011;271:124-133

34. Lumeng CN, Saltiel AR: Inflammatory links between obesity and metabolic disease. Journal of Clinical Investigation 2011;121:2111-2117

35. Weisberg SP, McCann D, Desai M, Rosenbaum M, Leibel RL, Ferrante AW, Jr.: Obesity is associated with macrophage accumulation in adipose tissue. The Journal of clinical investigation 2003;112:1796-1808

36. Lumeng CN, Bodzin JL, Saltiel AR: Obesity induces a phenotypic switch in adipose tissue macrophage polarization. The Journal of clinical investigation 2007;117:175-184

37. Elgazar-Carmon V, Rudich A, Hadad N, Levy R: Neutrophils transiently infiltrate intra-abdominal fat early in the course of high-fat feeding. Journal of lipid research 2008;49:1894-1903

38. Talukdar S, Oh DY, Bandyopadhyay G, Li D, Xu J, McNelis J, Lu M, Li P, Yan Q, Zhu Y, Ofrecio J, Lin M, Brenner MB, Olefsky JM: Neutrophils mediate insulin resistance in mice fed a high-fat diet through secreted elastase. Nature medicine 2012;18:1407-1412

39. Wu D, Molofsky AB, Liang H-E, Ricardo-Gonzalez RR, Jouihan HA, Bando JK, Chawla A, Locksley RM: Eosinophils Sustain Adipose Alternatively Activated Macrophages Associated with Glucose Homeostasis. Science 2011;332:243-247

40. Feuerer M, Herrero L, Cipolletta D, Naaz A, Wong J, Nayer A, Lee J, Goldfine AB, Benoist C, Shoelson S, Mathis D: Lean, but not obese, fat is enriched for a unique population of regulatory T cells that affect metabolic parameters. Nature medicine 2009;15:930-939

41. Nishimura S, Manabe I, Nagasaki M, Eto K, Yamashita H, Ohsugi M, Otsu M, Hara K, Ueki K, Sugiura S, Yoshimura K, Kadowaki T, Nagai R: CD8+ effector T cells contribute to macrophage recruitment and adipose tissue inflammation in obesity. Nature medicine 2009;15:914-920

42. Chatzigeorgiou A, Karalis KP, Bornstein SR, Chavakis T: Lymphocytes in obesity-related adipose tissue inflammation. Diabetologia 2012;55:2583-2592

43. Winer S, Chan Y, Paltser G, Truong D, Tsui H, Bahrami J, Dorfman R, Wang Y, Zielenski J, Mastronardi F, Maezawa Y, Drucker DJ, Engleman E, Winer D, Dosch HM: Normalization of obesity-associated insulin resistance through immunotherapy. Nature medicine 2009;15:921-929

44. Winer S, Winer DA: The adaptive immune system as a fundamental regulator of adipose tissue inflammation and insulin resistance. Immunology & Cell Biology 2012;90:755-762

45. Winer DA, Winer S, Shen L, Wadia PP, Yantha J, Paltser G, Tsui H, Wu P, Davidson MG, Alonso MN, Leong HX, Glassford A, Caimol M, Kenkel JA, Tedder TF, McLaughlin T, Miklos DB, Dosch HM, Engleman EG: B cells promote insulin resistance through modulation of T cells and production of pathogenic IgG antibodies. Nature medicine 2011;17:610-617

46. Chawla A, Nguyen KD, Goh YPS: Macrophage-mediated inflammation in metabolic disease. Nature Reviews Immunology 2011;11:738-749

47. Tian Xiao Y, Ganeshan K, Hong C, Nguyen Khoa D, Qiu Y, Kim J, Tangirala Rajendra K, Tonotonoz P, Chawla A: Thermoneutral Housing Accelerates Metabolic Inflammation to Potentiate Atherosclerosis but Not Insulin Resistance. Cell Metabolism 2016;23:165-178

48. Stemmer K, Kotzbeck P, Zani F, Bauer M, Neff C, Muller TD, Pfluger PT, Seeley RJ, Divanovic S: Thermoneutral housing is a critical factor for immune function and diet-induced obesity in C57BL/6 nude mice. International Journal of Obesity 2015;39:791-797

49. Kooijman S, van den Berg R, Ramkisoensing A, Boon MR, Kuipers EN, Loef M, Zonneveld TCM, Lucassen EA, Sips HCM, Chatzispyrou IA, Houtkooper RH, Meijer JH, Coomans CP, Biermasz NR, Rensen PCN: Prolonged daily light exposure increases body fat mass through attenuation of brown adipose tissue activity. Proceedings of the National Academy of Sciences 2015;112:6748-6753

50. Orozco-Solis R, Aguilar-Arnal L, Murakami M, Peruquetti R, Ramadori G, Coppari R, Sassone-Corsi P: The Circadian Clock in the Ventromedial Hypothalamus Controls Cyclic Energy Expenditure. Cell Metabolism 2016;23:467-478

51. Martínez de Morentin Pablo B, González-García I, Martins L, Lage R, Fernández-Mallo D, Martínez-Sánchez N, Ruíz-Pino F, Liu J, Morgan Donald A, Pinilla L, Gallego R, Saha Asish K, Kalsbeek A, Fliers E, Bisschop Peter H, Diéguez C, Nogueiras R, Rahmouni K, Tena-Sempere M, López M: Estradiol Regulates Brown Adipose Tissue Thermogenesis via Hypothalamic AMPK. Cell Metabolism 2014;20:41-53

52. Rogers NH, Perfield JW, Strissel KJ, Obin MS, Greenberg AS: Reduced Energy Expenditure and Increased Inflammation Are Early Events in the Development of Ovariectomy-Induced Obesity. Endocrinology 2009;150:2161-2168

53. Hatori M, Vollmers C, Zarrinpar A, DiTacchio L, Bushong Eric A, Gill S, Leblanc M, Chaix A, Joens M, Fitzpatrick James AJ, Ellisman Mark H, Panda S: Time-Restricted Feeding without Reducing Caloric Intake Prevents Metabolic Diseases in Mice Fed a High-Fat Diet. Cell Metabolism 2012;15:848-860

54. Nguyen KD, Qiu Y, Cui X, Goh YP, Mwangi J, David T, Mukundan L, Brombacher F, Locksley RM, Chawla A: Alternatively activated macrophages produce catecholamines to sustain adaptive thermogenesis. Nature 2011;480:104-108

55. McGregor RA, Kwon EY, Shin SK, Jung UJ, Kim E, Park JHY, Yu R, Yun JW, Choi MS: Time-course microarrays reveal modulation of developmental, lipid metabolism and immune gene networks in intrascapular brown adipose tissue during the development of diet-induced obesity. International Journal of Obesity 2013;37:1524-1531

56. Qiu Y, Nguyen Khoa D, Odegaard Justin I, Cui X, Tian X, Locksley Richard M, Palmiter Richard D, Chawla A: Eosinophils and Type 2 Cytokine Signaling in Macrophages Orchestrate Development of Functional Beige Fat. Cell 2014;157:1292-1308

57. Rao RR, Long JZ, White JP, Svensson KJ, Lou J, Lokurkar I, Jedrychowski MP, Ruas JL, Wrann CD, Lo JC, Camera DM, Lachey J, Gygi S, Seehra J, Hawley JA, Spiegelman BM: Meteorin-like Is a Hormone that Regulates Immune-Adipose Interactions to Increase Beige Fat Thermogenesis. Cell 2014;157:1279-1291

58. Brestoff JR, Artis D: Immune Regulation of Metabolic Homeostasis in Health and Disease. Cell 2015;161:146-160

59. Wellen KE, Hotamisligil GS: Inflammation, stress, and diabetes. The Journal of clinical investigation 2005;115:1111-1119

60. White MF: The insulin signalling system and the IRS proteins. Diabetologia 1997;40 Suppl 2:S2-17

61. Saltiel AR, Pessin JE: Insulin signaling pathways in time and space. Trends in cell biology 2002;12:65-71

62. Dandona P, Aljada A, Bandyopadhyay A: Inflammation: the link between insulin resistance, obesity and diabetes. Trends in immunology 2004;25:4-7

63. Hotamisligil GS, Shargill NS, Spiegelman BM: Adipose expression of tumor necrosis factor-alpha: direct role in obesity-linked insulin resistance. Science 1993;259:87-91

64. Hotamisligil GS, Peraldi P, Budavari A, Ellis R, White MF, Spiegelman BM: IRS-1-mediated inhibition of insulin receptor tyrosine kinase

activity in TNF-alpha- and obesity-induced insulin resistance. Science 1996;271:665-668

65. Adeli K, Taghibiglou C, Van Iderstine SC, Lewis GF: Mechanisms of hepatic very low-density lipoprotein overproduction in insulin resistance. Trends in cardiovascular medicine 2001;11:170-176

66. Libby P: Inflammation in atherosclerosis. Nature 2002;420:868-874

67. Hansson GK, Hermansson A: The immune system in atherosclerosis. Nature immunology 2011;12:204-212

68. Oorni K, Posio P, Ala-Korpela M, Jauhiainen M, Kovanen PT: Sphingomyelinase induces aggregation and fusion of small very low-density lipoprotein and intermediate-density lipoprotein particles and increases their retention to human arterial proteoglycans. Arteriosclerosis, thrombosis, and vascular biology 2005;25:1678-1683

69. Wooton-Kee CR, Boyanovsky BB, Nasser MS, de Villiers WJ, Webb NR: Group V sPLA2 hydrolysis of low-density lipoprotein results in spontaneous particle aggregation and promotes macrophage foam cell formation. Arteriosclerosis, thrombosis, and vascular biology 2004;24:762-767

70. Barath P, Fishbein MC, Cao J, Berenson J, Helfant RH, Forrester JS: Detection and localization of tumor necrosis factor in human atheroma. The American journal of cardiology 1990;65:297-302

71. Libby P, Lichtman AH, Hansson GK: Immune effector mechanisms implicated in atherosclerosis: from mice to humans. Immunity 2013;38:1092-1104

72. Clinton SK, Underwood R, Hayes L, Sherman ML, Kufe DW, Libby P: Macrophage colony-stimulating factor gene expression in vascular cells and in experimental and human atherosclerosis. The American journal of pathology 1992;140:301-316

73. van Diepen JA, Berbee JF, Havekes LM, Rensen PC: Interactions between inflammation and lipid metabolism: relevance for efficacy of anti-inflammatory drugs in the treatment of atherosclerosis. Atherosclerosis 2013;228:306-315

74. Khovidhunkit W, Kim MS, Memon RA, Shigenaga JK, Moser AH, Feingold KR, Grunfeld C: Effects of infection and inflammation on lipid and lipoprotein metabolism: mechanisms and consequences to the host. Journal of lipid research 2004;45:1169-1196

75. Shoelson SE, Lee J, Goldfine AB: Inflammation and insulin resistance. The Journal of clinical investigation 2006;116:1793-1801

76. Xu W, Deng YY, Yang L, Zhao S, Liu J, Zhao Z, Wang L, Maharjan P, Gao S, Tian Y, Zhuo X, Zhao Y, Zhou J, Yuan Z, Wu Y: Metformin ameliorates the proinflammatory state in patients with carotid artery atherosclerosis through sirtuin 1 induction. Translational research : the journal of laboratory and clinical medicine 2015;166:451-458

77. Goldberg RB, Temprosa MG, Mather KJ, Orchard TJ, Kitabchi AE, Watson KE: Lifestyle and metformin interventions have a durable effect to lower CRP and tPA levels in the diabetes prevention program except in those who develop diabetes. Diabetes care 2014;37:2253-2260

78. Greenwood J, Steinman L, Zamvil SS: Statin therapy and autoimmune disease: from protein prenylation to immunomodulation. Nature reviews Immunology 2006;6:358-370

Chapter 2

BCG lowers plasma cholesterol levels and delays atherosclerotic lesion progression in mice

Andrea D. van Dam, Siroon Bekkering, Malou Crasborn, Lianne van Beek,
Susan M. van den Berg, Frank Vrieling, Simone A. Joosten,
Vanessa van Harmelen, Menno P.J. de Winther, Dieter Lütjohann,
Esther Lutgens, Mariëtte R. Boon, Niels P. Riksen,
Patrick C.N. Rensen, Jimmy F.P. Berbée

ABSTRACT

Bacille-Calmette-Guérin (BCG), prepared from attenuated live *Mycobacterium bovis*, modulates atherosclerosis development as currently explained by immunomodulatory mechanisms. However, whether BCG is pro- or anti-atherogenic remains inconclusive as the effect of BCG on cholesterol metabolism, the main driver of atherosclerosis development, has remained underexposed in previous studies. Therefore, we aimed to elucidate the effect of BCG on cholesterol metabolism in addition to inflammation and atherosclerosis development in *APOE*3-Leiden.CETP* mice, a well-established model of human-like lipoprotein metabolism. To this end, hyperlipidemic *APOE*3-Leiden.CETP* mice were fed a Western-type diet containing 0.1% cholesterol and were terminated 6 weeks after a single intravenous injection with BCG (0.75 mg; $5x10^6$ CFU). BCG-treated mice exhibited hepatic mycobacterial infection and hepatomegaly. The enlarged liver (+53%, p=0.001) coincided with severe immune cell infiltration and a higher cholesterol content (+31%, p=0.03). Moreover, BCG reduced plasma total cholesterol levels (-34%, p=0.003), which was confined to reduced nonHDL-cholesterol levels (-36%, p=0.002). This was due to accelerated plasma clearance of cholesterol from intravenously injected [^{14}C]cholesteryl oleate-labelled VLDL-like particles ($t_{1/2}$ -41%, p=0.002) as a result of elevated hepatic uptake (+25%, p=0.05) as well as reduced intestinal cholestanol and sterol absorption (up to -37%, p=0.003). Ultimately, BCG decreased foam cell formation of peritoneal macrophages (-18%, p=0.02) and delayed atherosclerotic lesion progression in the aortic root of the heart. BCG tended to decrease atherosclerotic lesion area (-59%, p=0.08) and reduced lesion severity. In conclusion, BCG reduces plasma nonHDL-cholesterol levels and delays atherosclerotic lesion formation in hyperlipidemic mice.

INTRODUCTION

Cardiovascular disease is the leading cause of death in Western countries, and atherosclerosis is the pathology underlying most cardiovascular events. The main risk factor for the development of atherosclerosis is hypercholesterolemia, as excess cholesterol initiates foam cell formation in the arterial wall. Subsequently, inflammatory processes including recruitment of innate and adaptive immune cells contribute to further development of the plaque, which may eventually lead to plaque rupture and/or vessel occlusion (1). A variety of bacteria and viruses (2), but also bacterial components such as lipopolysaccharide (3), have been suggested to be implicated in atherosclerosis development. In this respect, Bacille-Calmette-Guérin (BCG), prepared from attenuated live *Mycobacterium bovis* and the only licensed vaccine against tuberculosis (4), is of special interest since BCG is used worldwide for vaccination.

Interestingly, animal studies have shown that BCG modulates atherosclerosis development. However, the data on whether BCG reduces or enhances atherosclerosis development are conflicting. BCG injection in rabbits in which plasma cholesterol levels were maintained constant (*i.e.* by individual adjustment of the percentage of cholesterol in the diet) increased lymphocyte and monocyte activation and hence atherosclerosis development (5). In contrast, repeated injections of killed BCG reduced atherosclerosis in LDL receptor-knockout (*Ldlr*$^{-/-}$) and apolipoprotein E-knockout (*Apoe*$^{-/-}$) mice, but did not significantly modulate plasma cholesterol levels. The reduced atherosclerosis development was accompanied by enhanced circulating IL-10 levels and reduced serum levels of pro-inflammatory cytokines (6). Although these pro- and anti-atherogenic effects have been attributed to immunomodulatory effects of BCG, the effect of BCG on the metabolism of cholesterol, the main driver of atherosclerosis development, has remained underexposed.

Therefore, in the current study we aimed to elucidate the effect of BCG on cholesterol metabolism and atherosclerosis development in *APOE*3-Leiden.CETP* (*E3L.CETP*) transgenic mice. These mice have a humanized lipoprotein profile due to expression of human cholesterol ester transfer protein (CETP), which transfers cholesteryl esters from HDL to LDL and VLDL in exchange for triglycerides, and a mutation of the human *APOE*3* gene, which attenuates clearance of cholesterol-enriched lipoprotein remnants without abrogating the apoE-LDLR clearance pathway (7-9). We show that BCG markedly reduces plasma cholesterol levels as a result of accelerated hepatic uptake of cholesterol-enriched lipoprotein remnants and reduced intestinal cholesterol absorption. Finally, BCG reduces foam cell formation and delays atherosclerotic plaque formation.

MATERIALS AND METHODS

Mice, diet and BCG treatment

Female *E3L.CETP* mice were obtained as previously described (7, 8). At the start of the experiment mice were 10-12 weeks of age and housed under standard conditions with a 12:12 h light-dark cycle and free access to food and water. Mice were fed a Western-type diet containing 0.1% cholesterol (WTD; Hope Farms, The Netherlands). After a run-in period of 3 weeks with WTD, mice were randomized according to body weight, plasma total cholesterol (TC) and plasma triglycerides (TG), and received an intravenous injection with a human dose of Bacille-Calmette-Guérin (BCG) vaccine SSI (0.75 mg; 5×10^6 CFU in 100 μL PBS; SSI Denmark) (10). Mice were terminated 6 weeks after the injection. Mouse experiments were performed in accordance with the Institute for Laboratory Animal Research Guide for the Care and Use of Laboratory Animals and had received approval from the University Ethical Review Board (Leiden University Medical Center, The Netherlands).

Mycobacterial culture

Blood, splenocytes and bone marrow were incubated both in BBL Bactec MGIT tubes (245113, BD and Company, NJ, USA) and on Lowenstein-Jensen + PACT plates (220501, BD and Company, NJ, USA) at 36°C. Bacterial growth in the BBL Bactec MGIT tubes was measured weekly using the BD BACTEC™-MicroMGIT Fluorescence Reader according to the manufacturer's instructions. Lowenstein-Jensen plates were checked once a week for growth of colonies. When positive, standard Ziehl-Neelsen (ZN) staining [z1] was performed to confirm presence of mycobacteria.

Liver histology

Livers were fixed in 4% paraformaldehyde, dehydrated in 70% EtOH, and embedded in paraffin. Hematoxylin-eosin (HE) and ZN stainings were performed on sections (5 μm) using standard protocols. Immunohistochemical detection of F4/80 was done on paraffin-embedded sections that were treated with proteinase K, by using a primary rat anti-

Table 1: *Primer sequences of forward and reverse primers (5′ → 3′).*

Gene	Forward primer	Reverse primer
Apob	GCCCATTGTGGACAAGTTGATC	CCAGGACTTGGAGGTCTTGGA
Cd3	AACACGTACTTGTACCTGAAAGCTC	GATGATTATGGCTACTGCTGTCA
Cd4	ACACACCTGTGCAAGAAGCA	GCTCTTGTTGGTTGGGAATC
Cd8	GGCTCTGGCTGGTCTTCA	GACGAAGGGGTCTGAATGAG
F4/80	CTTTGGCTATGGGCTTCCAGTC	GCAAGGAGGACAGAGTTTATCGTG
Gapdh	GGGGCTGGCATTGCTCTCAA	TTGCTCAGTGTCCTTGCTGGGG
Hmgcoar	CCGGCAACAACAAGATCTGTG	ATGTACAGGATGGCGATGCA
Ldlr	GCATCAGCTTGGACAAGGTGT	GGGAACAGCCACCATTGTTG
Tnf	AGCCCACGTCGTAGCAAACCAC	TCGGGGCAGCCTTGTCCCTT

mouse F4/80 monoclonal Ab (MCA497; 1/600, Serotec, UK) and a secondary goat anti-rat immunoglobulin peroxidase (MP-7444, Vector Laboratories Inc., CA, USA). The peroxidase activity was revealed with NovaRed (SK-4800, Vector Laboratories Inc.) and slides were counterstained with hematoxylin. The area positive for F4/80 was quantified using ImageJ Software.

RNA purification and quantitative RT-PCR
RNA was extracted from snap-frozen mouse livers using Tripure RNA Isolation reagent (Roche, The Netherlands) according to manufacturer's instructions. RNA concentrations were measured using NanoDrop and RNA was reverse transcribed using Moloney Murine Leukemia Virus Reverse Transcriptase (Promega, The Netherlands) for quantitative RT-PCR (qRT-PCR) to produce cDNA. Expression levels of genes were determined by qRT-PCR, using gene-specific primers (**Table 1**) and SYBR green supermix (Biorad, The Netherlands). mRNA expression was normalized to *Gapdh* mRNA content and expressed as fold change compared with control mice using the ΔΔCT method.

Flow cytometry
Circulating white blood cells were analysed using flow cytometry. After lysis of red blood cells, pelleted cells were resuspended in FACS buffer and stained for 30 minutes at 4°C in the dark with the fluorescently labelled antibodies listed in **Table 2**. Cells were measured on an LSR II flow cytometer (BD Biosciences, CA, USA). Data were analysed using FlowJo software (Treestar, OR, USA).

Isolation and ex vivo stimulation of cells
Resident peritoneal macrophages were isolated from mice by washing the peritoneal cavity with ice-cold sterile PBS. Pelleted cells were resuspended in RPMI 1640 Dutch-modified culture medium (Life Technologies/Invitrogen, The Netherlands) supplemented with 10

Table 2: *Antibodies used for flow cytometry.*

Antibody	Fluorochrome	Dilution	Clone, supplier
CD45.2	FITC	1:100	104, BioLegend
CD3	APC	1:100	145-2C11, eBioscience
CD4	Qdot605	1:1000	RM-4-5, BioLegend
CD8a	PerCPCy5.5	1:100	53-6.7, BioLegend
CD25	PeCy7	1:300	PC61.5, eBioScience
CD44	eFluor450	1:300	IM7, eBioScience
CD22.2	PE	1:200	Cy34.1, BD Biosciences
Cd11b	Pacific Blue	1:150	M1/70, BioLegend
Cd115-Biotin	n.a.	1:100	AFS98, eBioScience
Streptavidin	PeCy5	1:100	SAV, eBioScience
Gr-1	PeCy7	1:1500	RB6-8C5, Biolegend

mM glutamine, 10 mM pyruvate (Invitrogen) and 10 µg/mL gentamicin (Centrafarm, The Netherlands) and stimulated with 10 ng/mL LPS (*E. coli* serotype 055:B5, further purified as described previously (11); Sigma-Aldrich, MO, USA) for 24 h. Supernatants were collected for determination of cytokine secretion.

Splenocytes were resuspended in RPMI and stimulated with 10 ng/mL LPS or heat-inactivated *C. albicans* (MYA-3573 UC 820, ATCC, Germany). Supernatants were collected at 48 h or 5 days for measurement of innate or adaptive cytokines.

Bone marrow cells were resuspended in Dulbecco's Modified Eagle Medium (Gibco, Invitrogen, CA, USA) supplemented with 30% L929 medium, 10% FCS, 1% nonessential amino acids, 1% 100 U/mL penicillin and 100 mg/mL streptomycin for differentiation into macrophages. On day 6, the bone marrow-derived macrophages (BMDMs) were harvested and stimulated with 10 ng/mL LPS for 24 h. Supernatants were collected for cytokine measurements.

Cytokine measurements

Mouse IL-6 (CMC0063, Life technologies, The Netherlands), IL-10 and interferon γ (IFNγ; DY417 and DY485, R&D Systems Europe, UK) were measured using commercial ELISA kits according to manufacturers' instructions. Mouse tumor necrosis factor alpha (TNF) and IL-1β were measured using specific radioimmunoassays (RIA) as described previously (12).

Food intake and body weight and composition measurements

Food intake and body weight were measured weekly with a scale, and body composition was measured using an EchoMRI-100 analyzer (EchoMRI, TX, USA).

Determination of plasma and liver lipids

At the indicated time points, 4 h-fasted (from 8:00 am to 12:00 pm) blood samples were collected through tail vein bleeding and isolated plasma was assayed for TC and TG by using commercially available enzymatic kits (Roche Diagnostics, Germany). For determination of HDL-cholesterol, apoB-containing particles were precipitated from plasma with 20% polyethylene glycol in 200 mM glycine buffer (pH 10) and TC was measured in the supernatant.

Lipids were extracted from the liver following a protocol modified from Bligh and Dyer (13). Liver samples were homogenized in 10 µL ice-cold CH_3OH/mg tissue. Lipids were extracted into an organic phase by the addition of 1,800 µL CH_3OH:$CHCl_3$ (1:3 v/v) to 45 µL homogenate and subsequent centrifugation. The lower organic phase was evaporated, lipids were resuspended in 2% Triton X-100, and TC and TG content was assayed as described above. Phospholipids (PL) were determined using an enzymatic colorimetric kit (Instruchemie, The Netherlands).

Table 3: *Primary antibodies used for Western blot.*

Primary antibody	Dilution	Supplier
LDLR	1:1000	AF2255, R&D Systems
SR-BI	1:1000	Ab396, Abcam Inc
α/β-Tubulin	1:1000	#2148, Cell Signaling

In vivo clearance of VLDL-like particles

VLDL-like TG-rich particles (80 nm) labelled with glycerol tri[^{3}H]oleate (TO) and [^{14}C] cholesteryl oleate (CO) were prepared and characterized as described previously (9, 14). Mice were fasted for 4 h (from 8:00 am to 12:00 pm) and injected with 200 µL of VLDL-like particles (1.0 mg TG per mouse) via the tail vein. Blood samples were drawn from the tail vein at the indicated times after injection to determine the plasma decay of [^{3}H]TO and [^{14}C]CO. After 15 min, mice were killed by cervical dislocation and perfused with ice-cold PBS through the heart. Organs were harvested and weighed, dissolved in Tissue Solubilizer (Amersham Biosciences, The Netherlands) overnight at 56°C and analysed for ^{3}H- and ^{14}C-activity.

Extraction and analysis of hepatic cholestanol and sterols

Total cholesterol, markers for hepatic cholesterol synthesis (*i.e.* lanosterol, desmosterol and lathosterol) as well as markers for intestinal cholesterol absorption (*i.e.* cholestanol, campesterol and sitosterol) were extracted from liver by chloroform-methanol and analysed by GC-flame ionization detection and GC-MS as reported previously (15). Dry weight of liver samples was determined after they were dried to constant weight overnight in a Speedvac (Servant Instruments Inc., NY, USA). Data are expressed as ratio to hepatic total cholesterol levels.

Western blot

Pieces of snap-frozen liver tissue (~50 mg) were lysed, protein was isolated, and Western blots were performed as previously described (16). Primary antibodies and dilutions are listed in **Table 3**. Protein content was corrected for the housekeeping protein Tubulin.

Assessment of foam cell formation

Foam cell formation was assessed by culturing 1×10^5 cells/well either in control medium or medium supplemented with 50 **µ**g/mL oxidized human LDL (oxLDL, prepared as described previously (17)) for 48 h. Supernatants were removed and cells were lysed (0.5% Triton-X100). Uptake of oxidized LDL was assessed by measuring intracellular human apoB with ELISA as described before (17).

Atherosclerosis quantification

Hearts were collected, fixed in 4% paraformaldehyde, dehydrated in 70% EtOH, embedded in paraffin and cross-sectioned (5 μm) perpendicular to the axis of the aorta throughout the aortic root area, starting at the point where the open aortic valve leaflets appear. Per mouse, four sections with 50 μm intervals were used for atherosclerosis measurements. Sections were stained with haematoxylin-phloxine-saffron (HPS) for histological analysis. Lesions were categorized for lesion severity according to the guidelines of the American Heart Association adapted for mice (18). Various types of lesions were discerned: mild lesions (types 1-3), severe lesions (types 4-5) and valve lesions. Lesion area was determined using ImageJ Software (9). Detection of macrophage-positive area was performed with rat monoclonal anti-MAC-3 antibody (BD Pharmingen, CA, USA) and Vector Impress anti-rat (Vector Laboratories Inc.). The immunostaining was amplified using Vector Laboratories Elite ABC kit and peroxidase activity was visualized with NovaRed (Vector Laboratories Inc.). Sirius red (Chroma, Germany) was used to stain for collagen. The stability index was determined by dividing the Sirius red-positive area by the MAC-3-positive area.

Statistical Analysis

All data are expressed as means ± SEM. Groups were compared with a two-tailed unpaired Student's t-test unless stated otherwise. Groups were considered statistically significant if $p < 0.05$.

RESULTS

BCG induces mycobacterial infection in hyperlipidemic mice

E3L.CETP mice were fed a Western-type diet containing 0.1% cholesterol (WTD) and received a single intravenous BCG injection. After six weeks, blood and various organs were cultured to investigate whether viable BCG was still present. Blood of BCG-treated mice tested negative for mycobacteria. However, livers, spleens and bone marrow of BCG-treated mice were positive for mycobacteria (**Suppl. Fig. 1** and data not shown), indicating ongoing infection.

BCG induces hepatic inflammation

Since BCG induced hepatic mycobacterial infection and the liver plays a key role in lipid metabolism, we further studied the livers of the BCG-treated animals. Liver weight was increased in BCG-treated mice (+53%, **Fig. 1A**). In these livers, severe leukocyte infiltration (**Fig. 1B**) and accumulation of F4/80-positive cells (**Fig. 1C**) was observed. This coincided with increased expression of inflammatory markers including *F4/80* and *Tnf* as well as the T cell markers *Cd3*, *Cd4* and *Cd8* (**Fig. 1D**). Besides hepatomegaly, BCG-treated mice also exhibited an enlarged spleen (+149%, **Fig. 1A**).
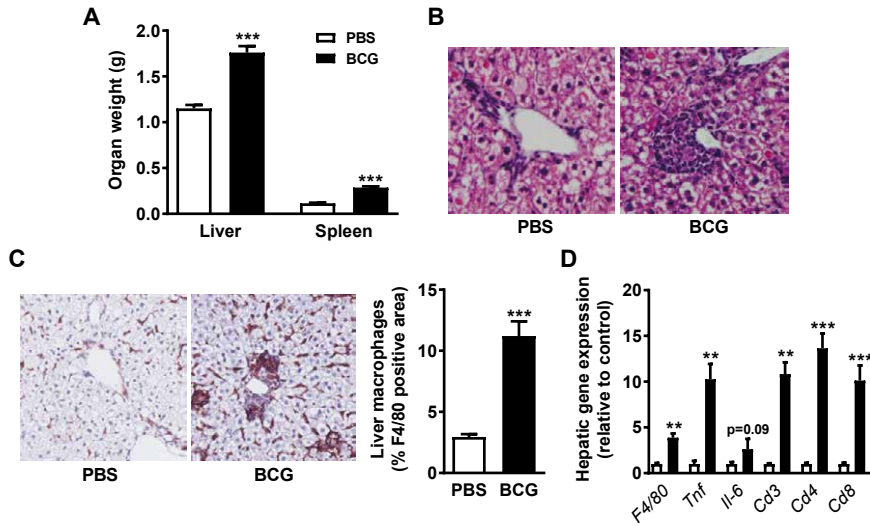
Figure 1. BCG induces hepatic inflammation. *E3L.CETP mice fed a WTD were treated with PBS or BCG (0.75 mg; 5x10^6 CFU; i.v.). Upon sacrifice after 6 weeks, liver and spleen were collected and weighed (A). Haematoxylin and Eosin (B) and F4/80 staining (C) of liver sections was performed. Representative pictures are shown. The relative content of F4/80 positive cells was quantified (C). Hepatic mRNA expression of the indicated inflammatory genes was determined (D). Values represent means ± SEM (n=6). **p<0.01 ***p<0.001 vs. PBS.*

BCG induces overall immune activation

Given the inflammatory state of the liver, we assessed the effect of BCG on circulating white blood cells by flow cytometry. Within the CD45$^+$ white blood cells, BCG did not significantly affect the relative monocyte or granulocyte content (**Suppl. Fig. 2A, B**), but did reduce the percentage of B cells (-33%, **Suppl. Fig. 2C**). The percentage of total T cells remained similar upon BCG vaccination (**Suppl. Fig. 2D**), but BCG increased T helper cells (+11%, **Fig. 2A**) without altering cytotoxic T cells (**Fig. 2D**). Activation of T helper cells was not affected by BCG (**Fig. 2B**), but the memory T helper cells tended to be higher (+59%, **Fig. 2C**). More pronounced effects on activation and memory were found within the cytotoxic T cells, as BCG induced both activation (+204%, **Fig. 2E**) and memory (+84%, **Fig. 2F**) of cytotoxic T cells. Overall, these findings suggest that BCG induces activation of circulating immune cells.

To determine the inflammatory status of tissue macrophages, we performed *ex vivo* stimulation of peritoneal macrophages, splenocytes and bone marrow-derived macrophages and measured cytokine secretion. BCG increased the number of macrophages in the peritoneal cavity (+37%, **Fig. 2G**). Even after correcting for the number of cells, the peritoneal macrophages of BCG-treated mice produced more inflammatory cytokines upon LPS stimulation than macrophages from untreated animals (*i.e.* TNF, IL-1β; **Fig. 2H-K**), suggesting an increased innate inflammatory phenotype.
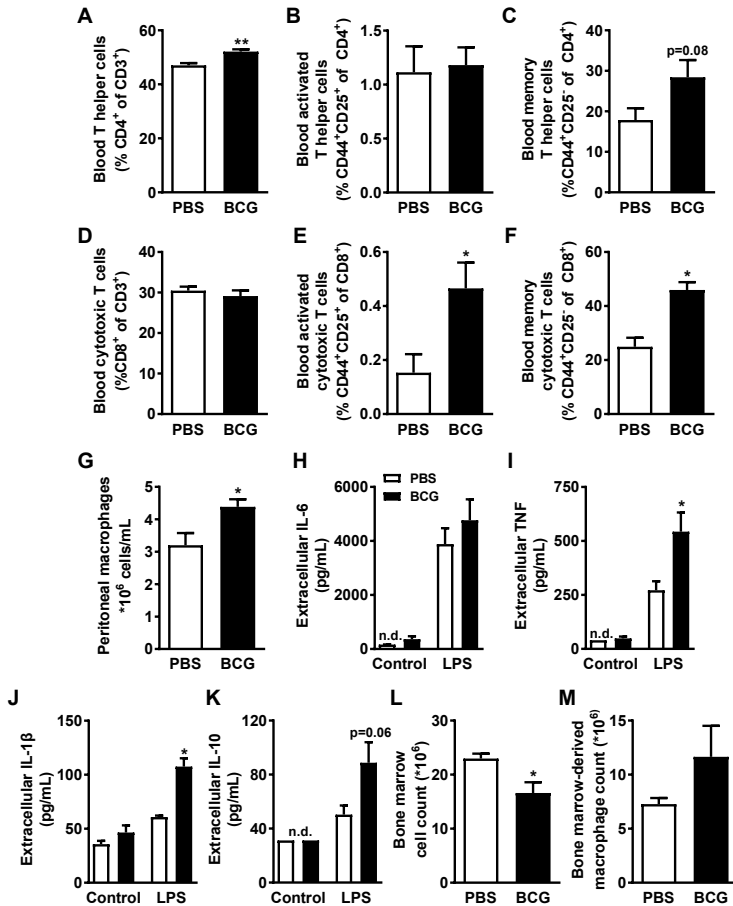
Figure 2. BCG increases immune activation. *E3L.CETP mice fed a WTD were treated with PBS or BCG (0.75 mg; 5x10^6 CFU; i.v.). After 6 weeks, blood, peritoneal macrophages and bone marrow were collected. Within the CD3+ T cell fraction, percentage of CD4+ (A) and CD8+ (D) cells were determined. Within the CD4+ and CD8+ T cell fractions, percentages of activated T cells (CD44+CD25+; B, E) and memory T cells (CD44+CD25-; C, F) were determined. Peritoneal macrophages were counted (G) and stimulated with LPS. Production of IL-6 (H), TNF (I), IL-1β (J) and IL-10 (K) was measured. Bone marrow cells were counted before (L) and after differentiation into macrophages (M). Values represent means ± SEM (n=6). *p<0.05 **p<0.01 vs. PBS.*

Splenocytes from BCG-treated mice also produced more inflammatory cytokines upon LPS stimulation (*i.e.* IL-6, TNF, IL-10; **Suppl. Fig. 2E-G**), confirming the inflammatory phenotype. Interestingly, upon adaptive immune response stimulation (*i.e.* with *C. Albicans*) splenocytes also produced more IFNγ (**Suppl. Fig. 2H**), suggesting that BCG activates CD4+ and CD8+ T cells in the spleen, in line with our observations on circulating cells.

Bone marrow cell counts were lower in mice treated with BCG (-28%, **Fig. 2L**). After adjusting for the number of cells, bone marrow-derived macrophages (BMDMs) from BCG treated mice did not exhibit lower capacity to proliferate (**Fig. 2M**), suggesting that the reduced bone marrow cell counts reflect hematopoietic stem and progenitor cell exhaustion. LPS stimulation of BMDMs did not reveal alterations in cytokine production (data not shown). Taken together, BCG infection resulted in increased overall immune activation.

BCG lowers body fat but increases liver lipid content

To assess the effect of BCG on the metabolic phenotype of *E3L.CETP* mice, body weight and composition were measured over the 6-week period after BCG administration. Total body weight (**Fig. 3A**) and food intake (**Fig. 3B**) were not affected by BCG. After 6 weeks, lean body mass remained unaffected (**Fig. 3C**), but fat mass tended to be lower in BCG-treated animals (-32%, **Fig. 3D**), which was corroborated by a reduced weight of the gonadal white

Figure 3. BCG increases liver lipids. *E3L.CETP mice fed a WTD were treated with PBS or BCG (0.75 mg; 5x10^6 CFU; i.v.). Body weight (A), food intake (B), lean mass (C), fat mass (D), gonadal white adipose tissue weight (E) were measured at the indicated time points. Lipids were extracted from liver and liver triglycerides (TG), liver total cholesterol (TC) and liver phospholipids (PL) were measured (F). Values represent means ± SEM (n=5-6). *p<0.05 **p<0.01 vs. PBS. gWAT, gonadal white adipose tissue.*
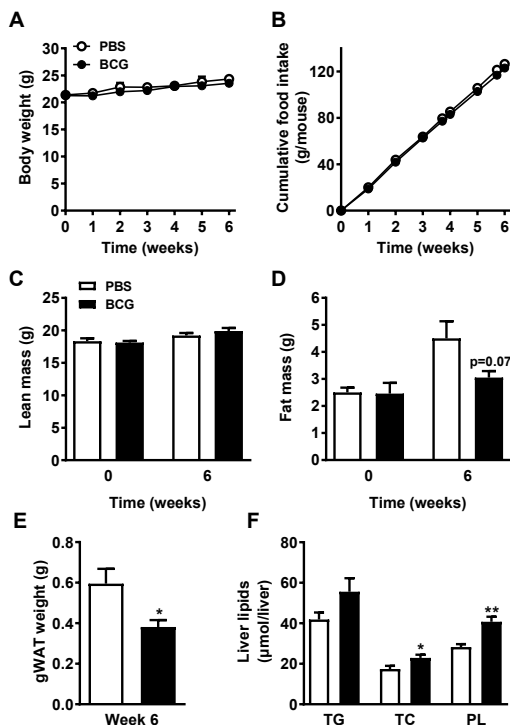
fat pads (-36%, **Fig. 3E**). In line with the increase in liver weight, BCG-treated mice exhibited increased liver lipid content (*i.e.* TG, cholesterol and phospholipids), although the increase in TG content did not reach statistical significance (**Fig. 3F**).

BCG lowers plasma cholesterol by accelerating hepatic uptake of cholesterol-enriched lipoprotein remnants and reducing intestinal cholesterol absorption

As hypercholesterolemia is the main risk factor for atherosclerosis development, we studied the effect of BCG on plasma lipid levels. BCG tended to decrease plasma TG levels after 6 weeks (-34%, **Fig. 4A**), and consistently reduced plasma total cholesterol (TC) levels during the study (-34% at the endpoint, **Fig. 4B**) when compared to the PBS-treated group. This reduction in TC was confined to lowering of the nonHDL-cholesterol fraction (**Fig. 4C**). To investigate whether the reduced plasma TC levels were due to increased clearance of lipoprotein remnant cholesterol, we assessed the plasma clearance and organ uptake of glycerol tri[^{3}H]oleate (TO)- and [^{14}C]cholesteryl oleate (CO)-double-labelled VLDL-like particles *in vivo*. Plasma clearance of [^{3}H]TO was comparable between the groups (**Fig. 4D**, $t_{1/2}$ = 3.0 *vs.* 3.4 min, p=0.09), and no obvious effects on organ uptake of ^{3}H-activity were found apart from an increased uptake by the spleen (+109%, **Fig. 4E**). In contrast, BCG markedly accelerated plasma clearance of [^{14}C]CO (**Fig. 4F**, $t_{1/2}$ = 5.0 *vs.* 8.5 min, p=0.002), mainly due to increased uptake of [^{14}C]CO by the liver (+25%, p=0.05) and to a lesser extent also by the spleen (+214%, **Fig. 4G**). The increase in liver and spleen weight are key to this increased [^{14}C]CO-uptake, as uptake of [^{14}C]CO by liver and spleen did not differ when expressed per gram organ (data not shown). These data support the notion that BCG reduces plasma TC levels by enhancing hepatic uptake of cholesterol-enriched lipoprotein remnants.

Besides increased cholesterol clearance, reduced hepatic cholesterol synthesis or intestinal cholesterol absorption could underlie the reduced plasma cholesterol levels. To assess whether BCG affects hepatic cholesterol synthesis, we determined the cholesterol precursors lanosterol, desmosterol and lathosterol in the liver (**Fig. 4H**). The ratios of lanosterol and desmosterol to total cholesterol were increased (+53 and +79%) upon BCG treatment, whereas the ratio of lathosterol to cholesterol remained unchanged. This suggests increased rather than decreased hepatic cholesterol synthesis. As measures of intestinal cholesterol absorption, we measured cholestanol, campesterol and sitosterol in the liver (**Fig. 4I**). Interestingly, the ratios of cholestanol and campestanol to total cholesterol were decreased (-28% and -37%), whereas the ratio of sitosterol to total cholesterol remained similar. These data indicate that BCG reduces intestinal cholesterol absorption.

We next assessed gene expression and protein content in the liver upon BCG treatment. BCG did not affect genes involved in cholesterol metabolism, including *Ldlr*, *Apob* and *Hmgcoar*, nor LDLR and SR-BI protein content (data not shown).
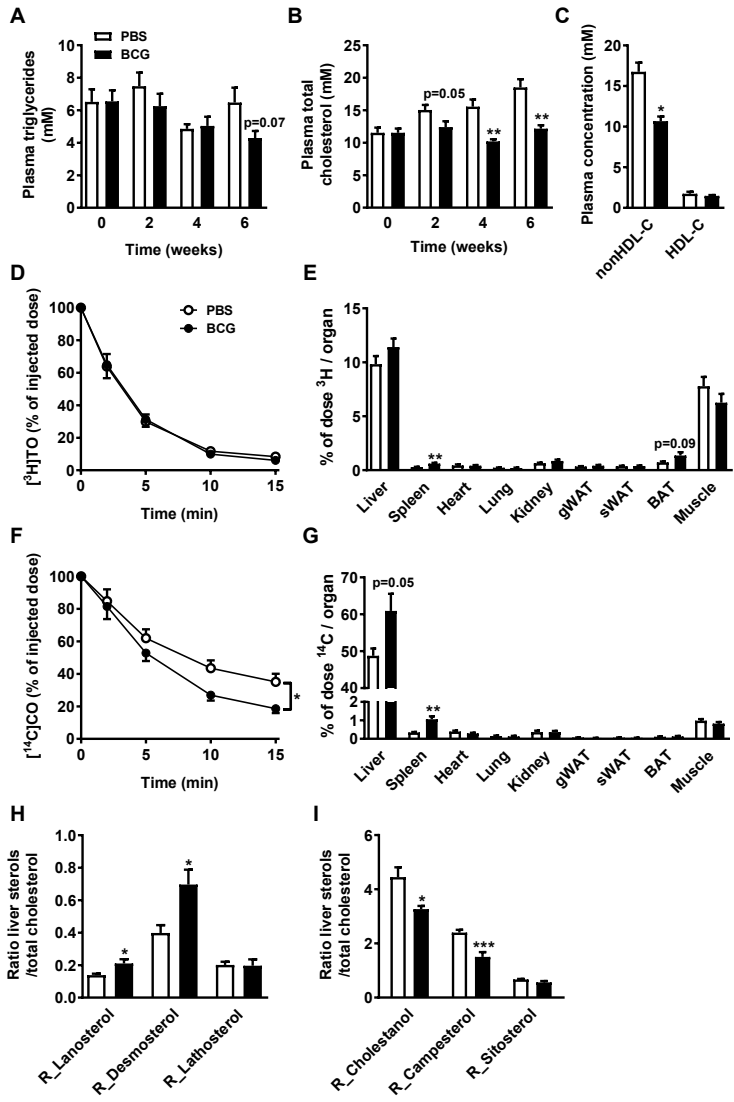
Figure 4. BCG increases plasma cholesterol clearance towards the liver and reduces intestinal cholesterol absorption. *E3L.CETP mice fed a WTD were treated with PBS or BCG (0.75 mg; 5×10^6 CFU; i.v.). Plasma triglycerides (A) and total cholesterol (B) were analysed at the indicated time points. After 6 weeks of treatment also plasma nonHDL-cholesterol and HDL-cholesterol were determined (C). After 6 weeks, mice were injected with glycerol tri[^{3}H]oleate and [^{14}C]cholesteryl oleate double-labelled VLDL-like particles and clearance from plasma (D, F) and uptake by organs and tissues at 15 min after injection were determined by analysing ^{3}H- and ^{14}C-activity (E, G). Cholanol and sterols were extracted from liver and expressed as ratios to cholesterol or per mg dry tissue weight (H, I). Values represent means ± SEM (n=4-6). Interaction between plasma clearance of ^{3}H- and ^{14}C-activity and time was analysed by two-way ANOVA. *p<0.05 **p<0.01 vs. PBS. nonHDL-C, nonHDL-cholesterol; HDL-C, HDL-cholesterol; gWAT, gonadal white adipose tissue; sWAT, subcutaneous white adipose tissue; BAT, brown adipose tissue.*
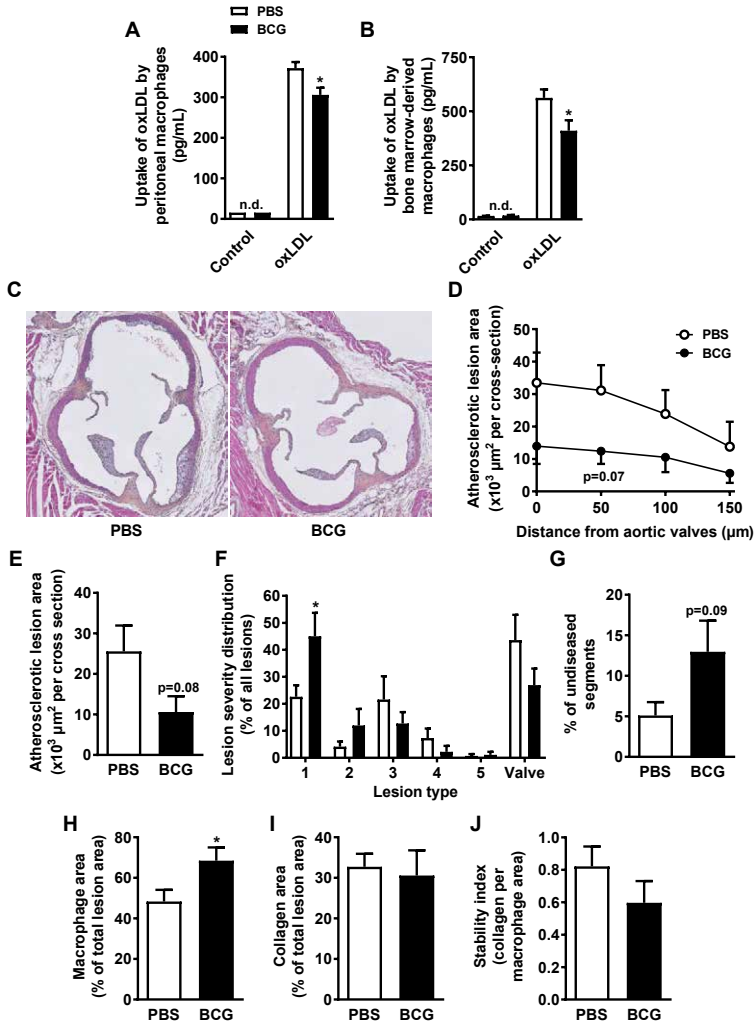
Figure 5. BCG decreases atherosclerosis development. *E3L.CETP mice fed a WTD were treated with PBS or BCG (0.75 mg; 5x10⁶ CFU; i.v.). After 6 weeks, peritoneal macrophages (A) and bone marrow-derived macrophages (B) were incubated with oxLDL and uptake was measured. Hearts were collected and slides of the valve area of the aortic root of were stained with haematoxylin – phloxine – saffron (C). Atherosclerotic lesion area as a function of distance was determined (D) and the mean lesion area was calculated from the four cross-sections from D (E). Lesions were categorized according to lesion severity (F) and the percentage of non-diseased segments was scored (G). The macrophage (H) and collagen (I) content of the lesions was determined, and the stability index (collagen/macrophage content of the lesions) was calculated (J). Values represent means ± SEM (n=6). *p<0.05 vs. PBS.*

BCG delays atherosclerosis development

Since BCG markedly increased immune activation, but lowered plasma cholesterol levels, we investigated the effects of BCG on foam cell formation and atherosclerosis development. BCG reduced the *ex vivo* uptake of oxLDL by peritoneal macrophages (-18%, **Fig. 5A**) and BMDMs (-27%, **Fig. 5B**), suggesting reduced foam cell formation and an overall anti-atherogenic phenotype of macrophages after BCG treatment.

We therefore determined atherosclerotic lesion area of the lesions in the aortic root of the heart 6 weeks after BCG administration. Interestingly, BCG tended to reduce atherosclerotic lesion area throughout the aortic root (**Fig. 5C, D**) as well as the mean atherosclerotic lesion area (-59%, **Fig. 5E**). Although lesion severity was generally mild, BCG still induced a shift towards a reduced lesion severity (**Fig. 5F**). In addition, the number of non-diseased segments tended to be higher after BCG treatment (+155%, **Fig. 5G**). In line with the reduced lesion severity, BCG increased the macrophage content of the lesions (+43%, **Fig. 5H**). Collagen content (**Fig. 5I**) and lesion stability (ratio collagen/macrophage area, **Fig. 5J**) were not affected by BCG. When only type 3 lesions were compared between groups, the macrophage content and lesion stability were unaffected (data not shown), indicating that BCG did not induce a more inflammatory or unstable phenotype of the lesions. Together, our findings indicate that BCG administration decreases plasma cholesterol levels and delays atherosclerosis development.

DISCUSSION

BCG has been shown to modulate atherosclerosis development through immunomodulatory mechanisms (5, 6), but its effect on cholesterol metabolism, the main determinant of atherosclerosis, has not been investigated before. In the current study, we show that BCG administration in hyperlipidemic *E3L.CETP* mice induced an overall inflammatory phenotype, as shown by hepatic infection and inflammation, and activation of circulating T cells as well as peritoneal macrophages and splenocytes. Furthermore, BCG markedly decreased plasma nonHDL-cholesterol levels by enhancing hepatic clearance of cholesterol and reduced foam cell formation *ex vivo*. As a result of these anti-atherogenic characteristics, BCG delayed atherosclerosis progression and reduced lesion severity.

We found BCG to be present in the liver, spleen and bone marrow 6 weeks after administration, indicating that the mycobacterium disseminated to these organs. In humans, dissemination of BCG can occur upon vaccination (19-21) and disseminated BCG infections can manifest in bladder cancer patients as a side effect of intravesical treatment with BCG (22). Our finding that the liver and spleen were enlarged in the BCG-treated group has also been observed in humans upon disseminated BCG infection (21, 23) and extrapulmonary tuberculosis (24, 25). Together, these reports indicate that our study can be translated to the human situation.

Besides increased immune activation, we observed a large reduction of plasma nonHDL-cholesterol levels upon BCG administration, which was accompanied by elevated hepatic

uptake of circulating cholesterol-enriched lipoprotein remnants and reduced intestinal cholesterol absorption. Since plasma HDL-cholesterol nor hepatic SR-BI content were altered, it seems unlikely that BCG influences reverse cholesterol transport. An underlying mechanism for the reduced plasma nonHDL-cholesterol levels could be that accumulated immune cells (26) as well as mycobacteria (27-30), both of which we detected in the liver, are responsible for the increased hepatic lipoprotein remnant uptake. Immune cells use lipids as an energy source and cholesterol is indispensable as a membrane component for cell growth, proliferation and membrane remodelling (26, 31, 32). Mycobacteria use host cholesterol for entry into macrophages and as a source of carbon and energy, as they cannot synthesize cholesterol themselves (27, 28, 33). Therefore, host cholesterol is essential for the persistence of infection (27-29). For *mycobacterium leprae*, which also infects macrophages and uses host cholesterol for survival, it was recently shown that infected macrophages take up LDL by upregulation of LDLR (34). Furthermore, *Ldlr* expression was shown to be upregulated in caseous human pulmonary tuberculosis granulomas (35), supporting the possibility that upregulation of LDLR specifically in infected tissue macrophages underlies the increased cholesterol uptake in our study. An additional cause of the reduced plasma nonHDL-cholesterol levels is the reduced intestinal cholesterol absorption as evidenced by reduced cholestanol and plant sterol levels in the liver. Intestinal absorption can be dysregulated by systemic or intra-abdominal inflammation, which is also observed in coeliac disease, Crohn's disease (36) and cystic fibrosis patients (37, 38). Evidently, BCG infection and subsequent inflammation also lead to reduced cholesterol absorption.

Several pieces of evidence suggest that mycobacteria modulate lipid metabolism in humans as well. For instance, cholesterol levels in Nigerian adults with tuberculosis are lower when compared to healthy controls (39). Deniz *et al.* (40) also show that serum total cholesterol, HDL-cholesterol and LDL-cholesterol concentrations are lower in patients with pulmonary tuberculosis. Moreover, *M. tuberculosis* uses fatty acids from host triglycerides as a lipid source (41) and tuberculosis patients exhibit lower serum medium-chain fatty acids (42). Unfortunately, to our knowledge, no data exist on plasma cholesterol levels in patients with disseminated BCG infection.

Ultimately, BCG tended to reduce atherosclerotic lesion area by more than half, and delayed the onset and progression of atherosclerosis evidenced by 1) the increased number of non-diseased segments; 2) the higher percentage of mild type 1 lesions; 3) the increased macrophage content of the lesions, indicative for mild type 1 and 2 lesions. Although the latter could also point to a more inflammatory phenotype of the lesions, this was contradicted by the fact that the macrophage content and lesion stability index within type 3 lesions only did not differ between the groups. Previous studies that investigated the effect of BCG on atherosclerosis focussed on the immunomodulatory effects of BCG and were not properly designed to investigate the effect of BCG on cholesterol metabolism. In one study performed in rabbits, plasma cholesterol level of each individual rabbit was maintained at a specific level by adjusting the cholesterol content in the diet (5), excluding the possibility to investigate the effects of BCG on cholesterol metabolism. Ovchinnikova *et*

al. (6) studied the effect of BCG that was killed by extensive freeze-drying on atherosclerosis and did not find changes in plasma cholesterol levels upon BCG treatment in *Apoe*^{-/-} mice and *Ldlr*^{-/-} mice. However, even though *Apoe*^{-/-} and *Ldlr*^{-/-} mice are the most widely used atherosclerosis models, they lack a functional hepatic ApoE-LDLR axis, the predominant route by which cholesterol-enriched lipoprotein remnants are cleared from the circulation (9). Based on our study in *E3L.CETP* mice, with a functional ApoE-LDLR pathway for lipoprotein remnant clearance, we conclude that the cholesterol lowering effect of BCG overrules the effect of immune activation during the development of atherosclerosis, resulting in delayed atherosclerotic plaque formation.

Carotid atherosclerosis is increased in patients with chronic infections and interestingly, the atherosclerosis risk is highest in those with the most prominent inflammatory response, indicating that systemic inflammation contributes to atherosclerosis (43). However, Giral *et al.* (44) compared hypercholesterolemic patients with and without a history of tuberculosis and found that past tuberculosis is not associated with atherosclerosis development. Whether mycobacterial infection has beneficial effects on atherosclerosis in humans related to a reduction in plasma cholesterol remains to be investigated.

In conclusion, our data demonstrate that BCG infection lowers plasma nonHDL-cholesterol levels by accelerating hepatic uptake of cholesterol-enriched lipoprotein remnants and reducing intestinal absorption of dietary cholesterol. Furthermore, BCG delays atherosclerotic plaque formation despite increased immune activation, most likely due to lowering of nonHDL-cholesterol. Because BCG is used as a vaccine for tuberculosis worldwide, the effect of BCG on atherosclerosis in humans is an interesting field of future studies.


ACKNOWLEDGMENTS

FUNDING

REFERENCES

2

1. Libby P, Lichtman AH, Hansson GK: Immune effector mechanisms implicated in atherosclerosis: from mice to humans. Immunity 2013;38:1092-1104

2. Rosenfeld ME, Campbell LA: Pathogens and atherosclerosis: update on the potential contribution of multiple infectious organisms to the pathogenesis of atherosclerosis. Thromb Haemost 2011;106:858-867

3. Westerterp M, Berbee JF, Pires NM, van Mierlo GJ, Kleemann R, Romijn JA, Havekes LM, Rensen PC: Apolipoprotein C-I is crucially involved in lipopolysaccharide-induced atherosclerosis development in apolipoprotein E-knockout mice. Circulation 2007;116:2173-2181

4. Bali P, Tousif S, Das G, van Kaer L: Strategies to improve BCG vaccine efficacy. Immunotherapy 2015;7:945-948

5. Lamb DJ, Eales LJ, Ferns GA: Immunization with bacillus Calmette-Guerin vaccine increases aortic atherosclerosis in the cholesterol-fed rabbit. Atherosclerosis 1999;143:105-113

6. Ovchinnikova OA, Berge N, Kang C, Urien C, Ketelhuth DF, Pottier J, Drouet L, Hansson GK, Marchal G, Back M, Schwartz-Cornil I, Lagranderie M: Mycobacterium bovis BCG killed by extended freeze-drying induces an immunoregulatory profile and protects against atherosclerosis. J Intern Med 2014;275:49-58

7. Westerterp M, van der Hoogt CC, de Haan W, Offerman EH, Dallinga-Thie GM, Jukema JW, Havekes LM, Rensen PC: Cholesteryl ester transfer protein decreases high-density lipoprotein and severely aggravates atherosclerosis in APOE*3-Leiden mice. Arterioscler Thromb Vasc Biol 2006;26:2552-2559

8. de Haan W, van der Hoogt CC, Westerterp M, Hoekstra M, Dallinga-Thie GM, Princen HM, Romijn JA, Jukema JW, Havekes LM, Rensen PC: Atorvastatin increases HDL cholesterol by reducing CETP expression in cholesterol-fed APOE*3-Leiden.CETP mice. Atherosclerosis 2008;197:57-63

9. Berbee JF, Boon MR, Khedoe PP, Bartelt A, Schlein C, Worthmann A, Kooijman S, Hoeke G, Mol IM, John C, Jung C, Vazirpanah N, Brouwers LP, Gordts PL, Esko JD, Hiemstra PS, Havekes LM, Scheja L, Heeren J, Rensen PC: Brown fat activation reduces hypercholesterolaemia and protects from atherosclerosis development. Nat Commun 2015;6:6356

10. Kleinnijenhuis J, Quintin J, Preijers F, Joosten LA, Ifrim DC, Saeed S, Jacobs C, van LJ, de JD, Stunnenberg HG, Xavier RJ, van der Meer JW, van CR, Netea MG: Bacille Calmette-Guerin induces NOD2-dependent nonspecific protection from reinfection via epigenetic reprogramming of monocytes. Proc Natl Acad Sci U S A 2012;109:17537-17542

11. Hirschfeld M, Ma Y, Weis JH, Vogel SN, Weis JJ: Cutting edge: repurification of lipopolysaccharide eliminates signaling through both human and murine toll-like receptor 2. J Immunol 2000;165:618-622

12. Netea MG, Demacker PN, Kullberg BJ, Boerman OC, Verschueren I, Stalenhoef AF, van der Meer JW: Low-density lipoprotein receptor-deficient mice are protected against lethal endotoxemia and severe gram-negative infections. J Clin Invest 1996;97:1366-1372

13. Bligh EG, Dyer WJ: A rapid method of total lipid extraction and purification. Can J Biochem Physiol 1959;37:911-917

14. Rensen PC, van Dijk MC, Havenaar EC, Bijsterbosch MK, Kruijt JK, van Berkel TJ: Selective liver targeting of antivirals by recombinant chylomicrons--a new therapeutic approach to hepatitis B. Nat Med 1995;1:221-225

15. Lutjohann D, Stroick M, Bertsch T, Kuhl S, Lindenthal B, Thelen K, Andersson U, Bjorkhem I, Bergmann KK, Fassbender K: High doses of simvastatin, pravastatin, and cholesterol reduce brain cholesterol synthesis in guinea pigs. Steroids 2004;69:431-438

16. Boon MR, Kooijman S, van Dam AD, Pelgrom LR, Berbee JF, Visseren CA, van Aggele RC, van den Hoek AM, Sips HC, Lombes M, Havekes LM, Tamsma JT, Guigas B, Meijer OC, Jukema JW, Rensen PC: Peripheral cannabinoid 1 receptor blockade activates brown adipose tissue and diminishes dyslipidemia and obesity. FASEB J 2014;28:5361-5375

17. van Tits LJ, Stienstra R, van Lent PL, Netea MG, Joosten LA, Stalenhoef AF: Oxidized LDL enhances pro-inflammatory responses of alternatively activated M2 macrophages: a crucial role for Kruppel-like factor 2. Atherosclerosis 2011;214:345-349

18. Wong MC, van Diepen JA, Hu L, Guigas B, de Boer HC, van Puijvelde GH, Kuiper J, van Zonneveld AJ, Shoelson SE, Voshol PJ, Romijn JA, Havekes LM, Tamsma JT, Rensen PC, Hiemstra PS, Berbee JF: Hepatocyte-specific IKKbeta expression aggravates atherosclerosis development in APOE*3-Leiden mice. Atherosclerosis 2012;220:362-368

19. Katzir Z, Okon E, Ludmirski A, Sherman Y, Haas H: Generalized lymphadenitis following B.C.G. vaccination in an immunocompetent 12-year-old boy. Eur J Pediatr 1984;141:165-167

20. Talbot EA, Perkins MD, Silva SF, Frothingham R: Disseminated bacille Calmette-Guerin disease after vaccination: case report and review. Clin Infect Dis 1997;24:1139-1146

21. Shoaran M, Najafi M, Jalilian R, Rezaei N: Granulomatous hepatitis as a rare complication of Bacillus Calmette-Guerin vaccination. Ann Saudi Med 2013;33:627-629

22. Patel SG, Cohen A, Weiner AB, Steinberg GD: Intravesical therapy for bladder cancer. Expert Opin Pharmacother 2015;16:889-901

23. Gottke MU, Wong P, Muhn C, Jabbari M, Morin S: Hepatitis in disseminated bacillus Calmette-Guerin infection. Can J Gastroenterol 2000;14:333-336

24. Guidi R, Bolli V, Lanza C, Biagetti C, Osimani P, de Benedictis FM: Macronodular hepatosplenic tuberculosis. Acta Radiol Short Rep 2012;1

25. Alghamdi AA, Awan FS, Maniyar IH, Alghamdi NA: Unusual manifestation of extrapulmonary tuberculosis. Case Rep Med 2013;2013:353798

26. Getz GS, Reardon CA: The mutual interplay of lipid metabolism and the cells of the immune system in relation to atherosclerosis. Clin Lipidol 2014;9:657-671

27. Ouellet H, Johnston JB, de Montellano PR: Cholesterol catabolism as a therapeutic target in Mycobacterium tuberculosis. Trends Microbiol 2011;19:530-539

28. Wipperman MF, Sampson NS, Thomas ST: Pathogen roid rage: cholesterol utilization by Mycobacterium tuberculosis. Crit Rev Biochem Mol Biol 2014;49:269-293

29. Pandey AK, Sassetti CM: Mycobacterial persistence requires the utilization of host cholesterol. Proc Natl Acad Sci U S A 2008;105:4376-4380

30. Lovewell RR, Sassetti CM, van der Ven BC: Chewing the fat: lipid metabolism and homeostasis during M. tuberculosis infection. Curr Opin Microbiol 2015;29:30-36

31. Heiniger HJ, Marshall JD: Cholesterol synthesis in polyclonally activated cytotoxic lymphocytes and its requirement for differentiation and proliferation. Proc Natl Acad Sci U S A 1982;79:3823-3827

32. Dabrowski MP, Peel WE, Thomson AE: Plasma membrane cholesterol regulates human lymphocyte cytotoxic function. Eur J Immunol 1980;10:821-827

33. Gatfield J, Pieters J: Essential role for cholesterol in entry of mycobacteria into

macrophages. Science 2000;288:1647-1650

34. Mattos KA, Oliveira VC, Berredo-Pinho M, Amaral JJ, Antunes LC, Melo RC, Acosta CC, Moura DF, Olmo R, Han J, Rosa PS, Almeida PE, Finlay BB, Borchers CH, Sarno EN, Bozza PT, Atella GC, Pessolani MC: Mycobacterium leprae intracellular survival relies on cholesterol accumulation in infected macrophages: a potential target for new drugs for leprosy treatment. Cell Microbiol 2014;16:797-815

35. Kim MJ, Wainwright HC, Locketz M, Bekker LG, Walther GB, Dittrich C, Visser A, Wang W, Hsu FF, Wiehart U, Tsenova L, Kaplan G, Russell DG: Caseation of human tuberculosis granulomas correlates with elevated host lipid metabolism. EMBO Mol Med 2010;2:258-274

36. van der Heide F: Acquired causes of intestinal malabsorption. Best Pract Res Clin Gastroenterol 2016;30:213-224

37. Wouthuyzen-Bakker M, Bodewes FA, Verkade HJ: Persistent fat malabsorption in cystic fibrosis; lessons from patients and mice. J Cyst Fibros 2011;10:150-158

38. Gelzo M, Sica C, Elce A, Dello RA, Iacotucci P, Carnovale V, Raia V, Salvatore D, Corso G, Castaldo G: Reduced absorption and enhanced synthesis of cholesterol in patients with cystic fibrosis: a preliminary study of plasma sterols. Clin Chem Lab Med 2016;54:1461-1466

39. Taylor GO, Bamgboye AE: Serum cholesterol and diseases in Nigerians. Am J Clin Nutr 1979;32:2540-2545

40. Deniz O, Gumus S, Yaman H, Ciftci F, Ors F, Cakir E, Tozkoparan E, Bilgic H, Ekiz K: Serum total cholesterol, HDL-C and LDL-C concentrations significantly correlate with the radiological extent of disease and the degree of smear positivity in patients with pulmonary tuberculosis. Clin Biochem 2007;40:162-166

41. Daniel J, Maamar H, Deb C, Sirakova TD, Kolattukudy PE: Mycobacterium tuberculosis uses host triacylglycerol to accumulate lipid droplets and acquires a dormancy-like phenotype in lipid-loaded macrophages. PLoS Pathog 2011;7:e1002093

42. Weiner J, III, Parida SK, Maertzdorf J, Black GF, Repsilber D, Telaar A, Mohney RP, Arndt-Sullivan C, Ganoza CA, Fae KC, Walzl G, Kaufmann SH: Biomarkers of inflammation, immunosuppression and stress with active disease are revealed by metabolomic profiling of tuberculosis patients. PLoS One 2012;7:e40221

43. Kiechl S, Egger G, Mayr M, Wiedermann CJ, Bonora E, Oberhollenzer F, Muggeo M, Xu Q, Wick G, Poewe W, Willeit J: Chronic infections and the risk of carotid atherosclerosis: prospective results from a large population study. Circulation 2001;103:1064-1070

44. Giral P, Kahn JF, Andre JM, Carreau V, Dourmap C, Bruckert E, Chapman MJ: Carotid atherosclerosis is not related to past tuberculosis in hypercholesterolemic patients. Atherosclerosis 2007;190:150-155

2

2
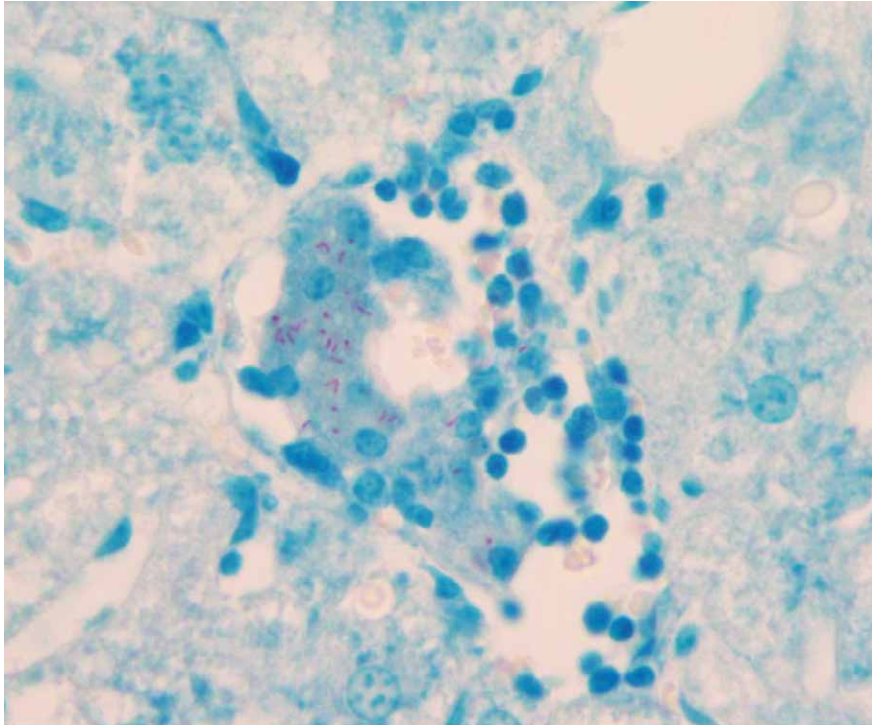
Supplementary figure 1. *E3L.CETP mice fed a WTD were treated with PBS or BCG (0.75 mg; 5x10^{6} CFU; i.v.) at baseline (t=0 weeks). Upon sacrifice after 6 weeks, livers were collected and Ziehl-Neelsen (ZN) staining of liver sections was performed. A representative liver section of a BCG-treated mouse is shown.*
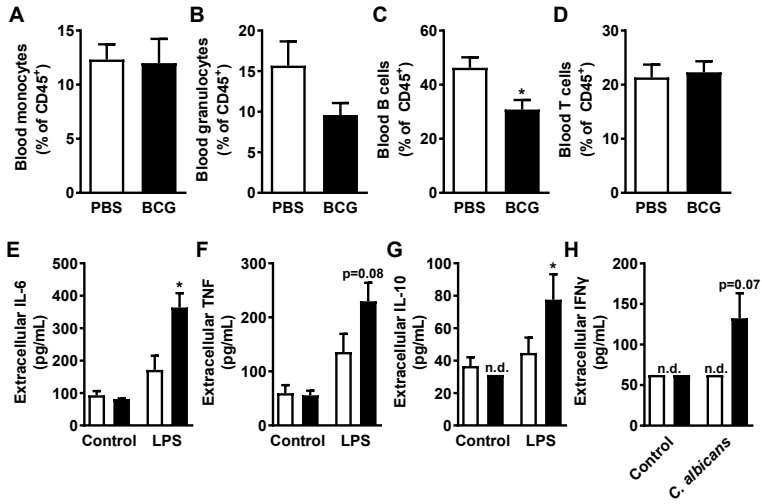
Supplementary figure 2. *E3L.CETP mice fed a WTD were treated with PBS or BCG (0.75 mg; 5x10^{6} CFU; i.v.) at baseline (t=0 weeks). After 6 weeks, blood and splenocytes were collected. Within the CD45+ cells in the blood, percentage of monocytes (A), granulocytes (B), B cells (C) and CD3+ T cells (D) was measured. Isolated splenocytes were stimulated with LPS for innate cytokines or C. albicans for adaptive cytokines. Production of IL-6 (E), TNF (F), IL-10 (G) and IFNγ (H) was measured. Values represent means ± SEM (n=6). *p<0.05 vs. PBS.*

Chapter 3

IgG is elevated in obese white adipose tissue but does not induce glucose intolerance via Fcγ-receptor or complement

Andrea D. van Dam, Lianne van Beek, Amanda C.M. Pronk,
Susan M. van den Berg, Frits Koning, Cees van Kooten, Patrick C.N. Rensen,
Mariëtte R. Boon, J. Sjef Verbeek, Ko Willems van Dijk, Vanessa van Harmelen

ABSTRACT

During the development of obesity, B cells accumulate in white adipose tissue (WAT) and produce IgG, which may contribute to the development of glucose intolerance. IgG signals by binding to Fcγ receptors (FcγR) and by activating the complement system. The aim of our study was to investigate whether activation of FcγR and/or complement C3 mediates the development of high fat diet-induced glucose intolerance. We studied mice lacking all four FcγRs (FcγRI/II/III/IV$^{-/-}$), only the inhibitory FcγRIIb (FcγRIIb$^{-/-}$), only the central component of the complement system C3 (C3$^{-/-}$), and mice lacking all FcγRs as well as C3 (FcγRI/II/III/IV/C3$^{-/-}$). These mouse models and wild-type control mice were fed a high-fat diet (HFD) for 15 weeks to induce obesity. Body weight and composition as well as glucose metabolism were assessed. The adipose tissue was characterized for adipocyte functionality and inflammation. In obese WAT of wild-type mice, B cells (+142%, $p<0.01$) and IgG (+128% $p<0.01$) were increased compared to lean WAT. Of all mouse models lacking IgG effector pathways, only C3$^{-/-}$ mice showed reduced HFD-induced weight gain as compared to controls (-18%, $p<0.01$). Surprisingly, FcγRI/II/III/IV$^{-/-}$ mice had deteriorated glucose tolerance (AUC +125%, $p<0.001$) despite reduced leukocyte number (-30%, $p<0.05$) in gonadal WAT (gWAT), whereas glucose tolerance and leukocytes within gWAT in the other models were unaffected compared to controls. Although IgG in gWAT was increased (+44 to +174%, $p<0.05$) in all mice lacking FcγRIIb (FcγRI/II/III/IV$^{-/-}$, FcγRIIb$^{-/-}$ and FcγRI/II/III/IV/C3$^{-/-}$), only FcγRI/II/III/IV/C3$^{-/-}$ mice exhibited appreciable alterations in immune cell infiltrate in gWAT, *e.g.* increased macrophages (+36%, $p<0.001$). In conclusion, FcγRIIb deficiency increases adipose tissue IgG, but FcγR and/or C3 deficiency does not protect against HFD-induced glucose intolerance or reduce adipose tissue inflammation. This indicates that if obesity-induced IgG contributes to the development of glucose intolerance, this is not mediated by FcγR or complement activation.

INTRODUCTION

White adipose tissue (WAT) inflammation is a hallmark of obesity-associated insulin resistance (1). Expanding adipose tissue releases increased levels of fatty acids and inflammatory (adipo)cytokines, which impair insulin signaling proteins and thereby decrease insulin sensitivity (2). These inflammatory mediators originate from hypertrophic adipocytes as well as from several types of immune cells residing in the adipose tissue (3). During obesity, additional immune cells infiltrate and accumulate in the adipose tissue (4, 5). Macrophages are the most abundant immune cells in mouse adipose tissue. They acquire a more pro-inflammatory phenotype during obesity and aggregate around necrotic adipocytes in so-called crown-like structures (6). Neutrophils, eosinophils and mast cells also contribute to inflammation and insulin resistance in adipose tissue (7-9). Besides, T cell infiltration occurs during obesity and various T cell populations differently affect obesity-associated insulin resistance (10), although they mostly contribute to metabolic dysfunction by recruitment of macrophages (11, 12). Moreover, B cells infiltrate obese adipose tissue (5, 13) and promote obesity-associated glucose intolerance by several mechanisms (13). Firstly, they induce secretion of the pro-inflammatory cytokine IFNγ by T cells, which induces pro-inflammatory macrophage polarization. In addition, B cells themselves produce cytokines that modulate insulin resistance. However, a unique function of B cells is the production of antibodies that have recently also been demonstrated to promote insulin resistance (13).

Of the 5 classes of antibodies produced by B cells in mammals, IgG is the major class of antibodies in the blood. IgG activates complement, and binds Fc receptors (FcRs) on macrophages and neutrophils, upon which pathogens coated with IgG are phagocytosed by these cells (14). Intriguingly, obesity is associated with higher IgG production and IgG-positive B cells in adipose tissue. Furthermore, transfer of IgG from obese high-fat diet (HFD)-fed mice to obese HFD-fed mice lacking B cells not only altered local inflammatory cytokine production and promoted pro-inflammatory macrophage polarization, but also deteriorated glucose tolerance. The latter seems to be mediated by an Fc-mediated process (*i.e.* FcRs or complement), since transfer of IgG lacking the Fc-binding portion did not affect glucose tolerance (13).

Innate immune effector cells express different FcRs specific for the diverse antibody subclasses. Fcγ receptors (FcγRs) bind IgG and the murine FcγR family includes FcγRI, FcγRIIb, FcγRIII and FcγRIV. FcγRI is the receptor with the highest affinity for the Fc fragment of IgG. FcγRI, FcγRIII and FcγRIV are activating receptors, which mediate phagocytosis, antigen presentation and killing of infected cells, whereas FcγRIIb is an inhibitory receptor. IgG also has different subclasses with varying affinity and specificity for the FcγRs (*i.e.* IgG1, IgG2a, IgG2b and IgG3) (15). In obese adipose tissue, IgG is enriched in crown-like structures, implicating that they are involved in the clearance of necrotic adipocytes. It is possible that in these crown-like structures, interactions between antibodies and FcRs on innate immune effector cells induce pro-inflammatory cytokine release. However, whether and which of the FcR are responsible for the effects of IgG on glucose metabolism remains

3

unknown (13). In addition to FcR binding and activation, antigen-bound IgG activates complement, which has also been shown to mediate insulin resistance by affecting adipose tissue macrophages (16).

In the current study, we aimed to elucidate whether activation of FcγR and/or complement mediates the development of adipose tissue inflammation and high fat diet-induced glucose intolerance. To this end, we investigated glucose metabolism in several mouse models lacking either all four FcγRs, only the inhibitory FcγR, the central component of the complement system C3, or all four FcγRs combined with C3. We show that absence of IgG effector pathways rather deteriorates than improves glucose intolerance. This implicates that if obesity-associated IgG contributes to the development of glucose intolerance, IgG does not seem to act via FcγR or complement activation.

MATERIALS AND METHODS

Mice and diet

Wild-type male mice (C57Bl/6J background) were purchased from Charles River (Maastricht, The Netherlands) and used as controls for the experiments with FcγRI/II/III/IV$^{-/-}$, C3$^{-/-}$ and FcγRI/II/III/IV/C3$^{-/-}$ mice. FcγRI/II/III/IV$^{-/-}$ (Fransen & Van Maaren 2016, submitted) and FcγRIIb$^{-/-}$ (17) mice were obtained as previously described. FcγRIIb$^{fl/fl}$ mice were used as controls for the FcγRIIb$^{-/-}$ mice. The complement C3$^{-/-}$ strain (18) was kindly provided by Mike Carroll (Harvard Medical School, Boston, MA). This strain was crossed with the FcγRI/II/III/IV$^{-/-}$ mice to obtain FcγRI/II/III/IV/C3$^{-/-}$ mice. FcγRIIb$^{fl/fl}$ mice and all knockout models had a C57Bl/6J background and were bred at the Leiden University Medical Center (Leiden, The Netherlands). At the start of each experiment, male mice were 8-12 weeks of age and housed under standard conditions with a 12:12 h light-dark cycle and free access to food and water. Mice were fed a high-fat diet (HFD; lard, 45% kcal% fat (D12451) or 60% kcal% fat (D12492) in the study with FcγRI/II/III/IV$^{-/-}$ mice; Research Diet Services, Wijk bij Duurstede, The Netherlands). After 15 weeks, mice were terminated and perfused with ice-cold PBS through the heart. Mouse experiments were performed in accordance with the Institute for Laboratory Animal Research Guide for the Care and Use of Laboratory Animals and had received approval from the University Ethical Review Board (Leiden University Medical Center, The Netherlands).

Body weight and composition measurements

At indicated time points, body weight was measured weekly with a scale and body composition was measured using an EchoMRI-100 analyzer (EchoMRI, TX, USA).

Adipocyte, stromal vascular fraction and leukocyte isolation

Gonadal white adipose tissue was dissected, rinsed in PBS and minced. Tissues were digested in a collagenase mixture (0.5 g/L collagenase (Type 1) in DMEM/F12 (pH 7.4) with 20 g/L of dialyzed bovine serum albumin (BSA, fraction V, Sigma, St Louis, USA)) for 1 h at

Table 1. *Antibodies used for flow cytometry.*

Antibody	Fluorochrome	Dilution	Clone, supplier
CD45.2	FITC	1:100	104, BioLegend
CD3	APC	1:100	145-2C11, eBioscience
CD4	Qdot605	1:1 000	RM-4-5, BioLegend
CD8a	PerCPCy5.5	1:100	53-6.7, BioLegend
CD19	PE	1:200	1D3, eBioscience
CD22.2	PE	1:200	Cy34.1, BD Biosciences
Cd11b	Pacific Blue	1:150	M1/70, BioLegend
F4/80	PE	1:200	BM8, eBioscience

37°C, and filtered through a 236-μm nylon mesh. Upon centrifugation of the suspension (10 min, 200 g), adipocytes were isolated from the surface for assessment of lipolysis. The pelleted stromal vascular fraction and blood samples were treated with red blood cell lysis buffer (BD Biosciences, CA, USA) and cells were counted using an automated cell counter (TC10, Bio-Rad Laboratories Inc., Veenendaal, The Netherlands). Cells were fixed in 0.5% paraformaldehyde and stored in FACS buffer (PBS, 0.02% sodium azide, 0.5% FCS) in the dark at 4°C for analysis by flow cytometry within one week.

Flow cytometry

Stromal vascular cells and circulating white blood cells were stained for 30 min at 4°C in the dark with the fluorescently labelled antibodies listed in **Table 1**. Cells were measured on an LSR II flow cytometer (BD Biosciences, CA, USA). Data were analysed using FlowJo software (Treestar, OR, USA).

Gonadal white adipose tissue histology

Gonadal white adipose tissue was fixed in 4% paraformaldehyde, dehydrated in 70% EtOH, and embedded in paraffin. Immunohistochemical detection of IgG and F4/80 was done on paraffin-embedded sections (5 μm). For detection of IgG, a biotinylated horse-anti-mouse IgG (BA-2000, 1/1250, Vector Laboratories Inc., CA, USA) and Vectastain ABC (PK-6100, Vector Laboratories Inc., CA, USA) were used. Detection of F4/80 was done by using a primary rat anti-mouse F4/80 monoclonal Ab (MCA497; 1/600, Serotec, UK) and a secondary goat anti-rat immunoglobulin peroxidase (MP-7444, Vector Laboratories Inc., CA, USA). Peroxidase activity in both stainings was revealed with NovaRed (SK-4800, Vector Laboratories Inc.). Slides were counterstained with hematoxylin. The areas positive for IgG or F4/80 were quantified using ImageJ Software.

Determination of plasma parameters

At the indicated time points, 6 h-fasted (from 8:00 am to 14:00 pm) blood samples were collected by tail vein bleeding into chilled capillaries that were coated with paraoxon (Sigma-Aldrich) to prevent ongoing lipolysis (19) and isolated plasma was assayed for

glucose, insulin, triglycerides and free fatty acids. Glucose was measured using an enzymatic kit from Instruchemie (Delfzijl, The Netherlands), and insulin by ELISA (Crystal Chem Inc., Downers Grove, IL). TG was measured by a commercially available enzymatic kit (Roche Diagnostics, Germany). Free fatty acids were measured using the NEFA C kit (Wako Diagnostics; Instruchemie, Delfzijl, The Netherlands).

Intravenous glucose tolerance test

After 6 or 8 weeks of HFD, mice were fasted for 6 h (from 8:00 am to 14:00 pm), a baseline blood sample was obtained by tail vein bleeding and mice were intravenously injected with D-glucose (2 g/kg body weight). Additional blood samples were drawn at indicated time points after glucose injection and plasma glucose was measured as described above.

Adipocyte lipolysis assay

Basal and stimulated lipolysis and the anti-lipolytic effect of insulin on gonadal adipocytes was measured by incubating isolated adipocytes (approx. 10 000 cells/mL) for 2 h at 37°C, with DMEM/F12 with 2% (v/v) BSA and 8-bromo-cAMP (10^{-3} M; Sigma, St. Louis, MO) with or without insulin (10^{-9} M). Glycerol concentrations were determined as a measure for lipolysis, using a free glycerol kit (Sigma, St. Louis, MO) and the hydrogen peroxide sensitive fluorescence dye Amplex Ultra Red, as previously described (20).

RNA purification and quantitative RT-PCR

RNA was extracted from snap-frozen gonadal white adipose tissue using Tripure RNA Isolation reagent (Roche, The Netherlands) according to manufacturer's instructions. RNA concentrations were measured using NanoDrop and RNA was reverse transcribed using Moloney Murine Leukemia Virus Reverse Transcriptase (Promega, The Netherlands) for quantitative RT-PCR (qRT-PCR) to produce cDNA. Expression levels of genes were determined by qRT-PCR, using gene-specific primers (**Table 2**) and SYBR green supermix (Biorad, The Netherlands). mRNA expression was normalized to *36b4* and *mCyclo* mRNA content and expressed as fold change compared with control mice using the ΔΔCT method.

Statistical analysis

All data are expressed as means ± SD. Groups were compared with a two-tailed unpaired Student's t-test or a two-way ANOVA for repeated measurements, as indicated. Differences were considered statistically significant if $p < 0.05$.

Table 2. *Primer sequences of forward and reverse primers (5' → 3').*

Gene	Forward primer	Reverse primer
36b4	GGACCCGAGAAGACCTCCTT	GCACATCACTCAGAATTTCAATGG
Il-6	ACCACGGCCTTCCCTACTTC	CTCATTTCCACGATTTCCCAG
Il-10	GACAACATACTGCTAACCGACTC	ATCACTCTTCACCTGCTCCACT
Mcp1	CACTCACCTGCTGCTACTCA	GCTTGGTGACAAAAACTACAGC
mCyclo	ACTGAATGGCTGGATGGCAA	TGTCCACAGTCGGAAATGGT
Tnfα	GATCGGTCCCCAAAGGGATG	CACTTGGTGGTTTGCTACGAC

RESULTS

B cells and IgG are enriched in obese adipose tissue

To examine the presence of B cells and IgG in gWAT, we used flow cytometry to quantify the percentage of B cells (CD19^{+}) within the leukocyte population (CD45^{+} cells) of the stromal vascular fraction (SVF) of gWAT of obese (>40 g) compared to lean (<30 g) mice that had been fed an HFD. In addition, we quantified IgG by immunohistochemistry in gWAT of these mice. The percentage of B cells was increased in gWAT of obese compared to lean mice (+142%, p<0.01, **Fig. 1A**). IgG staining in gWAT as percentage of total WAT area was also higher in obese versus lean mice (+128%, p<0.01, **Fig. 1B**). IgG was located around adipocytes and co-localized with cells positive for the macrophage marker F4/80 (**Fig. 1C**), suggesting that IgG primarily interacts with macrophages in the adipose tissue.

FcγRI/II/III/IV deficiency deteriorates glucose metabolism during HFD-induced obesity

We next studied the necessity of FcγRs in the development of HFD-induced obesity and glucose intolerance. Hereto, mice lacking all four FcγRs (FcγRI/II/III/IV^{-/-}) were fed an HFD for 15 weeks. Body weight (**Fig. 2A**), fat mass (**Fig. 2B**) and weight of several WAT depots (**Fig. 2C**) of FcγRI/II/III/IV^{-/-} mice were not different from control mice. FcγRI/II/III/IV^{-/-} mice had slightly more lean mass upon 15 weeks of HFD (+6%, p<0.05, **Fig. 1D**). Fasting plasma levels of glucose (**Fig. 2E**), triglycerides (**Fig. S1A**) and free fatty acids (**Fig. S1B**) during HFD did not differ between the two groups. However, after 6 weeks of HFD-feeding, plasma insulin levels were increased (+84%, p<0.05, **Fig. 2F**) and glucose tolerance as measured by an intravenous glucose tolerance test was deteriorated (AUC +125%, p<0.001, **Fig. 1G**) in FcγRI/II/III/IV^{-/-} mice compared to controls. To assess whether the reduced whole-body glucose tolerance was due to insulin resistance in white adipocytes, intracellular lipolysis was assessed *ex vivo*. Adipocytes isolated from gWAT of FcγRI/II/III/IV^{-/-} and control mice showed similar basal lipolysis and 8b-cAMP-stimulated lipolysis. Inhibition of lipolysis by

3
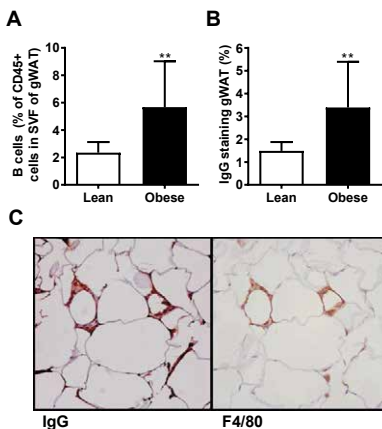
Figure 1. B cells and IgG in gWAT increase during HFD-induced obesity. *Male wild-type C57BL/6J mice were fed an HFD for different amounts of time varying between 4 and 34 weeks. Mice were categorized by body weight, with <30 g defined as lean (n=6-7) and >40 g defined as obese (n=12-13). The percentage of B cells (CD19^{+}) of CD45^{+} cells in SVF of gWAT was determined by flow cytometry (A). IgG staining of gWAT sections was performed and % of IgG staining was quantified (B). Histological IgG staining (left) and F4/80 staining (right) on gWAT. Values represent means ± SD. **p<0.01 vs. lean.*

insulin was also comparable between groups (**Fig. S1C**), suggesting that WAT may not be responsible for the deteriorated glucose tolerance in FcγRI/II/III/IV$^{-/-}$ mice.

FcγRI/II/III/IV deficiency increases adipose tissue IgG without affecting immune cell composition

To assess whether the absence of FcγRs affects adipose tissue IgG, IgG was quantified by immunohistochemistry on gWAT from FcγRI/II/III/IV$^{-/-}$ and control mice. Interestingly, adipose tissue IgG was increased in the FcγRI/II/III/IV$^{-/-}$ group (+44%, p<0.05, **Fig. 2H**). Immune cell composition in gWAT was not affected as FcγRI/II/III/IV$^{-/-}$ and control mice exhibited comparable percentages of leukocytes (CD45$^+$ cells) within the SVF (data not shown), and B cells (CD19$^+$), T cells (CD3$^+$) and macrophages (F4/80$^+$) within the leukocyte population (**Fig. 2I**). However, total cell count of the isolated SVF from gWAT was lower in the FcγRI/II/III/IV$^{-/-}$ group (-30%, p<0.01, **Fig. 2J**), indicating that the absolute numbers of immune cells in gWAT were lower than in control mice. This did not result in a less inflammatory milieu in gWAT, as expression of several inflammatory genes (*Mcp1, Tnfα, Il-6, Il-10*) was similar in FcγRI/II/III/IV$^{-/-}$ and control mice (**Fig. S1D**).

In blood, total cell count (data not shown) and percentages of B cells (CD22.2$^+$) and T cells within the leukocyte population were unaffected by FcγRI/II/III/IV deficiency (**Fig. S1E**), but within the T cell population, percentage of T helper cells (CD4$^+$) was lower (-8%, p<0.05) and the percentage of cytotoxic T cells (CD8$^+$) was higher (+8%, p<0.001) in FcγRI/II/III/IV$^{-/-}$ compared to control mice (**Fig. S1F**). This resulted in a lower CD4:CD8 ratio in FcγRI/II/III/IV$^{-/-}$ than in control mice (-15%, p<0.001, **Fig. 2K**), indicating increased systemic inflammation. In summary, FcγRI/II/III/IV$^{-/-}$ mice exhibited similar body weight but deteriorated glucose metabolism compared to controls, together with higher IgG levels but similar immune cell composition in WAT.

FcγRIIb deficiency does not affect glucose metabolism during HFD-induced obesity

We then assessed whether deficiency of only the inhibitory FcγR (FcγRIIb) would affect HFD-induced obesity and glucose intolerance. To this end, FcγRIIb$^{fl/fl}$ (control) and FcγRIIb$^{-/-}$ mice were fed an HFD for 15 weeks. Body weight (**Fig. 3A**) and total fat mass (**Fig. 3B**) were not different between FcγRIIb$^{-/-}$ and control mice, but weight of the gWAT fat pad was lower in FcγRIIb-deficient animals (-18%, p<0.05, **Fig. 3C**). FcγRIIb$^{-/-}$ mice showed higher lean mass on chow diet before the diet intervention (+9%, p<0.05, **Fig. 3D**), but this difference was nullified after HFD feeding. Fasting plasma glucose (**Fig. 3E**), insulin (**Fig. 3F**), triglyceride (**Fig. S2A**) and free fatty acid (**Fig. S2B**) levels did not differ between the two groups. Glucose tolerance after 8 weeks of HFD-feeding (**Fig. 3G**) and *ex vivo* lipolysis of gWAT adipocytes (**Fig. S2C**) were not different between the FcγRIIb$^{-/-}$ and control groups, suggesting that the inhibitory FcγR does not play a role in HFD-induced glucose intolerance.
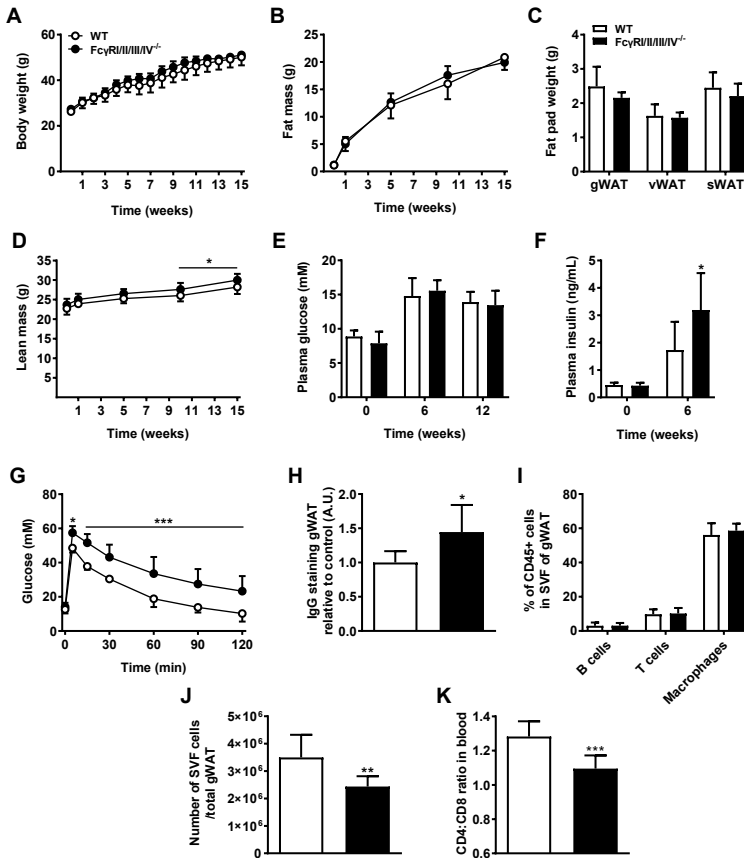
Figure 2. FcγRI/II/III/IV deficiency deteriorates glucose tolerance, increases IgG and decreases immune cells in gWAT during HFD-induced obesity. *FcγRI/II/III/IV$^{-/-}$ and wild-type control mice were fed an HFD for 15 weeks. Body weight (A), fat mass (B), WAT depot weight (C), lean mass (D), plasma glucose (E) and insulin (F) were analysed at the indicated time points. After 6 weeks, mice were injected intravenously with glucose and clearance from plasma was determined by measuring plasma glucose at 5, 15, 30, 60, 90 and 120 min after injection (G). IgG staining of gWAT sections was performed and quantified (H). The percentage of B cells (CD19$^+$), T cells (CD3$^+$) and macrophages (F4/80$^+$) of CD45$^+$ cells in SVF of gWAT was determined by flow cytometry (I). Total numbers of SVF cells per gWAT were counted (J). Within the CD3$^+$ T cell fraction in blood, the ratio of CD4$^+$ and CD8$^+$ cells was determined (K). Values represent means ± SD. *p<0.05, **p<0.01, ***p<0.001 vs. control (n=7-8) as measured by a two-way ANOVA in D, G or by a two-tailed unpaired Student's t-test in F, H, J, K. WT, wild-type; gWAT, gonadal white adipose tissue; vWAT, visceral white adipose tissue; sWAT, subcutaneous white adipose tissue; SVF, stromal vascular fraction.*

FcγRIIb deficiency increases adipose tissue IgG without affecting immune cell composition

Like in FcγRI/II/III/IV$^{-/-}$ mice, presence of IgG in gWAT of the FcγRIIb$^{-/-}$ mice was higher compared to controls (+94%, p<0.05, **Fig. 3H**), suggesting that lack of the inhibitory FcγR mediated this effect. FcγRIIb$^{-/-}$ mice had similar percentages of leukocytes (CD45$^+$ cells) within the SVF (data not shown), but exhibited a higher percentage of B cells (CD19$^+$, +95%, p<0.05, **Fig. 3I**) within the leukocyte population in gWAT. The percentage of T cells (CD3$^+$) within the leukocyte population of gWAT did not differ between FcγRIIb$^{-/-}$ mice and controls, but the percentage of macrophages (F4/80$^+$) was decreased in the FcγRIIb$^{-/-}$ group (-13%, p<0.05, **Fig. 3I**). Total cell count of the isolated SVF from gWAT was similar in FcγRI/II/III/IV$^{-/-}$ and control mice (**Fig. 3J**), as was the expression of inflammatory genes (*Mcp1, Tnfα, Il-6, Il-10*) in gWAT (**Fig. S2D**). Thus, FcγRIIb$^{-/-}$ mice had similar body weight and glucose tolerance compared to controls, together with higher IgG levels and slight alterations within the leukocyte population in WAT.

Complement C3 deficiency protects against HFD-induced obesity but does not improve glucose intolerance

In addition to signaling through FcγRs, IgG activates complement. To study the involvement of complement C3 in the development of HFD-induced obesity and glucose intolerance, mice lacking the central component of the complement system (C3$^{-/-}$) were fed an HFD for 15 weeks. Lack of C3 decreased HFD-induced body weight gain compared to control mice (-18%, p<0.01, **Fig. 4A**). This effect was primarily due to decreased accumulation of fat mass (**Fig. 4B**), reflected by less weight of the various WAT depots (-23 to -11%, p<0.06, **Fig. 4C**) of C3$^{-/-}$ compared to control mice. Lean mass of C3$^{-/-}$ mice was already lower at the beginning of the diet intervention (-5%, p<0.05), and this difference remained throughout the study (-6%, P<0.01 after 15 weeks of HFD, **Fig. 4D**). Both triglyceride (-29%, p<0.01, **Fig. S3A**) and free fatty acid (-22%, p<0.05, **Fig. S3B**) levels were lower in C3$^{-/-}$ mice before the diet intervention. Despite lower body weight, fasting plasma glucose (**Fig. 4E**) and insulin (**Fig. 3F**) levels were not different in C3$^{-/-}$ mice compared to controls. C3$^{-/-}$ mice did not exhibit different glucose tolerance (**Fig. 4G**) or *ex vivo* lipolysis of gWAT adipocytes, indicating that C3 deficiency does not affect glucose tolerance or adipocyte lipid metabolism.

Complement C3 deficiency does not alter immune cell composition

Even though complement C3$^{-/-}$ mice showed pronounced differences in body composition compared to controls, C3$^{-/-}$ mice exhibited similar percentages of leukocytes (CD45$^+$ cells) within the SVF (data not shown), and similar fractions of B cells (CD22.2$^+$), T cells (CD3$^+$) and macrophages (F4/80$^+$) within the leukocyte population of gWAT (**Fig. 4H**). Total cell count of the stromal vascular fraction isolated from gWAT was also the same between the two groups (**Fig. 4I**), as was inflammatory gene expression (*Mcp1, Tnfα, Il-6, Il-10*) in gWAT (**Fig. S3D**).

In blood, total cell count (data not shown) and percentages of B cells and T cells within the leukocyte population were unaffected in C3$^{-/-}$ mice (**Fig. S3E**), but within the T
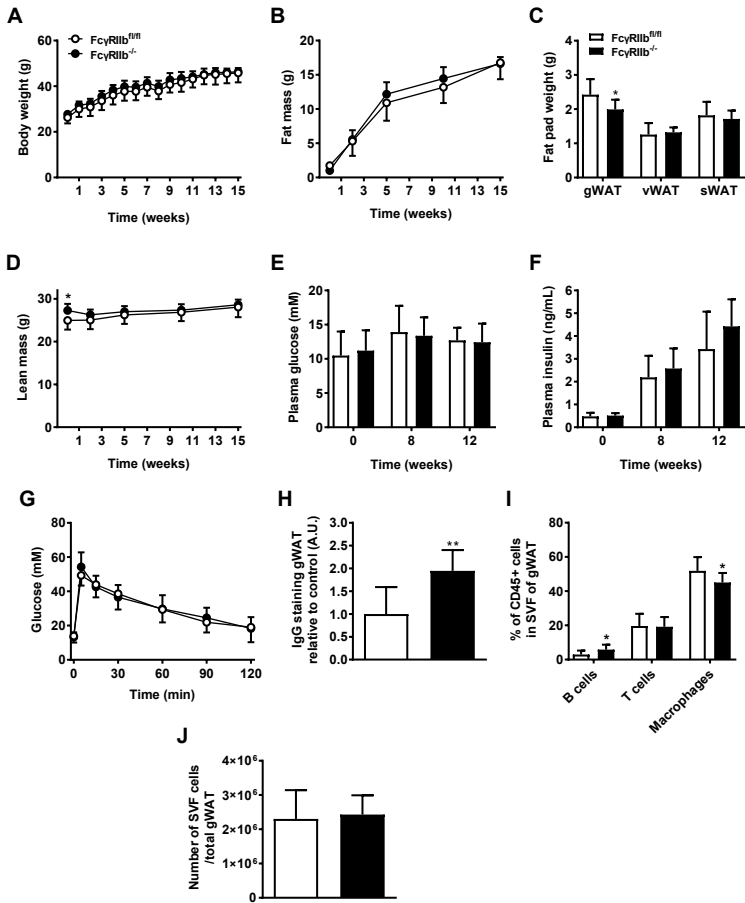
Figure 3. FcγRIIb deficiency does not affect glucose tolerance but increases IgG and slightly alters immune cell composition in gWAT during HFD-induced obesity. *FcγRIIb⁻/⁻ and FcγRIIbᶠˡ/ᶠˡ control mice were fed an HFD for 15 weeks. Body weight (A), fat mass (B), WAT depot weight (C), lean mass (D), plasma glucose (E) and insulin (F) were analysed at the indicated time points. After 8 weeks, mice were injected intravenously with glucose and clearance from plasma was determined by measuring plasma glucose at 5, 15, 30, 60, 90 and 120 min after injection (G). IgG staining of gWAT sections was performed and quantified (H). The percentage of B cells (CD19⁺), T cells (CD3⁺) and macrophages (F4/80⁺) of CD45⁺ cells in SVF of gWAT was determined by flow cytometry (I). Total numbers of SVF cells per gWAT were counted (J). Values represent means ± SD. *p<0.05, **p<0.01, ***p<0.001 vs. control (n=11-12) as measured by a two-way ANOVA in D or by a two-tailed unpaired Student's t-test in C, H, I. gWAT, gonadal white adipose tissue; vWAT, visceral white adipose tissue; sWAT, subcutaneous white adipose tissue; SVF, stromal vascular fraction.*

cell population, the percentage of cytotoxic T cells (CD8$^+$) was higher in C3$^{-/-}$ compared to control mice (+10%, p<0.01, **Fig. S3F**). As a result, C3$^{-/-}$ mice exhibited a lower CD4:CD8 ratio (-14%, p<0.05, **Fig. 4J**), representative of increased systemic inflammation. All in all, C3$^{-/-}$ mice had lower body weight but similar glucose tolerance and immune cell composition in WAT as compared to controls.

Deficiency of FcγRI/II/III/IV as well as complement C3 decreases insulin sensitivity during HFD-induced obesity

To exclude the possibility that either FcγRs or complement C3 are sufficient to mediate the effects of IgG signaling on glucose tolerance or that one of the pathways could compensate for lack of the other, mice lacking both C3 and all FcγRs (FcγRI/II/III/IV/C3$^{-/-}$) were fed an HFD for 15 weeks. Body weight, fat mass and lean mass of FcγRI/II/III/IV/C3$^{-/-}$ and control mice was similar after 15 weeks of HFD (**Fig. 5A-D**), although FcγRI/II/III/IV/C3$^{-/-}$ mice showed a transient increase in fat mass compared to controls (**Fig. 5B**). Plasma triglyceride levels (**Fig. S4A**) were not different between the two groups and free fatty acid levels transiently decreased (-18%, p<0.01, **Fig. S4B**) in FcγRI/II/III/IV/C3$^{-/-}$ mice compared to controls. Interestingly, FcγRI/II/III/IV/C3$^{-/-}$ mice also had transiently higher glucose levels after 6 weeks of HFD (+23%, p<0.001, **Fig. 5E**). Plasma insulin levels were higher at baseline (+18%, p<0.05) and after 6 weeks of HFD (+40%, p<0.01, **Fig. 5F**), indicating decreased insulin sensitivity in FcγRI/II/III/IV/C3$^{-/-}$ mice. However, glucose tolerance was not different after 6 weeks of HFD (**Fig. 5G**), suggesting that the increased insulin levels sufficiently compensated for the reduced insulin sensitivity to maintain normoglycemia. *Ex vivo* lipolysis of gWAT adipocytes did not differ between FcγRI/II/III/IV/C3$^{-/-}$ and control mice (**Fig. S4C**), suggesting that the decreased insulin sensitivity was not specific to WAT.

FcγRI/II/III/IV and complement C3 deficiency increases adipose tissue IgG and macrophages

Similar to FcγRI/II/III/IV$^{-/-}$ and FcγRIIb$^{-/-}$ mice, the quantity of IgG in gWAT of the FcγRI/II/III/IV/C3$^{-/-}$ mice was higher compared to controls (+174%, p<0.001, **Fig. 5H**). The leukocyte fraction (CD45$^+$ cells) within the SVF (data not shown) and percentage of B cells (CD22.2$^+$) within the leukocyte population in gWAT were comparable between the two groups. The percentage of T cells (CD3$^+$) was decreased (-20%, p<0.05) and the percentage of macrophages (F4/80$^+$) was increased (+36%, p<0.001) in FcγRI/II/III/IV/C3$^{-/-}$ mice compared to controls (**Fig. 5I**), while the total number of stromal vascular cells isolated from gWAT (**Fig. 5J**) and inflammatory gene expression (*Mcp1, Tnf*α*, Il-6, Il-10*) in gWAT (**Fig. S4D**) did not differ between the groups.

In blood, no differences were found in total cell count (data not shown), percentages of B and T cells within the leukocyte population (**Fig. S4E**), nor in the ratio of T helper (CD4$^+$) and cytotoxic T cells (CD8$^+$) within the T cell population (**Fig. S4F** and **5K**), indicating that systemic inflammation was not different between the groups. In summary, FcγRI/II/III/IV/C3$^{-/-}$ mice had similar body weight and glucose tolerance compared to controls, but higher IgG levels and altered in immune cell composition in WAT.
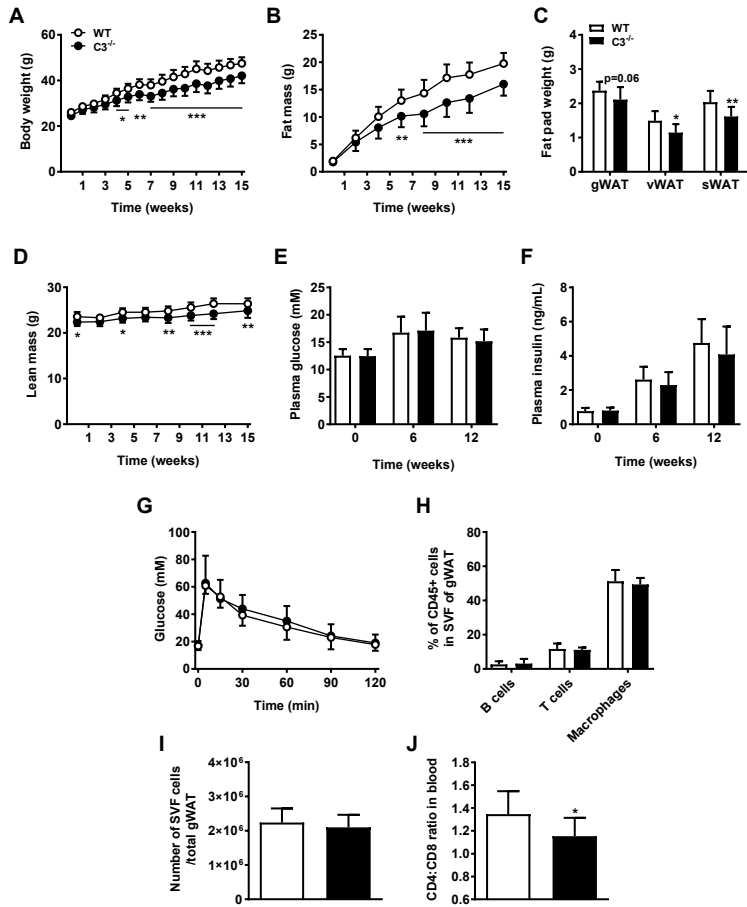
Figure 4. Complement C3 deficiency protects against weight gain but does not affect glucose tolerance or immune cell composition in gWAT during HFD-induced obesity. *Complement C3^{-/-} and wild-type control mice were fed an HFD for 15 weeks. Body weight (A), fat mass (B), WAT depot weight (C), lean mass (D), plasma glucose (E) and insulin (F) were analysed at the indicated time points. After 6 weeks, mice were injected intravenously with glucose and clearance from plasma was determined by measuring plasma glucose at 5, 15, 30, 60, 90 and 120 min after injection (G). The percentage of B cells (CD22.2^{+}), T cells (CD3^{+}) and macrophages (F4/80^{+}) of CD45^{+} cells in SVF of gWAT was determined by flow cytometry (H). Total numbers of SVF cells per gWAT were counted (I). Within the CD3^{+} T cell fraction in blood, the ratio of CD4^{+} and CD8^{+} cells was determined (J). Values represent means ± SD. *p<0.05, **p<0.01, ***p<0.001 vs. control (n=10-12) as measured by a two-way ANOVA in A, B, D or by a two-tailed unpaired Student's t-test in C, J. WT, wild-type; gWAT, gonadal white adipose tissue; vWAT, visceral white adipose tissue; sWAT, subcutaneous white adipose tissue; SVF, stromal vascular fraction.*
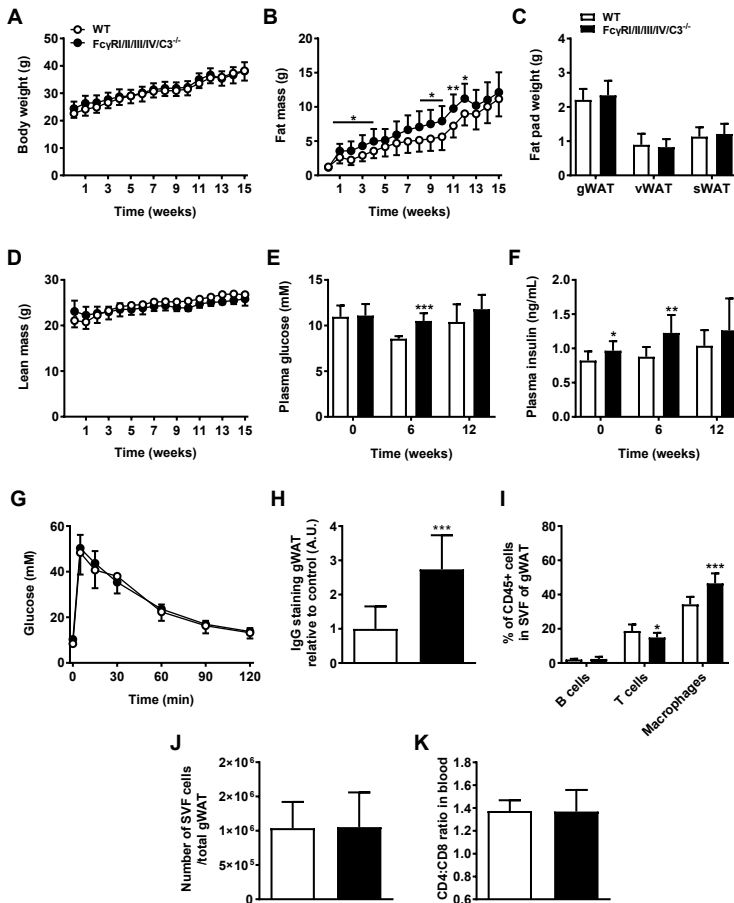
Figure 5. Deficiency of both FcγRI/II/III/IV and complement C3 elevates plasma insulin and increases IgG and macrophages in gWAT during HFD-induced obesity. *FcγRI/II/III/IV/C3$^{-/-}$ and wild-type control mice were fed an HFD for 15 weeks. Body weight (A), fat mass (B), WAT depot weight (C), lean mass (D), plasma glucose (E) and insulin (F) were analysed at the indicated time points. After 6 weeks, mice were injected intravenously with glucose and clearance from plasma was determined by measuring plasma glucose at 5, 15, 30, 60, 90 and 120 min after injection (G). IgG staining of gWAT sections was performed and quantified (H). The percentage of B cells (CD22.2$^+$), T cells (CD3$^+$) and macrophages (F4/80$^+$) of CD45$^+$ cells in SVF of gWAT was determined by flow cytometry (I). Total numbers of SVF cells per gWAT were counted (J). Within the CD3$^+$ T cell fraction in blood, the ratio of CD4$^+$ and CD8$^+$ cells was determined (K). Values represent means ± SD. *p<0.05, **p<0.01, ***p<0.001 vs. control (n=9-10) as measured by a two-way ANOVA in A, B, D or by a two-tailed unpaired Student's t-test in C, J. WT, wild-type; gWAT, gonadal white adipose tissue; vWAT, visceral white adipose tissue; sWAT, subcutaneous white adipose tissue; SVF, stromal vascular fraction.*

DISCUSSION

IgG in obese adipose tissue has been shown to decrease glucose tolerance, but the signaling pathway mediating these effects remains unknown (13). By using mouse models deficient for all four FcγRs (FcγRI/II/III/IV$^{-/-}$), only the inhibitory FcγRIIb (FcγRIIb$^{-/-}$), only the central component of the complement system C3 (C3$^{-/-}$), and all FcγRs combined with C3 (FcγRI/II/III/IV/C3$^{-/-}$), we show that deficiency for FcγR and/or complement C3, both of which are important for the effector functions of IgG, does not ameliorate the development of glucose intolerance in diet-induced obesity.

We observed that obese adipose tissue is enriched for B cells and IgG, as compared to lean adipose tissue, and we found that IgG co-localizes with macrophages in crown-like structures within the adipose tissue, which confirms previous reports (13, 21). It would be interesting to uncover to which antigens IgG responds in the adipose tissue. Adipocytes are known to present lipid antigens to immune cells (22) and it has also been reported that HFD-fed mice have higher levels of circulating IgG against modified LDL compared to mice fed a low fat diet (23). Winer *et al.* (13) searched for IgG antigens in serum of obese insulin-resistant *vs.* insulin-sensitive men and found mostly differences in intracellular self-antigens that are ubiquitously expressed in many tissues. Thus, the antigens to which obesity-induced IgG responds remain unknown and uncovering them is of high therapeutic value.

In our study, FcγRI/II/III/IV$^{-/-}$ mice lacking all IgG receptors exhibited deteriorated rather than improved glucose tolerance. This is in contrast to what we expected based on the data of Winer *et al.* (13). They showed that transfer of IgG from diet-induced obese wild-type mice to diet-induced obese B cell deficient mice deteriorated glucose tolerance whereas transfer of IgG lacking the Fc region did not, indicating that the pathogenic effects of IgG are mediated by FcγR or complement. However, the Fc region is important for extension of the half-life of IgG (24), raising the possibility that the lack of effect in the latter experiment is due to increased clearance of IgG. Since insulin sensitivity in the white adipocytes was not affected in our FcγRI/II/III/IV$^{-/-}$ mice, we speculate that other organs such as muscle could be responsible for the deterioration of glucose tolerance we found. FcRs are important for immune complex clearance (25) and lack of FcγRs may lead to accumulation of immune complexes in tissues and subsequent induction of pro-inflammatory responses and pathology (26). Indeed, we show that FcγRI/II/III/IV$^{-/-}$ mice had increased systemic inflammation as evidenced by more cytotoxic T cells in blood. To our knowledge, deficiency of all four FcγR in relation to obesity has not been studied to date. We have previously shown that in mice lacking the FcRγ-chain, the γ-subunit necessary for signaling and cell surface expression of activating FcγR and FcεRI, the development of obesity and glucose intolerance was reduced. However, these effects could be due to IgE (the ligand for FcεRI) or other non-IgG-effects, as the y-subunit is not exclusively associated with Fc-receptors (27). The FcγRI/II/III/IV$^{-/-}$ model is Fc-receptor-specific and therefore suitable to study specific effects of IgG signaling. FcγRIIb deficient mice did not show abnormal glucose

tolerance, indicating that the stimulating FcγRs were responsible for the deteriorated glucose metabolism that we observed in FcγRI/II/III/IV^{-/-} mice.

Since absence of FcγRs did not improve glucose tolerance in obese mice, we studied whether complement C3 is the pathway mediating the pathogenic effects of IgG. We found decreased body weight and fat mass due to less fat in several WAT depots in C3^{-/-} mice, which is in accordance with previous reports establishing that C3^{-/-} mice on an HFD have reduced weight of the WAT depots (28). We found that the decreased total body weight was partly due to lower lean mass of C3^{-/-} mice compared to controls. C3^{-/-} mice are known to have decreased birth weight (29), which is associated with reduced lean mass later in life (30) and thus coincides with our finding. Despite lower body weight, C3^{-/-} mice did not exhibit different glucose tolerance compared to controls after HFD. Disparate data on the effects of C3 deficiency on glucose tolerance have been reported. C3^{-/-} compared to wild-type mice on different backgrounds (C57Bl/6 and 129Sv) displayed similar insulin but lower plasma glucose levels (31). Murray *et al.* (28) also found lower fasting glucose levels in female C3^{-/-} mice on a chow diet and after 4 weeks of HFD compared to controls. However, after 16 weeks of HFD, fasting glucose and glucose tolerance did not differ anymore (28). The same group has also reported comparable fasting glucose and insulin levels in C3^{-/-} and wild-type mice on a chow diet (32), which is in line with what we found and suggests that complement C3 does not act on glucose levels or tolerance.

Mice lacking both FcγRs and C3 showed increased plasma insulin, possibly due to absence of FcγRs as FcγRI/II/III/IV^{-/-} mice also exhibited increased plasma insulin. However, no effects on glucose tolerance were found. This excludes the possibility that presence of either FcγRs or C3 is sufficient to mediate the development of glucose intolerance during obesity. Redundant roles for FcγR and C3 have been demonstrated before in autoimmune hypopigmentation. In the model for this pathology, FcR or C3 deficiency alone did not prevent development of antibody-mediated hypopigmentation, whereas a combined deficiency did (33).

Of note, all our models lacking the inhibitory FcγRIIb displayed higher IgG levels in adipose tissue compared to control mice. This is probably explained by the fact that this receptor mediates a negative feedback loop to dampen B cell activity and antibody production (15) and in agreement with the higher antibody titres in FcγRIIb^{-/-} mice upon immunization with antigens (34). Strikingly, FcγRI/II/III/IV^{-/-}, FcγRIIb^{-/-} and C3^{-/-} mice did not exhibit any or only showed negligible alterations in percentage of adipose tissue B cells, T cells and macrophages. FcγRI/II/III/IV^{-/-} mice even had reduced numbers of SVCs in adipose tissue, which is unexpected given the deteriorated glucose tolerance we found and therefore reinforces our hypothesis that other organs besides the adipose tissue may be the cause of the phenotype observed. Only FcγRI/II/III/IV/C3^{-/-} mice exhibited an appreciable increase in adipose tissue macrophages, but this was not accompanied by metabolic derangements. The lack of differences in inflammation between our immune deficient models and controls suggests that if obesity-associated IgG signals via FcγRs or complement, these pathways may be inferior to or compensated by other inflammatory processes occurring during obesity. Mice lacking B and T cells show a marked increase in macrophages and natural

killer cells in adipose tissue while the onset of obesity and the state of insulin resistance is unaffected compared to wild-type mice fed an HFD (21). In this light, one could argue that the role of B cells as a whole and therefore also IgG effector pathways are expendable in the development of glucose intolerance. Counter-regulatory mechanisms within the immune system may stretch beyond up- or downregulation of entire immune cell populations, as elevated inflammatory cytokine responses can already rescue deficiency of others (35). The higher cytotoxic T cell percentages we observed in blood of FcγRI/II/III/IV^{-/-} and C3^{-/-} mice may be the result of such compensatory inflammatory mechanisms.

In conclusion, our data demonstrate that B cells and IgG in adipose tissue increase in diet-induced obesity, and lack of FcγRIIb further increases IgG in adipose tissue. However, FcγR and/or complement C3 deficiency does not ameliorate the development of HFD-induced glucose intolerance. These data suggest that if HFD-induced IgG contributes to the development of glucose intolerance, this is not mediated by FcγRs or complement. Future research is necessary to identify the antigens that IgG in adipose tissue binds and will also reveal whether IgG-induced pathology in obesity is mediated by other mechanisms, for example the deposition of immune complexes.

ACKNOWLEDGEMENTS

FUNDING

REFERENCES

1. Xu H, Barnes GT, Yang Q, Tan G, Yang D, Chou CJ, Sole J, Nichols A, Ross JS, Tartaglia LA, Chen H: Chronic inflammation in fat plays a crucial role in the development of obesity-related insulin resistance. The Journal of clinical investigation 2003;112:1821-1830

2. Arkan MC, Hevener AL, Greten FR, Maeda S, Li ZW, Long JM, Wynshaw-Boris A, Poli G, Olefsky J, Karin M: IKK-beta links inflammation to obesity-induced insulin resistance. Nature medicine 2005;11:191-198

3. Ouchi N, Parker JL, Lugus JJ, Walsh K: Adipokines in inflammation and metabolic disease. Nature reviews Immunology 2011;11:85-97

4. Weisberg SP, McCann D, Desai M, Rosenbaum M, Leibel RL, Ferrante AW, Jr.: Obesity is associated with macrophage accumulation in adipose tissue. J Clin Invest 2003;112:1796-1808

5. van Beek L, van Klinken JB, Pronk AC, van Dam AD, Dirven E, Rensen PC, Koning F, Willems van Dijk K, van Harmelen V: The limited storage capacity of gonadal adipose tissue directs the development of metabolic disorders in male C57Bl/6J mice. Diabetologia 2015;58:1601-1609

6. Lumeng CN, Bodzin JL, Saltiel AR: Obesity induces a phenotypic switch in adipose tissue macrophage polarization. The Journal of clinical investigation 2007;117:175-184

7. Talukdar S, Oh DY, Bandyopadhyay G, Li D, Xu J, McNelis J, Lu M, Li P, Yan Q, Zhu Y, Ofrecio J, Lin M, Brenner MB, Olefsky JM: Neutrophils mediate insulin resistance in mice fed a high-fat diet through secreted elastase. Nature medicine 2012;18:1407-1412

8. Liu J, Divoux A, Sun J, Zhang J, Clement K, Glickman JN, Sukhova GK, Wolters PJ, Du J, Gorgun CZ, Doria A, Libby P, Blumberg RS, Kahn BB, Hotamisligil GS, Shi GP: Genetic deficiency and pharmacological stabilization of mast cells reduce diet-induced obesity and diabetes in mice. Nature medicine 2009;15:940-945

9. Wu D, Molofsky AB, Liang HE, Ricardo-Gonzalez RR, Jouihan HA, Bando JK, Chawla A, Locksley RM: Eosinophils sustain adipose alternatively activated macrophages associated with glucose homeostasis. Science (New York, NY) 2011;332:243-247

10. Seijkens T, Kusters P, Chatzigeorgiou A, Chavakis T, Lutgens E: Immune cell crosstalk in obesity: a key role for costimulation? Diabetes 2014;63:3982-3991

11. Winer S, Chan Y, Paltser G, Truong D, Tsui H, Bahrami J, Dorfman R, Wang Y, Zielenski J, Mastronardi F, Maezawa Y, Drucker DJ, Engleman E, Winer D, Dosch HM: Normalization of obesity-associated insulin resistance through immunotherapy. Nature medicine 2009;15:921-929

12. Nishimura S, Manabe I, Nagasaki M, Eto K, Yamashita H, Ohsugi M, Otsu M, Hara K, Ueki K, Sugiura S, Yoshimura K, Kadowaki T, Nagai R: CD8+ effector T cells contribute to macrophage recruitment and adipose tissue inflammation in obesity. Nature medicine 2009;15:914-920

13. Winer DA, Winer S, Shen L, Wadia PP, Yantha J, Paltser G, Tsui H, Wu P, Davidson MG, Alonso MN, Leong HX, Glassford A, Caimol M, Kenkel JA, Tedder TF, McLaughlin T, Miklos DB, Dosch HM, Engleman EG: B cells promote insulin resistance through modulation of T cells and production of pathogenic IgG antibodies. Nature medicine 2011;17:610-617

14. Alberts B. JA, Lewis J., Raff M., Roberts K., Walter P.: *Molecular Biology of the Cell*. New York, Garland Science, 2002

15. Nimmerjahn F, Ravetch JV: Fcgamma receptors as regulators of immune responses. Nature reviews Immunology 2008;8:34-47

3

16. Mamane Y, Chung Chan C, Lavallee G, Morin N, Xu LJ, Huang J, Gordon R, Thomas W, Lamb J, Schadt EE, Kennedy BP, Mancini JA: The C3a anaphylatoxin receptor is a key mediator of insulin resistance and functions by modulating adipose tissue macrophage infiltration and activation. Diabetes 2009;58:2006-2017

17. Boross P, Arandhara VL, Martin-Ramirez J, Santiago-Raber ML, Carlucci F, Flierman R, van der Kaa J, Breukel C, Claassens JW, Camps M, Lubberts E, Salvatori D, Rastaldi MP, Ossendorp F, Daha MR, Cook HT, Izui S, Botto M, Verbeek JS: The inhibiting Fc receptor for IgG, FcgammaRIIB, is a modifier of autoimmune susceptibility. Journal of immunology 2011;187:1304-1313

18. Wessels MR, Butko P, Ma M, Warren HB, Lage AL, Carroll MC: Studies of group B streptococcal infection in mice deficient in complement component C3 or C4 demonstrate an essential role for complement in both innate and acquired immunity. Proceedings of the National Academy of Sciences of the United States of America 1995;92:11490-11494

19. Zambon A, Hashimoto SI, Brunzell JD: Analysis of techniques to obtain plasma for measurement of levels of free fatty acids. Journal of lipid research 1993;34:1021-1028

20. Clark AM, Sousa KM, Jennings C, MacDougald OA, Kennedy RT: Continuous-flow enzyme assay on a microfluidic chip for monitoring glycerol secretion from cultured adipocytes. Anal Chem 2009;81:2350-2356

21. Duffaut C, Galitzky J, Lafontan M, Bouloumie A: Unexpected trafficking of immune cells within the adipose tissue during the onset of obesity. Biochemical and biophysical research communications 2009;384:482-485

22. Huh JY, Kim JI, Park YJ, Hwang IJ, Lee YS, Sohn JH, Lee SK, Alfadda AA, Kim SS, Choi SH, Lee DS, Park SH, Seong RH, Choi CS, Kim JB: A novel function of adipocytes in lipid antigen presentation to iNKT cells. Molecular and cellular biology 2013;33:328-339

23. Wolf D, Jehle F, Ortiz Rodriguez A, Dufner B, Hoppe N, Colberg C, Lozhkin A, Bassler N, Rupprecht B, Wiedemann A, Hilgendorf I, Stachon P, Willecke F, Febbraio M, von zur Muhlen C, Binder CJ, Bode C, Zirlik A, Peter K: CD40L deficiency attenuates diet-induced adipose tissue inflammation by impairing immune cell accumulation and production of pathogenic IgG-antibodies. PloS one 2012;7:e33026

24. Ghetie V, Ward ES: Multiple roles for the major histocompatibility complex class I- related receptor FcRn. Annual review of immunology 2000;18:739-766

25. van Lent P, Nabbe KC, Boross P, Blom AB, Roth J, Holthuysen A, Sloetjes A, Verbeek S, van den Berg W: The inhibitory receptor FcgammaRII reduces joint inflammation and destruction in experimental immune complex-mediated arthritides not only by inhibition of FcgammaRI/III but also by efficient clearance and endocytosis of immune complexes. The American journal of pathology 2003;163:1839-1848

26. Rodriguez-Iturbe B, Haas M: Post-Streptococcal Glomerulonephritis. In *Streptococcus pyogenes: Basic Biology to Clinical Manifestations* Ferretti JJ, Stevens DL, Fischetti VA, Eds. Oklahoma City, University of Oklahoma Health Sciences Center, 2016

27. van Beek L, Vroegrijk IO, Katiraei S, Heemskerk MM, van Dam AD, Kooijman S, Rensen PC, Koning F, Verbeek JS, Willems van Dijk K, van Harmelen V: FcRgamma-chain deficiency reduces the development of diet-induced obesity. Obesity (Silver Spring, Md) 2015;23:2435-2444

28. Murray I, Havel PJ, Sniderman AD, Cianflone K: Reduced body weight, adipose tissue, and leptin levels despite increased energy intake in female mice lacking acylation-stimulating protein. Endocrinology 2000;141:1041-1049

29. Chow WN, Lee YL, Wong PC, Chung MK, Lee KF,

Yeung WS: Complement 3 deficiency impairs early pregnancy in mice. Molecular reproduction and development 2009;76:647-655

30. Yliharsila H, Kajantie E, Osmond C, Forsen T, Barker DJ, Eriksson JG: Birth size, adult body composition and muscle strength in later life. International journal of obesity (2005) 2007;31:1392-1399

31. Cianflone K, Xia Z, Chen LY: Critical review of acylation-stimulating protein physiology in humans and rodents. Biochimica et biophysica acta 2003;1609:127-143

32. Murray I, Sniderman AD, Cianflone K: Mice lacking acylation stimulating protein (ASP) have delayed postprandial triglyceride clearance. Journal of lipid research 1999;40:1671-1676

33. Trcka J, Moroi Y, Clynes RA, Goldberg SM, Bergtold A, Perales MA, Ma M, Ferrone CR, Carroll MC, Ravetch JV, Houghton AN: Redundant and alternative roles for activating Fc receptors and complement in an antibody-dependent model of autoimmune vitiligo. Immunity 2002;16:861-868

34. Takai T, Ono M, Hikida M, Ohmori H, Ravetch JV: Augmented humoral and anaphylactic responses in Fc gamma RII-deficient mice. Nature 1996;379:346-349

35. Mayer-Barber KD, Yan B: Clash of the Cytokine Titans: counter-regulation of interleukin-1 and type I interferon-mediated inflammatory responses. Cellular & molecular immunology 2017;14:22-35

3

3
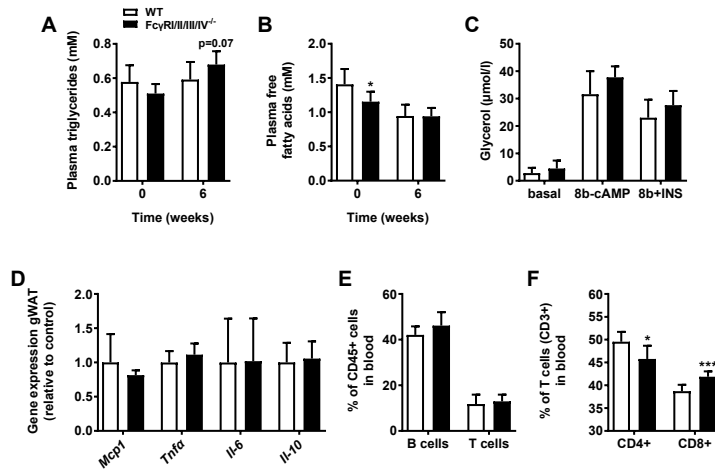
Supplementary figure 1. *FcγRI/II/III/IV^{-/-} and wild-type control mice were fed an HFD for 15 weeks. Plasma triglycerides (A) and free fatty acids (B) were analysed at the indicated time points. Basal, 8b-cAMP-stimulated and insulin inhibition of 8b-cAMP-stimulated ex vivo glycerol release (index of lipolysis) from isolated gonadal white adipocytes were determined (C). GWAT mRNA expression of the indicated inflammatory genes was determined (D). Within the CD45^{+} cell population in blood, the percentages of B cells (CD19^{+}) and T cells (CD3^{+}) were determined (E). Within the CD3^{+} T cell fraction in blood, the percentages of CD4^{+} and CD8^{+} cells were determined (K). Values represent means ± SD. *p<0.05, ***p<0.001 vs. control (n=7-8) as measured by a two-tailed unpaired Student's t-test. WT, wild-type; gWAT, gonadal white adipose tissue.*
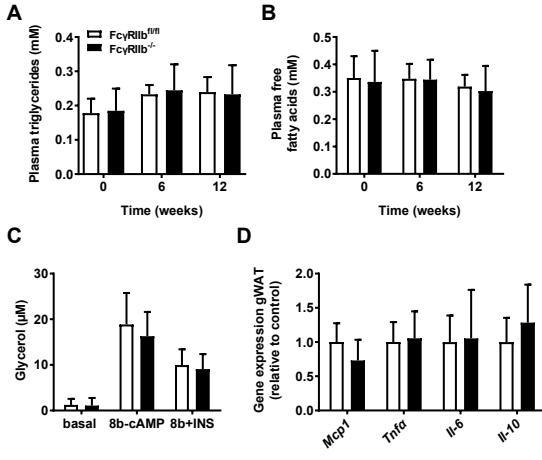
Supplementary figure 2. *FcγRIIb$^{-/-}$ and FcγRIIb$^{fl/fl}$ control mice were fed an HFD for 15 weeks. Plasma triglycerides (A) and free fatty acids (B) were analysed at the indicated time points. Basal, 8b-cAMP-stimulated and insulin inhibition of 8b-cAMP-stimulated ex vivo glycerol release (index of lipolysis) from isolated gonadal white adipocytes were determined (C). GWAT mRNA expression of the indicated inflammatory genes was determined (D). Values represent means ± SD. gWAT, gonadal white adipose tissue.*
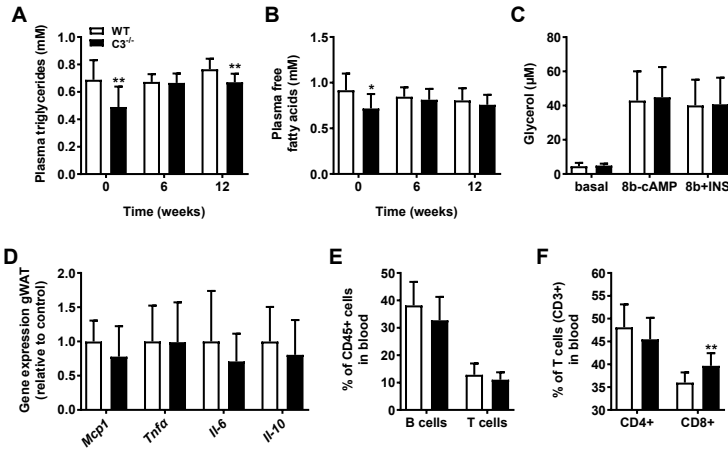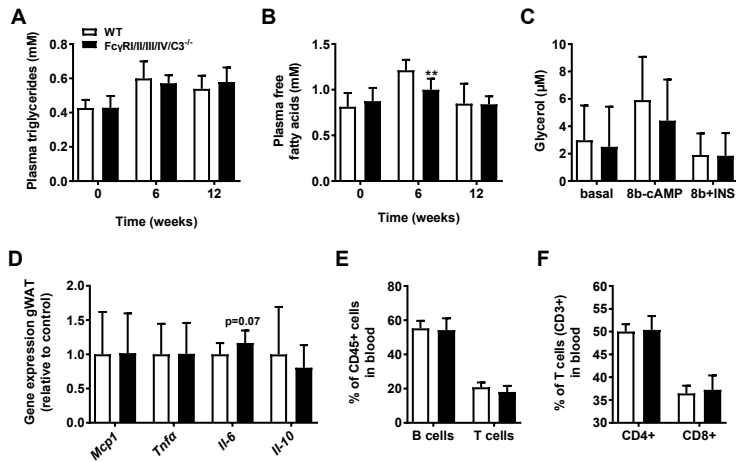

Supplementary figure 3. *Complement C3$^{-/-}$ and wild-type control mice were fed an HFD for 15 weeks. Plasma triglycerides (A) and free fatty acids (B) were analysed at the indicated time points. Basal, 8b-cAMP-stimulated and insulin inhibition of 8b-cAMP-stimulated ex vivo glycerol release (index of lipolysis) from isolated gonadal white adipocytes were determined (C). GWAT mRNA expression of the indicated inflammatory genes was determined (D). Within the CD45$^+$ cell population in blood, the percentages of B cells (CD22.2$^+$) and T cells (CD3$^+$) were determined (E). Within the CD3$^+$ T cell fraction in blood, the percentages of CD4$^+$ and CD8$^+$ cells were determined (K). Values represent means ± SD. *p<0.05, **p<0.01 vs. control (n=10-12) as measured by a two-tailed unpaired Student's t-test. WT, wild-type; gWAT, gonadal white adipose tissue.*

Supplementary figure 4. *FcγRI/II/III/IV/C3^{-/-} and wild-type control mice were fed an HFD for 15 weeks. Plasma triglycerides (A) and free fatty acids (B) were analysed at the indicated time points. Basal, 8b-cAMP-stimulated and insulin inhibition of 8b-cAMP-stimulated ex vivo glycerol release (index of lipolysis) from isolated gonadal white adipocytes were determined (C). GWAT mRNA expression of the indicated inflammatory genes was determined (D). Within the CD45^{+} cell population in blood, the percentages of B cells (CD22.2^{+}) and T cells (CD3^{+}) were determined (E). Within the CD3^{+} T cell fraction in blood, the percentages of CD4^{+} and CD8^{+} cells were determined (K). Values represent means ± SD. **p<0.01 vs. control (n=10) as measured by a two-tailed unpaired Student's t-test. WT, wild-type; gWAT, gonadal white adipose tissue.*

Chapter 4

South Asians have lower expression of interferon signaling genes in white adipose tissue and skeletal muscle compared to white Caucasians

Andrea D. van Dam, Mark J.W. Hanssen, Robin van Eenige,
Edwin Quinten, Hetty C. Sips, Cindy J.M. Hülsman, Ingrid M. Jazet,
Wouter D. van Marken Lichtenbelt, Tom H.M. Ottenhoff,
Mariëlle C. Haks, Patrick C.N. Rensen, Mariëtte R. Boon

ABSTRACT

South Asians have a higher risk of developing type 2 diabetes compared to white Caucasians. Since inflammation plays an important role in type 2 diabetes development, we assessed inflammatory state in South Asians compared to white Caucasians. We assessed transcriptomic levels of 144 inflammatory, immune-regulating and immune cell subset markers in blood, skeletal muscle and white adipose tissue (WAT) of overweight pre-diabetic Dutch South Asian and matched white Caucasian men using a focused multiplex gene expression profiling technique. In South Asians, expression of especially interferon signaling genes was lower, both in muscle (*IFIT3*, *IFI44*; -45-51%) and in WAT (*IFI35*, *IFI44*, *IFIT2*, *IFIT3*, *IFIT5*, *OAS1*, *STAT1*; -13-40%). Of note, *IL5* expression was also lower in WAT (-66%). In conclusion, South Asians have lower expression levels of interferon signaling genes in skeletal muscle and WAT. Future studies should investigate the relevance of interferon signaling for type 2 diabetes development.

4

INTRODUCTION

South Asians, who originate from the Indian subcontinent, make up 20% of the world population and have a higher risk of developing type 2 diabetes when compared to white Caucasians (1). Albeit central obesity and insulin resistance are more prevalent in South Asians than in white Caucasians (1), these predisposing classical risk factors cannot fully explain their excess risk of developing type 2 diabetes. Despite the clear link between inflammation and the pathogenesis of type 2 diabetes (2), comprehensive data on the inflammatory state in South Asians are lacking. Therefore, the aim of the current study was to compare transcriptomic levels of a large panel of inflammatory, immune-regulating and immune cell subset markers in blood, skeletal muscle and WAT of overweight, pre-diabetic South Asian and matched white Caucasian men.

MATERIALS AND METHODS

Participants

Ten Dutch overweight (body mass index (BMI) between 25 and 35 kg/m²), pre-diabetic middle-aged (35-55 y) South Asian males and ten BMI- and age-matched Dutch white Caucasian males were included in this study. Pre-diabetes was defined as fasting plasma glucose levels between 5.6 and 6.9 mmol/L or plasma glucose levels between 7.8 and 11.1 mmol/L at 2 hours after an oral glucose tolerance test. Ethnicity was specified as having four grandparents of white Caucasian or South Asian origin. Exclusion criteria included type 2 diabetes, smoking, vigorous exercise, liver or kidney dysfunction, hypo- or hyperthyroidism, uncontrolled hypertension and the use of beta-blockers. Three South Asians used antihypertensive medication before and during the study. The study was originally designed to assess the effect of L-arginine on energy expenditure and mitochondrial function, for which a part of this study will be published elsewhere (Hanssen & Boon).

Study approval

This study was approved by the Ethics Committee of Maastricht University Medical Center and the Leiden University Medical Center (The Netherlands). Procedures were conducted according to the principles of the Declaration of Helsinki. All participants provided written informed consent. Trial registration number: NCT02291458 (Hanssen & Boon).

Study design

Subjects were given placebo or L-arginine (Argimax®, Hankintatukku Oy) for six weeks (9 g/day, divided over three quantities per day after breakfast, lunch and dinner) in a randomized double-blind cross-over design with a four-week washout period in between. Subjects were instructed to abstain from heavy physical exercise during the last 2 days of the treatment period, and standardized evening meals were consumed before the experimental days. Each intervention period was followed by 2 study days. On the first study day, a 4h-fasted

blood sample was drawn and resting energy expenditure was measured during 45 min at thermoneutrality (*i.e.* 29.9±0.1°C) and during 90 min of cold exposure (*i.e.* 23.9±0.4°C) via a face-mask connected to an indirect calorimeter (EZcal, IDEE). Furthermore, a cold-induced [^{18}F]fluorodeoxyglucose (FDG) PET-CT scan was conducted to assess brown adipose tissue (BAT) volume and activity. On the second day, skeletal muscle biopsies (approx. 75-100 mg) were taken from the *musculus vastus lateralis* and subcutaneous white adipose tissue (WAT) biopsies were taken from the umbilical region under localized anesthesia in the morning after an overnight fast. Dual-energy X-ray absorptiometry (DEXA) was performed to assess body composition. The study was performed between November 2014 and October 2015 in Maastricht, The Netherlands (Hanssen & Boon). From all subjects, measurements after placebo treatment were used to study the transcriptomic levels of inflammatory, immune-regulating and immune cell subset markers in South Asians *vs.* white Caucasians.

RNA isolation and dual-color RT-MLPA assay

Muscle and WAT biopsies were homogenized in 1 mL TriPure RNA Isolation reagent (Roche, The Netherlands) and RNA was extracted according to manufacturer's instructions. Whole blood was collected in venipuncture PAXgene collection tubes and total RNA was extracted and purified using the PAXgene Blood miRNA kit (PreAnalytix). A dual-color Reverse Transcriptase Multiplex Ligation-dependent Probe Amplification (dcRT-MLPA) assay (3, 4) was performed on blood, WAT and skeletal muscle tissue. Briefly, for each target-specific sequence, a specific RT primer was designed located immediately downstream of the left and right hand half-probe target sequence. Following reverse transcription, left and right hand half-probes were hybridized to the cDNA at 60°C overnight. Annealed half-probes were ligated and subsequently amplified by PCR. PCR amplification products were 1:10 diluted in HiDi formamide-containing 400HD ROX size standard and analysed on an Applied Biosystems 3730 capillary sequencer in GeneScan mode (Baseclear). Trace data were analyzed using the GeneMapper 5.0 software package (Applied Biosystems). The areas of each assigned peak (in arbitrary units) were exported for further analysis in Microsoft Excel. Data were normalized to *GAPDH* and signals below the threshold value for noise cutoff in GeneMapper (log2 transformed peak area 7.64) were assigned the threshold value for noise cut-off (5, 6).

Statistical analysis

All data are expressed as means ± SEM. If some but not all subjects within a group showed an expression level below the detection limit, the value corresponding to the limit of detection divided by 2 was used for calculation of the mean and statistical analysis. If data were normally distributed as assessed by a Shapiro-Wilk test, log-transformed data were compared with a two-tailed unpaired Student's t-test and if not normally distributed with a Mann-Whitney U test. Correlations were analysed by linear regression analysis. IBM SPSS Statistics 23.0 was used for analyses and differences and correlations were considered statistically significant if $p<0.05$.

RESULTS

Clinical characteristics
White Caucasians and South Asians had comparable age, BMI and fasting glucose, though South Asians tended to be shorter (-2.8%; p=0.06) (**Table 1**).

Markers of inflammation in blood
Transcriptomic profiles of immune markers in blood are listed in **Supplementary Table 1**. Several markers were expressed higher in South Asians, including *GNLY* (+79%), *NOD2* (+40%), *IL2RA* (+33%), *CCL5* (+32%), *NLRP3* (+27%) and *PRF1* (+23%). In contrast, expression of *CCL19* (-47%), *IL6* (-30%), *FPR1* (-29%), *DSE* (-24%), *CXCL10* (-22%) and *TGFBR2* (-12%) was lower in the blood of South Asians.

Markers of inflammation in muscle and WAT
In muscle, the expression of many immune markers was below the detection limit (**Supplementary Table 1**). Nevertheless, expression levels of individual genes like *LAG3* (+79%), *TNIP1* (+49%), *IL23A* (+39%) and *NLRC4* (+32%) were higher in South Asians. The two genes most significantly lower expressed in South Asians were interferon signaling genes *IFI44* (-51%) and *IFIT3* (-45%) (**Fig. 1A**). In addition, *CTLA4* (-44%), *CXCL10* (-39%), *NCAM1* (-38%), *TNFRSF1A* (-38%), *IL13* (-36%), *SEC14L1* (-33%) and *TGFB1* (-14%) were lower expressed.

Table 1. Baseline metabolic characteristics and body composition after 6 weeks placebo treatment of white Caucasians and South Asians. *Body composition was determined by DEXA. BMI, body mass index; OGTT, oral glucose tolerance test. Data are presented as mean ± SEM.*

	White Caucasians n=10	South Asians n=10	P-value
Age (years)	47.5 ± 2.0	46.5 ± 2.3	0.744
Height (m)	1.81 ± 0.02	1.76 ± 0.02	0.061
Weight (kg)	99.9 ± 4.0	93.0 ± 3.8	0.223
BMI (kg/m²)	30.7 ± 1.2	30.1 ± 1.1	0.723
Fasting glucose (mmol/L)	5.7 ± 0.2	5.6 ± 0.2	0.939
OGTT2h glucose (mmol/L)	7.4 ± 0.6	6.6 ± 0.5	0.282
HbA1c (%; mmol/mol)	5.4 ± 0.1; 36.0 ± 0.9	5.7 ± 0.1; 38.3 ± 1.3	0.149
Total cholesterol (mmol/L)	5.60 ± 0.29	5.51 ± 0.24	0.819
TG (mmol/L)	1.72 ± 0.20	1.95 ± 0.41	0.628
Fat percentage (%)	30.1 ± 1.0	31.2 ± 1.3	0.540
Lean mass percentage (%)	67.6 ± 1.0	66.3 ± 1.3	0.458
Trunk/limb fat mass ratio	1.2 ± 0.1	1.2 ± 0.1	0.698
Visceral adipose tissue mass (g)	714 ± 79	689 ± 36	0.771
Visceral adipose tissue volume (cm³)	772 ± 86	745 ± 39	0.768

4
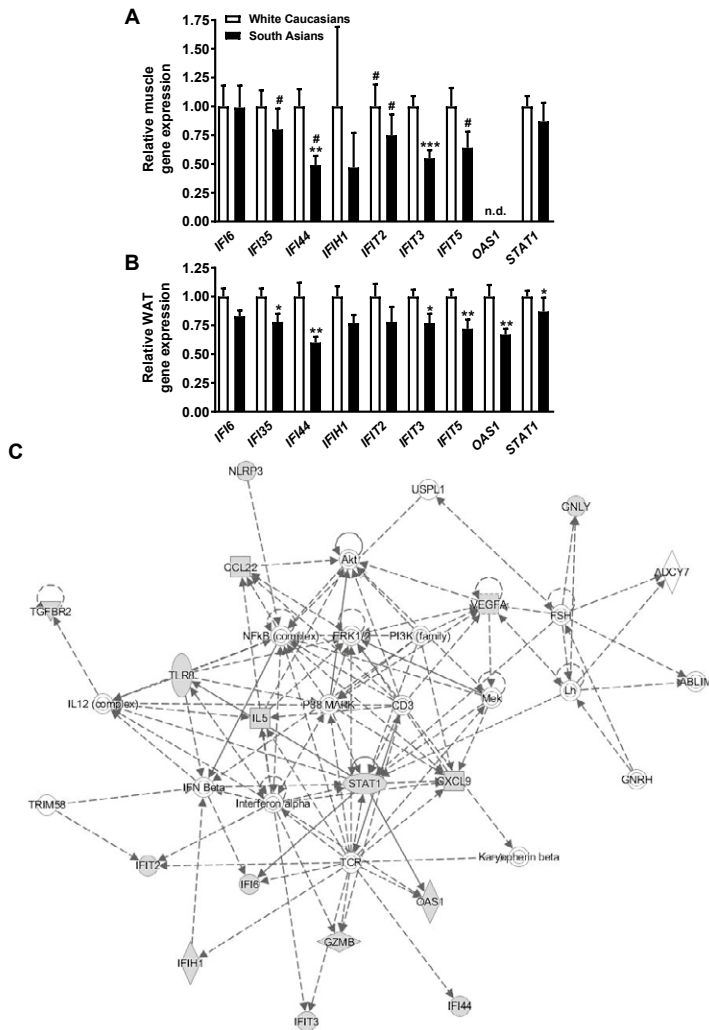
Figure 1. Interferon signaling gene expression is lower in muscle and white adipose tissue of South Asians compared to white Caucasians. *Relative interferon signaling gene expression in (A) muscle and (B) white adipose tissue of white Caucasians and South Asians. N.d., not detectable; WAT, white adipose tissue. Data are presented as mean ± SEM. *p<0.05, **p<0.01, ***p<0.001 compared to white Caucasians, #Gene expression of 4 or more individuals was not detectable. (C) Ingenuity Pathway Analysis (IPA) was performed on the list of genes with a (tendency for; p<0.1) different expression between South Asians and white Caucasians, which are marked with grey symbols in the network. Genes in uncoloured symbols were not analysed or identified as differentially expressed in our experiment and were integrated into the computationally generated network based on the evidence stored in the IPA knowledge memory indicating relevance to this network. The top canonical pathway was interferon signaling. Gene and gene relationship symbols: square, cytokine; vertical diamond, enzyme; horizontal diamond, peptidase; double circle, group or complex; dashed square, growth factor; triangle, kinase; horizontal oval, transcription factor; vertical oval, transmembrane receptor; single circle, other; arrow, acts on; continuous line, direct interaction; dashed line, indirect interaction.*
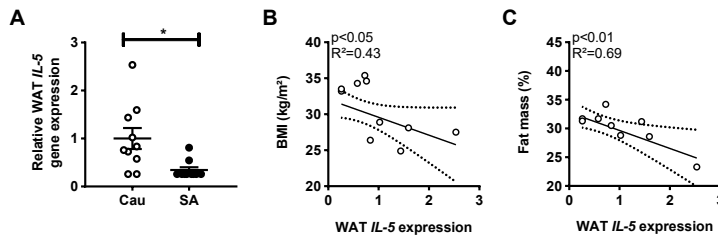
Figure 2. *IL5* gene expression is lower in white adipose tissue of South Asians compared to white Caucasians. *(A) Relative IL5 mRNA expression in white adipose tissue (WAT) of white Caucasians and South Asians. Data are presented as mean ± SEM. *p<0.05 compared to white Caucasians. Correlation of (B) body mass index (BMI) and (C) fat mass with IL5 mRNA expression in WAT of white Caucasians. WAT, white adipose tissue; WC, white Caucasians; SA, South Asians; BMI, body mass index.*

In WAT, several immune markers having a diverse range of immunological functions were differentially expressed between ethnicities including *GNLY* (+58%), *BPI* (-46%), *CCL22* (-34%), *CXCL9* (-28%) and *TGFBR2* (-17%) (**Supplementary Table 1**). Interestingly, in line with skeletal muscle, out of the 12 genes with significantly lower expression in South Asians, 7 were interferon signaling genes, including *IFI35* (-22%), *IFI44* (-40%), *IFIT2* (-22%), *IFIT3* (-23%), *IFIT5* (-28%), *OAS1* (-33%) and *STAT1* (-13%). *IFI6* (-17%) and *IFIH1* (-23%) expression also tended to be reduced (**Fig. 1B**).

To identify the signaling pathways that are differently regulated in WAT, genes with a tendency for different expression between South Asians and white Caucasians (p<0.1) were fed into Ingenuity Pathway Analysis (IPA). The top canonical pathway enriched with differentially expressed genes between the two ethnicities was interferon signaling (**Fig. 1C**), confirming our analysis of individual genes that are differentially expressed in WAT of South Asians and white Caucasians.

Of note, the most differently expressed gene in WAT of South Asians was *IL5* (-66%), which was mainly due to a lack of *IL5* expression in most South Asians (**Fig. 2A**). Remarkably, *IL5* expression in WAT of only white Caucasians (as expression was undetectable in South Asians), negatively correlated with BMI (R^2=0.43, p<0.05) and fat mass (R^2=0.69, p<0.01; **Fig. 2B-C**).

DISCUSSION

We demonstrate that many immune markers involved in a range of immunological functions in blood, muscle and WAT are differentially expressed in South Asians compared to white Caucasians. The most pronounced differences included lower expression of interferon signaling genes (skeletal muscle and WAT) and *IL5* (WAT) in South Asians.

Despite the high risk of type 2 diabetes in South Asians and the clear link between inflammation and type 2 diabetes, inflammation in South Asians has not been extensively studied. South Asians have higher plasma CRP levels compared to white Caucasians, suggesting a more pro-inflammatory state. Moreover, South Asians generally have more visceral adipose tissue, which is an important source of pro-inflammatory cytokines (7). One previous study observed similar CD68 protein content but lower CCL2 levels in muscle of South Asians compared to white Caucasians (8). Although we did not determine *CD68* expression, many macrophage markers including *CCL2* were undetectable in muscle of both ethnicities.

The most striking finding of the current study was that in both WAT and muscle, interferon signaling genes were consistently lower expressed in South Asians. Ingenuity pathway analysis corroborated the finding that the anti-inflammatory type 1 interferon signaling pathways, *i.e.* interferon α and β, were lower expressed in South Asians. Interestingly, adipose tissue-specific knockout of *interferon (α+β) receptor 1* in mice deteriorates high-fat diet induced weight gain, insulin resistance and glucose intolerance (9). On the other hand, IFNβ1 induces cellular glucose uptake via the PI3K/Akt pathway (10) and overexpression of *Ifnβ1* suppresses adipose tissue inflammation and protects against diet-induced obesity and glucose intolerance (11). Together, this indicates that impaired interferon signaling in South Asians may, at least partly, cause their predisposition for development of obesity as well as type 2 diabetes.

In addition, *IL5* expression was markedly lower expressed in WAT of South Asians. *IL5* is produced by group 2 innate lymphoid cells (ILC2s) and is essential for mobilizing eosinophils in the bone marrow and regulating homing and migration of eosinophils into tissues. *IL5* transgenic mice are hypereosinophilic and have reduced fat mass and improved glucose tolerance (12), which is in accordance with our data showing that *IL5* expression in adipose tissue of white Caucasians negatively correlates with fat mass. ILC2s also promote browning of WAT (13) and may thereby enhance energy expenditure and protect against obesity and associated disorders. Based on the findings in rodents, we speculate that low *IL5* expression in South Asians may be accompanied by low adipose tissue eosinophils, reduced browning and its unfavorable consequences such as higher fat mass and reduced glucose tolerance.

Limitations of our study are the small sample size and the placebo treatment that participants received in the context of the L-arginine treatment this trial was originally designed for. As we only assessed gene expression levels, further research into the immune system of South Asians would also benefit from performing analysis of protein levels and flow cytometry. Strengths of our study are the extensiveness of the panel of immune

markers measured, not only in blood, but also in two important metabolic tissues within the same individuals. Furthermore, the individuals of different ethnicities were well-matched for metabolic parameters that could interfere with inflammation, such as age and BMI.

In conclusion, the immune system in blood, muscle and WAT is differently primed in South Asians compared to white Caucasians, with a consistent lower expression of interferon signaling genes in metabolic tissues of South Asians as the most prominent feature. Whether interferon signaling in metabolic tissues directly influences glucose metabolism in humans and whether this could be a target to treat insulin resistance or reduce the risk of type 2 diabetes in South Asians is an interesting field of future investigation.

ACKNOWLEDGEMENTS

FUNDING

REFERENCES

1. Raji A, Seely EW, Arky RA, Simonson DC: Body fat distribution and insulin resistance in healthy Asian Indians and Caucasians. The Journal of clinical endocrinology and metabolism 2001;86:5366-5371

2. Boon MR, Bakker LE, van der Linden RA, van Ouwerkerk AF, de Goeje PL, Counotte J, Jazet IM, Rensen PC: High prevalence of cardiovascular disease in South Asians: Central role for brown adipose tissue? Critical reviews in clinical laboratory sciences 2015;52:150-157

3. Haks MC, Goeman JJ, Magis-Escurra C, Ottenhoff TH: Focused human gene expression profiling using dual-color reverse transcriptase multiplex ligation-dependent probe amplification. Vaccine 2015;33:5282-5288

4. Joosten SA, Goeman JJ, Sutherland JS, Opmeer L, de Boer KG, Jacobsen M, Kaufmann SH, Finos L, Magis-Escurra C, Ota MO, Ottenhoff TH, Haks MC: Identification of biomarkers for tuberculosis disease using a novel dual-color RT-MLPA assay. Genes and immunity 2012;13:71-82

5. Boon MR, Bakker LE, Haks MC, Quinten E, Schaart G, Van Beek L, Wang Y, Van Schinkel L, Van Harmelen V, Meinders AE, Ottenhoff TH, Van Dijk KW, Guigas B, Jazet IM, Rensen PC: Short-term high-fat diet increases macrophage markers in skeletal muscle accompanied by impaired insulin signalling in healthy male subjects. Clinical science (London, England : 1979) 2015;128:143-151

6. van der Lans AA, Boon MR, Haks MC, Quinten E, Schaart G, Ottenhoff TH, van Marken Lichtenbelt WD: Cold acclimation affects immune composition in skeletal muscle of healthy lean subjects. Physiological reports 2015;3:e12394

7. Chambers JC, Eda S, Bassett P, Karim Y, Thompson SG, Gallimore JR, Pepys MB, Kooner JS: C-reactive protein, insulin resistance, central obesity, and coronary heart disease risk in Indian Asians from the United Kingdom compared with European whites. Circulation 2001;104:145-150

8. Samaan MC, Anand SS, Sharma AM, Bonner A, Beyene J, Samjoo I, Tarnopolsky MA: Adiposity and immune-muscle crosstalk in South Asians & Europeans: A cross-sectional study. Scientific reports 2015;5:14521

9. Wieser V, Adolph TE, Grander C, Grabherr F, Enrich B, Moser P, Moschen AR, Kaser S, Tilg H: Adipose type I interferon signalling protects against metabolic dysfunction. Gut 2016; in press

10. Burke JD, Platanias LC, Fish EN: Beta interferon regulation of glucose metabolism is PI3K/Akt dependent and important for antiviral activity against coxsackievirus B3. Journal of virology 2014;88:3485-3495

11. Alsaggar M, Mills M, Liu D: Interferon beta overexpression attenuates adipose tissue inflammation and high-fat diet-induced obesity and maintains glucose homeostasis. Gene therapy 2016;24:60-66

12. Wu D, Molofsky AB, Liang HE, Ricardo-Gonzalez RR, Jouihan HA, Bando JK, Chawla A, Locksley RM: Eosinophils sustain adipose alternatively activated macrophages associated with glucose homeostasis. Science (New York, NY) 2011;332:243-247

13. Brestoff JR, Kim BS, Saenz SA, Stine RR, Monticelli LA, Sonnenberg GF, Thome JJ, Farber DL, Lutfy K, Seale P, Artis D: Group 2 innate lymphoid cells promote beiging of white adipose tissue and limit obesity. Nature 2015;519:242-246

4

SUPPLEMENTARY APPENDIX

Supplementary Table 1. Relative gene expression levels of immune markers in blood, skeletal muscle and white adipose tissue (WAT) of white Caucasians and South Asians. *N.d., not detectable. Data are presented as mean ± SEM, n=10 per group. *p<0.05, **p<0.01, ***p<0.001 compared to white Caucasians, #Gene expression of 4 or more individuals was not detectable.*

Gene	Blood		Muscle		WAT	
	White Caucasians	South Asians	White Caucasians	South Asians	White Caucasians	South Asians
Immune cell subset markers						
BLR1	1.00 ± 0.10	1.20 ± 0.11	1.00 ± 0.15#	0.87 ± 0.11#	1.00 ± 0.15	1.12 ± 0.18
CD19	1.00 ± 0.10	1.09 ± 0.12	n.d.#	n.d.#	n.d.#	n.d.#
NCAM1	1.00 ± 0.20	1.27 ± 0.17	1.00 ± 0.13	**0.62 ± 0.10#***	1.00 ± 0.19	0.86 ± 0.17
T cell subsets						
CD3E	1.00 ± 0.13	1.22 ± 0.07	n.d.#	n.d.#	1.00 ± 0.20#	1.38 ± 0.18
CD4	1.00 ± 0.06	0.97 ± 0.04	n.d.#	n.d.#	1.00 ± 0.07	0.89 ± 0.05
CD8A	1.00 ± 0.26	1.38 ± 0.24	n.d.#	n.d.#	n.d.#	n.d.#
CCR7	1.00 ± 0.16	1.14 ± 0.09	1.00 ± 0.17#	1.80 ± 0.38	1.00 ± 0.00#	1.14 ± 0.14#
PTPRCv1	1.00 ± 0.09	1.17 ± 0.08	n.d.#	n.d.#	1.00 ± 0.21#	0.78 ± 0.16#
PTPRCv2	1.00 ± 0.11	1.08 ± 0.06	n.d.#	n.d.#	1.00 ± 0.14	0.92 ± 0.10
AIRE	1.00 ± 0.13	0.80 ± 0.09	n.d.#	n.d.#	1.00 ± 0.11	1.06 ± 0.09
Th1 response						
CXCL10	1.00 ± 0.10	**0.78 ± 0.06***	1.00 ± 0.11	**0.61 ± 0.08#***	1.00 ± 0.10	0.93 ± 0.13
IFNG	n.d.#	n.d.#	n.d.#	n.d.#	n.d.#	n.d.#
IL1B	1.00 ± 0.10	0.88 ± 0.04	n.d.#	n.d.#	1.00 ± 0.17#	1.29 ± 0.19#
IL2	n.d.#	n.d.#	n.d.#	n.d.#	n.d.#	n.d.#
IL15	n.d.#	n.d.#	n.d.#	n.d.#	1.00 ± 0.13#	0.81 ± 0.00#
TBX21	1.00 ± 0.18#	0.95 ± 0.16#	n.d.#	n.d.#	n.d.#	n.d.#
TNF	1.00 ± 0.07	0.94 ± 0.04	1.00 ± 0.07	1.11 ± 0.10	1.00 ± 0.05	0.91 ± 0.07
Th2 response						
GATA3	1.00 ± 0.11	1.23 ± 0.08	n.d.#	n.d.#	1.00 ± 0.13#	1.30 ± 0.18#
IL4	1.00 ± 0.41#	0.38 ± 0.00#	n.d.#	n.d.#	1.00 ± 0.16#	0.77 ± 0.00#
IL4d2	1.00 ± 0.18	0.98 ± 0.13	n.d.#	n.d.#	1.00 ± 0.19#	0.94 ± 0.13
IL5	1.00 ± 0.16	0.80 ± 0.05	n.d.#	n.d.#	1.00 ± 0.22	**0.34 ± 0.06#****
IL6	1.00 ± 0.09	**0.70 ± 0.05***	1.00 ± 0.10#	1.04 ± 0.14#	1.00 ± 0.16	0.98 ± 0.09
IL9	1.00 ± 0.12	0.84 ± 0.07	n.d.#	n.d.#	1.00 ± 0.09	1.04 ± 0.10
IL13	n.d.#	n.d.#	1.00 ± 0.09	**0.64 ± 0.10***	1.00 ± 0.00#	1.23 ± 0.23#

4

Gene	Blood		Muscle		WAT	
	White Caucasians	South Asians	White Caucasians	South Asians	White Caucasians	South Asians
Th17 response						
IL17A	n.d.#	n.d.#	n.d.#	n.d.#	1.00 ± 0.00#	2.21 ± 0.99#
RORC	1.00 ± 0.26#	0.74 ± 0.00#	1.00 ± 0.14	0.80 ± 0.06	n.d.#	n.d.#
NEDD4L	1.00 ± 0.06	1.19 ± 0.09	1.00 ± 0.14	0.91 ± 0.08	1.00 ± 0.07	0.95 ± 0.08
IL22RA1	1.00 ± 0.11	1.10 ± 0.05	n.d.#	n.d.#	n.d.#	n.d.#
Treg markers						
CTLA4	1.00 ± 0.06	1.02 ± 0.04	1.00 ± 0.14	**0.56 ± 0.22***	1.00 ± 0.08	1.04 ± 0.08
FOXP3	1.00 ± 0.14	1.15 ± 0.07	n.d.#	n.d.#	1.00 ± 0.15	1.04 ± 0.12
IL10	1.00 ± 0.12	1.12 ± 0.08	n.d.#	n.d.#	1.00 ± 0.11	0.94 ± 0.08
IL2RA	1.00 ± 0.08	**1.33 ± 0.08****	n.d.#	n.d.#	1.00 ± 0.22#	1.06 ± 0.19#
IL7R	1.00 ± 0.11	1.11 ± 0.06	n.d.#	n.d.#	1.00 ± 0.11	0.96 ± 0.08
LAG3	1.00 ± 0.00#	1.33 ± 0.33#	1.00 ± 0.33	**1.79 ± 0.24***	n.d.#	n.d.#
TGFB1	1.00 ± 0.05	1.00 ± 0.03	1.00 ± 0.04	**0.86 ± 0.06***	1.00 ± 0.04	0.95 ± 0.04
TNFRSF18	1.00 ± 0.08	0.90 ± 0.14	n.d.#	n.d.#	1.00 ± 0.19#	1.11 ± 0.17#
Cytotoxicity markers						
GNLY	1.00 ± 0.17	**1.79 ± 0.19****	1.00 ± 0.00#	1.37 ± 0.19#	1.00 ± 0.23	**1.58 ± 0.23***
GZMA	1.00 ± 0.16	1.08 ± 0.13	n.d.#	n.d.#	1.00 ± 0.07	0.97 ± 0.09
GZMB	1.00 ± 0.21	1.32 ± 0.11	n.d.#	n.d.#	1.00 ± 0.13	1.37 ± 0.15
PRF1	1.00 ± 0.19	**1.23 ± 0.08***	n.d.#	n.d.#	1.00 ± 0.15	1.04 ± 0.18
Antimicrobial activity						
LTF	1.00 ± 0.22	0.58 ± 0.13	n.d.#	n.d.#	1.00 ± 0.40#	0.69 ± 0.25#
Macrophage markers						
CD14	1.00 ± 0.07	0.84 ± 0.04	1.00 ± 0.15	0.96 ± 0.25	1.00 ± 0.07	0.87 ± 0.08
CD163	1.00 ± 0.08	0.80 ± 0.04	1.00 ± 0.23	0.72 ± 0.33#	1.00 ± 0.07	0.83 ± 0.08
CD209	1.00 ± 0.08	0.99 ± 0.05	1.00 ± 0.15	1.10 ± 0.07	1.00 ± 0.09	0.99 ± 0.07
CCL2	1.00 ± 0.19#	0.92 ± 0.18#	n.d.#	n.d.#	1.00 ± 0.12	1.17 ± 0.24
CCL3	1.00 ± 0.08	1.07 ± 0.09	1.00 ± 0.51	0.38 ± 0.10	1.00 ± 0.07	1.23 ± 0.27
CCL4	1.00 ± 0.07	0.95 ± 0.04	n.d.#	n.d.#	1.00 ± 0.03	0.94 ± 0.04
CCL5	1.00 ± 0.11	**1.32 ± 0.09***	1.00 ± 0.17#	0.96 ± 0.14#	1.00 ± 0.11	1.07 ± 0.12
CCL22	1.00 ± 0.15	0.87 ± 0.05	n.d.#	n.d.#	1.00 ± 0.08	**0.66 ± 0.07****
CXCL13	1.00 ± 0.13	0.75 ± 0.22#	n.d.#	n.d.#	1.00 ± 0.20#	1.27 ± 0.27
IL12A	1.00 ± 0.15#	0.92 ± 0.14#	1.00 ± 0.25#	0.75 ± 0.00#	1.00 ± 0.16#	1.04 ± 0.20#
IL12B	1.00 ± 0.11	0.96 ± 0.05	1.00 ± 0.00#	1.14 ± 0.14#	1.00 ± 0.09	1.03 ± 0.10
IL23A	1.00 ± 0.03	1.05 ± 0.03	1.00 ± 0.09	**1.39 ± 0.10****	1.00 ± 0.04	1.00 ± 0.03
Scavenger receptors						
MARCO	1.00 ± 0.20	0.48 ± 0.14#	n.d.#	n.d.#	1.00 ± 0.43#	0.50 ± 0.12#

Gene	Blood		Muscle		WAT	
	White Caucasians	South Asians	White Caucasians	South Asians	White Caucasians	South Asians
Pattern recognition receptors						
CLEC7A	1.00 ± 0.09	0.86 ± 0.07	n.d.#	n.d.#	1.00 ± 0.15	0.79 ± 0.07
MRC1	n.d.#	n.d.#	n.d.#	n.d.#	1.00 ± 0.09	0.91 ± 0.09
MRC2	n.d.#	n.d.#	n.d.#	n.d.#	1.00 ± 0.11	1.00 ± 0.09
NOD1	1.00 ± 0.11	1.22 ± 0.09	n.d.#	n.d.#	1.00 ± 0.06	0.94 ± 0.06
NOD2	1.00 ± 0.14	**1.40 ± 0.06****	n.d.#	n.d.#	n.d.#	n.d.#
TLR1	1.00 ± 0.10	0.98 ± 0.07	n.d.#	n.d.#	1.00 ± 0.09	0.90 ± 0.10
TLR2	1.00 ± 0.12	0.91 ± 0.05	n.d.#	n.d.#	n.d.#	n.d.#
TLR3	1.00 ± 0.22#	0.90 ± 0.13	n.d.#	n.d.#	1.00 ± 0.04	0.98 ± 0.07
TLR4	1.00 ± 0.09	0.95 ± 0.06	n.d.#	n.d.#	1.00 ± 0.05	0.95 ± 0.05
TLR5	1.00 ± 0.14	0.85 ± 0.08	1.00 ± 0.47#	0.97 ± 0.16	1.00 ± 0.19#	2.68 ± 1.66#
TLR6	1.00 ± 0.09	0.88 ± 0.06	n.d.#	n.d.#	1.00 ± 0.12	1.19 ± 0.12
TLR7	1.00 ± 0.11	1.11 ± 0.07	1.00 ± 0.18#	0.96 ± 0.15#	1.00 ± 0.06	1.06 ± 0.09
TLR8	1.00 ± 0.20	1.06 ± 0.18	n.d.#	n.d.#	1.00 ± 0.25#	1.36 ± 0.16
TLR9	1.00 ± 0.51#	0.37 ± 0.30#	1.00 ± 0.10	1.21 ± 0.09	1.00 ± 0.11	0.96 ± 0.09
TLR10	n.d.#	n.d.#	n.d.#	n.d.#	n.d.#	n.d.#
Inflammasome components						
NLRC4	1.00 ± 0.07	0.99 ± 0.04	1.00 ± 0.10	**1.32 ± 0.10***	1.00 ± 0.05	1.07 ± 0.08
NLRP1	1.00 ± 0.10	1.06 ± 0.06	1.00 ± 0.00#	1.54 ± 0.23#	1.00 ± 0.06	0.94 ± 0.08
NLRP2	1.00 ± 0.16	0.90 ± 0.07	1.00 ± 0.16	1.22 ± 0.12	1.00 ± 0.09	1.01 ± 0.12
NLRP3	1.00 ± 0.07	**1.27 ± 0.06***	n.d.#	n.d.#	1.00 ± 0.14#	0.63 ± 0.09#
NLRP4	1.00 ± 0.10	0.76 ± 0.10	n.d.#	n.d.#	1.00 ± 0.10	1.05 ± 0.13
NLRP6	1.00 ± 0.13#	0.90 ± 0.09#	n.d.#	n.d.#	n.d.#	n.d.#
NLRP7	n.d.#	n.d.#	n.d.#	n.d.#	n.d.#	n.d.#
NLRP10	n.d.#	n.d.#	n.d.#	n.d.#	n.d.#	n.d.#
NLRP11	n.d.#	n.d.#	n.d.#	n.d.#	n.d.#	n.d.#
NLRP12	1.00 ± 0.10	0.92 ± 0.05	n.d.#	n.d.#	n.d.#	n.d.#
NLRP13	1.00 ± 0.30	1.08 ± 0.47	n.d.#	n.d.#	1.00 ± 0.08	0.80 ± 0.15#

4

Gene	Blood		Muscle		WAT	
	White Caucasians	South Asians	White Caucasians	South Asians	White Caucasians	South Asians
IFN signaling genes						
CD274	1.00 ± 0.09	1.03 ± 0.11	1.00 ± 0.25#	1.46 ± 0.23	1.00 ± 0.13#	1.06 ± 0.15#
FCGR1A	1.00 ± 0.15	1.37 ± 0.51	n.d.#	n.d.#	1.00 ± 0.16#	1.33 ± 0.24#
GBP1	1.00 ± 0.26	1.12 ± 0.20	n.d.#	n.d.#	1.00 ± 0.19#	0.98 ± 0.31#
GBP2	1.00 ± 0.11	1.10 ± 0.11	1.00 ± 0.14	0.90 ± 0.18	1.00 ± 0.08	0.90 ± 0.07
GBP5	1.00 ± 0.19	1.17 ± 0.17	n.d.#	n.d.#	1.00 ± 0.13	0.97 ± 0.14
IFI6	1.00 ± 0.42	0.72 ± 0.09	1.00 ± 0.18	0.99 ± 0.19	1.00 ± 0.07	0.83 ± 0.05
IFI16	1.00 ± 0.10	1.04 ± 0.09	1.00 ± 0.17	0.93 ± 0.18	1.00 ± 0.06	0.96 ± 0.05
IFI35	1.00 ± 0.14	0.99 ± 0.11	1.00 ± 0.14	0.80 ± 0.18#	1.00 ± 0.07	**0.78 ± 0.07***
IFI44	1.00 ± 0.48	0.54 ± 0.10	1.00 ± 0.15	**0.49 ± 0.08#****	1.00 ± 0.12	**0.60 ± 0.05****
IFI44L	1.00 ± 0.54	0.45 ± 0.09	1.00 ± 0.24#	0.58 ± 0.09#	1.00 ± 0.19	0.66 ± 0.09
IFIH1	1.00 ± 0.21	0.98 ± 0.09	1.00 ± 0.69	0.47 ± 0.30	1.00 ± 0.09	0.77 ± 0.07
IFIT2	1.00 ± 0.26	0.77 ± 0.09	1.00 ± 0.19#	0.75 ± 0.18#	1.00 ± 0.11	**0.78 ± 0.13***
IFIT3	1.00 ± 0.29	0.73 ± 0.11	1.00 ± 0.09	**0.55 ± 0.07*****	1.00 ± 0.06	**0.77 ± 0.08***
IFIT5	1.00 ± 0.26	0.79 ± 0.10	1.00 ± 0.16	0.64 ± 0.14#	1.00 ± 0.06	**0.72 ± 0.08****
IFITM3	1.00 ± 0.28	0.57 ± 0.10	1.00 ± 0.18	0.83 ± 0.14	1.00 ± 0.06	0.94 ± 0.07
INDO	1.00 ± 0.13	0.73 ± 0.10	n.d.#	n.d.#	1.00 ± 0.12#	0.88 ± 0.00#
IRF7	1.00 ± 0.16	0.80 ± 0.07	n.d.#	n.d.#	1.00 ± 0.15#	0.94 ± 0.17#
OAS1	1.00 ± 0.36	0.68 ± 0.09	n.d.#	n.d.#	1.00 ± 0.10	**0.67 ± 0.05****
OAS2	1.00 ± 0.37	0.68 ± 0.06	n.d.#	n.d.#	1.00 ± 0.16	0.70 ± 0.12#
OAS3	1.00 ± 0.48	0.50 ± 0.07	n.d.#	n.d.#	1.00 ± 0.14	0.77 ± 0.09
SOCS1	1.00 ± 0.07	0.87 ± 0.07	1.00 ± 0.22#	0.92 ± 0.24#	1.00 ± 0.08	0.91 ± 0.09
STAT1	1.00 ± 0.16	1.18 ± 0.10	1.00 ± 0.09	0.87 ± 0.16	1.00 ± 0.05	**0.87 ± 0.12***
STAT2	1.00 ± 0.16	1.07 ± 0.10	1.00 ± 0.14#	0.98 ± 0.12#	1.00 ± 0.05	0.97 ± 0.12
TAP1	1.00 ± 0.11	1.08 ± 0.10	1.00 ± 0.23#	0.95 ± 0.15#	1.00 ± 0.09	0.90 ± 0.10
TAP2	1.00 ± 0.12	1.08 ± 0.12	n.d.#	n.d.#	1.00 ± 0.08	0.92 ± 0.16
Apoptosis / Survival						
CASP8	1.00 ± 0.05	1.09 ± 0.07	n.d.#	n.d.#	1.00 ± 0.07	0.95 ± 0.06
BCL2	1.00 ± 0.12	1.19 ± 0.12	1.00 ± 0.21	0.47 ± 0.08	1.00 ± 0.06	1.08 ± 0.11
FASLG	1.00 ± 0.00#	1.13 ± 0.13#	n.d.#	n.d.#	n.d.#	n.d.#
FLCN1	1.00 ± 0.16#	1.03 ± 0.22#	n.d.#	n.d.#	1.00 ± 0.07	0.81 ± 0.09
TNFRSF1A	1.00 ± 0.07	0.99 ± 0.04	1.00 ± 0.14	**0.62 ± 0.12#***	1.00 ± 0.02	1.02 ± 0.06
TNFRSF1B	1.00 ± 0.06	0.93 ± 0.05	n.d.#	n.d.#	1.00 ± 0.09	0.86 ± 0.06
Small GTPases / (Rho)GTPase activating proteins						
ASAP1	1.00 ± 0.05	1.08 ± 0.05	1.00 ± 0.24	1.05 ± 0.31	1.00 ± 0.05	0.87 ± 0.09
RAB13	1.00 ± 0.19	1.11 ± 0.24	1.00 ± 0.14#	0.86 ± 0.14#	1.00 ± 0.05	0.90 ± 0.05
RAB24	1.00 ± 0.07	1.20 ± 0.24	1.00 ± 0.00#	1.21 ± 0.14#	1.00 ± 0.06	0.93 ± 0.08
RAB33A	1.00 ± 0.21	0.85 ± 0.05	1.00 ± 0.15#	0.92 ± 0.14#	1.00 ± 0.16#	2.20 ± 0.80#
TAGAP	1.00 ± 0.08	1.12 ± 0.07	n.d.#	n.d.#	1.00 ± 0.17	0.88 ± 0.13
TBC1D7	1.00 ± 0.17#	0.82 ± 0.13#	n.d.#	n.d.#	1.00 ± 0.15#	0.99 ± 0.15#

Gene	Blood		Muscle		WAT	
	White Caucasians	South Asians	White Caucasians	South Asians	White Caucasians	South Asians
Chemokines						
CCL11	n.d.#	n.d.#	n.d.#	n.d.#	1.00 ± 0.46#	2.51 ± 1.97#
CCL13	n.d.#	n.d.#	n.d.#	n.d.#	1.00 ± 0.37	0.96 ± 0.23
CCL19	1.00 ± 0.08	**0.53 ± 0.10***	1.00 ± 0.10#	1.17 ± 0.19#	1.00 ± 0.15	1.17 ± 0.18
CXCL9	1.00 ± 0.13#	0.84 ± 0.10#	n.d.#	n.d.#	1.00 ± 0.09	**0.72 ± 0.11***
CX3CL1	n.d.#	n.d.#	1.00 ± 0.22#	0.69 ± 0.00#	1.00 ± 0.14	0.86 ± 0.10
Cell growth / proliferation						
BMP6	1.00 ± 0.06	0.94 ± 0.06	1.00 ± 0.15	0.88 ± 0.25	1.00 ± 0.11	1.03 ± 0.09
TGFBR2	1.00 ± 0.05	**0.88 ± 0.09***	1.00 ± 0.13#	0.96 ± 0.16#	1.00 ± 0.06	**0.83 ± 0.04***
AREG	n.d.#	n.d.#	n.d.#	n.d.#	n.d.#	n.d.#
EGF	1.00 ± 0.18	0.85 ± 0.14	1.00 ± 0.16	1.23 ± 0.40#	1.00 ± 0.12	1.06 ± 0.16
VEGF	1.00 ± 0.22#	0.50 ± 0.00#	1.00 ± 0.27	1.09 ± 0.33	1.00 ± 0.15	0.70 ± 0.06
Cell activation						
HCK	1.00 ± 0.04	0.92 ± 0.03	n.d.#	n.d.#	1.00 ± 0.11	0.92 ± 0.11
LYN	1.00 ± 0.06	1.02 ± 0.04	n.d.#	n.d.#	1.00 ± 0.08	0.89 ± 0.10
SLAMF7	1.00 ± 0.16	1.23 ± 0.10	n.d.#	n.d.#	1.00 ± 0.11	1.02 ± 0.15
Transcriptional regulators / activators						
CAMTA1	n.d.#	n.d.#	n.d.#	n.d.#	n.d.#	n.d.#
TWIST1	n.d.#	n.d.#	n.d.#	n.d.#	1.00 ± 0.16#	1.05 ± 0.12
ZNF331	1.00 ± 0.25#	0.84 ± 0.12	n.d.#	n.d.#	1.00 ± 0.07	0.88 ± 0.06
ZNF532	1.00 ± 0.18	1.06 ± 0.28#	n.d.#	n.d.#	1.00 ± 0.05	0.92 ± 0.05
Intracellular transport						
SEC14L1	1.00 ± 0.05	0.95 ± 0.08	1.00 ± 0.12	**0.67 ± 0.07***	1.00 ± 0.10	0.86 ± 0.04
KIF1B	1.00 ± 0.04	1.05 ± 0.06	1.00 ± 0.12	0.94 ± 0.20	1.00 ± 0.04	0.93 ± 0.05
Inflammation						
DSE	1.00 ± 0.09	**0.76 ± 0.06***	1.00 ± 0.21	0.67 ± 0.16#	1.00 ± 0.09	1.07 ± 0.07
MMP9	1.00 ± 0.22	0.67 ± 0.10	n.d.#	n.d.#	1.00 ± 0.19	1.33 ± 0.43
SPP1	n.d.#	n.d.#	n.d.#	n.d.#	1.00 ± 0.30	0.82 ± 0.30
TIMP2	1.00 ± 0.06	0.97 ± 0.04	1.00 ± 0.13	0.68 ± 0.07	1.00 ± 0.07	1.02 ± 0.06
TNIP1	1.00 ± 0.07	1.01 ± 0.05	1.00 ± 0.31	**1.49 ± 0.41***	1.00 ± 0.08	0.92 ± 0.07
FPR1	1.00 ± 0.05	**0.71 ± 0.06****	1.00 ± 0.24#	0.47 ± 0.00#	1.00 ± 0.08	0.83 ± 0.09
BPI	1.00 ± 0.13	0.88 ± 0.05	1.00 ± 0.21#	0.55 ± 0.08#	1.00 ± 0.14	**0.54 ± 0.06****
Mitochondrial Stress / Proteasome						
HPRT	1.00 ± 0.12	1.25 ± 0.09	n.d.#	n.d.#	1.00 ± 0.12	1.13 ± 0.17

Chapter | **5**

Salsalate activates
brown adipose tissue in mice

Andrea D. van Dam, Kimberly J. Nahon, Sander Kooijman,
Susan M. van den Berg, Anish A. Kanhai, Takuya Kikuchi,
Mattijs M. Heemskerk, Vanessa van Harmelen, Marc Lombès,
Anita M. van den Hoek, Menno P.J. de Winther, Esther Lutgens,
Bruno Guigas, Patrick C.N. Rensen, Mariëtte R. Boon

ABSTRACT

Salsalate improves glucose intolerance and dyslipidemia in type 2 diabetes patients, but the mechanism is still unknown. The aim of the present study was to unravel the molecular mechanisms involved in these beneficial metabolic effects of salsalate by treating mice with salsalate during and after development of high fat diet-induced obesity. We found that salsalate attenuated and reversed high fat diet-induced weight gain, in particular fat mass accumulation, improved glucose tolerance and lowered plasma triglyceride (TG) levels. Mechanistically, salsalate selectively promoted the uptake of fatty acids from glycerol tri[^{3}H]oleate-labeled lipoprotein-like emulsion particles by brown adipose tissue (BAT), decreased the intracellular lipid content in BAT and increased rectal temperature, all pointing to more active BAT. Treatment of differentiated T37i brown adipocytes with salsalate increased uncoupled respiration in cells. Moreover, salsalate upregulated *Ucp1* expression and enhanced glycerol release, a dual effect that was abolished by inhibition of protein kinase A (PKA). In conclusion, salsalate activates BAT, presumably by directly activating brown adipocytes via the PKA pathway, suggesting a novel mechanism that may explain its beneficial metabolic effects in type 2 diabetes patients.

5

INTRODUCTION

Salsalate is a nonsteroidal anti-inflammatory drug belonging to the salicylate class of drugs. Salicylates are originally derived from plants, in which they function as part of the immune system to combat infections. Nowadays, synthetic compounds that break down to salicylates *in vivo,* including aspirin and salsalate, have largely replaced salicylate (1). In humans, salicylates have strong anti-inflammatory effects and have therefore been applied in the clinic for several decades to treat pain and inflammation caused by rheumatoid arthritis (2, 3).

Studies have shown that salicylates exhibit beneficial metabolic effects as well. A recent trial has demonstrated that salsalate lowers HbA1c levels, fasting blood glucose and circulating triglycerides (TG) in type 2 diabetes patients (4). Furthermore, salsalate increases energy expenditure in human subjects (5). In contrast to aspirin, salsalate is not associated with an increased risk of gastrointestinal bleeding and therefore relatively safe for long-term clinical experience. Thus, it is considered a promising anti-diabetic drug (3). The mechanisms underlying the beneficial metabolic effects of salsalate remain largely unknown, partly because its receptor has not been identified yet (6). Salicylates have been shown to activate AMP-activated protein kinase (AMPK) in liver, muscle and white adipose tissue (WAT), suggesting a role of this energy-sensing kinase in the mechanism of action of the drug (1). However, salicylate still improves glucose metabolism in mice lacking the regulatory AMPK-β1 subunit, suggesting involvement of other pathways as well (1).

The objective of the current study was to investigate the mechanism(s) underlying the beneficial effects of salsalate on lipid and glucose metabolism by treating APOE*3-Leiden.CETP (E3L.CETP) transgenic mice, a well-established model for human-like lipoprotein metabolism (7-9), with salsalate mixed through the high fat diet (HFD). We found that salsalate both prevented and reduced HFD-induced weight gain by lowering fat mass accumulation, and improved glucose and lipid metabolism. Mechanistic studies showed that these effects were accompanied by increased activity of brown adipose tissue (BAT). Taken together, our data indicate that BAT may contribute to the beneficial effects of salsalate on lipid and glucose metabolism and corroborate previous findings that targeting BAT may be a valuable strategy to correct metabolic derangements.

MATERIALS AND METHODS

Mice, diet and salsalate treatment

APOE*3-Leiden cholesteryl ester transfer protein (E3L.CETP) mice were obtained as previously described (7-9). To assess the effect of salsalate on progression of obesity, dyslipidemia and hyperglycemia, 10-week old male E3L.CETP mice were randomized to receive an HFD (Research Diets, 45% kcal lard fat) without or with 0.5% (w/w) salsalate (2-carboxyphenyl salicylate, TCI Europe N.V.) for 12 weeks. To assess the effect of salsalate on regression of obesity and associated metabolic disorders, 10-week old male diet-

induced (12 weeks HFD) obese E3L.CETP mice received salsalate (0.5% w/w) for 4 weeks. To investigate the effect of salsalate independent of the E3L.CETP background in a progression setting, 10-week old male wild-type (WT) mice (C57Bl/6J background; Charles River, USA) were randomized to receive an HFD without or with salsalate for 4 weeks.

Mice were individually housed at 21°C or 28°C (WT mice). To mask the bitter taste of salsalate, anise (3.33%, w/w) was added to the diet of both groups in all studies (10). Mouse experiments were performed in accordance with the Institute for Laboratory Animal Research Guide for the Care and Use of Laboratory Animals and have received approval from the University Ethical Review Board (Leiden University Medical Center, Leiden, The Netherlands).

Body weight and body composition measurements

Body weight was measured with a scale and body composition using EchoMRI (EchoMRI-100, Houston, Texas, USA).

Determination of plasma parameters

Upon randomisation and at 4 week intervals during treatment, 6 h fasted blood was collected and assayed for triglycerides (TG), total cholesterol (TC) and free fatty acids (FFA) as described before (11, 12). Glucose was measured using an enzymatic kits from Instruchemie (Delfzijl) and insulin by ELISA (Crystal Chem. Inc., Downers Grove, IL).

Intravenous Glucose Tolerance Test (ivGTT)

Mice were fasted for 6 h, a baseline blood sample was obtained, and mice were intravenously injected with 10 μl/g body weight of glucose dissolved in PBS (200 mg/mL). Additional blood samples were taken at t = 5, 15, 30, 60, 90 and 120 min. Capillaries were placed on ice and centrifuged, and glucose levels were measured as described above.

In vivo clearance of radiolabeled lipoprotein-like emulsion particles

Lipoprotein-like TG-rich emulsion particles (80 nm) labeled with glycerol tri[^{3}H]oleate (triolein, [^{3}H]TO) were prepared and characterized as described previously (13). Mice were fasted for 6 h (from 7.00 am to 13.00 pm) and injected with 200 μl of emulsion particles (1.0 mg TG per mouse) via the tail vein (t = 0). After 15 min, mice were sacrificed by cervical dislocation and perfused with ice-cold PBS through the heart. Thereafter, organs were harvested, weighed and the uptake of [^{3}H]TO-derived radioactivity was quantified and expressed per gram wet tissue weight.

Rectal temperature measurement

Rectal temperature was measured between 3.00 and 4.00 p.m. using a rectal probe attached to a digital thermometer (BAT-12 Microprobe Thermometer, Physitemp, Clifton, NJ).

Histology

Interscapular BAT and gonadal WAT were removed and fixed in 4% paraformaldehyde, dehydrated in 70% EtOH and embedded in paraffin. Haematoxylin and eosin (H&E) staining was done using standard protocols. The area of intracellular lipid vacuoles in BAT was quantified using Image J (NIH, US).

Quantification of TG content in BAT

Lipids were extracted from BAT following a modified protocol from Bligh and Dyer (14). BAT samples (~50 mg) were homogenized in 10 µL of ice-cold CH_3OH per mg tissue. Lipids were extracted into an organic phase by addition of 1800 µL of $CH_3OH:CHCl_3$ (1:3 v/v) to 45 µL homogenate and subsequent centrifugation. The lower organic phase was evaporated, lipids were resuspended in 2% Triton X-100 and TG content was assayed (see above). BAT lipids were reported per mg protein (Pierce BCA Protein Assay Kit).

Isolation of stromal vascular fraction and flow cytometry

Gonadal WAT was removed, rinsed in PBS and minced. Tissues were digested in a collagenase mixture (DMEM with 20 mM HEPES, Collagenase XI and Collagenase I, Sigma) for 45 min at 37°C and passed through a 70-µm nylon mesh. The suspension was centrifuged (6 min, 1,250 rpm) and the pelleted stromal vascular fraction (SVF) was resuspended in FACS buffer. Fc blocking (CD16/32 antibody) was performed prior to a 30 min staining with fluorescently labeled primary antibodies for CD45, CD11b, Ly6G, F4/80, CD11c, CD206, Gr-1, CD19, CD3, CD4, CD8, CD25 and FoxP3 (BioLegend, e-Bioscience or BD). SVF was analyzed by flow cytometry with a BD FacsCANTO II flow cytometer and FlowJo software.

Analysis of DNA content

DNA content in gonadal WAT samples was quantified as previously described (15).

Culture and differentiation of white and brown adipocytes

3T3-L1 (American Type Culture Collection, Manassas, VA) and T37i cells (16, 17) were cultured and differentiated as described before. Differentiated cells were treated with salsalate (SML0070, Sigma), sodium salicylate (S2007, Sigma), AICA riboside (AICAR; ab120358, Abcam), noradrenalin (A7257, Sigma), CL316243 (Tocris Bioscience, Bristol, UK) or vehicle (DMSO) for 15 min or 8 h. H89 (H-5239, LC Laboratories) was added 1 h before initiation of salsalate treatment. Supernatant was collected for determination of glycerol concentration (Instruchemie, Delfzijl) and cells were harvested for RNA or protein analysis as described below.

Oxygen consumption measurements

A Seahorse Bioscience XF96 extracellular flux analyzer (Seahorse Biosciences, North Billerica, MA) was used to measure oxygen consumption rate (OCR) in differentiated T37i cells. On day 8 of differentiation, cells were trypsinized and seeded in a 96-well Seahorse assay plate. The next day, the ATP synthase inhibitor oligomycin, vehicle, salsalate and

Table 1: *Primary antibodies for Western blot.*

Primary antibody	Residue	Supplier	Reference	Dilution
ACC	-	Cell Signaling	#3662	1:1000
pACC	Ser79	Cell Signaling	#3661	1:1000
AMPKα	-	Cell Signaling	#2532	1:1000
pAMPKα	Thr172	Cell Signaling	#2535	1:1000
pHSL	Ser563	Cell Signaling	#4139	1:1000
pHSL	Ser565	Cell Signaling	#4137	1:1000
PKA substrates	Ser/Thr	Cell Signaling	#9621	1:1000
UCP1	-	Sigma	U6382	1:5000
α/β Tubulin	-	Cell Signaling	#2148	1:1000

5

Table 2: *Primer sequences of forward and reverse primers (5′ → 3′).*

Gene	Forward primer	Reverse Primer
36b4	GGACCCGAGAAGACCTCCTT	GCACATCACTCAGAATTTCAATGG
Acc1	AACGTGCAATCCGATTTGTT	GAGCAGTTCTGGGAGTTTCG
Acc2	AGATGGCCGATCAGTACGTC	GGGGACCTAGGAAAGCAATC
Adrb3	TGAAACAGCAGACAGGGACA	AGTCTGTCAGCTTCCCTCCA
Cd36	GCAAAGAACAGCAGCAAAATC	CAGTGAAGGCTCAAAGATGG
Cpt1a	AGGAGACAAGAACCCCAACA	AAGGAATGCAGGTCCACATC
Elovl3	TGTTGGCCAGACCTACATGA	ATCCGTGTAGATGGCAAAGC
F4/80	CTTTGGCTATGGGCTTCCAGTC	GCAAGGAGGACAGAGTTTATCGTG
Fasn	CACAGGCATCAATGTCAACC	TTTGGGAAGTCCTCAGCAAC
Fizz1	CCTGCCCTGCTGGGATGACT	GGGCAGTGGTCCAGTCAACGA
Mcp1	GCATCTGCCCTAAGGTCTTCA	TTCACTGTCACACTGGTCACTCCTA
Nos2	TCCTGGACATTACGACCCCT	CTCTGAGGGCTGACACAAGG
Ppargc1α	TGCTAGCGGTTCTCACAGAG	AGTGCTAAGACCGCTGCATT
Pparα	CAACCCGCCTTTTGTCATAC	CCTCTGCCTCTTTGTCTTCG
Scd1	GCTCTACACCTGCCTCTTCGGGAT	TCCAGAGGCGATGAGCCCCG
Srebp1c	CTGGCTGAGGCGGGATGA	TACGGGCCACAAGAAGTAGA
Ucp1	TCAGGATTGGCCTCTACGAC	TGCATTCTGACCTTCACGAC
Ym1	ACAATTAGTACTGGCCCACCAGGAA	TCCTTGAGCCACTGAGCCTTCA
β2m	TGACCGGCTTGTATGCTATC	CAGTGTGAGCCAGGATATA

CL316243 were preloaded in the reagent delivery chambers and pneumatically injected into the wells. Oligomycin was injected to a final concentration of 1.5 μM and the OCR was measured 3 times after mixing. Then, vehicle (0.1% DMSO), salsalate and/or CL316243 were injected and the OCR was measured 6 times in 30 minutes. All OCR measurements were normalized to cell count using Cyquant (Invitrogen).

Western blot analysis

Pieces of snap-frozen mouse tissues (approx. 50 mg) or T37i cells (grown in 3.8 cm^2 wells) were lysed, protein was isolated and Western blots were performed as previously described (11). Primary antibodies and dilutions are listed in **Table 1**. Protein content was corrected for a control mix on each blot and for the housekeeping protein tubulin.

RNA purification and qRT-PCR

RNA was extracted from snap-frozen mouse tissues (approx. 25 mg) or T37i cells (grown in 3.8 cm^2 wells) using Tripure RNA Isolation reagent (Roche). Total RNA (1-2 μg) was reverse transcribed using Moloney Murine Leukemia Virus (M-MLV) Reverse Transcriptase (Sigma) for qRT-PCR to produce cDNA. mRNA expression was normalized to *β2-microglobulin* (*β2m*) and *36b4* mRNA content and expressed as fold change compared to control mice using the ∆∆CT method. The primers sequences used are listed in **Table 2**.

Statistical analysis

All data are expressed as mean ± SEM, unless stated otherwise. Groups were compared with a two-tailed unpaired Student's test and considered statistically significant if $p < 0.05$.

RESULTS

Salsalate prevents high fat diet-induced obesity

To investigate the effect of salsalate on the development of obesity, male E3L.CETP mice were fed an HFD with or without salsalate for 12 weeks (*i.e.* progression study). Salsalate prevented the HFD-induced increase in body mass seen in the control group (-80%, 1.6±2.6 vs. 7.9±5.5 g, $p < 0.01$; **Fig. 1A**), which was due to a decreased gain in fat mass (-60%, 3.1±2.4 vs. 7.8±4.2, $p < 0.05$; **Fig. 1B**) rather than lean mass (**Fig. 1C**). Although salsalate persistently prevented mice from gaining fat mass throughout the treatment period, salsalate decreased food intake only during the first three days (**Fig. 1D**).

Salsalate prevents high fat diet-induced deterioration of glucose and triglyceride metabolism

Next, we assessed whether salsalate protects mice from developing HFD-induced glucose intolerance and dyslipidemia. Although salsalate did not affect fasting glucose levels (**Fig. 2A**), it reduced insulin levels after 4 weeks (-41%, $p < 0.05$), 8 weeks (-47%, p=0.07) and 12 weeks (-67%, $p < 0.05$; **Fig. 2B**) of treatment. In addition, salsalate improved glucose

A Control / Salsalate — Body weight (g) vs Time (weeks)

B Fat mass (g) vs Time (weeks)

C Lean mass (g) vs Time (weeks)

D Food intake (g/24h) vs Time (weeks)
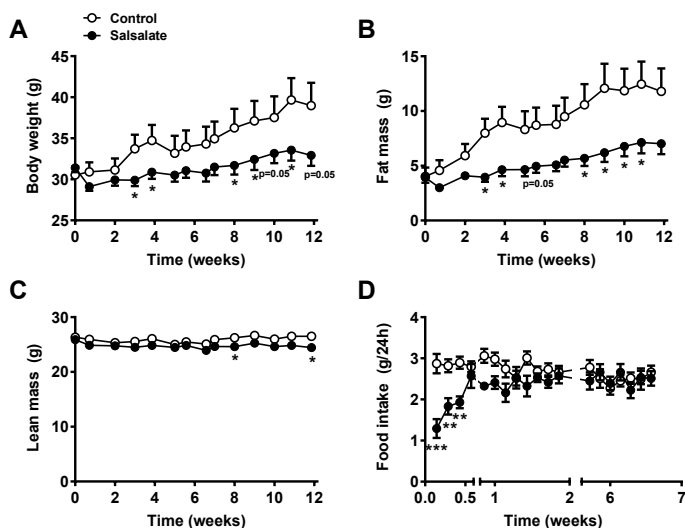
Figure 1. Salsalate prevents obesity and fat mass accumulation in E3L.CETP mice fed a high fat diet.
*10-week old male E3L.CETP mice were fed a high fat diet (HFD) without (open circles) or with (closed circles) salsalate for 12 weeks (A-D). Body weight (A), fat mass (B) and lean mass (C) were monitored throughout the experiment. Food intake was measured daily in the first two weeks and in the 6th week of the experiment (D). Values represent means ± SEM (n=9-10). * p<0.05, ** p<0.01, *** p<0.001 vs control.*

tolerance (**Fig. 2C**), as evidenced by a reduction of the area under the curve of glucose concentrations during an ivGTT (AUC -25%, p<0.05; **Fig. 2D**). Salsalate did not affect plasma TC levels **(Fig. 2E)** throughout the treatment period but decreased plasma TG levels at 8 weeks (-43%, p<0.01) and 12 weeks (-47%, p<0.05; **Fig. 2F**).

To elucidate which metabolic organs were involved in the TG-lowering effect of salsalate, the tissue-specific uptake of FA derived from intravenously injected [³H]TO-labeled lipoprotein-like emulsion particles was determined. Salsalate tended to increase the uptake of [³H]TO-derived activity by dorsocervical BAT (dcBAT), although significance was not reached, probably due to the substantial interindividual variation (**Fig. 2G**).

Salsalate reverses high fat diet-induced obesity and improves glucose and triglyceride metabolism

We investigated the potential of salsalate to reverse diet-induced obesity (DIO) in E3L.CETP mice (regression study). In this setting, salsalate lowered body weight (**Fig. 3A**) mainly due to a reduction in fat mass (**Fig. 3B**). Furthermore, salsalate reduced fasting glucose (-30%, p<0.01; **Fig. 3C**) and TG levels (-46%, p<0.05; **Fig. 3D**). Salsalate increased the uptake of [³H]TO-derived activity predominantly by iBAT (+156%, p<0.01) and dcBAT (+102%, p<0.05) and to some extent by the liver (+38%, p<0.01) (**Fig. 3E**). These data suggest that salsalate
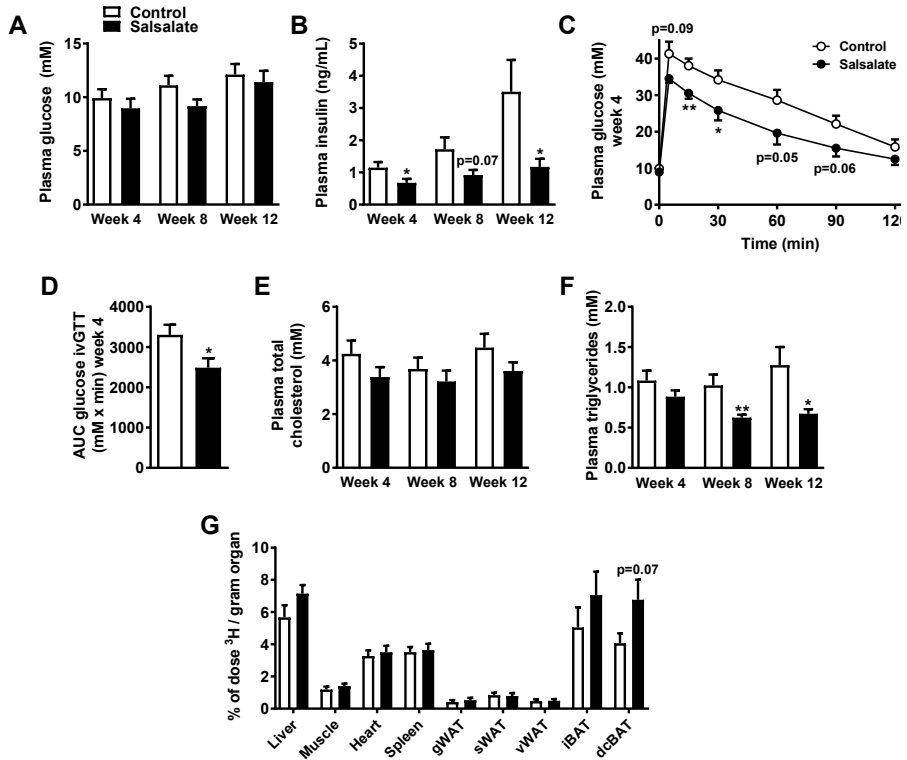
Figure 2. Salsalate prevents high fat diet-induced deterioration of glucose and triglyceride metabolism in E3L.CETP mice fed a high fat diet. *10-week old male E3L.CETP mice were fed a high fat diet (HFD) without (open bars/circles) or with (closed bars/circles) salsalate for 12 weeks (A-G). Blood samples from 6 h-fasted mice were collected by tail vein bleeding at different time points and plasma glucose (A), insulin (B), total cholesterol (E) and triglyceride (F) levels were determined. After 4 weeks, 6 h-fasted mice were injected i.v. with glucose and additional blood samples were taken at 5, 15, 30, 60, 90 and 120 min after injection (C-D). A clearance experiment was performed in which 6 h-fasted mice were i.v. injected with [³H] TO-labeled lipoprotein-like emulsion particles. After 15 min, mice were sacrificed and uptake of [³H]TO-derived activity was determined in the organs (G). AUC = area under the curve. Values represent means ± SEM (n=9-10). * p<0.05, ** p<0.01 vs control. sWAT, subcutaneous white adipose tissue; vWAT, visceral white adipose tissue.*

activates BAT, which is further supported by the observation that rectal temperature was raised (+0.5°C, p<0.05; **Fig. 3F**) upon salsalate treatment. Moreover, salsalate reduced interscapular BAT weight (-50%, p<0.01; **Fig. 3G**), indicating reduced fat accumulation within the tissue. Indeed, lipid droplet content was lower (**Fig. 3H, I, J**), pointing to higher intracellular lipolysis (18).
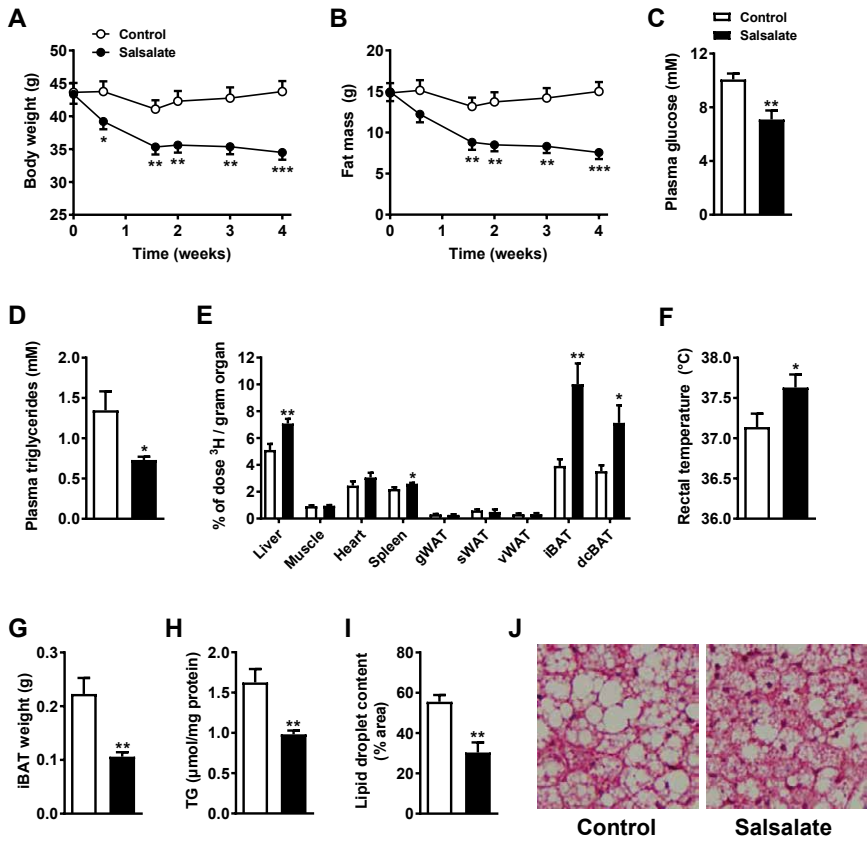
Figure 3. Salsalate reverses high fat diet-induced obesity and deterioration of glucose and triglyceride metabolism and enhances lipoprotein-TG derived fatty acid uptake by liver and brown adipose tissue in E3L.CETP mice fed a high fat diet. *10-week old male E3L.CETP mice were fed an HFD for 12 weeks to render them obese and subsequently fed an HFD without (open bars/circles) or with (closed bars/circles) salsalate for 4 weeks (A-I). Body weight (A) and fat mass (B) were monitored throughout the treatment period. After the treatment period, blood samples from 6 h-fasted mice were collected by tail vein bleeding and plasma glucose (C) and triglyceride (D) levels were determined. A clearance experiment was performed in which 6 h-fasted mice were i.v. injected with [³H]TO-labeled lipoprotein-like emulsion particles. After 15 min, mice were sacrificed and uptake of [³H]TO-derived activity was determined in the organs (E). Rectal temperature was determined after 4 weeks of treatment (F). Upon sacrifice, interscapular brown adipose tissue (iBAT) was collected and weighed (G). Lipids were extracted from BAT and TG content was measured (H). Haematoxylin and Eosin (H&E) staining of BAT sections was performed and relative content of lipid vacuoles in BAT tissue sections were quantified (I), representative pictures are shown (J). Values represent means ± SEM (n=9-10). * p<0.05, ** p<0.01, *** p<0.001 vs control. sWAT, subcutaneous white adipose tissue; vWAT, visceral white adipose tissue.*

Salsalate prevents body weight gain and activates brown adipose tissue irrespective of the transgenic background

To exclude that the effects of salsalate were specific to the E3L.CETP transgenic model, male WT mice were fed an HFD with or without salsalate for 4 weeks. We confirmed that salsalate treatment had similar effects on body weight, body composition and food intake (**Suppl. Fig. 1A-D**). Prevention of adiposity despite equal food intake suggests that either physical activity or energy expenditure is enhanced. Indeed, salsalate increased EE during the dark phase (+10%, p<0.05; **Suppl. Fig. 1E**). This was especially due to a higher glucose oxidation (+29%, p<0.001; **Suppl. Fig. 1F**), whereas fat oxidation did not differ (**Suppl. Fig. 1G**). Accordingly, respiratory exchange ratio (RER) was higher during the dark phase (**Suppl. Fig. 1H**). Physical activity was not affected (**Suppl. Fig. 1I**), suggesting that the energetic loss is mainly explained by increased energy expenditure.

Comparable to our findings in E3L.CETP mice, salsalate reduced plasma insulin levels (**Suppl. Fig. 2A**) and improved glucose tolerance (**Suppl. Fig. 2B-D**). This was probably achieved via an insulin-independent mechanism, as no differences in glucose levels were found between the treatment groups upon an insulin challenge (**Suppl. Fig. 2E**). Of note, AMPK phosphorylation in muscle was enhanced upon salsalate treatment (+43%, p<0.05), as was phosphorylation of its downstream target ACC (+75%, p<0.05; **Suppl. Fig. 2**F).

In WT mice, salsalate also reduced plasma triglyceride levels (**Suppl. Fig. 2G**). This was not due to lowered intestinal TG absorption, since salsalate-treated mice did not have significantly lower plasma TG levels in response to an oral olive oil gavage (**Suppl. Fig. 2H**) and FFA content in feces collected in the third week of treatment was unaltered (**Suppl. Fig. 2I**). Neither VLDL-TG (**Suppl. Fig. 2J**) nor VLDL[^{35}S]apoB production (**Suppl. Fig. 2K**) were affected upon 4 weeks of salsalate treatment, further supporting a role for BAT in the TG-lowering effect of salsalate. Indeed, comparable to the effects seen in E3L.CETP mice, salsalate reduced interscapular BAT weight (-42%, p<0.001; **Fig. 4A**), lowered lipid content (-29%, p<0.05**; Fig. 4B, C**) and tended to increase the uptake of [^{3}H]TO-derived activity by the BAT depots (**Suppl. Fig. 3C**).

Under thermoneutral conditions, salsalate still prevented the development of high fat diet-induced obesity (**Suppl. Fig. 3A,B**). However, thermoneutrality ablated the salsalate-induced tendency towards an increased TG uptake by BAT (**Suppl. Fig. 3C**) and prevented the reduction in plasma TG levels seen at room temperature (**Suppl. Fig. 3D**). Thus, noradrenergic input (*i.e.* slight cold sensing at room temperature) seems necessary to bring about salsalate-induced TG uptake by BAT.

To further elucidate the mechanisms by which salsalate activates BAT and regulates intracellular lipolysis, we measured mRNA and (phosphorylated) protein levels in BAT of mice housed at 21°C upon treatment. Salsalate did not affect *Ucp1* mRNA expression (data not shown) nor UCP1 protein content (**Fig. 4D**). Salsalate tended to increase the PKA-mediated lipolysis-stimulating phosphorylation of HSL on the Ser563 residue (+77%, p=0.06) but not AMPK-mediated phosphorylation of HSL on the Ser565 residue (19) (**Fig. 4D**), suggesting increased PKA signaling in BAT. Despite the fact that phosphorylation of ACC, the downstream target of AMPK, was increased, we did not observe significant differences in AMPK expression or phosphorylation (**Fig. 4D**).

5
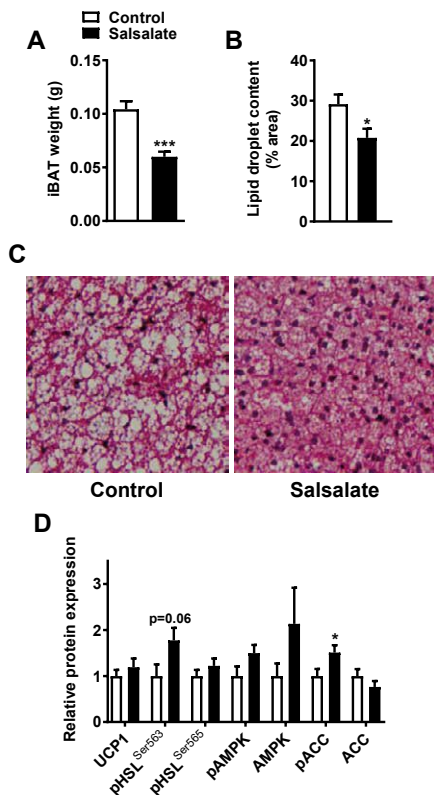
Figure 4. Salsalate activates brown adipose tissue in wild type mice fed a high fat diet. *10-week old male C57Bl/6J mice were fed a high fat diet (HFD) without (open bars) or with (closed bars) salsalate for 4 weeks. Upon sacrifice, interscapular brown adipose tissue (iBAT) was collected and weighed (A). Haematoxylin and Eosin (H&E) staining of BAT sections was performed and relative content of lipid vacuoles in BAT tissue sections were quantified (B), representative pictures are shown (C). Protein content was determined by Western blot (D). Values represent means ± SEM (n=6-8). * p<0.05, *** p<0.001 vs control.*

Salsalate reduces WAT cell size and lowers inflammation in wild type mice fed a high fat diet

Since salsalate massively reduced fat mass, we assessed the phenotype of WAT in more detail. In line with the decreased total fat mass (**Figs. 1B, 3B, S1B**), salsalate reduced the weight of the gonadal WAT (gWAT) fat pad (-49%, p<0.001; **Fig. 5A**). Histological analysis showed that salsalate reduced adipocyte size (-44%, p<0.01; **Figs. 5B, C**), while total cell number, as assessed by DNA content, did not differ (data not shown).

Since salsalate is an anti-inflammatory compound, we investigated the immune cell composition of gWAT by flow cytometry. We did not observe a change in the percentage of CD45+ cells within the stromal vascular fraction (SVF), nor in relative monocyte, macrophage, granulocyte, T- and B-cell content (data not shown). However, we found less pro-inflammatory (CD11c+) M1 macrophages and more anti-inflammatory (CD206+) M2 macrophages within the F4/80+ fraction (**Fig. 5D, E**). Accordingly, salsalate decreased *F4/80* and *Mcp1* mRNA expression in gWAT (**Fig. 5F**), confirming fewer pro-inflammatory macrophages and less recruitment of pro-inflammatory macrophages (20, 21) in gWAT
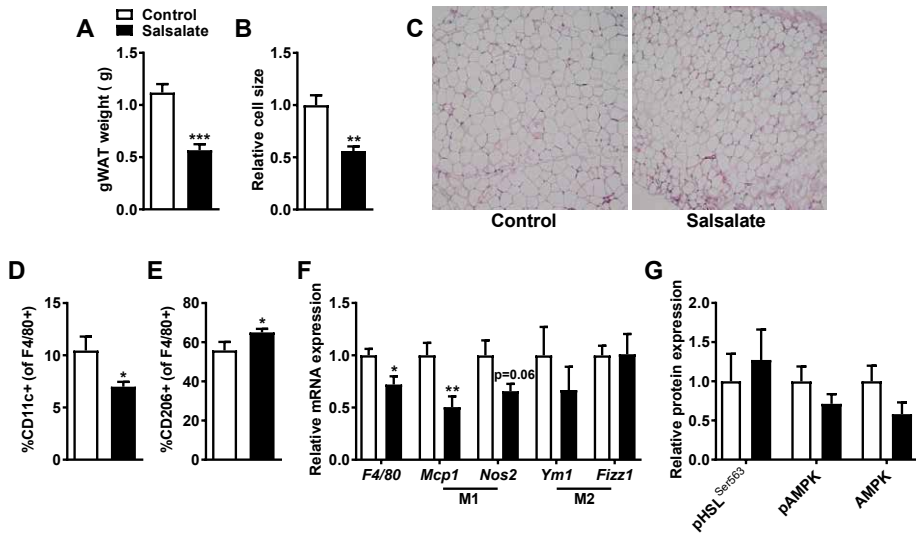
Figure 5. Salsalate reduces white adipocyte cell size and lowers inflammation in WAT of wild type mice fed a high fat diet. *10-week old male wild type mice were fed a high fat diet (HFD) without (open bars) or with (closed bars) salsalate for 4 weeks. Gonadal white adipose tissue (gWAT) was collected and weighed (A). Haematoxylin and Eosin (H&E) staining of gWAT sections was performed and relative cell size of white adipocytes in gWAT tissue sections was quantified (B), representative pictures are shown (C). Percentage of macrophages (%CD11b⁺Ly6G⁻F4/80⁺) of CD45⁺ cells in stromal vascular fraction (SVF) of gWAT were determined by flow cytometry. Within the macrophage fraction, pro-inflammatory M1 macrophages (CD11c⁺) (D) and anti-inflammatory M2 macrophages (CD206⁺) (E) were measured. mRNA expression in of inflammatory markers (F) in gWAT was determined by qRT-PCR. Protein content was determined by Western blot (G). Values represent means ± SEM (n=6-8). * p<0.05, ** p<0.01, *** p<0.001 vs control.*

of salsalate treated mice. Thus, besides preventing fat accumulation in WAT, salsalate prevented HFD-induced skewing of macrophages towards a pro-inflammatory phenotype.

Next, we studied whether the diminished adipocyte size following salsalate treatment could be the result of increased TG lipolysis. Phosphorylation levels of HSL on the Ser563 residue (phosphorylated by PKA; **Fig. 5G**) in gWAT did not differ, nor did plasma free fatty acid (FFA) levels (data not shown). Moreover, *in vitro* stimulation of 3T3-L1 cells with salsalate did not influence Ser563-HSL phosphorylation (**Suppl. Fig. 4A**) and even repressed the glycerol concentration in the supernatant (**Suppl. Fig. 4B**). Of the oxidation genes we measured in gWAT, only *Acc2* was upregulated upon salsalate treatment, suggesting slightly enhanced oxidation in gWAT (**Suppl. Fig. 5A**). The phosphorylation state nor the expression of AMPK was altered (**Fig. 5G**) in gWAT. We also investigated markers of lipogenesis in gWAT, but only found an upregulation of *Acc1* expression (**Suppl. Fig. 5B**). Collectively, these data indicate that it is unlikely that lipolysis, oxidation or lipogenesis in WAT is the primary mechanism responsible for the prevention of fat mass accumulation following salsalate treatment.

Salsalate directly activates brown adipocytes in vitro

Since our collective data suggested that the improvement in triglyceride metabolism by salsalate could be due to activation of BAT, we investigated whether salsalate directly activates brown adipocytes and which intracellular mechanism(s) are involved. Strikingly, treatment of differentiated T37i adipocytes with salsalate increased uncoupled respiration (**Fig. 6A**). In line with this, increasing concentrations of salsalate resulted in a dose-dependent increase in *Ucp1* expression (up to +227%, p<0.001; **Fig. 6B**) as well as glycerol release (up to +92%, p<0.001; **Fig. 6C**). Accordingly, salsalate decreased lipid content in the cells, as shown by Nile Red staining (-18%, p<0.05; **Suppl. Fig. 6A**). Decreased *de novo* lipogenesis found upon treatment with salsalate (**Suppl. Fig. 6B**) could also contribute to this finding. Besides *Ucp1*, salsalate upregulated several other genes involved in BAT function (**Fig. 6D**).

The majority, but not all, of orally administered salsalate is metabolized to salicylate *in vivo*, resulting in plasma concentrations of 1-3 mM (1). Like salsalate, salicylate (1 mM) enhanced *Ucp1* expression in T37i brown adipocytes (+53%, p<0.01, **Suppl. Fig. 6C**). Salicylate (1 and 3 mM) also enhanced expression of *Pparα* (up to +304%, p<0.01) and its target gene (22) *Elovl3* (up to +224%, p<0.05; **Suppl. Fig. 6C**), while the higher dosage of salicylate (3 mM) enhanced glycerol release (+80%, p<0.01; **Suppl. Fig. 6D**).

Since salsalate is known to directly activate AMPK (1), we investigated this in brown adipocytes. However, salsalate did not increase phosphorylation of AMPK (**Fig. 6E**) nor ACC (data not shown) after stimulation for 15 min, 1 h or 8 h (data not shown). We therefore searched for another route by which salsalate may activate BAT.

As both AMPK and PKA regulate lipolysis in BAT by phosphorylation of HSL (23, 24), and our *in vivo* data indicated PKA-mediated phosphorylation of HSL on the Ser563 residue, we investigated whether salsalate activates the PKA-HSL route in brown adipocytes. Salsalate enhanced phosphorylation of the 30 kDa PKA substrate in brown adipocytes

Figure 6 (right page). Salsalate directly activates T37i brown adipocytes. *T37i cells were cultured and differentiated into mature brown adipocytes. Cells were treated with salsalate (300 μM) after addition of oligomycin and oxygen consumption rate was directly measured with an extracellular flux analyzer. Values represent means ± SEM of 11-13 independent wells (A). Cells were treated with increasing concentrations of salsalate for 8 h and Ucp1 mRNA expression (B) and glycerol release (C) were determined. Cells were treated with salsalate (300 μM) for 8 h and mRNA expression was determined (D). Cells were treated with salsalate (300 μM) or AICAR for 15 min and protein content was determined (E). Cells were treated with salsalate (300 μM) for 8 h and protein content was determined (F). Cells were treated with salsalate (300 μM) in the presence of H89 for 8 h and Ser563-HSL phosphorylation (G), Ucp1 mRNA expression (H) and glycerol release (I) were determined. Cells were treated with salsalate (300 μM) and CL316243 (10μM) after addition of oligomycin and oxygen consumption rate was directly measured with an extracellular flux analyzer. Values represent means ± SEM of 11-13 independent wells (J). Protein content was determined by Western Blot and mRNA expression was determined by qRT-PCR. OCR = oxygen consumption rate, OM = oligomycin. Values represent means ± SD of 3-6 independent sets of RNA, supernatant or protein. * p<0.05, ** p<0.01, *** p<0.001 vs control or CL316243, # p<0.05, ## p<0.01 vs salsalate.*
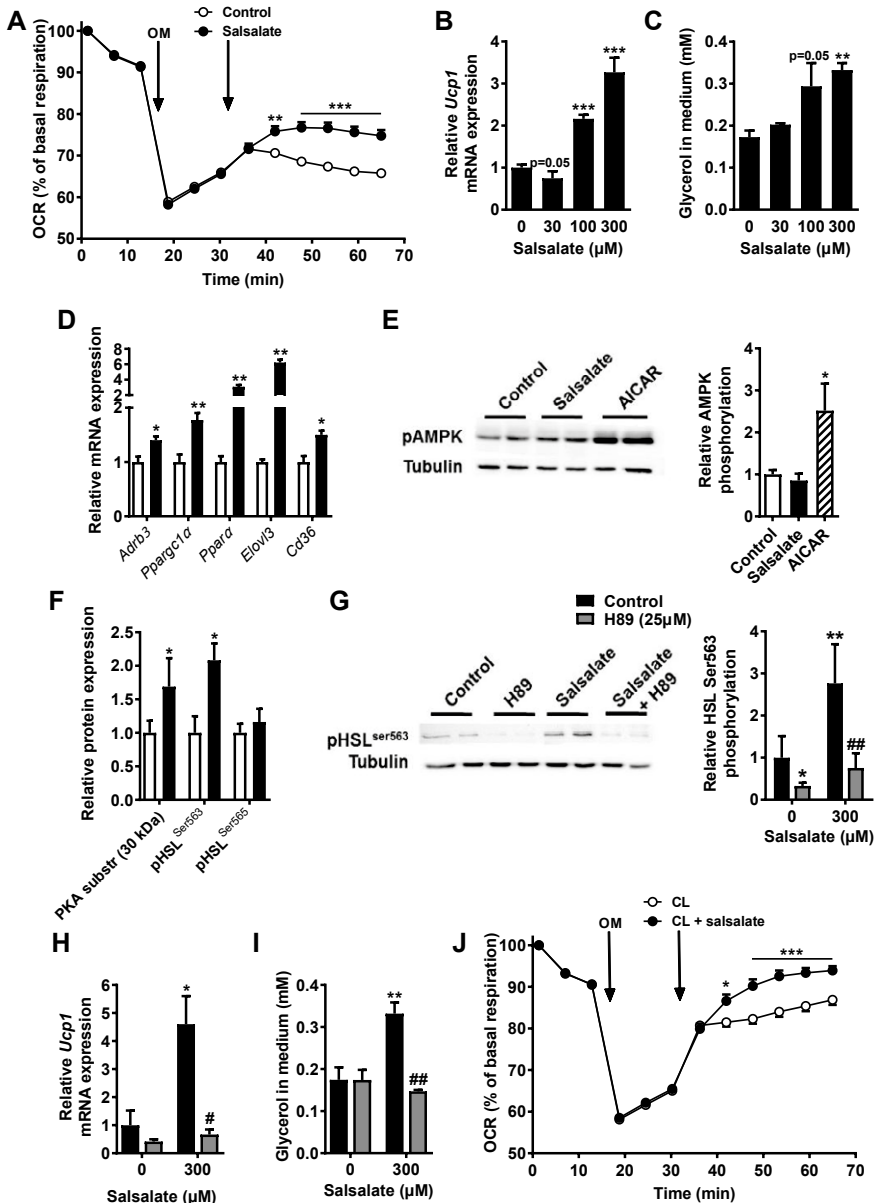
after 8 h of stimulation (+69%, p<0.05) and increased phosphorylation of HSL on Ser563, the PKA phosphorylation site of this lipolytic enzyme (+108%, p<0.05; **Fig. 6F**), while phosphorylation of HSL on Ser565, the AMPK phosphorylation site, was unaffected. To investigate the involvement of the PKA pathway for BAT activation by salsalate, we stimulated brown adipocytes with salsalate in the presence of the PKA inhibitor H89 (25 µM). H89 blunted the salsalate-induced Ser563-HSL phosphorylation (**Fig. 6G**), upregulation of *Ucp1* expression (**Fig. 6H**) and glycerol release (**Fig. 6I**), indicating that the PKA pathway is required for brown adipocyte activation by salsalate. These data are consistent with our observation that salsalate only increased TG uptake by BAT *in vivo* when mice are housed at room temperature, *i.e.* when adrenergic signalling is present.

Since PKA is a downstream target of β-adrenergic signalling, we investigated whether salsalate acts in synergism with β-adrenergic stimulation in T37i brown adipocytes. Although salsalate in combination with the β3-agonist CL316243 enhanced uncoupled respiration as compared to CL316243 alone, no synergistic effect was found (**Fig. 6J**). Furthermore, salsalate and NA showed an additive effect on *Ucp1* expression (**Suppl. Fig. 6E**). This suggests that increased β-adrenergic signalling is not required for the effects of salsalate, but since inhibition of PKA abolishes the effects of salsalate, basal β-adrenergic signalling is. Taken together, both our *in vitro* and *in vivo* data point to an interplay between β-adrenergic and salsalate-induced signalling.

5

DISCUSSION

Previous studies in humans and animals have shown that salsalate has beneficial metabolic effects by improving glucose tolerance and lowering plasma triglycerides (3, 4). The mechanisms responsible for these changes, however, remained unclear. In the present study, we show that chronic treatment of E3L.CETP and WT mice with salsalate recapitulates these beneficial metabolic effects and in addition prevents and reduces body weight gain, mainly by lowering fat mass accumulation. Moreover, we provide evidence from both *in vivo* and *in vitro* studies that salsalate activates BAT, an important player in energy metabolism. To the best of our knowledge, this is the first study reporting that activation of BAT may, at least partly, underlie the beneficial metabolic effects of salsalate.

The finding that salsalate prevented body weight gain and fat mass accumulation accompanied by a reduced white adipocyte size has been reported before in rats (25). Lower fat accumulation may be the consequence of a lower food intake or higher energy expenditure. Although we noticed that food intake was transiently reduced upon salsalate treatment in mice, the preventive effect on fat mass accumulation persisted throughout the studies. We found increased energy expenditure in our study, which is in line with studies in humans showing that salsalate treatment increases energy expenditure by +18% (2, 5), suggesting that the long term inhibiting effects of salsalate on body weight gain are caused by increased resting energy expenditure.

In our study, salsalate improved glucose tolerance via an insulin-independent mechanism and lowered plasma glucose and triglyceride levels, which is in line with findings in humans (2, 3). Recently, it has been shown that salicylate acutely stimulates phosphorylation of AMPK and simultaneously increases glucose transport, independent of insulin, into muscle in rat skeletal muscles *ex vivo* (26). Correspondingly, in our study, AMPK phosphorylation in muscle was enhanced upon salsalate treatment, as was phosphorylation of its downstream target ACC. Taken together, our data suggest that salsalate improves glucose tolerance by enhancing glucose oxidation and glucose uptake via an insulin-independent pathway. BAT, a metabolically active tissue that contributes to energy metabolism by uncoupling the electron transport chain from ATP synthesis through uncoupling protein-1 (UCP1), also has a key role in systemic glucose homeostasis by enhancing glucose clearance (27, 28). Although we do not have evidence for the possibility that salsalate improves glucose tolerance through BAT activation, we did show that the TG-lowering effect of salsalate was due to higher uptake of lipoprotein-TG-derived FA by BAT as intestinal TG absorption and hepatic VLDL production were unaffected in our experimental settings. We provide strong evidence that BAT was activated upon salsalate treatment, since we found reduced intracellular lipid content and higher rectal temperature *in vivo*, and higher uncoupled respiration, upregulation of the expression of thermogenic markers *Ucp1* and *Elovl3* and increased glycerol release upon salsalate treatment *in vitro.*

Regarding the mechanism through which salsalate activates BAT, we found slightly increased phosphorylation of AMPK's downstream target ACC in BAT *in vivo*, but not of AMPK itself. In T37i brown adipocytes *in vitro*, phosphorylation statuses of AMPK and ACC

were also unaffected. Although a recent study by Hawley *et al.* (1) showed that salicylate activates AMPK in the liver, muscle and adipose tissue, they also observed that the potency of salicylate to improve fasting glucose and insulin, glucose tolerance and insulin resistance were retained in mice lacking the β1 subunit of AMPK, demonstrating that other pathways are more important than the AMPK-mediated beneficial metabolic effects of salicylates.

Our data point more profoundly towards activation of the PKA-HSL pathway in BAT. We found that salsalate increased Ser563-HSL phosphorylation in BAT *in vivo* and in brown adipocytes *in vitro*, which points to an increase of PKA-mediated lipolysis. Indeed, salsalate treatment enhanced glycerol release *in vitro* and reduced the intracellular lipid content in BAT *in vivo*. The enhanced intracellular release of FA results in increased availability of substrate for oxidation that can also induce allosteric activation of UCP1 (29), both resulting in enhanced uncoupling, which we also demonstrated in brown adipocytes *in vitro*. Importantly, the fact that PKA inhibition blunted the salsalate-induced Ser563-HSL phosphorylation, *Ucp1* expression and glycerol release *in vitro* supports a necessity for this pathway in brown adipocyte activation.

Besides improving metabolism, salsalate is an effective anti-inflammatory agent in the clinic. With the current knowledge of a profound link between obesity, inflammation and type 2 diabetes, we also investigated the effects of salsalate on the inflammatory state of WAT. In gWAT, salsalate lowered *Mcp1* expression, an attraction factor of pro-inflammatory M1 macrophages, and prevented HFD-induced skewing of macrophages towards this phenotype. Previous research showed that high concentrations of salicylates inhibit NF-κB activity *in vitro*, a key transcription factor that regulates inflammation (30). In obese humans, salsalate lowers the inflammatory state, with a 34% reduction in circulating levels of C-reactive protein and declined NF-κB activity in WAT (31, 32). This reduction in inflammation might contribute to the improved glucose metabolism upon salsalate.

Since it is becoming increasingly clear that BAT activation and subsequent elevation of energy expenditure can lower body fat mass in human adults (33), drugs that target BAT are of great interest in the combat against obesity. Although some human studies suggested that salsalate does not affect body weight (4, 34), effects on fat mass have not been reported. As mice have a relatively larger amount of BAT compared to humans (35, 36), activation of BAT by salsalate in humans might translate into improved fat distribution, glucose and lipid metabolism without substantially affecting total body weight.

In conclusion, we show that salsalate exerts beneficial metabolic effects by directly activating BAT through modulation of the PKA pathway in BAT (**Fig. 7**). Further studies are warranted to investigate whether salsalate activates BAT in humans, thereby preventing obesity and associated disorders.
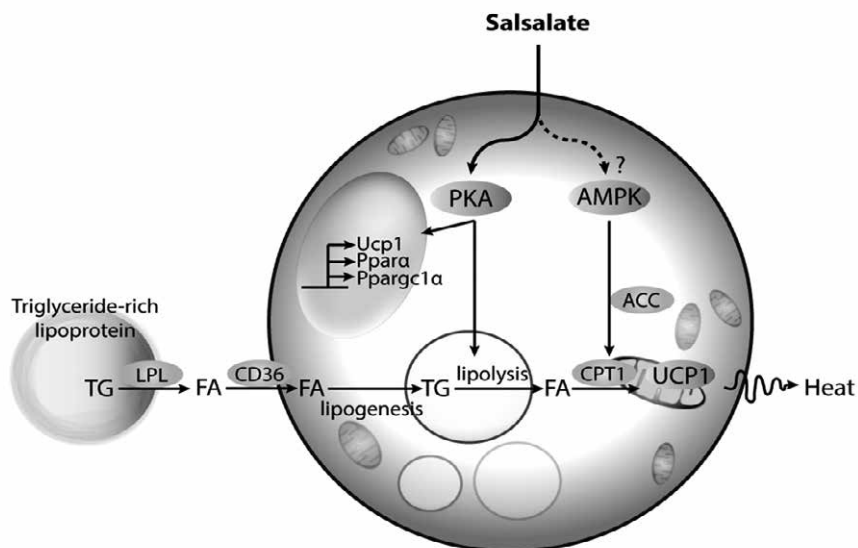
Figure 7. Proposed mechanism by which salsalate activates brown adipose tissue. *Salsalate improves intracellular lipolytic capacity of the brown adipocyte by increasing PKA-mediated HSL phosphorylation, thereby enhancing FA release from TG stored in lipid droplets. This leads to activation of UCP1, which uncouples ATP synthesis. Moreover, salsalate results in enhanced expression of Pparα, Ppargc1α, and Ucp1, altogether resulting in increased activity and uncoupling of ATP synthesis in BAT. A reduction in intracellular lipid content and upregulation of Cd36 in BAT enhances uptake of TG-derived FA from the plasma by BAT. This eventually results in lowering of circulating lipids and reduction in fat mass.*

ACKNOWLEDGEMENTS

FUNDING

REFERENCES

1. Hawley SA, Fullerton MD, Ross FA, Schertzer JD, Chevtzoff C, Walker KJ, Peggie MW, Zibrova D, Green KA, Mustard KJ, Kemp BE, Sakamoto K, Steinberg GR, Hardie DG: The ancient drug salicylate directly activates AMP-activated protein kinase. Science (New York, NY) 2012;336:918-922

2. Goldfine AB, Silver R, Aldhahi W, Cai D, Tatro E, Lee J, Shoelson SE: Use of salsalate to target inflammation in the treatment of insulin resistance and type 2 diabetes. Clinical and translational science 2008;1:36-43

3. Rumore MM, Kim KS: Potential role of salicylates in type 2 diabetes. The Annals of pharmacotherapy 2010;44:1207-1221

4. Goldfine AB, Fonseca V, Jablonski KA, Pyle L, Staten MA, Shoelson SE: The effects of salsalate on glycemic control in patients with type 2 diabetes: a randomized trial. Annals of internal medicine 2010;152:346-357

5. Meex RC, Phielix E, Moonen-Kornips E, Schrauwen P, Hesselink MK: Stimulation of human whole-body energy expenditure by salsalate is fueled by higher lipid oxidation under fasting conditions and by higher oxidative glucose disposal under insulin-stimulated conditions. The Journal of clinical endocrinology and metabolism 2011;96:1415-1423

6. Fu ZQ, Yan S, Saleh A, Wang W, Ruble J, Oka N, Mohan R, Spoel SH, Tada Y, Zheng N, Dong X: NPR3 and NPR4 are receptors for the immune signal salicylic acid in plants. Nature 2012;486:228-232

7. de Haan W, van der Hoogt CC, Westerterp M, Hoekstra M, Dallinga-Thie GM, Princen HM, Romijn JA, Jukema JW, Havekes LM, Rensen PC: Atorvastatin increases HDL cholesterol by reducing CETP expression in cholesterol-fed APOE*3-Leiden.CETP mice. Atherosclerosis 2008;197:57-63

8. van der Hoogt CC, de Haan W, Westerterp M, Hoekstra M, Dallinga-Thie GM, Romijn JA, Princen HM, Jukema JW, Havekes LM, Rensen PC: Fenofibrate increases HDL-cholesterol by reducing cholesteryl ester transfer protein expression. Journal of lipid research 2007;48:1763-1771

9. Westerterp M, van der Hoogt CC, de Haan W, Offerman EH, Dallinga-Thie GM, Jukema JW, Havekes LM, Rensen PC: Cholesteryl ester transfer protein decreases high-density lipoprotein and severely aggravates atherosclerosis in APOE*3-Leiden mice. Arteriosclerosis, thrombosis, and vascular biology 2006;26:2552-2559

10. Coomans CP, Geerling JJ, van den Berg SA, van Diepen HC, Garcia-Tardon N, Thomas A, Schroder-van der Elst JP, Ouwens DM, Pijl H, Rensen PC, Havekes LM, Guigas B, Romijn JA: The insulin sensitizing effect of topiramate involves KATP channel activation in the central nervous system. British journal of pharmacology 2013;170:908-918

11. Boon MR, Kooijman S, van Dam AD, Pelgrom LR, Berbée JF, Visseren CA, van Aggele RC, van den Hoek AM, Sips HC, Lombes M, Havekes LM, Tamsma JT, Guigas B, Meijer OC, Jukema JW, Rensen PC: Peripheral cannabinoid 1 receptor blockade activates brown adipose tissue and diminishes dyslipidemia and obesity. FASEB journal : official publication of the Federation of American Societies for Experimental Biology 2014;28:5361-5375

12. Zambon A, Hashimoto SI, Brunzell JD: Analysis of techniques to obtain plasma for measurement of levels of free fatty acids. Journal of lipid research 1993;34:1021-1028

13. Rensen PC, van Dijk MC, Havenaar EC, Bijsterbosch MK, Kruijt JK, van Berkel TJ: Selective liver targeting of antivirals by
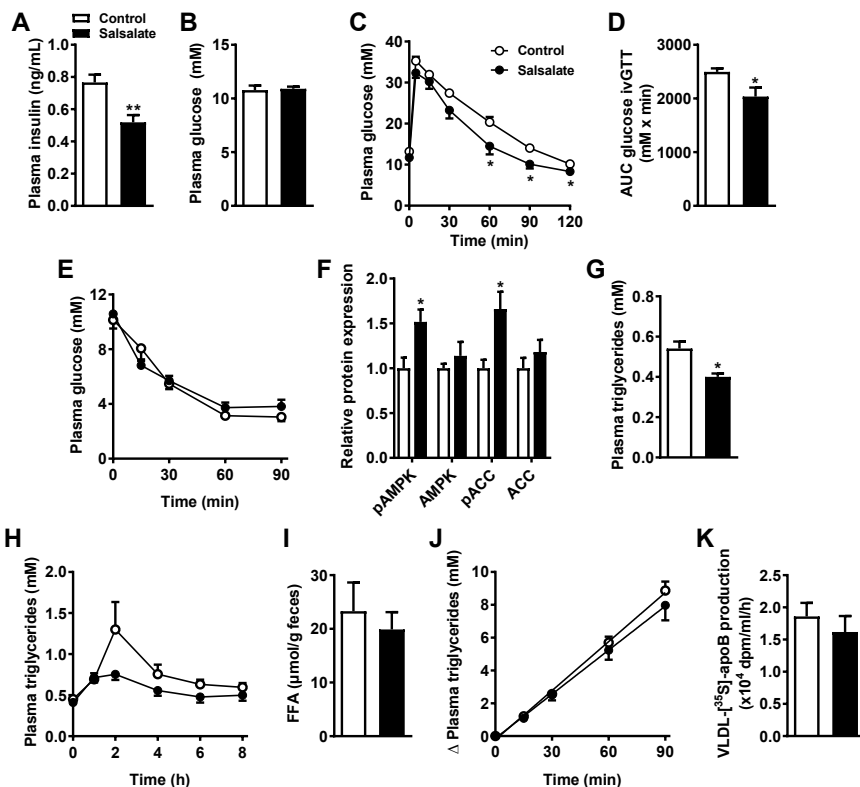
5

recombinant chylomicrons--a new therapeutic approach to hepatitis B. Nature medicine 1995;1:221-225

14. Bligh EG, Dyer WJ: A rapid method of total lipid extraction and purification. Canadian journal of biochemistry and physiology 1959;37:911-917

15. Cariou B, Postic C, Boudou P, Burcelin R, Kahn CR, Girard J, Burnol AF, Mauvais-Jarvis F: Cellular and molecular mechanisms of adipose tissue plasticity in muscle insulin receptor knockout mice. Endocrinology 2004;145:1926-1932

16. Zennaro MC, Le Menuet D, Viengchareun S, Walker F, Ricquier D, Lombes M: Hibernoma development in transgenic mice identifies brown adipose tissue as a novel target of aldosterone action. The Journal of clinical investigation 1998;101:1254-1260

17. van den Berghe N, Ouwens DM, Maassen JA, van Mackelenbergh MG, Sips HC, Krans HM: Activation of the Ras/mitogen-activated protein kinase signaling pathway alone is not sufficient to induce glucose uptake in 3T3-L1 adipocytes. Molecular and cellular biology 1994;14:2372-2377

18. Ortega-Molina A, Efeyan A, Lopez-Guadamillas E, Munoz-Martin M, Gomez-Lopez G, Canamero M, Mulero F, Pastor J, Martinez S, Romanos E, Mar Gonzalez-Barroso M, Rial E, Valverde AM, Bischoff JR, Serrano M: Pten positively regulates brown adipose function, energy expenditure, and longevity. Cell metabolism 2012;15:382-394

19. Watt MJ, Holmes AG, Pinnamaneni SK, Garnham AP, Steinberg GR, Kemp BE, Febbraio MA: Regulation of HSL serine phosphorylation in skeletal muscle and adipose tissue. American journal of physiology Endocrinology and metabolism 2006;290:E500-508

20. Kanda H, Tateya S, Tamori Y, Kotani K, Hiasa K, Kitazawa R, Kitazawa S, Miyachi H, Maeda S, Egashira K, Kasuga M: MCP-1 contributes to macrophage infiltration into adipose tissue,

insulin resistance, and hepatic steatosis in obesity. The Journal of clinical investigation 2006;116:1494-1505

21. Weisberg SP, McCann D, Desai M, Rosenbaum M, Leibel RL, Ferrante AW, Jr.: Obesity is associated with macrophage accumulation in adipose tissue. The Journal of clinical investigation 2003;112:1796-1808

22. Jakobsson A, Jorgensen JA, Jacobsson A: Differential regulation of fatty acid elongation enzymes in brown adipocytes implies a unique role for Elovl3 during increased fatty acid oxidation. American journal of physiology Endocrinology and metabolism 2005;289:E517-526

23. Geerling JJ, Boon MR, van der Zon GC, van den Berg SA, van den Hoek AM, Lombes M, Princen HM, Havekes LM, Rensen PC, Guigas B: Metformin lowers plasma triglycerides by promoting VLDL-triglyceride clearance by brown adipose tissue in mice. Diabetes 2014;63:880-891

24. Cannon B, Nedergaard J: Brown adipose tissue: function and physiological significance. Physiological reviews 2004;84:277-359

25. Cao Y, Dubois DC, Sun H, Almon RR, Jusko WJ: Modeling diabetes disease progression and salsalate intervention in Goto-Kakizaki rats. The Journal of pharmacology and experimental therapeutics 2011;339:896-904

26. Serizawa Y, Oshima R, Yoshida M, Sakon I, Kitani K, Goto A, Tsuda S, Hayashi T: Salicylate acutely stimulates 5'-AMP-activated protein kinase and insulin-independent glucose transport in rat skeletal muscles. Biochemical and biophysical research communications 2014;453:81-85

27. Stanford KI, Middelbeek RJ, Townsend KL, An D, Nygaard EB, Hitchcox KM, Markan KR, Nakano K, Hirshman MF, Tseng YH, Goodyear LJ: Brown adipose tissue regulates glucose homeostasis and insulin sensitivity. The Journal of clinical investigation 2013;123:215-223

5

28. Matsushita M, Yoneshiro T, Aita S, Kameya T, Sugie H, Saito M: Impact of brown adipose tissue on body fatness and glucose metabolism in healthy humans. International journal of obesity (2005) 2014;38:812-817

29. Fedorenko A, Lishko PV, Kirichok Y: Mechanism of fatty-acid-dependent UCP1 uncoupling in brown fat mitochondria. Cell 2012;151:400-413

30. Kopp E, Ghosh S: Inhibition of NF-kappa B by sodium salicylate and aspirin. Science (New York, NY) 1994;265:956-959

31. Goldfine AB, Fonseca V, Jablonski KA, Chen YD, Tipton L, Staten MA, Shoelson SE: Salicylate (salsalate) in patients with type 2 diabetes: a randomized trial. Annals of internal medicine 2013;159:1-12

32. Fleischman A, Shoelson SE, Bernier R, Goldfine AB: Salsalate improves glycemia and inflammatory parameters in obese young adults. Diabetes care 2008;31:289-294

33. Yoneshiro T, Aita S, Matsushita M, Kayahara T, Kameya T, Kawai Y, Iwanaga T, Saito M: Recruited brown adipose tissue as an antiobesity agent in humans. The Journal of clinical investigation 2013;123:3404-3408

34. Koska J, Ortega E, Bunt JC, Gasser A, Impson J, Hanson RL, Forbes J, de Courten B, Krakoff J: The effect of salsalate on insulin action and glucose tolerance in obese non-diabetic patients: results of a randomised double-blind placebo-controlled study. Diabetologia 2009;52:385-393

35. van Marken Lichtenbelt WD, Schrauwen P: Implications of nonshivering thermogenesis for energy balance regulation in humans. American journal of physiology Regulatory, integrative and comparative physiology 2011;301:R285-296

36. Vosselman MJ, van Marken Lichtenbelt WD, Schrauwen P: Energy dissipation in brown adipose tissue: from mice to men. Molecular and cellular endocrinology 2013;379:43-50

37. Van Klinken JB, van den Berg SA, Havekes LM, Willems Van Dijk K: Estimation of activity related energy expenditure and resting metabolic rate in freely moving mice from indirect calorimetry data. PloS one 2012;7:e36162

38. Redgrave TG, Roberts DC, West CE: Separation of plasma lipoproteins by density-gradient ultracentrifugation. Analytical biochemistry 1975;65:42-49

5

5
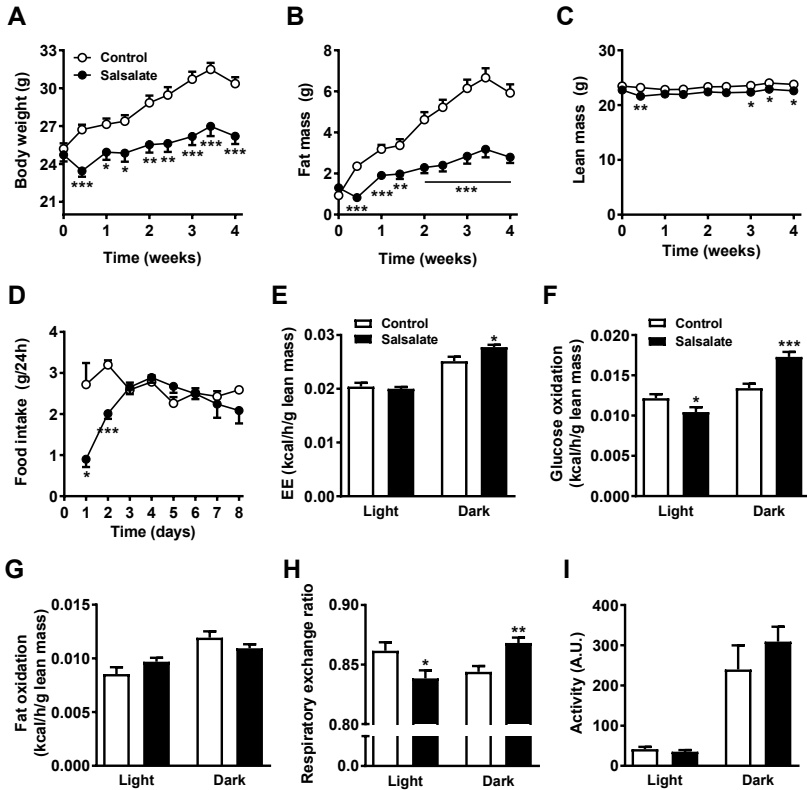
Supplementary figure 1. Salsalate prevents obesity and fat mass accumulation in wild type mice fed a high fat diet. *10-week old male wild type mice (C57Bl/6J background) were fed a high fat diet (HFD) without (open circles) or with (closed circles) salsalate for 4 weeks (A-D). Body weight (A), fat mass (B) and lean mass (C) were monitored throughout the experiment. Food intake was measured daily in the first week of the experiment (D). From day 5 to day 9 of salsalate treatment, mice were housed in fully automatic metabolic cages (LabMaster System; TSE Systems, Bad Homburg, Germany), which measured oxygen uptake (V_{O2}), carbon dioxide production (V_{CO2}) and caloric intake. Total energy expenditure (E) was calculated from V_{O2} and V_{CO2} using the Weir equation, and glucose oxidation (F) and fat oxidation (G) were calculated from V_{O2} and V_{CO2} as described previously (37). Respiratory exchange ratio (H) was also calculated from V_{O2} and V_{CO2}. Physical activity (I) was measured with infrared sensor frames. Measurements (E-H) were corrected for lean mass as determined by EchoMRI (EchoMRI-100, Houston, Texas, USA). EE = energy expenditure. Values represent means ± SEM (n=7-8). * p<0.05, ** p<0.01, *** p<0.001 vs control.*

A Control □ Salsalate ■
Plasma insulin (ng/mL)
**

B
Plasma glucose (mM)

C
Plasma glucose (mM)
○ Control ● Salsalate
Time (min)
*

D
AUC glucose ivGTT (mM × min)
*

E
Plasma glucose (mM)
Time (min)

F
Relative protein expression
pAMPK * AMPK pACC * ACC

G
Plasma triglycerides (mM)
*

H
Plasma triglycerides (mM)
Time (h)

I
FFA (μmol/g feces)

J
Δ Plasma triglycerides (mM)
Time (min)

K
VLDL-[^{35}S]-apoB production (×10^4 dpm/ml/h)

Supplementary figure 2. Salsalate improves glucose and triglyceride metabolism in wild type mice fed a high fat diet. *10-week old male wild type mice were fed a high fat diet (HFD) without (open circles/bars) or with (closed circles/bars) salsalate for 4 weeks. Blood samples from 6 h-fasted mice were collected by tail bleeding at different time points and plasma insulin (A), glucose (B) and triglyceride (G) levels were determined. After 4 weeks, 6 h fasted mice were i.v. injected with glucose and additional blood samples were taken at 5, 15, 30, 60, 90 and 120 min after injection (C-D). After 4 weeks, an insulin tolerance test was performed by injecting 6 h fasted mice i.p.with insulin (NovoRapid, Novo Nordisk, Denmark; 1 U/kg whole body mass) and measuring glucose at t = 15, 30, 60 and 90 min (E). Protein content in muscle was determined by Western blot (F). Postprandial triglyceride (TG) response was measured after 3 weeks of salsalate treatment. Animals were fasted for 6 h and a basal blood sample was drawn before an intragastric load of 200 μL olive oil (Carbonell, Traditional, Cordoba, Spain) was given. Blood samples were drawn 1, 2, 4, 6 and 8 h after the bolus via tail vein bleeding and plasma TG levels were measured (H). Feces was collected during the 3rd week of salsalate treatment. Feces was then weighed, freeze-dried and ground, and fecal fatty acids were determined by methyl esterification. To this end, 750 μL CH$_3$OH/NaOH (10 M)/H$_2$O (3:1:1 v/v) was added to the feces and samples were incubated and mixed in a thermomixer (600 rpm, 90°C) for 1 h. Then, 1050 μL of HCl (6 M)/hexane (3:7.7 v/v) was added before samples were vortexed and spun down 1 min at 14,000 rpm. The upper hexane layer was dried using N$_2$ and redissolved in 2% Triton X-100. Fatty acids were measured using the NEFA C kit (Wako Diagnostics, Instruchemie, Delfzijl) (I). After 4 weeks of salsalate treatment, hepatic VLDL production was determined. Mice were fasted for 4 h and anesthetized by intraperitoneal injection of 6.25 mg/kg acepromazine (Alfasan, Weesp), 6.25 mg/kg midazolam (Roche, Mijdrecht), and 0.31 mg/kg fentanyl (Janssen Pharmaceuticals, Tilburg). Mice were injected intravenously*

with Tran[³⁵S] label (20 μCi/mouse; MP Biomedicals, Eindhoven) to label newly produced apolipoprotein B (apoB). After 30 min, at t = 0 min, Triton WR-1339 (Sigma-Aldrich) was injected intravenously (0.5 mg/g body weight, 10% solution in PBS) to block serum VLDL clearance. Blood samples were drawn before (t = 0) and at 15, 30, 60, and 90 min after injection of Triton and used for determination of plasma TG concentration (J). After 120 min, mice were exsanguinated via the retro-orbital plexus. VLDL was isolated from serum after density gradient ultracentrifugation at d < 1.006 g/ml by aspiration (38) and examined for incorporated ³⁵S-activity as a measure of ApoB production rate (K). AUC = area under the curve; FFA = free fatty acids. Values represent means ± SEM (n=5-8). * p<0.05, ** p<0.01 vs control.

5
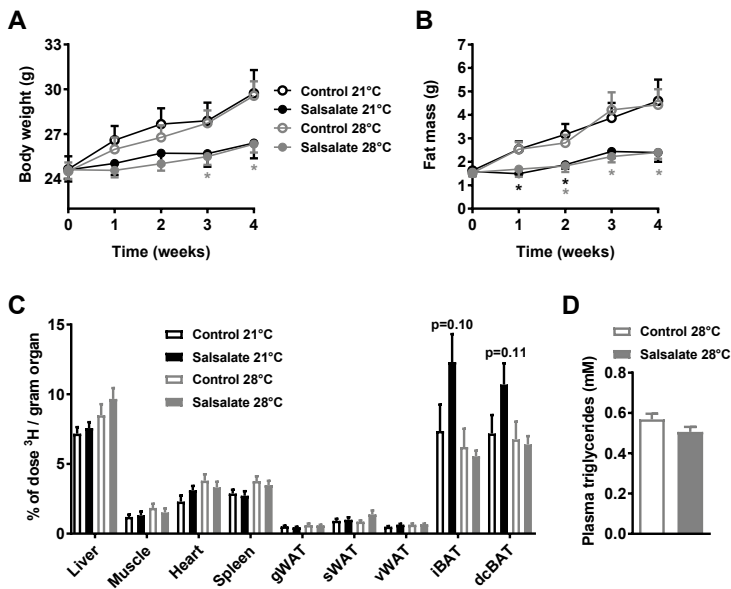
Supplementary figure 3. Effect of salsalate at thermoneutrality. *10-week old male wild type mice were housed at 21°C (black circles/bars) or 28°C (grey circles/bars) and fed a high fat diet (HFD) without (open circles/bars) or with (closed circles/bars) salsalate for 4 weeks. Body weight (A) and fat mass (B) were monitored throughout the experiment. A clearance experiment was performed in which 6 h-fasted mice were i.v. injected with [³H]TO-labeled lipoprotein-like emulsion particles. After 15 min, mice were sacrificed and uptake of [³H]TO-derived activity was determined in the organs (C). After 4 weeks of treatment, blood samples from 6 h-fasted mice were collected by tail bleeding and plasma triglyceride levels were determined (D). Values represent means ± SEM (n=7-8). * p<0.05 vs control. (g,s,v)WAT, gonadal, subcutaneous, visceral white adipose tissue; (i,dc)BAT, interscapular, dorsocervical brown adipose tissue.*
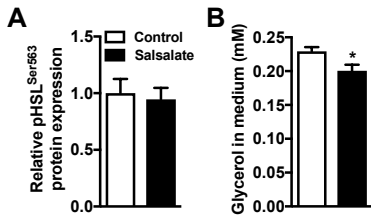
Supplementary figure 4. Effect of salsalate on 3T3-L1 cells. *3T3-L1 cells were cultured and differentiated into white adipocytes. White adipocytes were treated with 300 µM salsalate for 8 h. Protein content was determined by Western blot (A) and glycerol concentration in the culture medium was measured (B). Values represent means ± SD (n=3). * p<0.05 vs control.*
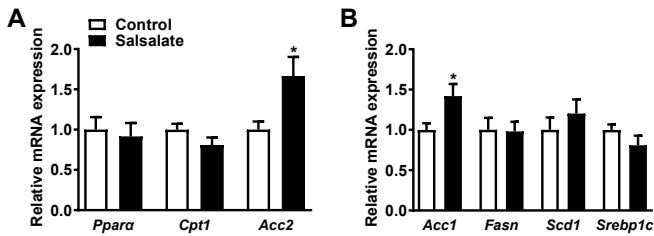
Supplementary figure 5. Effect of salsalate on genes involved in beta-oxidation and lipogenesis in gWAT of wild type mice fed a high fat diet. *10-week old male wild type mice were fed a high fat diet (HFD) without (open bars) or with (closed bars) salsalate for 4 weeks and gonadal white adipose tissue (gWAT) was collected. mRNA expression was determined by qRT-PCR (A-B). Values represent means ± SEM (n=7-8). * p<0.05 vs control.*
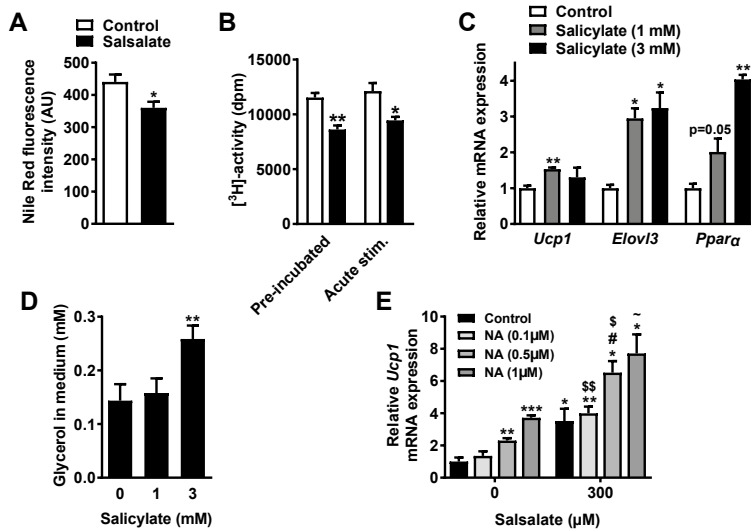
Supplementary figure 6. *In vitro* effects of salsalate and salicylate on T37i brown adipocytes. *T37i cells were cultured and differentiated into mature brown adipocytes. Cells (grown in 0.32 cm² wells) were treated with salsalate (300 μM) for 8 h, stained with 0.1 mg/mL Nile Red solution (Molecular probes, N-1142) for 2 h at 37°C and measured with a fluorimeter (Ex. 485 nm, Em. 590 nm). Values represent means ± SEM of 11 independent wells (A). To assess de novo lipogenesis, cells (grown in 3.8 cm² wells) were incubated at 37°C with HEPES buffer (29.8 g HEPES, 8.78 g NaCl, 4.66 g KCl, 1.12 g D-glucose, 18.8 g BSA, 0.132 g CaCl₂ in 1.125 L H₂O, pH 7.3), 100 nM insulin and [³H]glucose (~500,000 cpm). Cells were either pre-incubated with vehicle or salsalate for 6 h or the compound was added together with the [³H]glucose. After 2 h, cells were washed and 600 μL cold CHCl₃/CH₃OH (1:1 v/v) was added. Cells were left on ice for 30 min, upon which the supernatant was isolated. Next, 125 μL H₂O was added and the samples were mixed and spun for 10 min at 3,500 rpm. The CHCl₃ layer was isolated and evaporated under N₂ and incorporation of [³H]glucose-derived radioactivity was quantified. Values represent means ± SEM of 4-5 independent wells (B). Cells were treated with salicylate (1 or 3 mM) for 8 h and mRNA expression was determined by qRT-PCR (C). In addition, glycerol concentration in the medium was assessed (D). Cells were treated with salsalate (300 μM) in the presence of increasing concentrations of noradrenalin (0.1 – 1 μM) for 8 h and Ucp1 mRNA expression was determined (E). NA = noradrenalin. Values represent means ± SD of 3-4 independent sets of RNA. * p<0.05, ** p<0.01 vs control , $ p<0.05, $$ p<0.01 vs NA, ~ p<0.10 vs NA and salsalate.*

Chapter | **6**

GPR120 as a novel target to increase lipid oxidation and reduce obesity

Andrea D. van Dam, Geerte Hoeke, Maaike Schilperoort,
Erik A. van den Berg, Onno C. Meijer, Anne Reifel-Miller, Tamer Coskun,
Trond Ulven, Mark Christian, Mariëtte R. Boon, Patrick C.N. Rensen

ABSTRACT

The free fatty acid receptor GPR120 is highly expressed in white adipose tissue and brown adipose tissue (BAT), both of which play a major role in triglyceride metabolism. However, the effects of GPR120 on lipid metabolism and substrate utilization have not been studied to date. The aim of our current study was to assess the role of GPR120 in lipid metabolism. To this end, GPR120$^{-/-}$ and wild-type mice (C57BL/6 background) received a high-fat diet (HFD) for 8 weeks. Body composition was monitored by EchoMRI and fully automated metabolic cages were used to measure energy expenditure and substrate utilization. GPR120$^{-/-}$ mice had higher fat mass (+25%, p=0.05), lower physical activity (-49%, p<0.05) and lower energy expenditure during the dark phase (-5%, p<0.05), albeit that substrate utilization was not different (similar respiratory exchange ratio) compared to wild-type mice. GPR120 deficiency reduced the expression of *Ucp1*, *Prdm16* and *Ppara* in BAT (-38 to -59%, p<0.05) without reducing uptake of fatty acids derived from intravenously injected lipoprotein-like particles labeled with glycerol tri[^{3}H]oleate ([^{3}H]TO) by BAT. When wild-type mice were fed a HFD for 6 weeks and orally treated with the GPR120 agonist TUG891 (10 mg/kg daily) during the last 3 weeks of HFD feeding, TUG891 reduced fat mass after 2.5 weeks (-40%, p<0.05). To assess acute effects of the GPR120 agonist, wild-type mice on a chow diet were treated with i.p. TUG891 (35 mg/kg daily) for 5 days. Although i.p. TUG891 treatment did not increase total energy expenditure, the GPR120 agonist acutely increased fat oxidation (+331%, p<0.01) while reducing glucose oxidation (-18%, p<0.05), which was accompanied by a tendency for reduced fat mass already after 5 days (-19%, p=0.06). In conclusion, GPR120 deficiency increases fat mass without evident effects on triglyceride-rich lipoprotein turnover and GPR120 agonism reduces fat mass accompanied by increased fat oxidation. Therefore, stimulation of GPR120 holds therapeutic potential to combat obesity.

6

INTRODUCTION

G protein-coupled receptors (GPCRs) represent the largest family of transmembrane signaling receptors (1). A subclass of the GPCR family specifically binds free fatty acids (FFAs), which can act as signaling molecules to regulate various physiological processes. GPR120, also known as free fatty acid receptor 4 (FFAR4), is activated by medium and long chain fatty acids (2). Recent studies have revealed an important role for GPR120 in immune regulation, hormonal secretion and energy metabolism. For example, several studies showed that GPR120 mediates anti-inflammatory actions of ω-3 fatty acids (3-5). In white adipose tissue (WAT), GPR120 plays a role in adipocyte differentiation (6) and enhances glucose uptake, which contributes to improved insulin sensitivity (3). GPR120 deficiency leads to obesity, glucose intolerance and hepatic steatosis in mice fed a high-fat diet (7). In humans, individuals carrying a mutation associated with decreased GPR120 signaling have an increased risk of obesity (7). Together, these negative effects of reduced GPR120 signaling have led to high interest in the development of pharmacological compounds to activate this receptor (8, 9).

GPR120 is expressed in both WAT and brown adipose tissue (BAT). WAT is the most abundant adipose tissue type, found throughout the body in different subcutaneous and visceral depots (10). WAT is a major participant in energy regulation of the body, by storing excess ingested glucose and fatty acids in the form of triglycerides within adipocytes and by releasing fatty acids to meet the energy needs of other organs (11). In contrast to WAT, BAT combusts fatty acids to generate heat for maintenance of body temperature, defined as non-shivering thermogenesis. Brown adipocytes are smaller than white adipocytes, contain many mitochondria and typically contain multiple small lipid droplets (10). Thermogenesis is dependent on the presence of uncoupling protein 1 (UCP1), which is present in mitochondria and "uncouples" electron transport from ATP synthesis. As a consequence, heat is generated instead of ATP (12, 13). Interestingly, GPR120 is highly expressed in BAT and cold exposure even further increases its expression in BAT and subcutaneous (s)WAT (14), indicating a role for GPR120 in thermogenesis. Also, GPR120 expression increases in WAT of mice on a high-fat diet (6). Collectively, these data suggest GPR120 plays a role in both BAT and WAT physiology.

Although previous studies have focused on the metabolic effects of GPR120 signaling, most focused on the effects of GPR120 on gut hormone secretion and glucose metabolism. The aim of our current study was to assess the role of GPR120 in lipid metabolism and the therapeutic potential of a selective GPR120 agonist. To this end, we studied lipid metabolism in GPR120^{-/-} mice and treated wild-type mice with the GPR120 agonist TUG891. We found that GPR120 deficiency increases fat mass, reduces physical activity and reduces the expression of BAT-specific genes, but does not have pronounced effects on lipid metabolism. Interestingly, we found that specific stimulation of GPR120 with TUG891 increases fat oxidation and reduces fat mass. Taken together, our data indicate that GPR120 deficiency increases fat mass without evident effects on triglyceride-rich

6

lipoprotein turnover and GPR120 agonism reduces fat mass accompanied by increased fat oxidation. Therefore, GPR120 may be a promising target to reduce obesity.

MATERIALS AND METHODS

Animals, diet and treatment

All mice were approximately 12 weeks of age at the start of each experiment and individually housed under standard conditions with a 12:12 h light-dark cycle (from 7:00 h to 19:00 h) and free access to food and water. To assess the effect of GPR120 deficiency on the development of obesity, male GPR120^{-/-} mice and wild-type mice on a C57Bl/6 background were acquired from Taconic Biosciences. Mice received a high-fat diet (HFD; 45% kcal from lard fat, Research Diets) for 8 weeks, upon which they were sacrificed by cervical dislocation. Two wild-type mice were excluded due to severe infection during the study. One GPR120^{-/-} mouse was excluded because of unexplained weight loss after 4 weeks of HFD.

To investigate the effect of oral treatment with a GPR120 agonist on obesity, male C57Bl6/J mice (Charles River Laboratories) were fed a HFD for 3 weeks before initiation of treatment with TUG891 at 12 weeks of age. TUG891 was synthesized as described previously (15). Mice were treated with vehicle or TUG891 (10 mg/kg body weight, dissolved in 10% v/v DMSO, 10% w/v cremophor and 5% w/v mannitol in water, all from Sigma-Aldrich) by oral gavages daily at 15:00 h. Treatment lasted for 3 weeks, upon which the mice were sacrificed by cervical dislocation.

The acute effects of TUG891 on energy expenditure were assessed in male C57Bl6/J mice. First, mice were i.p. injected twice daily at 9:00 h and 16:00 h with vehicle or increasing doses of TUG891 (dissolved in 10% v/v DMSO in PBS) ranging from 15-50 mg/kg body weight as indicated over a period of 5 days. Thereafter, mice were i.p. injected once daily at 17:00 h with 35 mg/kg body weight TUG891 for 5 consecutive days. Mouse experiments were performed in accordance with the Institute for Laboratory Animal Research Guide for the Care and Use of Laboratory Animals and had received approval from the University Ethical Review Board (Leiden University Medical Center, The Netherlands).

Food intake, body weight, and body composition

At indicated time points, food intake and body weight were measured with a scale, and body composition was measured using an EchoMRI-100 analyzer (EchoMRI, TX, USA).

Energy metabolism

GPR120^{-/-} and wild-type control mice were housed in fully automatic metabolic cages (LabMaster System; TSE Systems) in the second week of HFD-feeding. Wild-type mice that received i.p. treatment with TUG891 were housed in metabolic cages during the entire treatment period. Metabolic cages measured oxygen uptake (V_{O2}) and carbon dioxide production (V_{CO2}). Respiratory exchange ratio (RER), glucose oxidation and fat oxidation were calculated from V_{O2} and V_{CO2} as described previously (16). Total energy expenditure was

calculated from V_{O2} and V_{CO2} using the Weir equation (17). Physical activity was measured with infrared sensor frames.

Histology of WAT and BAT

Subcutaneous WAT and interscapular BAT (iBAT) were removed, fixed in 4% paraformaldehyde, dehydrated in 70% EtOH, and embedded in paraffin. Hematoxylin-eosin (HE) stainings were performed on sections (5 μm) using standard protocols. The cell size of adipocytes in WAT and the area of intracellular lipid vacuoles in BAT were quantified using ImageJ software.

RNA purification and quantitative RT-PCR

RNA was extracted from snap-frozen iBAT using Tripure RNA Isolation reagent (Roche) according to manufacturer's instructions. RNA concentrations were measured using NanoDrop and RNA was reverse transcribed using Moloney Murine Leukemia Virus Reverse Transcriptase (Promega) for quantitative RT-PCR (qRT-PCR) to produce cDNA. Expression levels of genes were determined by qRT-PCR, using gene-specific primers (Table 1) and SYBR green supermix (Biorad). mRNA expression was normalized to *B2m* and *Gapdh* mRNA content and expressed as fold change compared with control mice using the ΔΔCT method.

6

Table 1. *Primer sequences of forward and reverse primers (5' → 3').*

Gene	Forward primer	Reverse primer
Angptl4	GGAAAGAGGCTTCCCAAGAT	TCCCAGGACTGGTTGAAGTC
Ap2	ACACCGAGATTTCCTTCAAACTG	CCATCTAGGGTTATGATGCTCTTCA
B2m	TGACCGGCTTGTATGCTATC	CAGTGTGAGCCAGGATATAG
Cd36	GCAAAGAACAGCAGCAAAATC	CAGTGAAGGCTCAAAGATGG
Cpt1a	GAGACTTCCAACGCATGACA	ATGGGTTGGGGTGATGTAGA
Elovl3	GGATGACGCCGTAGTCAGTA	GACAGAATGGACGCCAAAGT
Gapdh	GGGGCTGGCATTGCTCTCAA	TTGCTCAGTGTCCTTGCTGGGG
Glut1	AGCATCTTCGAGAAGGCAGG	ACAACAAACAGCGACACCAC
Glut4	CAGCGCCTGAGTCTTTTCTT	GGCATTGATAACCCCAATGT
Gpr120	ACATTGGATTGGCCCAACCGCA	TCCGCGATGCTTTCGTGATCTGT
Lpl	CCCTAAGGACCCCTGAAGAC	GGCCCGATACAACCAGTCTA
Pgc1a	TGCTAGCGGTTCTCACAGAG	AGTGCTAAGACCGCTGCATT
Ppara	ATGCCAGTACTGCCGTTTTC	GGCCTTGACCTTGTTCATGT
Pparγ	GTGCCAGTTTCGATCCGTAGA	GGCCAGCATCGTGTAGATGA
Prdm16	ACTTTGGATGGGAGCAGATG	CTCCAGGCTCGATGTCCTTA
Ucp1	TCAGGATTGGCCTCTACGAC	TGCATTCTGACCTTCACGAC
Vegfα	GGAGATCCTTCGAGGAGCACTT	GGCGATTTAGCAGCAGATATAAGAA

Plasma lipids and glucose

At the indicated time points, 4 h-fasted (from 8:00 to 12:00) blood samples were collected from GPR120^{-/-} and wild-type control mice and 6 h-fasted (from 8:00 to 14:00) blood samples were collected from mice that were orally treated with TUG891 or vehicle. This was done by tail vein bleeding into chilled capillaries that were coated with paraoxon (Sigma-Aldrich) to prevent ongoing lipolysis (18). Isolated plasma was assayed for triglycerides, glucose, and free fatty acids. Triglyceride and glucose levels were measured by commercially available enzymatic kits (from Roche Diagnostics and Instruchemie, respectively). Free fatty acids were measured using the NEFA C kit (Wako Diagnostics; Instruchemie).

Olive oil tolerance test

Postprandial triglyceride response was measured in GPR120^{-/-} and wild-type control mice after 6 weeks of HFD. Animals were fasted for 4 h (from 7:00 h to 11:00 h) and a basal blood sample was drawn before an intragastric load of 200 µL olive oil (Carbonell, Traditional, Spain) was given. Blood samples were drawn 1, 2, 4 and 8 h after the bolus via tail vein bleeding and plasma triglyceride and free fatty acid levels were measured as described above.

In vivo clearance of lipoprotein-like emulsion particles and glucose

Lipoprotein-like emulsion particles were prepared from 100 mg of total lipid, including glycerol trioleate (triolein; TO; 70 mg), egg yolk phosphatidylcholine (22.7 mg), lysophosphatidylcholine (2.3 mg), cholesteryl oleate (3.0 mg) and cholesterol (2.0 mg), with addition of [³H]TO (3.7 MBq). Lipids were sonicated and resulting particles fractionated by sequential density gradient ultracentrifugation steps (19). The emulsion fraction containing lipoprotein-like particles of 80 nm was isolated and mixed with 2-[1-¹⁴C]deoxy-D-glucose ([¹⁴C]DG; 4:1 ratio, based on radioactive count). Mice were fasted for 6 h (from 7:00 h to 13:00 h) and injected with 200 µL of [¹⁴C]DG and [³H]TO-labeled lipoprotein-like particles (1.0 mg triglycerides per mouse) via the tail vein. Blood samples were drawn from the tail vein at 2, 5, 10 and 15 minutes after injection to determine the plasma decay of [³H]TO and [¹⁴C]DG. After 15 min, mice were sacrificed by cervical dislocation and perfused with ice-cold PBS through the heart. Organs were harvested and weighed, dissolved in Tissue Solubilizer (Amersham Biosciences) overnight at 56°C and analyzed for ³H- and ¹⁴C-activity.

Statistical Analysis

All data are expressed as means ± SEM. Groups were compared with a two-tailed unpaired Student's t-test or a two-way ANOVA for repeated measurements, as indicated. Probability values less than 0.05 were considered statistically significant.

RESULTS

GPR120 deficiency increases HFD-induced fat accumulation and reduces physical activity

To investigate the consequences of GPR120 deficiency on the development of obesity, GPR120$^{-/-}$ and wild-type control mice were fed a HFD for 8 weeks. Body weight (**Fig. 1A**) was comparable between the groups throughout the study, although GPR120$^{-/-}$ mice exhibited less lean mass (23.5 *vs.* 25.7 g, p<0.05; **Fig. 1B**) and more fat mass (2.8 *vs.* 1.0 g, p<0.01; **Fig. 1C**) at the beginning of the HFD. The difference in lean mass disappeared while the difference in fat mass in GPR120$^{-/-}$ enlarged during the time course of HFD feeding. The increased fat mass was mainly due to an increase in the sWAT depot, while gWAT mass was comparable between GPR120$^{-/-}$ and control mice after 8 weeks of HFD (**Fig. 1D**). The iBAT depot was also larger but this does not contribute substantially to total body fat or weight. The increase in fat mass could not be explained by differences in food intake as cumulative food intake was lower in GPR120$^{-/-}$ mice compared to controls (**Fig. 1E**). Instead, total energy expenditure was lower in GPR120$^{-/-}$ animals during the dark phase (**Fig. 1F, G**). The latter could possibly be due to the markedly lower physical activity levels observed in GPR120$^{-/-}$ mice as compared to controls (**Fig. 1H, I**). Despite a lower energy expenditure, GPR120 deficiency did not affect substrate utilization, as the respiratory exchange ratio (RER) was similar in GPR120$^{-/-}$ and control mice (**Fig. 1J**).

GPR120 deficiency reduces BAT-specific gene expression

To further investigate the cause of the increased fat mass observed in GPR120$^{-/-}$ mice, we more closely assessed the sWAT and iBAT depots. In line with the increased sWAT depot weight, the average size of adipocytes in the sWAT depot of GPR120$^{-/-}$ mice tended to be larger than in controls (**Fig. 2A, B**). Albeit that lipid droplet content in iBAT was not significantly higher in GPR120$^{-/-}$ mice (**Fig. 2C, D**), markers of active BAT including *Ucp1*, *Elovl3*, *Prdm16*, *Ppara* and *Vegf* were all lower in GPR120$^{-/-}$ mice compared to controls (**Fig. 2E**). Of the markers involved in differentiation and mitochondrial function, only *aP2* was significantly lower in GPR120$^{-/-}$ mice (**Fig. 2F**). Interestingly, also many of the genes involved in substrate uptake were lower in GPR120$^{-/-}$ mice, including *Lpl*, *Angptl4*, *Glut1* and *Glut4* (**Fig. 2G**).

GPR120 deficiency does not affect plasma lipid metabolism

Since GPR120$^{-/-}$ mice displayed higher fat mass and lower markers of BAT activity, we studied whether the unfavorable metabolic phenotype of GPR120$^{-/-}$ mice coincided with deterioration of plasma lipid metabolism. After 8 weeks of HFD, plasma triglyceride (**Fig. 3A**), free fatty acid (**Fig. 3B**) and glucose levels (**Fig. 3C**) did not significantly differ between GPR120$^{-/-}$ and control mice. Likewise, GPR120 deficiency did not affect excursions of plasma triglyceride (**Fig. 3D**) and free fatty acid (**Fig. 3E**) levels in response to an oral olive oil gavage, suggesting unaltered plasma clearance of chylomicrons. To evaluate the relative contribution of organs in the plasma clearance of triglyceride-derived fatty acids, we next

6
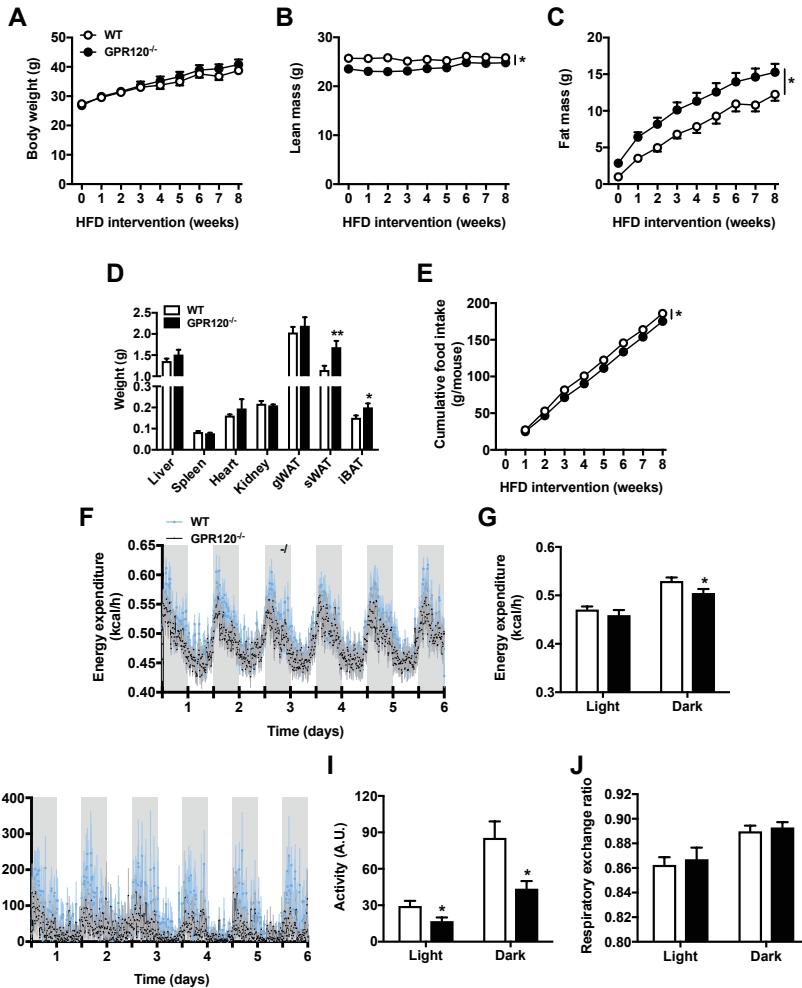
Figure 1. GPR120 deficiency increases HFD-induced fat accumulation and reduces physical activity.
GPR120$^{-/-}$ and wild-type (WT) mice were fed a high-fat diet (HFD) for 8 weeks. Body weight (A), lean mass (B), fat mass (C) and food intake (E) were measured weekly. At the end of the study, mice were sacrificed and organs were collected and weighed (D). In the second week of HFD, mice were housed in fully automatic metabolic cages (LabMaster System; TSE Systems), which measured oxygen uptake (V$_{O2}$) and carbon dioxide production (V$_{CO2}$). Total energy expenditure was calculated from V$_{O2}$ and V$_{CO2}$ using the Weir equation (F) and the average energy expenditure over the entire week was calculated for the light and dark phase separately (G). Physical activity was measured with infrared sensor frames (H) and the average physical activity over the entire week was calculated for the light and dark phase separately (I). Respiratory exchange ratio was calculated as the V$_{CO2}$ / V$_{O2}$ ratio (J). Values are presented as mean ± SEM (n=8-9). *p<0.05, **p<0.01 vs. WT.
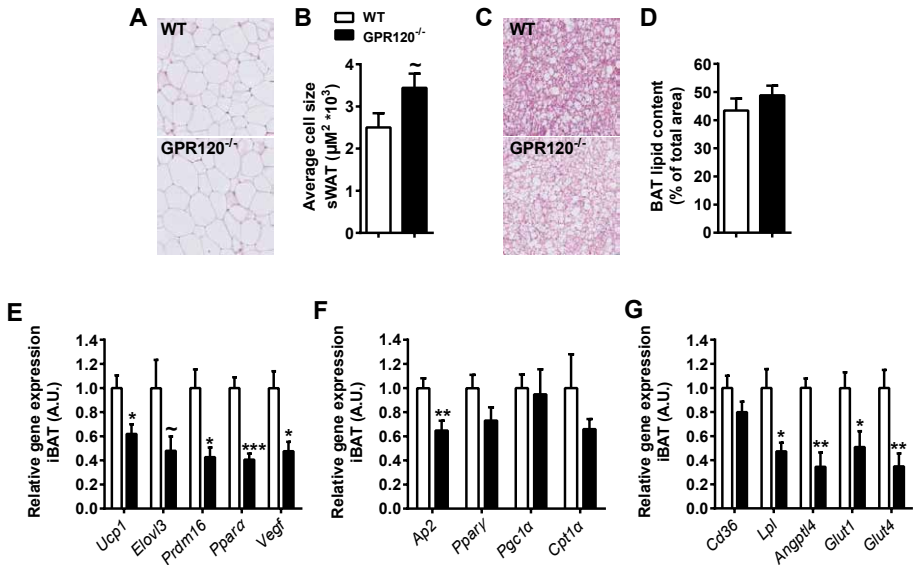
Figure 2. GPR120 deficiency reduces BAT-specific gene expression. *GPR120^{-/-} and wild-type (WT) mice were fed a high-fat diet (HFD) for 8 weeks. Haematoxylin and Eosin staining of sWAT and iBAT sections was performed, and representative figures are shown (A, C). The cell size of adipocytes in sWAT (B) and the lipid content of iBAT (D) were quantified and representative pictures are shown. mRNA expression of the indicated genes was determined in iBAT (E-G). Values are presented as mean ± SEM (n=7-9). *p<0.05, **p< 0.01, ***p< 0.001 vs. WT.*

assessed the plasma clearance and organ distribution of [3H]TO-labeled triglyceride-rich lipoprotein-like emulsion particles (**Fig. 3F**). While the clearance of [3H]TO from plasma was unaffected, the uptake of [3H]TO-derived oleate was higher in sWAT of GPR120^{-/-} mice (**Fig. 3G**). This was due to the larger amount of sWAT in GPR120^{-/-} mice, since uptake per gram sWAT was similar in both groups (data not shown). While the plasma clearance of [14C] deoxyglucose (DG) also did not differ between GPR120^{-/-} mice and controls (**Fig. 3H**), the uptake of [14C]DG by the kidneys and iBAT of GPR120^{-/-} mice was higher (**Fig. 3I**). Although this could suggest that deficiency of the lipid sensor GPR120 directs BAT to take up glucose, GPR120 deficiency does not have major impact on lipid metabolism.
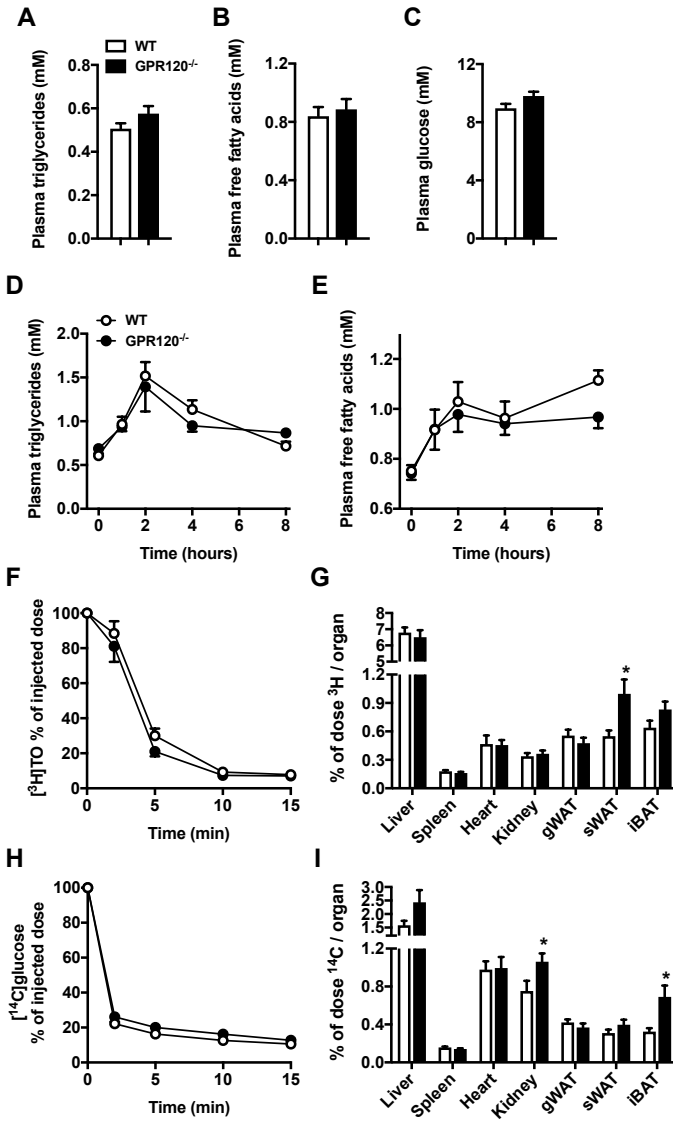
Figure 3. GPR120 deficiency does not affect plasma lipid metabolism. *GPR120^{-/-} and wild-type (WT) mice were fed a high-fat diet (HFD) for 8 weeks. At the end of the study, 6 h fasted blood samples were drawn and plasma triglycerides (A), free fatty acids (B) and glucose (C) were determined. After 6 weeks of HFD, a basal blood sample was drawn from 4 h-fasted mice upon which they received an oral bolus of olive oil. Subsequently, at 1, 2, 4 and 8 hours after the olive oil gavage, blood samples were taken and assayed for plasma triglycerides (D) and free fatty acids (E). After 8 weeks of HFD, mice were injected i.v. with glycerol tri[³H]oleate-labeled lipoprotein-like particles and [¹⁴C]deoxy-D-glucose, and clearance from plasma (F, H) and uptake by organs at 15 min after injection (G, I) were determined by analyzing ³H- and ¹⁴C-activity. Values are presented as mean ± SEM (n=8-9). *p<0.05 vs. WT.*
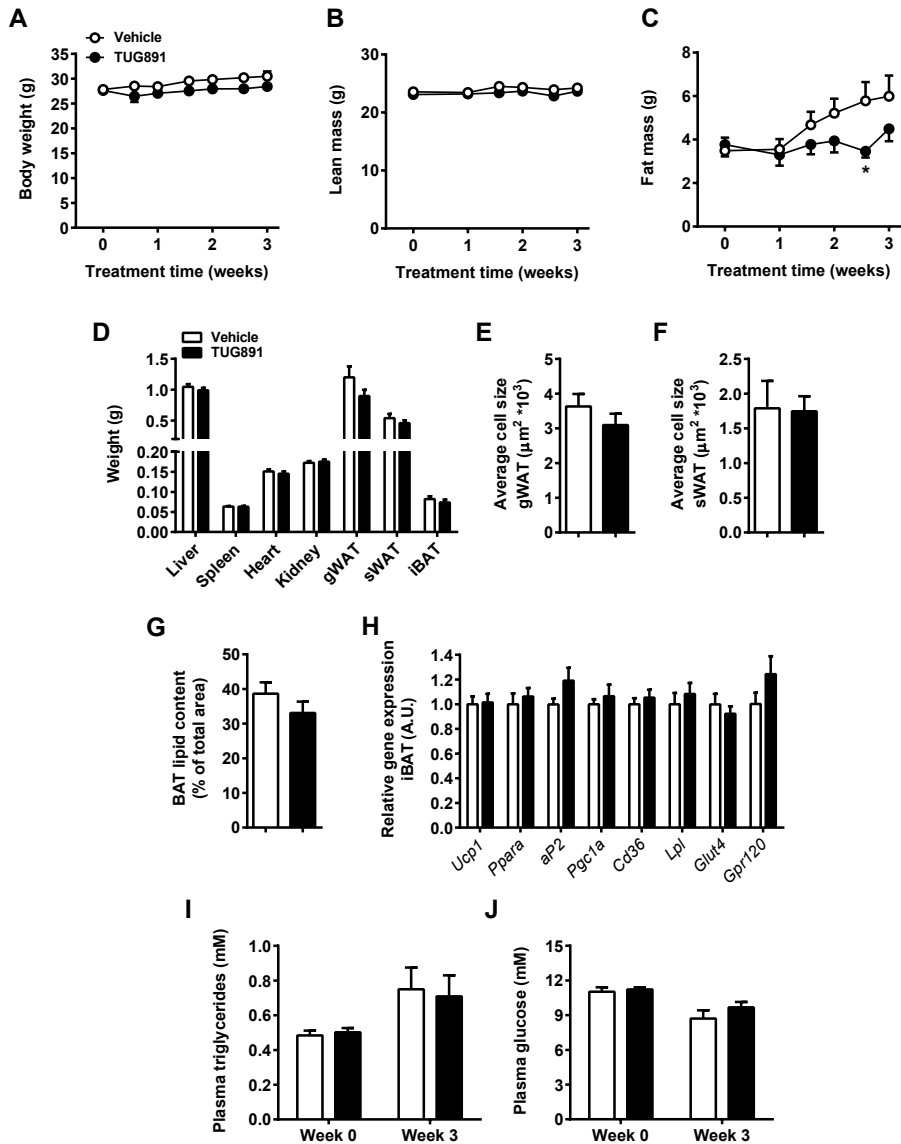
Figure 4. Oral treatment with GPR120 agonist TUG891 reduces fat mass. *Wild-type mice were fed a high-fat diet (HFD) for 6 weeks and treated orally with vehicle or 10 mg/kg body weight TUG891 during the last 3 weeks of HFD feeding. Body weight (A), lean mass (B) and fat mass (C) were measured once to twice weekly. At the end of the study, mice were sacrificed and organs were collected and weighed (D). Haematoxylin and Eosin staining of gWAT, sWAT and iBAT sections was performed, and the cell size of adipocytes in gWAT (E) and sWAT (F), and the lipid content of iBAT (G) were quantified. mRNA expression of the indicated genes was determined in iBAT (H). Before the start of TUG891 treatment and after 3 weeks, 6 h fasted blood samples were drawn and plasma triglycerides (I) and glucose (J) were determined. Values are presented as mean ± SEM (n=7-8). *p<0.05 vs. vehicle.*

Oral treatment with GPR120 agonist TUG891 reduces fat mass

To assess the therapeutic potential of targeting GPR120 to reduce fat mass, we next treated HFD-fed mice orally with the GPR120 agonist TUG891 (10 mg/kg daily) or vehicle for 3 weeks. Total body weight (**Fig. 4A**) and lean mass (**Fig. 4B**) were not affected by TUG891 treatment. However, fat mass was slightly reduced after 2.5 weeks of treatment (**Fig. 4C**). This was not due to a decrease in a specific adipose tissue depot, as gWAT, sWAT and iBAT weights were similar between TUG891-treated animals and vehicle-treated controls (**Fig. 4D**). Accordingly, TUG891 did not affect adipocyte cell size in gWAT (**Fig. 4E**) or sWAT (**Fig. 4F**), nor did it alter lipid droplet content (**Fig. 4G**) or gene expression (**Fig. 4H**) in iBAT. Plasma triglyceride (**Fig. 4E**) and glucose (**Fig. 4F**) levels were also unaffected by TUG891.

GPR120 agonist TUG891 acutely increases fat oxidation

Since GPR120 deficiency increased fat mass and reduced energy expenditure, and treatment with the GPR120 agonist TUG891 reduced fat mass in HFD-fed mice, we wanted to gain more insight into the mechanism behind the effect of GPR120 on energy utilization and fat mass. We first assessed the acute effects of TUG891 on energy expenditure and substrate utilization. Since the oral availability of compounds is often hindered by low and/ or slow intestinal absorption but no data on optimal dosing was available yet, we chose to treat mice on a normal chow diet i.p. with increasing doses of TUG891 (twice daily). Strikingly, TUG891 injection before onset of the dark phase acutely decreased RER (**Fig. 5A**), increased fat oxidation (**Fig. 5B**) and decreased glucose oxidation (**Fig. 5C**), whereas TUG891 treatment at the beginning of the light phase did not have pronounced effects on these parameters. No differences were observed in total energy expenditure (**Fig. 5D**) or physical activity (**Fig. 5E**). Based on these initial results, we selected the intermediate dose of 35 mg/kg TUG891 and administration time 2 h before the initiation of the dark phase because of the prominent effects on fat oxidation. We then investigated in a larger number of mice (n=8) on a chow diet the effects of this dose of TUG891 i.p. once daily for a period of 5 consecutive days on RER and fat mass. While TUG891 did not affect total energy expenditure (**Fig. 6A, B**) or physical activity (**Fig. 6C, D**), the GPR120 agonist reduced RER (**Fig. 6E, F**), increased fat oxidation (**Fig. 6G, H**) and decreased glucose oxidation (**Fig. 6I, J**) during the dark phase. Total body weight (**Fig. 7A**) and lean mass (**Fig. 7B**) were unaffected. However, in accordance with the increased fat oxidation, fat mass tended to be reduced already after 5 days of treatment with TUG891 (**Fig. 7C**).
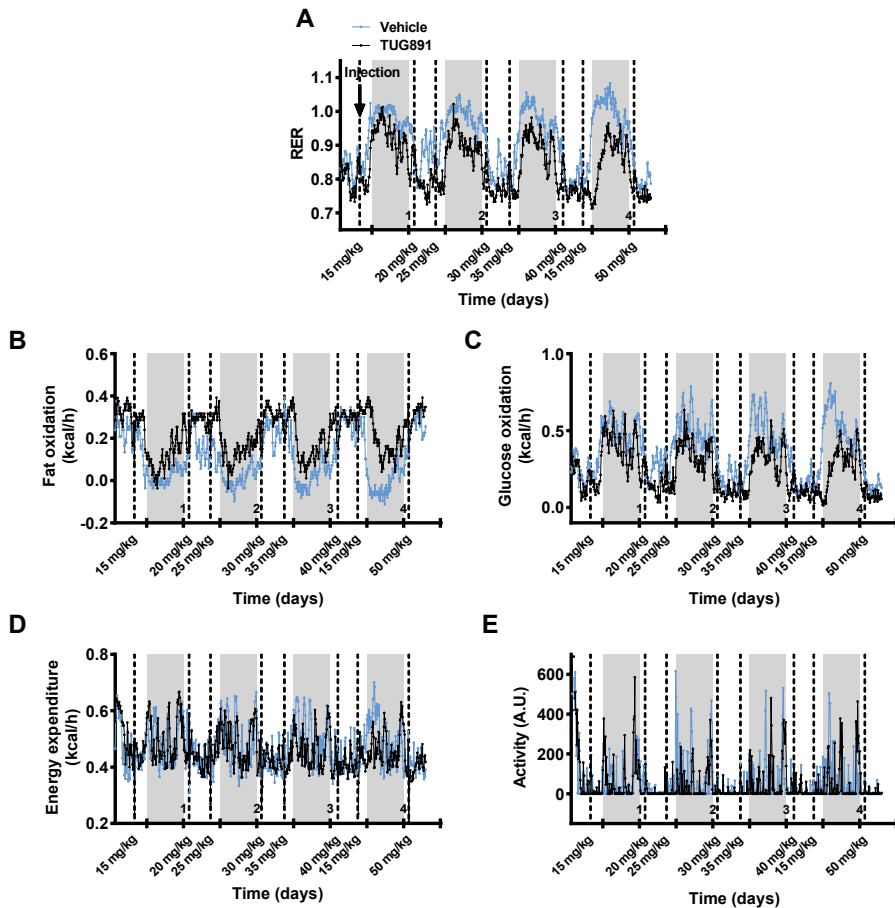
Figure 5. I.p. treatment with 35 mg/kg GPR120 agonist TUG891 acutely increases fat oxidation when injected before onset of the dark phase. *Wild-type mice were fed a chow diet and housed in fully automatic metabolic cages (LabMaster System; TSE Systems), which measured oxygen uptake (V_{O2}) and carbon dioxide production (V_{CO2}). Mice were i.p. injected (dotted line) twice daily at 9:00 and 16:00 with vehicle or increasing doses of TUG891 ranging from 15-50 mg/kg body weight as indicated over a period of 5 days. Respiratory exchange ratio (A), fat oxidation (B) and glucose oxidation (C) were calculated from V_{O2} and V_{CO2}. Total energy expenditure was also calculated from V_{O2} and V_{CO2} using the Weir equation (D). Physical activity was measured with infrared sensor frames (E). (n=1).*
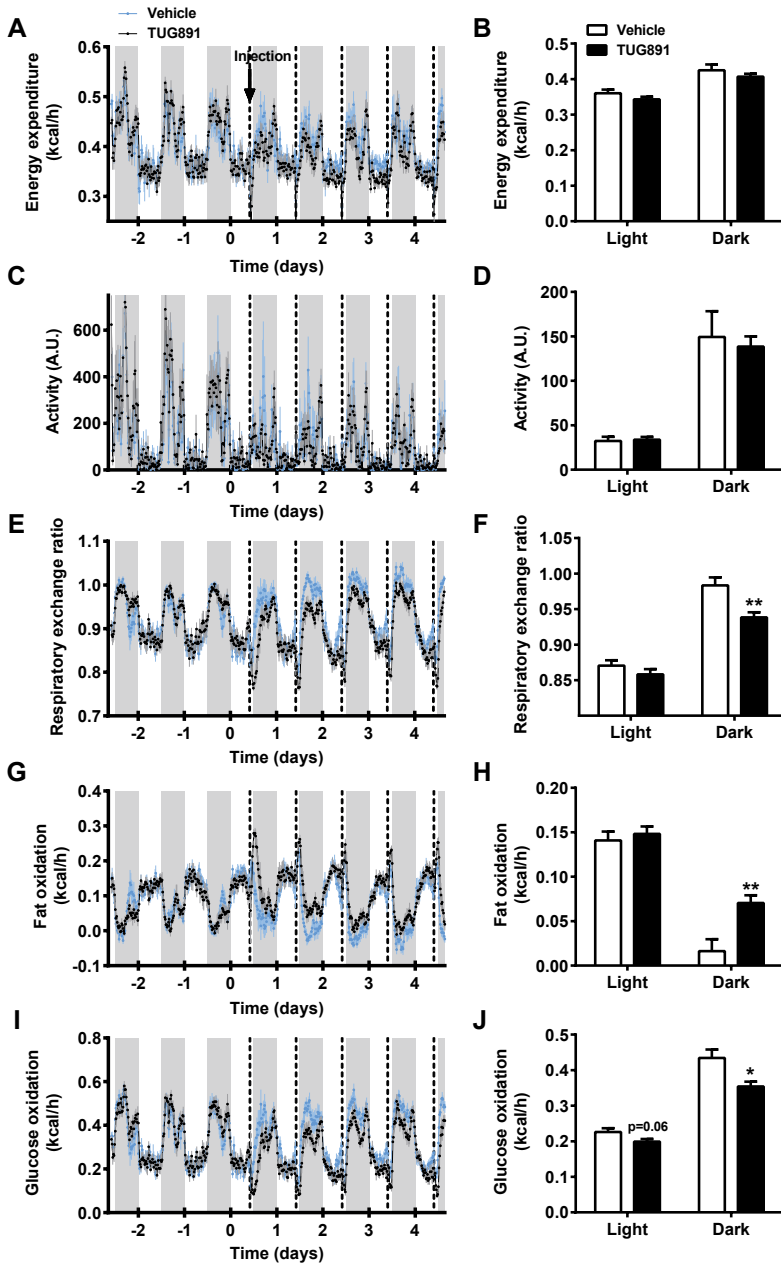
Figure 6 (left page). GPR120 agonist TUG891 acutely increases fat oxidation. *Wild-type mice were fed a chow diet and housed in fully automatic metabolic cages (LabMaster System; TSE Systems), which measured oxygen uptake (V_{O2}) and carbon dioxide production (V_{CO2}). Mice were i.p. injected once daily (dotted line) at 17:00 with 35 mg/kg body weight TUG891 for 5 consecutive days. Total energy expenditure was calculated from V_{O2} and V_{CO2} using the Weir equation (A) and the average energy expenditure over the treatment period was calculated for the light and dark phase separately (B). Physical activity was measured with infrared sensor frames (C) and the average physical activity over the treatment period was calculated for the light and dark phase separately (D). Respiratory exchange ratio was calculated as the V_{CO2} / V_{O2} ratio (E) and the average respiratory exchange ratio over the treatment period was calculated for the light and dark phase separately (F). Fat oxidation (G) and glucose oxidation (I) were also calculated from V_{O2} and V_{CO2} and the average fat and glucose oxidation over the treatment period was calculated for the light and dark phase separately (H, J). Values are presented as mean ± SEM (n=8). *p<0.05, **p<0.01 vs. vehicle.*
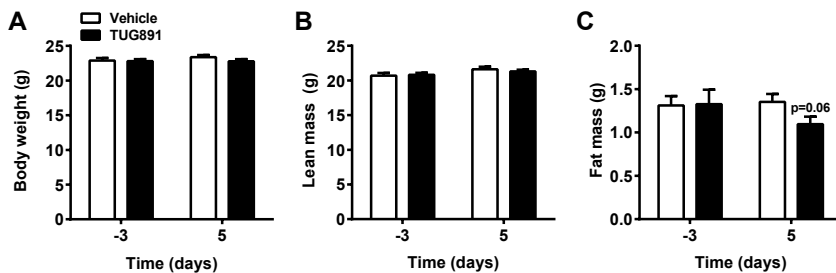
Figure 7. GPR120 agonist TUG891 tends to reduce fat mass. *Wild-type mice were fed a chow diet and i.p. injected once daily at 17:00 with vehicle or 35 mg/kg body weight TUG891 for 5 consecutive days. Body weight (A), lean mass (B) and fat mass (C) and were measured before and after TUG891 treatment. Values are represented as mean ± SEM (n=8).*

DISCUSSION

In the current study, we assessed the role of GPR120 in obesity development and lipid metabolism. We demonstrated that GPR120 deficiency, although not evidently influencing plasma lipid metabolism, increases HFD-induced fat mass and reduces energy expenditure. This coincided with lower physical activity and lower BAT-specific gene expression. In addition, GPR120 agonism reduced fat mass related to increased fat oxidation, which highlights the therapeutic potential of targeting GPR120 to reduce obesity.

We established that GPR120^{-/-} mice exhibited higher fat mass as compared to wild-type control mice. This corroborates previous findings by Ichimura *et al.* (7), who reported that GPR120^{-/-} mice on a HFD store more fat than wild-type controls. In our study, this increased fat mass of GPR120^{-/-} mice was not reflected by higher body weight. This is in contrast to the previous study in which the authors did find that GPR120 deficiency increased HFD-

induced body weight gain (7). This discrepancy may be explained by differences in age or strain of the mice, or even the facility in which experiments were performed. We found that GPR120^{-/-} mice had lower energy expenditure in the dark phase, which could contribute to their higher fat mass. Remarkably, lower energy expenditure in young GPR120^{-/-} mice was also reported previously, but only during the light phase (7).

The most striking effect of GPR120 deficiency we observed was lower physical activity levels during both the light and the dark phase, which may partly underlie the lower energy expenditure of GPR120^{-/-} mice. Although physical activity has not been investigated in relation to GPR120 before, reduced physical activity is often reported in mice that underwent orchidectomy (20, 21) or with androgen deficiency (21). Besides in adipose tissue, GPR120 is also highly expressed in the pituitary gland (6, 22). Moreover, GPR120 protein colocalizes with LHβ and FSHβ, being subunits of the gonadotropin hormones LH and FSH, respectively, in the pituitary gland (23). This suggests that GPR120 may stimulate gonadotropin secretion in the pituitary and thereby indirectly stimulate androgen production in the testes. In line with this hypothesis, fatty acids increase LH release from pituitary cells (22). However, it has also been described that the GPR40/120 agonist GW9508 does not induce LH release and the GPR40/120 antagonist GW1100 fails to inhibit fatty acid-induced LH release from pituitary cells, arguing against a role for GPR120 in the fatty acid-induced release of LH from the pituitary (22). Whether GPR120 regulates pituitary gonadotropin secretion *in vivo* and what the effect of GPR120 deficiency is on androgen levels is an interesting field of future investigation. As androgen deficiency exacerbates HFD-induced metabolic derangements in mice (21), low androgen levels could well be the mechanism behind the deteriorated metabolic phenotype (*i.e.* increased fat mass, less active BAT) we found in GPR120 deficient animals.

Another important contributor to energy expenditure is BAT. GPR120^{-/-} mice in our study exhibited increased iBAT mass and reduced gene expression of BAT markers and genes involved in substrate uptake by BAT, indicating that GPR120 deficiency indeed renders BAT less active. Surprisingly, GPR120 deficiency was not accompanied by higher plasma lipid levels, worsened olive oil tolerance or slower plasma lipid clearance. Others have found high and inducible mRNA expression of *Gpr120* in BAT upon cold, and impaired cold-induced browning in GPR120^{-/-} mice, both of which do suggest an important role of GPR120 in BAT activation (24). Thus, besides the lower physical activity we found in GPR120^{-/-} mice, lower BAT activity may in part underlie the higher fat accumulation in WAT. However, even though GPR120 agonism activates BAT, is involved in browning of WAT (24), and both BAT and browned WAT are important regulators of lipid metabolism (25), the presence of GPR120 on BAT does not seem to contribute to fatty acid uptake by BAT or to regulate plasma lipid levels in our study.

In line with the observation that deficiency for GPR120 increased fat mass, agonism of GPR120 using the agonist TUG891 decreased fat mass. We selected TUG891 because of its high selectivity for GPR120 over GPR40 compared to other agonists such as GW9508 and NCG21 (15, 26). An oral dose of 10 mg/kg daily reduced fat mass after 2.5 weeks of treatment, whereas an i.p. dose of 35 mg/kg daily already tended to reduce fat mass after

6

5 days of treatment. Obviously, the higher dose in the latter experiment is probably mainly responsible for this difference, although the fact that the orally treated mice were on a HFD and the dissimilar bioavailability of the compound upon oral *vs.* i.p. treatment (lower absorption of compounds upon oral administration decreases their bioavailability) likely also contributed to the varying effects on fat mass. Only one study describing treatment of rodents with TUG891 has been published to date. In this study, mice received a daily dose of 20 mg/kg TUG891 through the drinking water for 2 weeks, upon which reduced fat mass, improved glucose and insulin tolerance were observed (27). A disadvantage of this administration route is that GPR120, which is also expressed on the tongue, may be involved in taste preference (28, 29). When treating mice i.p. twice daily, we observed larger effects of TUG891 on substrate utilization when administered at the end of the light phase than when administered at the beginning of the light phase. Besides dose and administration route, it is becoming increasingly common to take into account the circadian timing of administration to maximize therapeutic efficacy (30). Since lipid metabolism is also under circadian regulation (31), we believe that timing of TUG891 administration is of great importance to optimize the intended effect and minimize possible (toxic) side effects associated with administration of many exogenous compounds.

When further investigating the mechanism behind the potential of TUG891 to decrease fat mass, increased fat oxidation directly after administration of TUG891 was observed. This increase in fat oxidation is likely due to increased BAT activity, as previous studies have demonstrated that BAT activation increases fatty acid uptake by BAT (25, 32), and stimulates lipid oxidation rather than glucose oxidation (25). Others have shown that the GPR40/120 agonist GW9508 activates BAT and increases oxygen consumption in mice. Whether TUG891 actually increases triglyceride-derived fatty acid uptake by BAT and whether the stimulation of fat oxidation is mediated by GPR120 should be assessed in future studies.

In humans, GPR120 is well expressed in both subcutaneous and omental adipose tissue (7). Besides, branched fatty acid esters of hydroxy fatty acids (FAHFAs), a novel class of endogenous lipids, signal through GPR120 and positively correlate with insulin sensitivity in humans (33). These findings strengthen the possibility that the metabolic effects of GPR120 activation are translatable to humans.

In conclusion, absence of the fatty acid receptor GPR120 deteriorates metabolic phenotype, evidenced by increased fat mass and reduced physical activity in HFD-fed mice, without evidently altering plasma lipid metabolism. The GPR120 agonist TUG891 increases fat oxidation and reduces fat mass, demonstrating that GPR120 agonism, and this specific compound, hold therapeutic potential to reduce obesity. Further research into the mechanisms behind the beneficial metabolic effects of TUG891 is warranted to further develop this compound for treatment of obesity.

6

FUNDING

6

REFERENCES

1. Kobilka BK: G protein coupled receptor structure and activation. Biochimica et biophysica acta 2007;1768:794-807

2. Hirasawa A, Tsumaya K, Awaji T, Katsuma S, Adachi T, Yamada M, Sugimoto Y, Miyazaki S, Tsujimoto G: Free fatty acids regulate gut incretin glucagon-like peptide-1 secretion through GPR120. Nature medicine 2005;11:90-94

3. Oh DY, Talukdar S, Bae EJ, Imamura T, Morinaga H, Fan W, Li P, Lu WJ, Watkins SM, Olefsky JM: GPR120 is an omega-3 fatty acid receptor mediating potent anti-inflammatory and insulin-sensitizing effects. Cell 2010;142:687-698

4. Li X, Yu Y, Funk CD: Cyclooxygenase-2 induction in macrophages is modulated by docosahexaenoic acid via interactions with free fatty acid receptor 4 (FFA4). FASEB journal : official publication of the Federation of American Societies for Experimental Biology 2013;27:4987-4997

5. Liu Y, Chen LY, Sokolowska M, Eberlein M, Alsaaty S, Martinez-Anton A, Logun C, Qi HY, Shelhamer JH: The fish oil ingredient, docosahexaenoic acid, activates cytosolic phospholipase A(2) via GPR120 receptor to produce prostaglandin E(2) and plays an anti-inflammatory role in macrophages. Immunology 2014;143:81-95

6. Gotoh C, Hong YH, Iga T, Hishikawa D, Suzuki Y, Song SH, Choi KC, Adachi T, Hirasawa A, Tsujimoto G, Sasaki S, Roh SG: The regulation of adipogenesis through GPR120. Biochemical and biophysical research communications 2007;354:591-597

7. Ichimura A, Hirasawa A, Poulain-Godefroy O, Bonnefond A, Hara T, Yengo L, Kimura I, Leloire A, Liu N, Iida K, Choquet H, Besnard P, Lecoeur C, Vivequin S, Ayukawa K, Takeuchi M, Ozawa K, Tauber M, Maffeis C, Morandi A, Buzzetti R, Elliott P, Pouta A, Jarvelin MR, Korner A, Kiess W, Pigeyre M, Caiazzo R, Van Hul W, Van Gaal L, Horber F, Balkau B, Levy-Marchal C, Rouskas K, Kouvatsi A, Hebebrand J, Hinney A, Scherag A, Pattou F, Meyre D, Koshimizu TA, Wolowczuk I, Tsujimoto G, Froguel P: Dysfunction of lipid sensor GPR120 leads to obesity in both mouse and human. Nature 2012;483:350-354

8. Milligan G, Ulven T, Murdoch H, Hudson BD: G-protein-coupled receptors for free fatty acids: nutritional and therapeutic targets. The British journal of nutrition 2014;111 Suppl 1:S3-7

9. Hudson BD, Ulven T, Milligan G: The therapeutic potential of allosteric ligands for free fatty acid sensitive GPCRs. Current topics in medicinal chemistry 2013;13:14-25

10. Cinti S: The adipose organ. Prostaglandins, leukotrienes, and essential fatty acids 2005;73:9-15

11. Kershaw EE, Flier JS: Adipose tissue as an endocrine organ. The Journal of clinical endocrinology and metabolism 2004;89:2548-2556

12. Cannon B, Nedergaard J: Brown adipose tissue: function and physiological significance. Physiological reviews 2004;84:277-359

13. Fedorenko A, Lishko PV, Kirichok Y: Mechanism of fatty-acid-dependent UCP1 uncoupling in brown fat mitochondria. Cell 2012;151:400-413

14. Rosell M, Kaforou M, Frontini A, Okolo A, Chan YW, Nikolopoulou E, Millership S, Fenech ME, MacIntyre D, Turner JO, Moore JD, Blackburn E, Gullick WJ, Cinti S, Montana G, Parker MG, Christian M: Brown and white adipose tissues: intrinsic differences in gene expression and response to cold exposure in mice. American journal of physiology Endocrinology and metabolism 2014;306:E945-964

15. Shimpukade B, Hudson BD, Hovgaard CK, Milligan G, Ulven T: Discovery of a potent and selective GPR120 agonist. Journal of medicinal

6

chemistry 2012;55:4511-4515

16. Van Klinken JB, van den Berg SA, Havekes LM, Willems Van Dijk K: Estimation of activity related energy expenditure and resting metabolic rate in freely moving mice from indirect calorimetry data. PloS one 2012;7:e36162

17. Weir JB: New methods for calculating metabolic rate with special reference to protein metabolism. The Journal of physiology 1949;109:1-9

18. Zambon A, Hashimoto SI, Brunzell JD: Analysis of techniques to obtain plasma for measurement of levels of free fatty acids. Journal of lipid research 1993;34:1021-1028

19. Rensen PC, Herijgers N, Netscher MH, Meskers SC, van Eck M, van Berkel TJ: Particle size determines the specificity of apolipoprotein E-containing triglyceride-rich emulsions for the LDL receptor versus hepatic remnant receptor in vivo. Journal of lipid research 1997;38:1070-1084

20. Ibebunjo C, Eash JK, Li C, Ma Q, Glass DJ: Voluntary running, skeletal muscle gene expression, and signaling inversely regulated by orchidectomy and testosterone replacement. American journal of physiology Endocrinology and metabolism 2011;300:E327-340

21. Dubois V, Laurent MR, Jardi F, Antonio L, Lemaire K, Goyvaerts L, Deldicque L, Carmeliet G, Decallonne B, Vanderschueren D, Claessens F: Androgen Deficiency Exacerbates High-Fat Diet-Induced Metabolic Alterations in Male Mice. Endocrinology 2016;157:648-665

22. Garrel G, Simon V, Denoyelle C, Cruciani-Guglielmacci C, Migrenne S, Counis R, Magnan C, Cohen-Tannoudji J: Unsaturated fatty acids stimulate LH secretion via novel PKCepsilon and -theta in gonadotrope cells and inhibit GnRH-induced LH release. Endocrinology 2011;152:3905-3916

23. Moriyama R, Deura C, Imoto S, Nose K, Fukushima N: Expression of the long-chain fatty acid receptor GPR120 in the gonadotropes of the mouse anterior pituitary gland. Histochemistry and cell biology 2015;143:21-27

24. Quesada-Lopez T, Cereijo R, Turatsinze JV, Planavila A, Cairo M, Gavalda-Navarro A, Peyrou M, Moure R, Iglesias R, Giralt M, Eizirik DL, Villarroya F: The lipid sensor GPR120 promotes brown fat activation and FGF21 release from adipocytes. Nature communications 2016;7:13479

25. Berbée JF, Boon MR, Khedoe PP, Bartelt A, Schlein C, Worthmann A, Kooijman S, Hoeke G, Mol IM, John C, Jung C, Vazirpanah N, Brouwers LP, Gordts PL, Esko JD, Hiemstra PS, Havekes LM, Scheja L, Heeren J, Rensen PC: Brown fat activation reduces hypercholesterolaemia and protects from atherosclerosis development. Nature communications 2015;6:6356

26. Hudson BD, Shimpukade B, Mackenzie AE, Butcher AJ, Pediani JD, Christiansen E, Heathcote H, Tobin AB, Ulven T, Milligan G: The pharmacology of TUG-891, a potent and selective agonist of the free fatty acid receptor 4 (FFA4/GPR120), demonstrates both potential opportunity and possible challenges to therapeutic agonism. Molecular pharmacology 2013;84:710-725

27. Gozal D, Qiao Z, Almendros I, Zheng J, Khalyfa A, Shimpukade B, Ulven T: Treatment with TUG891, a free fatty acid receptor 4 agonist, restores adipose tissue metabolic dysfunction following chronic sleep fragmentation in mice. International journal of obesity (2005) 2016;40:1143-1149

28. Cartoni C, Yasumatsu K, Ohkuri T, Shigemura N, Yoshida R, Godinot N, le Coutre J, Ninomiya Y, Damak S: Taste preference for fatty acids is mediated by GPR40 and GPR120. The Journal of neuroscience : the official journal of the Society for Neuroscience 2010;30:8376-8382

29. Ancel D, Bernard A, Subramaniam S, Hirasawa A, Tsujimoto G, Hashimoto T, Passilly-Degrace

P, Khan NA, Besnard P: The oral lipid sensor GPR120 is not indispensable for the orosensory detection of dietary lipids in mice. Journal of lipid research 2015;56:369-378

30. Selfridge JM, Gotoh T, Schiffhauer S, Liu J, Stauffer PE, Li A, Capelluto DG, Finkielstein CV: Chronotherapy: Intuitive, Sound, Founded...But Not Broadly Applied. Drugs 2016;76:1507-1521

31. Gooley JJ: Circadian regulation of lipid metabolism. The Proceedings of the Nutrition Society 2016;75:440-450

32. Khedoe PP, Hoeke G, Kooijman S, Dijk W, Buijs JT, Kersten S, Havekes LM, Hiemstra PS, Berbée JF, Boon MR, Rensen PC: Brown adipose tissue takes up plasma triglycerides mostly after lipolysis. Journal of lipid research 2015;56:51-59

33. Yore MM, Syed I, Moraes-Vieira PM, Zhang T, Herman MA, Homan EA, Patel RT, Lee J, Chen S, Peroni OD, Dhaneshwar AS, Hammarstedt A, Smith U, McGraw TE, Saghatelian A, Kahn BB: Discovery of a class of endogenous mammalian lipids with anti-diabetic and anti-inflammatory effects. Cell 2014;159:318-332

6

Chapter | **7**

General discussion
and future perspectives

GENERAL DISCUSSION AND FUTURE PERSPECTIVES

The current worldwide obesity epidemic requires novel preventive and curative strategies. These strategies should not only aim at reducing obesity, but above all combat its related morbidities including type 2 diabetes and cardiovascular disease. Obesity leads to higher plasma lipid levels (*i.e.* cholesterol and triglycerides) and systemic inflammation. An exciting challenge within the dynamic field of immunometabolism is unraveling the molecular mechanisms connecting accumulation of adipose tissue, the subsequent increase in plasma lipids and systemic inflammation, and ultimately the development of type 2 diabetes and cardiovascular disease. A better understanding of these mechanisms will provide novel therapeutic targets and possibilities to improve treatment options.

To gain more insight into the role of the immune system in obesity, insulin resistance, dyslipidemia and atherosclerosis, we studied the effects of a bacterial infection and antibodies (IgG) on these parameters in several mouse models. We also investigated mediators of inflammation in blood and tissues of South Asians, a population with a particularly high risk of developing type 2 diabetes. Furthermore, we determined the potential of an anti-inflammatory compound and a fatty acid receptor agonist to reduce obesity and inflammation, and to ultimately improve glucose and lipid metabolism in mice.

From this thesis, various novel perceptions on the link between obesity, the immune system, and development of type 2 diabetes and cardiovascular disease have arisen which will be discussed and interpreted in this final chapter. Furthermore, therapeutic implications and future options for the management of metabolic disease will be addressed. The figure in this chapter is a graphical representation of the results obtained in this thesis (**Fig. 1**).

INFLAMMATION, LIPID METABOLISM AND ATHEROSCLEROSIS

Obesity is associated with high plasma levels of low density lipoprotein (LDL) cholesterol (1, 2) and inflammation (3, 4). Together with inflammation, cholesterol is a main risk factor for atherosclerosis as excess cholesterol initiates plaque formation in the arterial wall. Oxidized LDL (oxLDL) cholesterol is taken up by macrophages, upon which the macrophages turn into foam cells. Moreover, oxLDL triggers inflammation, *e.g.* by activating endothelial cells of the vessel wall to express adhesion molecules and chemokines such as the monocyte chemoattractant protein-1 (MCP-1), and thereby further enhancing plaque development (5-8). In **chapter 2**, we discovered that mycobacterial infection with BCG in *APOE*3-Leiden.CETP* (*E3L.CETP*) mice, despite overall immune activation, reduced plasma cholesterol levels and ultimately tended to reduce atherosclerosis development. This is a peculiar finding since alterations in levels of plasma lipids and plasma inflammatory mediators usually go hand in hand. As reviewed by Van Diepen *et al.* (7), various classes of lipid-lowering drugs have anti-inflammatory properties that are mainly attributable to the reduced presence of lipids, although lipid-lowering drugs also directly interfere with

inflammatory pathways. In turn, some anti-inflammatory drugs alter lipids levels, although the effects are ambiguous. For example, the inhibitor of NF-κB salicylate lowers plasma triglycerides in type 2 diabetes patients but not in individuals with pre-type 2 diabetes, and IL-6 signaling inhibitors raise plasma triglycerides in patients with rheumatoid arthritis. More investigations are needed to unravel the specific effects of anti-inflammatory drugs on lipid metabolism (7).

Even though inflammation and lipid levels usually go up or down together, other conditions exist in which an immune response is associated with lower lipid levels. Hepatitis C virus (HCV) infection causes hypolipidemia (9, 10), but the mechanism by which HCV deregulates lipid metabolism is different from what we think the mechanisms behind the cholesterol lowering effects of BCG are. While we observed that BCG increased cholesterol clearance and reduced intestinal cholesterol absorption, without evidence for reduced hepatic cholesterol synthesis, HCV interferes with host cholesterol metabolism by exploiting the lipoprotein machinery during replication in the hepatocyte (11, 12), resulting in lower synthesis of cholesterol (13). Despite the cholesterol-lowering effects of HCV infection, HCV infection was often reported to be associated with atherosclerosis (14, 15). One of the possible mechanisms mediating this link could be the activation of inflammatory processes and cytokine imbalance. It must be noted however that the results of studies describing the association between HCV infection and atherogenesis are not uniform and controversy still exists on the direction of the association (16). Knowing the relative contribution of inflammatory processes and lipid metabolism is a prerequisite to justify the development and application of anti-inflammatory drugs for the treatment of atherosclerosis, but lipid metabolism and inflammatory processes are so intertwined that it is nearly impossible to dissect what their relative contributions to atherogenesis are.

To accurately assess the relative contribution of cholesterol and inflammation in atherosclerosis development, superior mouse models than the currently available ones are needed. *E3L* and *E3L.CETP* mice express a mutation of the human *APOE*3* gene besides their endogenous apoE. This attenuates clearance of cholesterol-enriched lipoprotein remnants via the LDLR pathway, resulting in a humanized lipoprotein profile (17-19). Most studies performed in *E3L* and/or *E3L.CETP* mice to date investigated the effect of lipid level-modulating compounds on atherosclerosis (20-22). In most studies, the plasma total cholesterol exposure correlated with measures of the atherosclerotic lesion area (as in (17)), which underscores the high degree of dependence of atherogenesis on cholesterol levels in these models. Only few studies demonstrated a reducing effect of a compound on atherosclerosis beyond and independent of the reduction achieved by lowering of cholesterol by the compound alone in *E3L* mice (23, 24). These conclusions were drawn from an experimental set-up in which a separate cholesterol-fed control group was taken along with lower cholesterol intake that resulted in plasma cholesterol levels that were comparable to the cholesterol-fed group that was treated with the compound. In mice treated with rosuvastatin, the expression of MCP-1 and tumor necrosis factor (TNF) was lower than in the group with matched plasma cholesterol levels, and atherosclerosis was also lower than in the group with matched plasma cholesterol levels, indicating an additional

anti-inflammatory and inhibitory effect of rosuvastatin on atherogenesis (23). In another study, salicylate reduced hepatic NF-κB activity and macrophage content in plaques further than matched cholesterol feeding did, also pointing to an effect of salicylate independent of its cholesterol-lowering effect (24). Only one study in *E3L.CETP* mice showed increased rather than decreased inflammatory state without any effect on plasma lipid levels upon parasympathetic denervation of the spleen, evidenced by increased dendritic cells, B cells and T cells in the spleen, increased expression of inflammatory cytokines in the liver and in peritoneal leukocytes and increased levels of the cytokines IL-1β and IL-6 in the circulation. Nevertheless, this did not aggravate atherosclerosis development (25). Taken together, modulation of inflammation independently of lipid metabolism has hardly been studied in *E3L* and/or *E3L.CETP* mice and since many interventions modulate both lipids and inflammation, these models are not recommended if one wants to assess a pro- or anti-inflammatory effect on atherosclerosis development independent of alterations in lipid levels.

Apoe^{-/-} and *Ldlr*^{-/-} mice are the most widely used mouse models for atherosclerosis. Since these mice lack a functional hepatic ApoE-LDLR axis, the predominant route by which cholesterol-enriched lipoprotein remnants are cleared from the circulation (17), they do not respond to lipid-lowering therapies (26). *Apoe*^{-/-} mice spontaneously develop atherosclerosis, even on a chow diet which does not contain cholesterol. In contrast, *Ldlr*^{-/-} mice have a modest elevation of plasma cholesterol compared to wild-type mice and exhibit slow atherosclerosis development. Nevertheless, when fed a diet rich in cholesterol, these mice also have strongly elevated cholesterol and accelerated atherogenesis (26). ApoE not only mediates lipoprotein clearance, but also has anti-inflammatory and immunomodulatory properties. Compared to wild-type mice, *Apoe*^{-/-} mice have higher expression of immunostimulatory cell surface molecules on macrophages, which results in enhanced T cell activation compared to wild-type mice (27). When stimulated with LPS, *Apoe*^{-/-} mice show a higher upregulation of the pro-inflammatory cytokines TNF, IL-6, IL-12 and interferon-γ in liver and spleen compared to wild-type mice. This may also be explained by the ability of apoE to bind and inactivate LPS (28, 29). *Ldlr*^{-/-}*apobec-1*^{-/-} mice, which also display high cholesterol levels, do not exhibit this inflated cytokine response upon LPS injection, indicating that the increase in pro-inflammatory cytokines in *Apoe*^{-/-} mice upon LPS is independent of hypercholesterolemia (30). A mechanism explaining more inflammation in *Apoe*^{-/-} mice is that lack of ApoE also reduces the uptake of apoptotic bodies by macrophages, resulting in more apoptotic bodies and macrophage recruitment in the liver, lungs, brain and possibly more organs compared to wild-type mice. In addition, the pro-inflammatory markers TNF and fibrinogen are higher in livers of *Apoe*^{-/-} mice compared to wild-types. When comparing macrophage content between wild-type, *Apoe*^{-/-} mice and *Ldlr*^{-/-} mice, which have a similar lipoprotein profile as *Apoe*^{-/-} mice, *Ldlr*^{-/-} mice do not show increased macrophages in the lungs and only exhibit a ~1.5-fold upregulation of hepatic macrophages that does not reach significance compared to wild-type mice. In contrast, *Apoe*^{-/-} mice have a ~3-fold higher macrophage content in both liver and lungs compared to wild-type mice, which equals ~2-fold increases compared to *Ldlr*^{-/-}

7

mice (31). The augmented immune activation and ectopic macrophage recruitment in *Apoe*$^{-/-}$ mice possibly contributes to atherosclerosis.

These differences in clearance of cholesterol-enriched lipoprotein remnants and inflammatory state between mouse models for atherosclerosis may explain why studies are sometimes conflicting. For example, BAT activation increases the selective uptake of fatty acids from triglyceride-rich lipoproteins into BAT, resulting in the formation of cholesterol-enriched remnants. In *Apoe*$^{-/-}$ and *Ldlr*$^{-/-}$ mice, in which these remnants cannot be cleared by the liver, this leads to enhanced atherogenesis (17, 32). In contrast, BAT activation in E3L.CETP mice accelerates the hepatic clearance of these cholesterol-enriched remnants, resulting in protection from atherosclerosis development (17), an effect that may be expected relevant for most humans with an intact apoE-LDLr clearance pathway for lipoprotein remnants. As for the effect of BCG on atherosclerosis (**chapter 2**), different studies have been performed in different animal models. Subcutaneous BCG injections in rabbits of which plasma cholesterol levels were maintained within a certain range by varying the cholesterol content of the diet per rabbit revealed more atherogenesis upon BCG treatment (33). A study in which *Ldlr*$^{-/-}$ and *Apoe*$^{-/-}$ mice were treated with subcutaneous injections of freeze-dried BCG showed less atherogenesis (34). Both of these studies justly concluded that the effects of BCG on atherogenesis went through immunomodulatory mechanisms since the cholesterol levels between BCG-treated and control mice were similar. The differences in outcome between the studies (more *vs.* less atherosclerosis) are possibly due to differences in immune responses of rabbits vs mice, the difference in BCG used (live attenuated *vs.* freeze-dried), the dosing and number of injections with BCG and the amount of cholesterol in the diet, since cholesterol is also a pro-inflammatory stimulus. If one would be interested to know whether the BCG-induced infection and associated inflammation we observed upon intravenous administration of live attenuated BCG, independently of its cholesterol-lowering effect, accelerates atherosclerosis, a new experiment would have to be done in which a group with matched low cholesterol levels is included. Alternatively, the experiment could be repeated in *Ldlr*$^{-/-}$ mice.

Sometimes, the differences between mouse models for atherosclerosis may help to gain mechanistic insight. Since *Ldlr*$^{-/-}$ mice lack hepatic clearance of cholesterol-enriched remnants and do not show immunological abnormalities like *Apoe*$^{-/-}$ mice do, *Ldlr*$^{-/-}$ might be the best model to study the effect of immunomodulatory effects independent of lipid metabolism on atherosclerosis. However, in the end we strive for models that are as comparable as possible to humans, with the ultimate aim to predict how a compound acts in man. In this light, rabbits and E3L.CETP mice are still the best option we currently have.

ADIPOSE TISSUE INFLAMMATION AND TYPE 2 DIABETES

Inflammation is also believed to be an important link between accumulation of adipose tissue and development of type 2 diabetes. White adipose tissue (WAT) harbours many types of immune cells, of which the numbers increase during obesity (35-39). The

chronic inflammation associated with obesity disturbs insulin signalling in the tissue, since inflammatory cytokines activate JNK and IKKβ signalling pathways. This results in inhibitory phosphorylation of insulin receptor substrate 1 and 2 (IRS1 and IRS2), proteins that transmit signals from the insulin receptor to intracellular signalling pathways (40, 41). This inhibition of insulin signalling induces insulin resistance in white adipose tissue and contributes to development of type 2 diabetes. Macrophages were the first and most abundant type of immune cells discovered to infiltrate obese WAT (36, 42), for which the majority of research on immune cells in adipose tissue focuses on macrophages. Adipose tissue macrophages fulfil conventional functions such as clearing cellular debris and taking part in tissue immune surveillance. Macrophages also have a lipid buffering function; during lipolysis (*e.g.* upon fasting or adrenergic activation), macrophages take up and store lipids released from adipocytes in order to ensure gradual lipid release into the circulation (43). Recent studies have also focused on the function of other immune cell types in WAT inflammation, such as B cells. B cells were first reported to be present in adipose tissue in 2005 (44), and were subsequently found to be recruited to adipose tissue during high-fat diet (HFD) feeding (45). Winer *et al.* (46) showed that IgG, an antibody produced by B cells that activates complement and binds Fc receptors (FcRs), promotes insulin resistance and glucose intolerance. In **chapter 3**, we confirm that adipose tissue B cells and IgG are more abundant in obese compared to lean adipose tissue (also see graphical representation in **Fig. 1** of this discussion). However, we showed that lack of FcγR and complement C3, the two pathways through which IgG signals, does not ameliorate the development of HFD-induced glucose intolerance. This implicates that presence of FcγR and complement C3 is not critical for the development obesity-associated glucose intolerance. When investigating adipose tissue inflammation, we found that mice lacking FcγR and complement C3 did not exhibit any or only marginal differences (*i.e.* increased number of macrophages in WAT only in mice lacking both FcγR and complement C3) in inflammation compared to controls. Perhaps, counter-regulatory mechanisms between different elements of the immune system prevent that effects on metabolic parameters are active in mice that lack FcγR or complement C3. Possibly, the number of natural killer cells or other immune cell types that we did not measure may be increased in adipose tissue, as has been shown in mice lacking B and T cells compared to wild-type mice fed a HFD (45). Counter-regulatory mechanisms within the immune system may stretch beyond up- or downregulation of entire immune cell populations, as elevated inflammatory cytokine responses can already compensate deficiency of others (47). Of note, our finding that deficiency of B cell-derived IgG downstream signalling pathways (*i.e.* FcγR and complement C3, **chapter 3**) does not ameliorate development of glucose intolerance is supported by the report that deficiency of B and T cells does not affect the onset of obesity and the state of insulin resistance in mice (45). Overall, the complexity and versatility of the immune system complicate the research into immune modulation of adipose tissue and metabolic disorders. Since removing B cells or B cell components without inducing compensatory effects by other constituents of the immune system is not possible, the precise role of B cells in WAT inflammation and insulin resistance remains obscure.

7

In **chapter 4**, our purpose was to gain insight into the inflammatory state of WAT (and also skeletal muscle and blood) in a population with a high risk of type 2 diabetes. Since South Asians have an exceptionally high risk to develop this disorder compared to white Caucasians (48), we compared transcriptomic levels of a large panel of inflammatory, immune-regulating and immune cell subset markers in blood, skeletal muscle and WAT of overweight, pre-diabetic South Asian and matched white Caucasian men. It is generally known that obesity is associated with the infiltration of several immune cell types in WAT including macrophages, T cells and B cells, which are held responsible for the induction of chronic low-grade inflammation and development of insulin resistance (41). For this reason, we had expected increased expression of markers for these cell types in WAT of South Asians compared to white Caucasians. Surprisingly, expression levels of the main markers for immune cell subsets such as CD3, CD4 (T cells), CD19 (B cells) and the monocyte/ macrophage markers CD14, CD163 and CCL5 were comparable in WAT of South Asians and white Caucasians. Nevertheless, we revealed that South Asians have lower expression of interferon signalling genes in WAT than white Caucasians. These interferon signalling genes are transcribed by transcription factors called interferon regulatory factors (IRFs) (49). Interestingly, IRFs (IRF1-IRF9) were recently found to be expressed in adipose tissue, where they regulate adipogenesis (50). Subsequently, IRF4 was discovered to promote lipolysis and inhibit lipogenesis in adipocytes, indicating that this factor is involved in lipid handling within the adipose tissue. Moreover, lack of IRF4 increases adiposity in mice (51, 52). In contrast to IRF4, IRF3 protects from HFD-induced obesity (53), suggesting that the different IRFs have opposing functions which might be explained if they compete for the same co-factors. Together, these data imply that altered regulation of upstream transcription factors for interferon signalling such as IRF3 and IRF4 could, at least in part, underlie the higher abdominal adiposity in South Asians compared to white Caucasians (48, 54). Besides, links between interferon signalling and glucose metabolism exist. *Ifnβ1* overexpression maintains healthy glucose homeostasis upon HFD feeding of mice (55) whereas IRF4 deficiency and adipose tissue-specific knockout of *Ifnar1* deteriorate insulin resistance and glucose tolerance (52, 56). As South Asians are more glucose intolerant than white Caucasians (57), these data support the possibility of a link between the reduced interferon signaling in their WAT (**chapter 4** and **Fig. 1** of this discussion) and deteriorated glucose metabolism.

Obviously, interferon signaling may not be the only cause of the disadvantageous metabolic phenotype of South Asians. From literature it is known that South Asian newborns are characterized by elevated E-selectin and CRP levels in the cord blood, which suggests that endothelial dysfunction and enhanced inflammation are already present at birth in this population (58). Healthy lean adolescent South Asians have less BAT volume than matched white Caucasians (59), although this diminished BAT phenotype was not observed in the current study with overweight, pre-diabetic older South Asian and matched white Caucasian men (Boon & Hanssen, unpublished data). Nevertheless, the South Asians in the current study had reduced mitochondrial function as measured in skeletal muscle, which is probably the main reason for their lower energy expenditure compared to white Caucasians

7

(Boon & Hanssen, unpublished data). This finding matches the 'mitochondrial efficiency hypothesis' postulated by Bhopal and Rafnsson (60), who propose that differences in environmental stressors such as a cold environment for white Caucasians and a food shortage for South Asians have led to differences in mitochondrial coupling efficiency. As a result, white Caucasians produce relatively large amounts of heat during oxidative phosphorylation while in South Asians the conversion of energy to adenosine triphosphate (ATP) rather than to heat is maximised. The latter is very unfavourable in the current environment with abundance of food and reduced need to be physically active (60). It would be very exciting to assess whether evolutionary pressure led to differences in genes that contribute to mitochondrial function and inflammation in South Asians in genome-wide association studies in South Asians and white Caucasians. In addition, the relation between reduced interferon signalling in South Asians and their reduced mitochondrial function, BAT activity, energy expenditure and worsened glucose intolerance is an interesting field of future investigation.

THERAPEUTIC IMPLICATIONS

Obesity is associated with hyperlipidaemia (1, 2) and systemic inflammation (3, 4), which in turn are closely involved in the development of obesity-associated metabolic disorders (61, 62). In the first part of this discussion, lowering of cholesterol has already been passed in review and this is an effective strategy to reduce atherosclerosis and cardiovascular disease. In this section, additional strategies to constrain development of obesity-associated disorders by lowering plasma lipids and/or reducing inflammation to decrease development of atherosclerosis and insulin resistance will be discussed.

Triglyceride combustion by BAT and beige WAT

A promising therapeutic approach to reduce plasma triglyceride levels is to increase combustion of fatty acids by BAT. Activation of β3-adrenergic receptors on brown adipocytes is the most well-known and potent way to induce thermogenesis and lipid combustion (63, 64) and β3-adrenergic receptor agonists such as CL-316243 potently induce lipid uptake by BAT in mice (17). Many other compounds have also been identified to activate BAT. Among these, rimonabant (65), metformin (66), glucagon-like peptide-1 receptor activation (67) and salsalate (**chapter 5**) also reduce plasma triglycerides. We showed that salsalate does this by directly activating BAT (**Fig. 1**), evidenced by increased uncoupled respiration and lipolysis in brown adipocytes. Although it was long thought that salicylates exert their beneficial metabolic effects through activation of AMPK (68, 69), we found evidence for an alternative intracellular mechanism dependent on the PKA pathway. A later report by Smith *et al.* (70) confirms that AMPK does not mediate the beneficial effects of salicylates. Although they primarily focussed on glucose metabolism rather than triglycerides, they showed that mice lacking the AMPK subunit that salicylates interact with still experience beneficial effects on glucose metabolism upon salicylate treatment. Interestingly, the same

group also provided evidence for a mechanism by which salicylate induces mitochondrial uncoupling independent of UCP1, possibly explained by the protonophoric effects of salicylates, *i.e.* the ability to move protons across lipid bilayers (70). The potential of salsalate to directly induce mitochondrial uncoupling in primary hepatocytes (70) may also explain why salsalate prevents non-alcoholic steatohepatitis (71). If salsalate indeed functions as a mitochondrial uncoupler in any cell type, this also clarifies how salsalate increases energy expenditure in human subjects (72). Other protonophoric compounds are probably effective to lower plasma triglycerides by activating BAT too. However, systemic treatment with mitochondrial uncouplers can be very dangerous; the mitochondrial uncoupler 2,4-dinitrophenol (DNP) induces weight loss but is associated with side effects like hyperthermia, tachycardia and death (73-75). In order to safely induce weight loss by activating BAT with mitochondrial uncouplers, improved ways to specifically target BAT would be warranted first.

A novel approach to activate BAT is via GPR120, a free fatty acid receptor that is activated by medium and long chain fatty acids (76). GPR120 is highly expressed in WAT and BAT and others have shown that GPR120 mediates anti-inflammatory actions of ω-3 fatty acids (77-79), plays a role in adipocyte differentiation (80), and enhances glucose uptake, which contributes to improved insulin sensitivity (77). Lack of GPR120 leads to obesity, glucose intolerance and hepatic steatosis (81). Our incentive to study whether stimulation of GPR120 could activate BAT was the fact that *Gpr120* expression in BAT increases upon cold exposure (82), which indicates a role for GPR120 in thermogenesis. We found that lack of GPR120 increased fat mass and reduced energy expenditure, but did not have evident effects on triglyceride-rich lipoprotein turnover. Promisingly, injections with the GPR120 agonist TUG891 increased fat oxidation and reduced fat mass (**chapter 6**). While we were performing these experiments, others already published that the GPR120 agonist GW9508 activates BAT (**Fig. 1**) (83). Although these are encouraging results, future studies (which will soon be performed by Schilperoort *et al.*) will have to elucidate whether BAT activation by GPR120 agonists also leads to enhanced triglyceride-derived fatty acid uptake by BAT and consequently lower plasma lipids.

An alternative therapeutic approach is to induce the formation of beige adipocytes in WAT, because beige adipocytes probably also use triglycerides for nonshivering thermogenesis like classic brown adipocytes do. This is supported by the fact that fatty acid uptake in beige WAT upon β3-adrenergic stimulation increases while the WAT depots shrink (17). Beiging of WAT is typically induced by cold and catecholamine stimulation (17, 84, 85), but many other stimuli that promote a beige phenotype are rapidly being discovered and include pharmacological activation of β3-adrenergic receptors (17, 64), thyroid hormone (86), glucagon-like peptide 1 receptor activation (67), fibroblast growth factor 21 (87), and bone morphogenetic protein 7 (88). Furthermore, various components of the immune system have been implicated to promote beiging, such as alternatively activated macrophages (89, 90), eosinophils (91) and ILC2s (92, 93). Several cytokines were identified to be involved in the underlying mechanisms and recent evidence also points towards a prominent role for interferon regulatory factors in the regulation of beiging (52, 53). Thus,

genesis and activation of beige adipocytes is an alternative pharmacological strategy to combust lipids and thereby reduce lipid levels in the blood.

Although it was long thought that beige adipocytes are derived from Myf5^{+} precursor cells whereas white adipocytes are not, the current model of the differentiation process seems more complex as Myf5^{+} cells can also differentiate into white adipocytes. More specific factors that mark brown/beige adipogenesis (*e.g.* the transcription factor Ebf2) are presently being discovered (94). Gaining a better understanding of adipocyte development is a prerequisite for the development of compounds that promote beige adipocyte differentiation and is under investigation.

Cholesterol lowering strategies

Whether triglycerides are an independent risk factor for cardiovascular disease is still under debate (95), but cholesterol certainly is the main risk factor for atherosclerosis development (6). Therefore, cholesterol-lowering strategies are effective in battling atherosclerosis. In **chapter 2**, we found that mycobacterial BCG infection lowered cholesterol partly by increasing hepatic uptake of cholesterol. We speculate that the accumulation of mycobacteria we detected in the liver could be responsible for this increased cholesterol uptake (**Fig. 1** of this discussion), as mycobacteria use host cholesterol as an energy source (96-99). Since humans cannot use cholesterol as an energy source like triglycerides, the most effective strategy to lower cholesterol levels in humans is inhibition of HMG-CoA reductase, which decreases cholesterol synthesis in the liver. Other approaches are inhibition of intestinal cholesterol absorption and sequestration of bile acids. Bile acid sequestrants bind bile acids in the intestine, thereby preventing their reabsorption and leading to increased fecal excretion. This reduces the bile acid pool in the liver and thereby stimulates bile acid synthesis from cholesterol. Consequently, hepatic uptake of cholesterol is increased to replenish hepatic cholesterol levels and plasma cholesterol levels are lowered. The most recent addition to cholesterol lowering drugs are proprotein convertase subtilisin kexin type 9 (PCSK9) inhibitors. PCSK9 binds to the LDL receptor (mainly in the liver), resulting in intracellular degradation of the receptor and a subsequent decrease in LDL receptors on the plasma membrane. By preventing PCSK9 binding to LDL receptors with PCSK9 inhibitors, LDL receptor degradation is prevented, which results in increased LDL receptor expression and enhanced hepatic uptake of LDL from the circulation (100). As discussed above, BAT activation not only has the potential to reduce plasma triglyceride levels (101, 102), but activation of BAT by β3-adrenergic receptor stimulation in *E3L.CETP* mice also lowers cholesterol levels by indirectly accelerating the hepatic clearance of cholesterol-enriched remnants (17). Although (temporarily) introducing a cholesterol-consuming bacterium is far from optimal considering the pathogenic nature of *e.g. Mycobacterium tuberculosis* or *Mycobacterium leprae* (103), it would be neat to find a novel strategy to combust cholesterol in a similar way as BAT is able to burn triglycerides.

7

Anti-inflammatory strategies

Taking into account the wide spectrum of inflammatory cells and cytokines that are elevated in obesity, targeting a single cell, factor or cytokine might not be efficient to reduce systemic inflammation and ways to manage the overall metabolic inflammation should be considered. In this light, salicylates, such as salsalate, are favourable as they inhibit the master regulatory protein complex of inflammation NF-κB and thereby transcription of many inflammatory cytokines (104). Despite the fact that salicylates were shown to lower glucose levels in diabetic individuals more than 100 years ago (4, 105), and since then a large amount of research was dedicated to the role of inflammation in both insulin resistance and atherosclerosis, salicylates have not been applied in the clinic to treat these disorders yet. In **chapter 5**, we show that salsalate not only improves glucose metabolism, but also reduces inflammation in WAT (**Fig. 1** of this discussion). Although we did not demonstrate a causal relationship between the reduced adipose tissue inflammation and the improved glucose metabolism observed, it does confirm that the two effects go together. Promisingly, salicylate was also shown to reduce atherosclerosis partly by quenching inflammation. As described above, this was proven by showing that salicylate treatment reduces hepatic NF-κB activity and macrophage content in plaques further than low cholesterol feeding (to achieve similar plasma cholesterol levels in the salicylate-treated and the control group) did (24).

Since South Asians have reduced expression of type 1 interferon signalling in WAT (**chapter 4**) and a disadvantageous metabolic phenotype including obesity and insulin resistance (106, 107), one could speculate that anti-inflammatory type 1 interferons would qualify to treat adipose tissue inflammation and/or insulin resistance and atherosclerosis in this population. Interferons are currently used to treat viral infections (108) but have never been applied or tested to treat metabolic inflammation. Although more insight into the link between interferon signalling in adipose tissue and metabolic health would be useful, investigating whether interferon treatment would be effective to reduce metabolic disease in humans does not entail a high risk because interferons are approved drugs (108).

In summary, type 2 diabetes and atherosclerosis are both characterized by systemic inflammation and a decent amount of evidence suggests that targeting inflammation with pharmacological interventions may improve these metabolic disorders.

TRANSLATIONAL CHALLENGES

Large quantities of studies aimed at reducing the obesity epidemic and related morbidities are currently being performed in mice, which ultimately need to be translated towards the human situation. For instance, anti-inflammatory strategies to reduce atherosclerosis and insulin resistance may deserve faster implementation in the clinic if only we could show how and to which extent the immune system exactly contributes to these metabolic derangements in humans. The fact that lipid metabolism and inflammation are intertwined (7) complicates progress within this field of research. HMG-CoA reductase inhibitors

(*i.e.* statins) reduce C-reactive protein (CRP, a marker of inflammation) levels besides lowering LDL cholesterol in clinical trials (109-111). When added to statins, the cholesterol absorption inhibitor ezetimibe also reduces CRP (112). It was recently reported that PCSK9 is directly involved in promoting inflammatory processes (113, 114) and thereby contributes to atherosclerosis independent of cholesterol, which suggests that even PCSK9 inhibition may reduce inflammation (114). Comparative studies into the differential effects of statins, ezetimibe and PCSK9 inhibitors on cholesterol levels, inflammatory markers and cardiovascular outcome may shed more light upon the relative contribution of inflammation and cholesterol on cardiovascular disease in humans. It would also be interesting to take along assessment of the inflammatory phenotype of WAT and skeletal muscles more often in clinical studies as we did in **chapter 4**, to gain a better understanding of potential anti-inflammatory effects of promising compounds on these tissues.

With regards to lowering triglycerides by activating BAT and beige WAT, combusting lipids this way prevents obesity and atherosclerosis in mice, but the translational value of these promising results from different mouse models for the human situation is still uncertain. Interscapular classical BAT in mice does not regress with age whereas adult humans no longer possess this classical BAT depot. Another difficulty in extrapolating mouse data to the human is the fact that humans are usually situated in a thermoneutral zone (±25°C) due to the wearing of clothes, while mice are often housed at room temperature (18-22°C) at which BAT is active. Housing mice in their thermoneutral condition (30°C) would be more comparable to the human situation, which is not always acknowledged. Future studies BAT activation and beiging in mice should therefore preferably be performed at 30°C.

Interestingly, mechanisms of beiging of WAT display more similarities between mice and humans. Hormones, immune cells or cytokines that induce beige adipocytes in mice are also present in humans, suggesting that beiging via those mechanisms can also occur in humans. For example, presence of ILC2s in human adipose tissue has been confirmed, suggesting that the circuit of ILC2s, eosinophils, type 2 cytokines and anti-inflammatory macrophages that induce beiging in mice, is also operational in human beiging (115). Severe beiging of WAT is also seen in patients with pheochromocytoma, a catecholamine-secreting tumor. This condition indeed leads to increased energy expenditure (116). Together, these observations support a similar mechanism behind beiging in humans and in mice, although beiging capacity and its contribution to energy expenditure in humans still needs to be determined in detail.

Potential drugs that induce beiging of WAT in humans are currently being tested in the clinic (117). A possible target would be the β3-adrenergic receptor, although it is not specific for brown adipocytes as it is expressed in a variety of organs. Until recently, β-adrenergic receptor agonists had not been shown to have major effects on energy balance. In 2015, it was shown that a latest generation β-adrenergic receptor agonist, mirabegron (approved to treat the overactive bladder), activated BAT evidenced by increased [^{18}F]fluorodeoxyglucose (FDG) uptake, and increased energy expenditure in healthy male subjects (118). As for targeting inflammation, the effects of salsalate (**chapter 5**) are currently being investigated in clinical trials (119-122). Promisingly, some studies show that salsalate improves glycemic
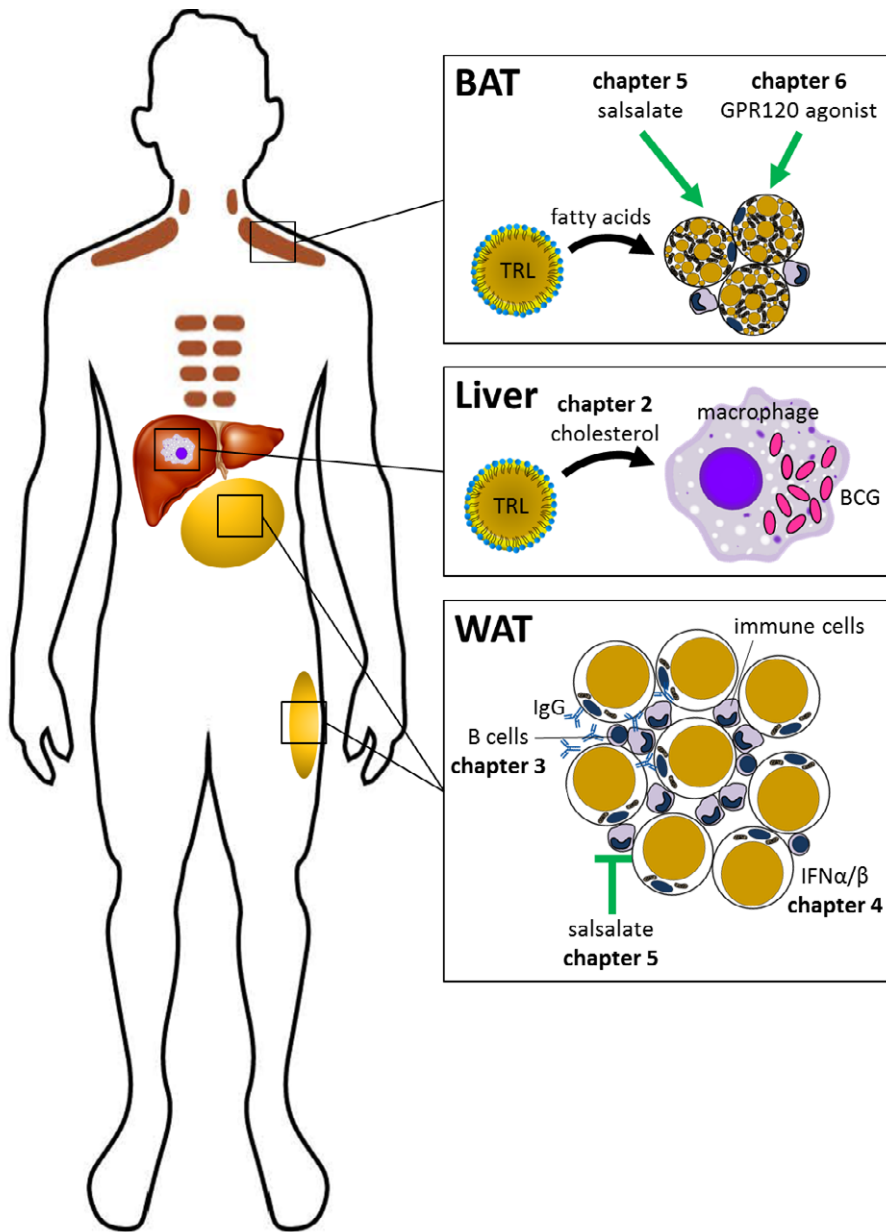
7

Figure 1. Immune modulation of adipose tissue and lipid metabolism. *See text for explanation. BAT, brown adipose tissue; BCG, Bacille-Calmette-Guérin; IFN, interferon; TRL, triglyceride-rich lipoprotein; WAT, white adipose tissue.*

control (123) and reduces systemic inflammation (119, 124, 125). However, salsalate did not reduce noncalcified coronary plaque volume in man (119), and thus the question remains whether reducing inflammation per se also reduces cardiovascular disease in humans.

Besides receptor-targeted drugs, diet and nutritional components can be considered as an alternative strategy to modulate thermogenesis and inflammation in humans. Although it is known that brown, beige and white adipocytes are fuelled by glucose and fatty acids, large knowledge gaps still exist. We still do not know whether different types of dietary fatty acids or carbohydrates elicit distinct effects on thermogenesis and inflammation. Whereas saturated fatty acids promote inflammation and are detrimental for metabolic health (126), n-3 fatty acids are anti-inflammatory and act beneficially (127). Whether dietary n-3 fatty acids activate BAT or promote beiging remains to be investigated. As for specific carbohydrates, hardly anything is known about their effects on BAT activity or beiging. Almost 30 years ago, Walgren *et al.* (128) showed that dietary carbohydrates increase noradrenaline turnover in heart and/or BAT of rats, unrelated to the type of carbohydrate (*i.e.* fructose, sucrose, dextrose, corn starch) (128). These promising data have not been followed up. Other nutritional components of interest may be amino acids. High plasma concentrations of branched-chain amino acids are found in obesity and type 2 diabetes, and they are associated with increased cardiovascular risk (129). In mice, dietary restriction for the amino acid methionine activates BAT (130). Together, this suggests that altered intake of amino acids could modulate metabolic health. Future research might shed light on the underexposed aspect of modulating inflammation and thermogenesis and ultimately metabolic health by nutritional components.

7

CONCLUDING REMARKS AND FUTURE PERSPECTIVES

The immune system plays an important role in brown and white adipose tissue and lipid metabolism and mechanisms behind the interactions between immune cells, adipocytes and lipids are gradually being uncovered. These mechanisms could yield targets to develop novel therapeutic strategies to lower plasma lipid levels, attenuate adipose tissue and systemic inflammation, and ultimately reduce atherosclerosis and insulin resistance. Currently, the most favourable novel approach to eliminate triglycerides and possibly also cholesterol is by increasing combustion of fatty acids in BAT or beige adipocytes in WAT. Combining this with anti-inflammatory therapies to restrain systemic and adipose tissue inflammation will probably further improve metabolic outcome by uncoupling obesity from its associated disorders that are mediated by inflammation. Since the immune system and its functioning are very complex, targeting central mediators of inflammation (*i.e.* transcription factors or upstream regulators of main inflammatory pathways such as NF-κB or IRFs) are probably preferred.

In order to find novel and effective therapeutic targets, the challenge is to identify the metabolic crosstalk between (brown, beige and white) adipocytes and immune cells and the order of events that occur during obesity development. Immune modulation of adipose

tissue and lipid metabolism will not come down to an individual immune cell type and will involve significant crosstalk between different cell types. Important questions to further address include: What are the immune regulatory effector molecules that are secreted by adipocytes to attract or regulate immune cells? How are browning and the immune system regulated in obesity? And how do these processes change during aging? And last but not least, it is of great importance to translate these findings towards the clinic in favour of developing effective and safe treatment options for the patient.

7

REFERENCES

1. Klop B, Elte JW, Cabezas MC: Dyslipidemia in obesity: mechanisms and potential targets. Nutrients 2013;5:1218-1240

2. Nordestgaard BG: Triglyceride-Rich Lipoproteins and Atherosclerotic Cardiovascular Disease: New Insights From Epidemiology, Genetics, and Biology. Circulation research 2016;118:547-563

3. Hotamisligil GS: Inflammation and metabolic disorders. Nature 2006;444:860-867

4. Shoelson SE, Lee J, Goldfine AB: Inflammation and insulin resistance. The Journal of clinical investigation 2006;116:1793-1801

5. Getz GS, Reardon CA: The mutual interplay of lipid metabolism and the cells of the immune system in relation to atherosclerosis. Clinical lipidology 2014;9:657-671

6. Steinberg D: Atherogenesis in perspective: hypercholesterolemia and inflammation as partners in crime. Nature medicine 2002;8:1211-1217

7. van Diepen JA, Berbee JF, Havekes LM, Rensen PC: Interactions between inflammation and lipid metabolism: relevance for efficacy of anti-inflammatory drugs in the treatment of atherosclerosis. Atherosclerosis 2013;228:306-315

8. Schaftenaar F, Frodermann V, Kuiper J, Lutgens E: Atherosclerosis: the interplay between lipids and immune cells. Curr Opin Lipidol 2016;27:209-215

9. Serfaty L, Andreani T, Giral P, Carbonell N, Chazouilleres O, Poupon R: Hepatitis C virus induced hypobetalipoproteinemia: a possible mechanism for steatosis in chronic hepatitis C. Journal of hepatology 2001;34:428-434

10. Miyazaki T, Honda A, Ikegami T, Saitoh Y, Hirayama T, Hara T, Doy M, Matsuzaki Y: Hepatitis C virus infection causes hypolipidemia regardless of hepatic damage or nutritional state: An epidemiological survey of a large

Japanese cohort. Hepatology research : the official journal of the Japan Society of Hepatology 2011;41:530-541

11. Grassi G, Di Caprio G, Fimia GM, Ippolito G, Tripodi M, Alonzi T: Hepatitis C virus relies on lipoproteins for its life cycle. World journal of gastroenterology 2016;22:1953-1965

12. Aizawa Y, Seki N, Nagano T, Abe H: Chronic hepatitis C virus infection and lipoprotein metabolism. World journal of gastroenterology 2015;21:10299-10313

13. Clark PJ, Thompson AJ, Vock DM, Kratz LE, Tolun AA, Muir AJ, McHutchison JG, Subramanian M, Millington DM, Kelley RI, Patel K: Hepatitis C virus selectively perturbs the distal cholesterol synthesis pathway in a genotype-specific manner. Hepatology (Baltimore, Md) 2012;56:49-56

14. Huang H, Kang R, Zhao Z: Is hepatitis C associated with atherosclerotic burden? A systematic review and meta-analysis. PloS one 2014;9:e106376

15. Olubamwo OO, Onyeka IN, Miettola J, Kauhanen J, Tuomainen TP: Hepatitis C as a risk factor for carotid atherosclerosis – a systematic review. Clinical physiology and functional imaging 2016;36:249-260

16. Ishizaka N, Ishizaka Y, Yamkado M: Atherosclerosis as a possible extrahepatic manifestation of chronic hepatitis C virus infection. Clinical Medicine Insights Cardiology 2014;8:1-5

17. Berbée JF, Boon MR, Khedoe PP, Bartelt A, Schlein C, Worthmann A, Kooijman S, Hoeke G, Mol IM, John C, Jung C, Vazirpanah N, Brouwers LP, Gordts PL, Esko JD, Hiemstra PS, Havekes LM, Scheja L, Heeren J, Rensen PC: Brown fat activation reduces hypercholesterolaemia and protects from atherosclerosis development. Nature communications 2015;6:6356

7

18. Westerterp M, van der Hoogt CC, de Haan W, Offerman EH, Dallinga-Thie GM, Jukema JW, Havekes LM, Rensen PC: Cholesteryl ester transfer protein decreases high-density lipoprotein and severely aggravates atherosclerosis in APOE*3-Leiden mice. Arteriosclerosis, thrombosis, and vascular biology 2006;26:2552-2559

19. van den Maagdenberg AM, Hofker MH, Krimpenfort PJ, de Bruijn I, van Vlijmen B, van der Boom H, Havekes LM, Frants RR: Transgenic mice carrying the apolipoprotein E3-Leiden gene exhibit hyperlipoproteinemia. The Journal of biological chemistry 1993;268:10540-10545

20. Berbee JF, Wong MC, Wang Y, van der Hoorn JW, Khedoe PP, van Klinken JB, Mol IM, Hiemstra PS, Tsikas D, Romijn JA, Havekes LM, Princen HM, Rensen PC: Resveratrol protects against atherosclerosis, but does not add to the antiatherogenic effect of atorvastatin, in APOE*3-Leiden.CETP mice. The Journal of nutritional biochemistry 2013;24:1423-1430

21. Kuhnast S, Louwe MC, Heemskerk MM, Pieterman EJ, van Klinken JB, van den Berg SA, Smit JW, Havekes LM, Rensen PC, van der Hoorn JW, Princen HM, Jukema JW: Niacin Reduces Atherosclerosis Development in APOE*3Leiden. CETP Mice Mainly by Reducing NonHDL-Cholesterol. PloS one 2013;8:e66467

22. Kuhnast S, van der Tuin SJ, van der Hoorn JW, van Klinken JB, Simic B, Pieterman E, Havekes LM, Landmesser U, Luscher TF, Willems van Dijk K, Rensen PC, Jukema JW, Princen HM: Anacetrapib reduces progression of atherosclerosis, mainly by reducing non-HDL-cholesterol, improves lesion stability and adds to the beneficial effects of atorvastatin. European heart journal 2015;36:39-48

23. Kleemann R, Princen HM, Emeis JJ, Jukema JW, Fontijn RD, Horrevoets AJ, Kooistra T, Havekes LM: Rosuvastatin reduces atherosclerosis development beyond and independent of its plasma cholesterol-lowering effect in APOE*3-Leiden transgenic mice: evidence for antiinflammatory effects of rosuvastatin. Circulation 2003;108:1368-1374

24. de Vries-van der Weij J, Toet K, Zadelaar S, Wielinga PY, Kleemann R, Rensen PC, Kooistra T: Anti-inflammatory salicylate beneficially modulates pre-existing atherosclerosis through quenching of NF-kappaB activity and lowering of cholesterol. Atherosclerosis 2010;213:241-246

25. Kooijman S, Meurs I, van Beek L, Khedoe PP, Giezekamp A, Pike-Overzet K, Cailotto C, van der Vliet J, van Harmelen V, Boeckxstaens G, Berbee JF, Rensen PC: Splenic autonomic denervation increases inflammatory status but does not aggravate atherosclerotic lesion development. American journal of physiology Heart and circulatory physiology 2015;309:H646-654

26. Zadelaar S, Kleemann R, Verschuren L, de Vries-Van der Weij J, van der Hoorn J, Princen HM, Kooistra T: Mouse models for atherosclerosis and pharmaceutical modifiers. Arteriosclerosis, thrombosis, and vascular biology 2007;27:1706-1721

27. Tenger C, Zhou X: Apolipoprotein E modulates immune activation by acting on the antigen-presenting cell. Immunology 2003;109:392-397

28. Rensen PC, Oosten M, Bilt E, Eck M, Kuiper J, Berkel TJ: Human recombinant apolipoprotein E redirects lipopolysaccharide from Kupffer cells to liver parenchymal cells in rats In vivo. The Journal of clinical investigation 1997;99:2438-2445

29. Van Oosten M, Rensen PC, Van Amersfoort ES, Van Eck M, Van Dam AM, Breve JJ, Vogel T, Panet A, Van Berkel TJ, Kuiper J: Apolipoprotein E protects against bacterial lipopolysaccharide-induced lethality. A new therapeutic approach to treat gram-negative sepsis. The Journal of biological chemistry 2001;276:8820-8824

30. Ali K, Middleton M, Pure E, Rader DJ: Apolipoprotein E suppresses the type I

7

inflammatory response in vivo. Circulation research 2005;97:922-927

31. Grainger DJ, Reckless J, McKilligin E: Apolipoprotein E modulates clearance of apoptotic bodies in vitro and in vivo, resulting in a systemic proinflammatory state in apolipoprotein E-deficient mice. Journal of immunology (Baltimore, Md : 1950) 2004;173:6366-6375

32. Dong M, Yang X, Lim S, Cao Z, Honek J, Lu H, Zhang C, Seki T, Hosaka K, Wahlberg E, Yang J, Zhang L, Lanne T, Sun B, Li X, Liu Y, Zhang Y, Cao Y: Cold exposure promotes atherosclerotic plaque growth and instability via UCP1-dependent lipolysis. Cell Metab 2013;18:118-129

33. Lamb DJ, Eales LJ, Ferns GA: Immunization with bacillus Calmette-Guerin vaccine increases aortic atherosclerosis in the cholesterol-fed rabbit. Atherosclerosis 1999;143:105-113

34. Ovchinnikova OA, Berge N, Kang C, Urien C, Ketelhuth DF, Pottier J, Drouet L, Hansson GK, Marchal G, Back M, Schwartz-Cornil I, Lagranderie M: Mycobacterium bovis BCG killed by extended freeze-drying induces an immunoregulatory profile and protects against atherosclerosis. Journal of internal medicine 2014;275:49-58

35. Lumeng CN, Bodzin JL, Saltiel AR: Obesity induces a phenotypic switch in adipose tissue macrophage polarization. The Journal of clinical investigation 2007;117:175-184

36. Weisberg SP, McCann D, Desai M, Rosenbaum M, Leibel RL, Ferrante AW, Jr.: Obesity is associated with macrophage accumulation in adipose tissue. The Journal of clinical investigation 2003;112:1796-1808

37. Elgazar-Carmon V, Rudich A, Hadad N, Levy R: Neutrophils transiently infiltrate intra-abdominal fat early in the course of high-fat feeding. Journal of lipid research 2008;49:1894-1903

38. Talukdar S, Oh DY, Bandyopadhyay G, Li D, Xu J, McNelis J, Lu M, Li P, Yan Q, Zhu Y, Ofrecio

J, Lin M, Brenner MB, Olefsky JM: Neutrophils mediate insulin resistance in mice fed a high-fat diet through secreted elastase. Nature medicine 2012;18:1407-1412

39. Wu D, Molofsky AB, Liang H-E, Ricardo-Gonzalez RR, Jouihan HA, Bando JK, Chawla A, Locksley RM: Eosinophils Sustain Adipose Alternatively Activated Macrophages Associated with Glucose Homeostasis. Science 2011;332:243-247

40. Lumeng CN, Saltiel AR: Inflammatory links between obesity and metabolic disease. Journal of Clinical Investigation 2011;121:2111-2117

41. Chawla A, Nguyen KD, Goh YPS: Macrophage-mediated inflammation in metabolic disease. Nature Reviews Immunology 2011;11:738-749

42. van Beek L, van Klinken JB, Pronk AC, van Dam AD, Dirven E, Rensen PC, Koning F, Willems van Dijk K, van Harmelen V: The limited storage capacity of gonadal adipose tissue directs the development of metabolic disorders in male C57Bl/6J mice. Diabetologia 2015;58:1601-1609

43. Boutens L, Stienstra R: Adipose tissue macrophages: going off track during obesity. Diabetologia 2016;59:879-894

44. Caspar-Bauguil S, Cousin B, Galinier A, Segafredo C, Nibbelink M, Andre M, Casteilla L, Penicaud L: Adipose tissues as an ancestral immune organ: site-specific change in obesity. FEBS letters 2005;579:3487-3492

45. Duffaut C, Galitzky J, Lafontan M, Bouloumie A: Unexpected trafficking of immune cells within the adipose tissue during the onset of obesity. Biochemical and biophysical research communications 2009;384:482-485

46. Winer DA, Winer S, Shen L, Wadia PP, Yantha J, Paltser G, Tsui H, Wu P, Davidson MG, Alonso MN, Leong HX, Glassford A, Caimol M, Kenkel JA, Tedder TF, McLaughlin T, Miklos DB, Dosch HM, Engleman EG: B cells promote insulin resistance through modulation of T cells and production

of pathogenic IgG antibodies. Nature medicine 2011;17:610-617

47. Mayer-Barber KD, Yan B: Clash of the Cytokine Titans: counter-regulation of interleukin-1 and type I interferon-mediated inflammatory responses. Cellular & molecular immunology 2017;14:22-35

48. Raji A, Seely EW, Arky RA, Simonson DC: Body fat distribution and insulin resistance in healthy Asian Indians and Caucasians. The Journal of clinical endocrinology and metabolism 2001;86:5366-5371

49. Ivashkiv LB, Donlin LT: Regulation of type I interferon responses. Nature reviews Immunology 2014;14:36-49

50. Eguchi J, Yan QW, Schones DE, Kamal M, Hsu CH, Zhang MQ, Crawford GE, Rosen ED: Interferon regulatory factors are transcriptional regulators of adipogenesis. Cell metabolism 2008;7:86-94

51. Eguchi J, Wang X, Yu S, Kershaw EE, Chiu PC, Dushay J, Estall JL, Klein U, Maratos-Flier E, Rosen ED: Transcriptional control of adipose lipid handling by IRF4. Cell metabolism 2011;13:249-259

52. Kong X, Banks A, Liu T, Kazak L, Rao RR, Cohen P, Wang X, Yu S, Lo JC, Tseng YH, Cypess AM, Xue R, Kleiner S, Kang S, Spiegelman BM, Rosen ED: IRF4 is a key thermogenic transcriptional partner of PGC-1alpha. Cell 2014;158:69-83

53. Kumari M, Wang X, Lantier L, Lyubetskaya A, Eguchi J, Kang S, Tenen D, Roh HC, Kong X, Kazak L, Ahmad R, Rosen ED: IRF3 promotes adipose inflammation and insulin resistance and represses browning. The Journal of clinical investigation 2016;126:2839-2854

54. Lear SA, Humphries KH, Kohli S, Birmingham CL: The use of BMI and waist circumference as surrogates of body fat differs by ethnicity. Obesity (Silver Spring, Md) 2007;15:2817-2824

55. Alsaggar M, Mills M, Liu D: Interferon beta overexpression attenuates adipose tissue inflammation and high-fat diet-induced obesity and maintains glucose homeostasis. Gene therapy 2016;24:60-66

56. Wieser V, Adolph TE, Grander C, Grabherr F, Enrich B, Moser P, Moschen AR, Kaser S, Tilg H: Adipose type I interferon signalling protects against metabolic dysfunction. Gut 2016; in press

57. McKeigue PM, Ferrie JE, Pierpoint T, Marmot MG: Association of early-onset coronary heart disease in South Asian men with glucose intolerance and hyperinsulinemia. Circulation 1993;87:152-161

58. Boon MR, Karamali NS, de Groot CJ, van Steijn L, Kanhai HH, van der Bent C, Berbee JF, Middelkoop B, Rensen PC, Tamsma JT: E-selectin is elevated in cord blood of South Asian neonates compared with Caucasian neonates. The Journal of pediatrics 2012;160:844-848. e841

59. Bakker LE, Boon MR, van der Linden RA, Arias-Bouda LP, van Klinken JB, Smit F, Verberne HJ, Jukema JW, Tamsma JT, Havekes LM, van Marken Lichtenbelt WD, Jazet IM, Rensen PC: Brown adipose tissue volume in healthy lean south Asian adults compared with white Caucasians: a prospective, case-controlled observational study. The lancet Diabetes & endocrinology 2014;2:210-217

60. Bhopal RS, Rafnsson SB: Could mitochondrial efficiency explain the susceptibility to adiposity, metabolic syndrome, diabetes and cardiovascular diseases in South Asian populations? International journal of epidemiology 2009;38:1072-1081

61. Shoelson SE, Herrero L, Naaz A: Obesity, inflammation, and insulin resistance. Gastroenterology 2007;132:2169-2180

62. Legein B, Temmerman L, Biessen EA, Lutgens E: Inflammation and immune system interactions in atherosclerosis. Cellular and molecular life sciences : CMLS 2013;70:3847-3869

7

63. Cannon B, Nedergaard J: Brown adipose tissue: function and physiological significance. Physiological reviews 2004;84:277-359

64. Cypess AM, Weiner LS, Roberts-Toler C, Franquet Elia E, Kessler SH, Kahn PA, English J, Chatman K, Trauger SA, Doria A, Kolodny GM: Activation of human brown adipose tissue by a beta3-adrenergic receptor agonist. Cell Metab 2015;21:33-38

65. Boon MR, Kooijman S, van Dam AD, Pelgrom LR, Berbée JF, Visseren CA, van Aggele RC, van den Hoek AM, Sips HC, Lombes M, Havekes LM, Tamsma JT, Guigas B, Meijer OC, Jukema JW, Rensen PC: Peripheral cannabinoid 1 receptor blockade activates brown adipose tissue and diminishes dyslipidemia and obesity. FASEB journal : official publication of the Federation of American Societies for Experimental Biology 2014;28:5361-5375

66. Geerling JJ, Boon MR, van der Zon GC, van den Berg SA, van den Hoek AM, Lombes M, Princen HM, Havekes LM, Rensen PC, Guigas B: Metformin lowers plasma triglycerides by promoting VLDL-triglyceride clearance by brown adipose tissue in mice. Diabetes 2014;63:880-891

67. Kooijman S, Wang Y, Parlevliet ET, Boon MR, Edelschaap D, Snaterse G, Pijl H, Romijn JA, Rensen PC: Central GLP-1 receptor signalling accelerates plasma clearance of triacylglycerol and glucose by activating brown adipose tissue in mice. Diabetologia 2015;58:2637-2646

68. Hawley SA, Fullerton MD, Ross FA, Schertzer JD, Chevtzoff C, Walker KJ, Peggie MW, Zibrova D, Green KA, Mustard KJ, Kemp BE, Sakamoto K, Steinberg GR, Hardie DG: The ancient drug salicylate directly activates AMP-activated protein kinase. Science 2012;336:918-922

69. Steinberg GR, Dandapani M, Hardie DG: AMPK: mediating the metabolic effects of salicylate-based drugs? Trends in endocrinology and metabolism: TEM 2013;24:481-487

70. Smith BK, Ford RJ, Desjardins EM, Green AE, Hughes MC, Houde VP, Day EA, Marcinko K, Crane JD, Mottillo EP, Perry CG, Kemp BE, Tarnopolsky MA, Steinberg GR: Salsalate (Salicylate) Uncouples Mitochondria, Improves Glucose Homeostasis, and Reduces Liver Lipids Independent of AMPK-beta1. Diabetes 2016;65:3352-3361

71. Liang W, Verschuren L, Mulder P, van der Hoorn JW, Verheij J, van Dam AD, Boon MR, Princen HM, Havekes LM, Kleemann R, van den Hoek AM: Salsalate attenuates diet induced non-alcoholic steatohepatitis in mice by decreasing lipogenic and inflammatory processes. British journal of pharmacology 2015;172:5293-5305

72. Meex RC, Phielix E, Moonen-Kornips E, Schrauwen P, Hesselink MK: Stimulation of human whole-body energy expenditure by salsalate is fueled by higher lipid oxidation under fasting conditions and by higher oxidative glucose disposal under insulin-stimulated conditions. The Journal of clinical endocrinology and metabolism 2011;96:1415-1423

73. Zack F, Blaas V, Goos C, Rentsch D, Buttner A: Death within 44 days of 2,4-dinitrophenol intake. International journal of legal medicine 2016;130:1237-1241

74. Ost M, Keipert S, Klaus S: Targeted mitochondrial uncoupling beyond UCP1 – The fine line between death and metabolic health. Biochimie 2017;134:77-85

75. Grundlingh J, Dargan PI, El-Zanfaly M, Wood DM: 2,4-dinitrophenol (DNP): a weight loss agent with significant acute toxicity and risk of death. Journal of medical toxicology : official journal of the American College of Medical Toxicology 2011;7:205-212

76. Hirasawa A, Tsumaya K, Awaji T, Katsuma S, Adachi T, Yamada M, Sugimoto Y, Miyazaki S, Tsujimoto G: Free fatty acids regulate gut incretin glucagon-like peptide-1 secretion through GPR120. Nature medicine 2005;11:90-94

7

77. Oh DY, Talukdar S, Bae EJ, Imamura T, Morinaga H, Fan W, Li P, Lu WJ, Watkins SM, Olefsky JM: GPR120 is an omega-3 fatty acid receptor mediating potent anti-inflammatory and insulin-sensitizing effects. Cell 2010;142:687-698

78. Li X, Yu Y, Funk CD: Cyclooxygenase-2 induction in macrophages is modulated by docosahexaenoic acid via interactions with free fatty acid receptor 4 (FFA4). FASEB journal : official publication of the Federation of American Societies for Experimental Biology 2013;27:4987-4997

79. Liu Y, Chen LY, Sokolowska M, Eberlein M, Alsaaty S, Martinez-Anton A, Logun C, Qi HY, Shelhamer JH: The fish oil ingredient, docosahexaenoic acid, activates cytosolic phospholipase A(2) via GPR120 receptor to produce prostaglandin E(2) and plays an anti-inflammatory role in macrophages. Immunology 2014;143:81-95

80. Gotoh C, Hong YH, Iga T, Hishikawa D, Suzuki Y, Song SH, Choi KC, Adachi T, Hirasawa A, Tsujimoto G, Sasaki S, Roh SG: The regulation of adipogenesis through GPR120. Biochemical and biophysical research communications 2007;354:591-597

81. Ichimura A, Hirasawa A, Poulain-Godefroy O, Bonnefond A, Hara T, Yengo L, Kimura I, Leloire A, Liu N, Iida K, Choquet H, Besnard P, Lecoeur C, Vivequin S, Ayukawa K, Takeuchi M, Ozawa K, Tauber M, Maffeis C, Morandi A, Buzzetti R, Elliott P, Pouta A, Jarvelin MR, Korner A, Kiess W, Pigeyre M, Caiazzo R, Van Hul W, Van Gaal L, Horber F, Balkau B, Levy-Marchal C, Rouskas K, Kouvatsi A, Hebebrand J, Hinney A, Scherag A, Pattou F, Meyre D, Koshimizu TA, Wolowczuk I, Tsujimoto G, Froguel P: Dysfunction of lipid sensor GPR120 leads to obesity in both mouse and human. Nature 2012;483:350-354

82. Rosell M, Kaforou M, Frontini A, Okolo A, Chan YW, Nikolopoulou E, Millership S, Fenech ME, MacIntyre D, Turner JO, Moore JD, Blackburn E, Gullick WJ, Cinti S, Montana G, Parker MG, Christian M: Brown and white adipose tissues: intrinsic differences in gene expression and response to cold exposure in mice. American journal of physiology Endocrinology and metabolism 2014;306:E945-964

83. Quesada-Lopez T, Cereijo R, Turatsinze JV, Planavila A, Cairo M, Gavalda-Navarro A, Peyrou M, Moure R, Iglesias R, Giralt M, Eizirik DL, Villarroya F: The lipid sensor GPR120 promotes brown fat activation and FGF21 release from adipocytes. Nature communications 2016;7:13479

84. Kuji I, Imabayashi E, Minagawa A, Matsuda H, Miyauchi T: Brown adipose tissue demonstrating intense FDG uptake in a patient with mediastinal pheochromocytoma. Annals of nuclear medicine 2008;22:231-235

85. Yamaga LY, Thom AF, Wagner J, Baroni RH, Hidal JT, Funari MG: The effect of catecholamines on the glucose uptake in brown adipose tissue demonstrated by (18)F-FDG PET/CT in a patient with adrenal pheochromocytoma. European journal of nuclear medicine and molecular imaging 2008;35:446-447

86. Lin JZ, Martagon AJ, Cimini SL, Gonzalez DD, Tinkey DW, Biter A, Baxter JD, Webb P, Gustafsson JA, Hartig SM, Phillips KJ: Pharmacological Activation of Thyroid Hormone Receptors Elicits a Functional Conversion of White to Brown Fat. Cell reports 2015;13:1528-1537

87. Fisher FM, Kleiner S, Douris N, Fox EC, Mepani RJ, Verdeguer F, Wu J, Kharitonenkov A, Flier JS, Maratos-Flier E, Spiegelman BM: FGF21 regulates PGC-1alpha and browning of white adipose tissues in adaptive thermogenesis. Genes & development 2012;26:271-281

88. Boon MR, van den Berg SA, Wang Y, van den Bossche J, Karkampouna S, Bauwens M, De Saint-Hubert M, van der Horst G, Vukicevic S, de Winther MP, Havekes LM, Jukema JW, Tamsma JT, van der Pluijm G, van Dijk KW,

Rensen PC: BMP7 activates brown adipose tissue and reduces diet-induced obesity only at subthermoneutrality. PloS one 2013;8:e74083

89. Nguyen KD, Qiu Y, Cui X, Goh YP, Mwangi J, David T, Mukundan L, Brombacher F, Locksley RM, Chawla A: Alternatively activated macrophages produce catecholamines to sustain adaptive thermogenesis. Nature 2011;480:104-108

90. Fabbiano S, Suarez-Zamorano N, Rigo D, Veyrat-Durebex C, Stevanovic Dokic A, Colin DJ, Trajkovski M: Caloric Restriction Leads to Browning of White Adipose Tissue through Type 2 Immune Signaling. Cell Metab 2016;24:434-446

91. Qiu Y, Nguyen KD, Odegaard JI, Cui X, Tian X, Locksley RM, Palmiter RD, Chawla A: Eosinophils and type 2 cytokine signaling in macrophages orchestrate development of functional beige fat. Cell 2014;157:1292-1308

92. Lee MW, Odegaard JI, Mukundan L, Qiu Y, Molofsky AB, Nussbaum JC, Yun K, Locksley RM, Chawla A: Activated type 2 innate lymphoid cells regulate beige fat biogenesis. Cell 2015;160:74-87

93. Brestoff JR, Kim BS, Saenz SA, Stine RR, Monticelli LA, Sonnenberg GF, Thome JJ, Farber DL, Lutfy K, Seale P, Artis D: Group 2 innate lymphoid cells promote beiging of white adipose tissue and limit obesity. Nature 2015;519:242-246

94. Sanchez-Gurmaches J, Hung CM, Guertin DA: Emerging Complexities in Adipocyte Origins and Identity. Trends in cell biology 2016;26:313-326

95. Goldberg IJ, Eckel RH, McPherson R: Triglycerides and heart disease: still a hypothesis? Arteriosclerosis, thrombosis, and vascular biology 2011;31:1716-1725

96. Ouellet H, Johnston JB, de Montellano PR: Cholesterol catabolism as a therapeutic target in Mycobacterium tuberculosis. Trends in microbiology 2011;19:530-539

97. Wipperman MF, Sampson NS, Thomas ST: Pathogen roid rage: cholesterol utilization by Mycobacterium tuberculosis. Critical reviews in biochemistry and molecular biology 2014;49:269-293

98. Pandey AK, Sassetti CM: Mycobacterial persistence requires the utilization of host cholesterol. Proceedings of the National Academy of Sciences of the United States of America 2008;105:4376-4380

99. Lovewell RR, Sassetti CM, VanderVen BC: Chewing the fat: lipid metabolism and homeostasis during M. tuberculosis infection. Current opinion in microbiology 2016;29:30-36

100. Feingold KR, Grunfeld C: Cholesterol Lowering Drugs. In *Endotext* De Groot LJ, Chrousos G, Dungan K, Feingold KR, Grossman A, Hershman JM, Koch C, Korbonits M, McLachlan R, New M, Purnell J, Rebar R, Singer F, Vinik A, Eds. South Dartmouth (MA), MDText.com, Inc., 2000

101. Khedoe PP, Hoeke G, Kooijman S, Dijk W, Buijs JT, Kersten S, Havekes LM, Hiemstra PS, Berbée JF, Boon MR, Rensen PC: Brown adipose tissue takes up plasma triglycerides mostly after lipolysis. Journal of lipid research 2015;56:51-59

102. Bartelt A, Bruns OT, Reimer R, Hohenberg H, Ittrich H, Peldschus K, Kaul MG, Tromsdorf UI, Weller H, Waurisch C, Eychmuller A, Gordts PL, Rinninger F, Bruegelmann K, Freund B, Nielsen P, Merkel M, Heeren J: Brown adipose tissue activity controls triglyceride clearance. Nature medicine 2011;17:200-205

103. Mattos KA, Oliveira VC, Berredo-Pinho M, Amaral JJ, Antunes LC, Melo RC, Acosta CC, Moura DF, Olmo R, Han J, Rosa PS, Almeida PE, Finlay BB, Borchers CH, Sarno EN, Bozza PT, Atella GC, Pessolani MC: Mycobacterium leprae intracellular survival relies on cholesterol accumulation in infected macrophages: a potential target for new drugs for leprosy treatment. Cellular microbiology 2014;16:797-815

7

104. Shoelson SE, Lee J, Yuan M: Inflammation and the IKK beta/I kappa B/NF-kappa B axis in obesity- and diet-induced insulin resistance. International journal of obesity and related metabolic disorders : journal of the International Association for the Study of Obesity 2003;27 Suppl 3:S49-52

105. Williamson RT: On the Treatment of Glycosuria and Diabetes Mellitus with Sodium Salicylate. British medical journal 1901;1:760-762

106. McKeigue PM, Shah B, Marmot MG: Relation of central obesity and insulin resistance with high diabetes prevalence and cardiovascular risk in South Asians. Lancet (London, England) 1991;337:382-386

107. Raji A, Gerhard-Herman MD, Warren M, Silverman SG, Raptopoulos V, Mantzoros CS, Simonson DC: Insulin resistance and vascular dysfunction in nondiabetic Asian Indians. The Journal of clinical endocrinology and metabolism 2004;89:3965-3972

108. De Clercq E, Li G: Approved Antiviral Drugs over the Past 50 Years. Clinical microbiology reviews 2016;29:695-747

109. Ridker PM: Moving beyond JUPITER: will inhibiting inflammation reduce vascular event rates? Current atherosclerosis reports 2013;15:295

110. Ridker PM, Danielson E, Fonseca FA, Genest J, Gotto AM, Jr., Kastelein JJ, Koenig W, Libby P, Lorenzatti AJ, MacFadyen JG, Nordestgaard BG, Shepherd J, Willerson JT, Glynn RJ: Rosuvastatin to prevent vascular events in men and women with elevated C-reactive protein. The New England journal of medicine 2008;359:2195-2207

111. Ridker PM, Danielson E, Fonseca FA, Genest J, Gotto AM, Jr., Kastelein JJ, Koenig W, Libby P, Lorenzatti AJ, Macfadyen JG, Nordestgaard BG, Shepherd J, Willerson JT, Glynn RJ: Reduction in C-reactive protein and LDL cholesterol and cardiovascular event rates after initiation of rosuvastatin: a prospective study of the JUPITER trial. Lancet (London, England) 2009;373:1175-1182

112. Bays HE, Neff D, Tomassini JE, Tershakovec AM: Ezetimibe: cholesterol lowering and beyond. Expert review of cardiovascular therapy 2008;6:447-470

113. Walley KR, Thain KR, Russell JA, Reilly MP, Meyer NJ, Ferguson JF, Christie JD, Nakada TA, Fjell CD, Thair SA, Cirstea MS, Boyd JH: PCSK9 is a critical regulator of the innate immune response and septic shock outcome. Science translational medicine 2014;6:258ra143

114. Cheng JM, Oemrawsingh RM, Garcia-Garcia HM, Boersma E, van Geuns RJ, Serruys PW, Kardys I, Akkerhuis KM: PCSK9 in relation to coronary plaque inflammation: Results of the ATHEROREMO-IVUS study. Atherosclerosis 2016;248:117-122

115. Brestoff JR, Kim BS, Saenz SA, Stine RR, Monticelli LA, Sonnenberg GF, Thome JJ, Farber DL, Lutfy K, Seale P, Artis D: Group 2 innate lymphoid cells promote beiging of white adipose tissue and limit obesity. Nature 2015;519:242-246

116. Frontini A, Vitali A, Perugini J, Murano I, Romiti C, Ricquier D, Guerrieri M, Cinti S: White-to-brown transdifferentiation of omental adipocytes in patients affected by pheochromocytoma. Biochimica et Biophysica Acta (BBA) – Molecular and Cell Biology of Lipids 2013;1831:950-959

117. Giordano A, Frontini A, Cinti S: Convertible visceral fat as a therapeutic target to curb obesity. Nature Reviews Drug Discovery 2016;15:405-424

118. Cypess AM, Weiner LS, Roberts-Toler C, Elía EF, Kessler SH, Kahn PA, English J, Chatman K, Trauger SA, Doria A, Kolodny GM: Activation of Human Brown Adipose Tissue by a β3-Adrenergic Receptor Agonist. Cell metabolism 2015;21:33-38

119. Hauser TH, Salastekar N, Schaefer EJ, Desai

7

T, Goldfine HL, Fowler KM, Weber GM, Welty F, Clouse M, Shoelson SE, Goldfine AB: Effect of Targeting Inflammation With Salsalate: The TINSAL-CVD Randomized Clinical Trial on Progression of Coronary Plaque in Overweight and Obese Patients Using Statins. JAMA cardiology 2016;1:413-423

120. Ariel D, Kim SH, Liu A, Abbasi F, Lamendola CA, Grove K, Tomasso V, Reaven GM: Salsalate-induced changes in lipid, lipoprotein, and apoprotein concentrations in overweight or obese, insulin-resistant, nondiabetic individuals. Journal of clinical lipidology 2015;9:658-663

121. Penesova A, Koska J, Ortega E, Bunt JC, Bogardus C, de Courten B: Salsalate has no effect on insulin secretion but decreases insulin clearance: a randomized, placebo-controlled trial in subjects without diabetes. Diabetes, obesity & metabolism 2015;17:608-612

122. Barzilay JI, Jablonski KA, Fonseca V, Shoelson SE, Goldfine AB, Strauch C, Monnier VM: The impact of salsalate treatment on serum levels of advanced glycation end products in type 2 diabetes. Diabetes care 2014;37:1083-1091

123. Goldfine AB, Fonseca V, Jablonski KA, Pyle L, Staten MA, Shoelson SE: The effects of salsalate on glycemic control in patients with type 2 diabetes: a randomized trial. Annals of internal medicine 2010;152:346-357

124. Goldfine AB, Fonseca V, Jablonski KA, Chen YD, Tipton L, Staten MA, Shoelson SE: Salicylate (salsalate) in patients with type 2 diabetes: a randomized trial. Annals of internal medicine 2013;159:1-12

125. Goldfine AB, Conlin PR, Halperin F, Koska J, Permana P, Schwenke D, Shoelson SE, Reaven PD: A randomised trial of salsalate for insulin resistance and cardiovascular risk factors in persons with abnormal glucose tolerance. Diabetologia 2013;56:714-723

126. Shi H, Kokoeva MV, Inouye K, Tzameli I, Yin H, Flier JS: TLR4 links innate immunity and fatty acid – induced insulin resistance. The Journal of clinical investigation 2006;116:3015-3025

127. Lee JY, Plakidas A, Lee WH, Heikkinen A, Chanmugam P, Bray G, Hwang DH: Differential modulation of Toll-like receptors by fatty acids: preferential inhibition by n-3 polyunsaturated fatty acids. Journal of lipid research 2003;44:479-486

128. Walgren MC, Young JB, Kaufman LN, Landsberg L: The effects of various carbohydrates on sympathetic activity in heart and interscapular brown adipose tissue of the rat. Metabolism 1987;36:585-594

129. Bifari F, Nisoli E: Branched-chain amino acids differently modulate catabolic and anabolic states in mammals: a pharmacological point of view. British journal of pharmacology 2016; in press

130. Wanders D, Burk DH, Cortez CC, Van NT, Stone KP, Baker M, Mendoza T, Mynatt RL, Gettys TW: UCP1 is an essential mediator of the effects of methionine restriction on energy balance but not insulin sensitivity. FASEB journal : official publication of the Federation of American Societies for Experimental Biology 2015;29:2603-2615

7

Addendum

SUMMARY

The worldwide prevalence of obesity is steadily increasing. Obesity leads to insulin resistance and atherosclerosis, which are the pathologies underlying type 2 diabetes and cardiovascular disease, respectively. Inflammation is an important factor connecting obesity to these disorders, but the exact mechanisms connecting obesity, the immune system, type 2 diabetes and cardiovascular disease are still under investigation. The research described in this thesis was performed 1) to gain more insight into the role of the immune system in obesity, dyslipidemia, insulin resistance and atherosclerosis, 2) to study whether inflammation contributes to the disadvantageous metabolic phenotype of a human population with a particularly high risk to develop type 2 diabetes and cardiovascular disease, and 3) to study the therapeutic potential of decreasing inflammation by pharmacological strategies to reduce obesity and improve glucose and lipid metabolism in pre-clinical models. **Chapter 1** serves as a general introduction to the different processes and players that are important in obesity and associated disorders, including regulation of lipid metabolism, the physiology of adipose tissue, and the interaction between the immune system and adipose tissue function.

We first studied the effect of a potent inflammatory trigger, *i.e.* Bacille-Calmette-Guérin (BCG), on lipid metabolism and atherosclerosis. BCG is prepared from attenuated live *Mycobacterium bovis* and modulates atherosclerosis development as currently explained by immunomodulatory mechanisms. However, whether BCG is pro- or anti-atherogenic remains inconclusive as the effect of BCG on cholesterol metabolism, the main driver of atherosclerosis development, has remained underexposed in previous studies. In **chapter 2**, we aimed to elucidate the effect of BCG on inflammation in relation to cholesterol metabolism and atherosclerosis development in a mouse model of human-like lipoprotein metabolism. To this end, we fed hyperlipidemic APOE*3-Leiden.CETP mice a Western-type diet and treated them with a single intravenous injection of BCG. We found that BCG-treated mice had hepatic mycobacterial infection and hepatomegaly. Enlargement of the liver coincided with severe immune cell infiltration and a higher cholesterol content. Moreover, BCG reduced plasma total cholesterol levels. This was due to accelerated hepatic clearance of cholesterol, as evident from clearance studies with intravenously injected [14C]cholesteryl oleate-labeled lipoprotein-like particles, and to reduced intestinal plant sterol and cholestanol absorption. Ultimately, BCG decreased the ability of peritoneal macrophages to become foam cells and tended to decrease atherosclerotic lesion area and reduced lesion severity in the aortic root of the heart: BCG delayed atherosclerotic lesion progression. Consequently, we concluded that BCG reduces the plasma levels of atherogenic lipoproteins and delays atherosclerotic lesion formation in hyperlipidemic mice.

In **chapter 3**, we switched our focus from immune modulation of lipid metabolism and atherosclerosis to glucose metabolism and type 2 diabetes. During the development of obesity, B cells accumulate in white adipose tissue (WAT) and produce IgG, which has previously been suggested to contribute to the development of glucose intolerance.

IgG signals by binding to Fcγ receptors (FcγR) and by activating the complement system (including C3). We aimed to study whether activation of FcγR and/or complement C3 mediates the development of high fat diet-induced glucose intolerance. To this end, we studied high-fat diet-fed mice lacking all four FcγRs, only the inhibitory FcγRIIb, only the central component of the complement system C3, and mice lacking all FcγRs as well as C3. We found that absence of the inhibitory FcγRIIb increases adipose tissue IgG, but that absence of FcγRs and/or C3 does not protect against high-fat diet induced glucose intolerance. We therefore concluded that if obesity-induced IgG contributes to the development of glucose intolerance, this is not mediated by FcγR or complement activation.

In **chapter 4**, we studied the inflammatory state of South Asians, a human population with a particularly high risk to develop glucose intolerance, compared to white Caucasians. More specifically, we compared mRNA expression of 144 markers of immune function in skeletal muscle and WAT of middle-aged overweight pre-diabetic Dutch South Asian and matched white Caucasian men. We found that expression of especially interferon signaling genes was lower in South Asians, both in muscle (IFIT3, IFI44) and WAT (IFI35, IFI44, IFIT2, IFIT3, IFIT5, OAS1, STAT1). Ingenuity pathway analysis highlighted the anti-inflammatory interferon α/β signaling pathway to be lower in South Asians. From this, we concluded that South Asians have impaired interferon signaling in metabolic tissues. Since recent evidence from rodent studies shows that impaired interferon α/β signaling in adipose tissue induces insulin resistance and glucose intolerance, impaired interferon signaling in South Asians may contribute to their high risk of type 2 diabetes.

In the next part of this thesis, we focused on the treatment of metabolic inflammation. The anti-inflammatory compound salsalate lowers glucose intolerance and dyslipidemia in type 2 diabetes patients, but the mechanism was still unknown. The aim of **chapter 5** was to unravel the molecular mechanisms involved in these beneficial metabolic effects of salsalate by treating mice with salsalate during and after development of high-fat diet-induced obesity. We found that salsalate attenuates and reverses high-fat diet-induced weight gain, in particular fat mass accumulation, improves glucose tolerance, and lowers plasma triglyceride levels. Mechanistically, salsalate selectively promotes the uptake of triglyceride-derived fatty acids by BAT, as evident from clearance studies with glycerol tri[³H]oleate-labeled lipoprotein-like emulsion particles, decreased the intracellular lipid content in BAT, and increased rectal temperature, all pointing to more active BAT. Moreover, treatment of T37i brown adipocytes *in vitro* with salsalate increased uncoupled respiration, expression of the uncoupling protein-1 (*Ucp1*) and lipolysis. These latter two effects were abolished by the inhibition of cAMP-dependent protein kinase A (PKA). We concluded that salsalate activates BAT, presumably by directly activating brown adipocytes via the PKA pathway. This suggests a novel mechanism that may explain its beneficial metabolic effects in type 2 diabetes patients.

Finally, we studied the therapeutic potential of targeting GPR120, a free fatty acid receptor that is highly expressed in BAT and WAT, is regulated by cold exposure, and is a mediator of anti-inflammatory and insulin-sensitizing effects. Since the effects of GPR120 on lipid metabolism and substrate utilization have not been studied to date, the aims

of **chapter 6** were to assess the role of GPR120 in lipid metabolism and to evaluate the therapeutic potential of a selective GPR120 agonist in energy consumption. When fed a high-fat diet, GPR120 deficient mice had higher fat mass, lower physical activity, and lower energy expenditure during the dark phase, while relative substrate utilization (*i.e.* glucose *vs.* fatty acids) did not differ compared to wild-type mice. GPR120 deficiency reduced expression of *Ucp1*, *Prdm16* and *Ppar*α, which are markers of BAT activity, thus suggesting less active BAT. Treatment with the GPR120 agonist TUG891 during high-fat diet-feeding reduced fat mass after 2.5 weeks. Furthermore, short-term treatment (5 days) with TUG891 on a chow diet acutely increased fat oxidation and reduced glucose oxidation, and already tended to reduce fat mass. From these data we concluded that GPR120 deficiency increases fat mass while GPR120 agonism reduces fat mass and increases fat oxidation. Therefore, stimulation of GPR120 holds therapeutic potential to combat obesity.

To conclude, we evaluated the results of this thesis in **chapter 7** and discussed the potential of targeting adipose tissue (and) inflammation to treat obesity-associated disorders such as type 2 diabetes and cardiovascular disease. Taken together, the studies described in this thesis have increased our understanding of the role of inflammation in adipose tissue function and lipid metabolism during the development of type 2 diabetes and cardiovascular disease. Moreover, novel potential therapeutic strategies were identified to combat obesity, metabolic inflammation and associated metabolic disorders, such as treatment with interferons, salsalate and GPR120 agonists.

SAMENVATTING

Obesitas komt wereldwijd steeds meer voor en leidt vaak tot insulineresistentie en aderverkalking. Insuline is het hormoon dat na een maaltijd door de alvleesklier geproduceerd wordt en suikeropname door metabole organen zoals spieren, lever en vetweefsel stimuleert. Als gevolg van verminderde werking van insuline (ofwel insulineresistentie) hoopt suiker op in het bloed en zo kan type 2 diabetes ontstaan. Aderverkalking komt juist door ophoping van vetten (cholesterol) en immuuncellen in de bloedvatwand. Aderverkalking kan uiteindelijk leiden tot een hart- of herseninfarct. Omdat type 2 diabetes en hart- en vaatziekten vaker voorkomen bij mensen met overgewicht, worden deze kwalen ook wel obesitas-gerelateerde stofwisselingsziekten genoemd.

In het geval van obesitas is niet alleen de vetstofwisseling verstoord, maar ook is het immuunsysteem actiever. Waarschijnlijk heeft het immuunsysteem een belangrijke rol bij de ontwikkeling van insulineresistentie en aderverkalking, maar hoe obesitas, het immuunsysteem en type 2 diabetes en hart- en vaatziekten precies met elkaar verbonden zijn is nog niet geheel bekend. Het onderzoek in dit proefschrift werd uitgevoerd om 1) meer inzicht te krijgen in de rol van het immuunsysteem in obesitas, een verstoorde vetstofwisseling, insulineresistentie en aderverkalking, 2) de activiteit van het immuunsysteem te onderzoeken in een groep mensen met een bijzonder hoog risico op het ontwikkelen van type 2 diabetes en hart- en vaatziekten, en 3) te onderzoeken of geneesmiddelen die het immuunsysteem remmen, een gunstig effect hebben op obesitas en de suiker- en vetstofwisseling in muizen.

Hoofdstuk 1 vormt een algemene introductie, waarin de verschillende organen en processen die betrokken zijn bij de ontwikkeling van obesitas en de daaraan gerelateerde ziekten zoals type 2 diabetes en hart- en vaatziekten, besproken worden. Obesitas ontstaat door een 'positieve energiebalans', waarbij de inname van energie (in de vorm van voedsel) hoger is dan het energieverbruik. De organen in ons lichaam gebruiken voornamelijk suikers en vetten als bron van energie, en na een maaltijd worden deze vanuit het voedsel via het bloed naar organen zoals het hart, spieren en vetweefsel getransporteerd. Suiker is oplosbaar in bloed, maar vetten niet. Daarom worden vetten uit het dieet door de darm in oplosbare pakketjes verpakt die we lipoproteïnen noemen, waarna ze alsnog via het bloed naar de organen worden gebracht. De meest voorkomende vetten in ons voedsel zijn triglyceriden en cholesterol. Triglyceriden zijn de vetten die door organen als energiebron worden gebruikt, en bij een overschot aan energie (ofwel een positieve energiebalans) wordt de energie (suikers én triglyceriden) na een chemische omzetting in de vorm van triglyceriden opgeslagen in vetcellen in ons vetweefsel. Cholesterol is geen bron van energie, maar een essentieel onderdeel van onze cellen en cruciaal voor de aanmaak van hormonen, vitamine D en galzuren.

Aangezien buitensporige opslag van vet kenmerkend is voor obesitas, is in dit proefschrift vooral onderzoek gedaan naar het vetweefsel. Er bestaan verschillende soorten vetweefsel, waaronder wit vet en bruin vet. Van wit vet heeft een mens wel 12-35 kg en de voornaamste functie van wit vet is de opslag van overtollige triglyceriden.

Bruin vet verbrandt juist triglyceriden om warmte te genereren, waardoor zoogdieren hun lichaamstemperatuur op peil kunnen houden. Van bruin vet hebben we maar 100-200 g. Interessant genoeg zitten er tussen de vetcellen in het witte vetweefsel ook heel veel immuuncellen. Tijdens de ontwikkeling van obesitas komen er veel meer immuuncellen naar het witte vet, die zorgen voor ontsteking van het vetweefsel. In het bruine vet komen ook immuuncellen voor, maar hierover is nog maar nauwelijks iets bekend. Wel staat vast dat overmatige activatie van het immuunsysteem of metabole ontsteking, zoals tijdens obesitas optreedt, kan bijdragen aan insulineresistentie en aderverkalking. Zo remt ontsteking de effecten van insuline en dragen immuuncellen bij aan de ontwikkeling van aderverkalking. Een overactief immuunsysteem bevordert dus zowel type 2 diabetes als hart- en vaatziekten.

Vaccinatie kan het immuunsysteem activeren, en via deze weg de ontwikkeling van aderverkalking beïnvloeden. Een vaccin dat wereldwijd gebruikt wordt is het anti-tuberculose vaccin Bacille-Calmette-Guérin (BCG) dat gemaakt is van verzwakte tuberculose-bacteriën. Eerder onderzoek naar de effecten van BCG op het immuunsysteem en aderverkalking gaf tegenstrijdige resultaten, aangezien verergering maar ook vermindering van aderverkalking werd gerapporteerd. Omdat aderverkalking niet alleen van het immuunsysteem maar ook sterk van cholesterol afhangt, onderzochten wij of BCG behalve het immuunsysteem ook de cholesterolstofwisseling beïnvloedt en daarmee ook de ontwikkeling van aderverkalking. De resultaten hiervan staan beschreven in **hoofdstuk 2**. We toonden aan dat een enkele injectie met BCG in muizen leidde tot een bacteriële infectie, een sterk vergrote lever en activatie van het immuunsysteem. In de levers van BCG-behandelde dieren zaten veel meer immuuncellen en cholesterol, terwijl in het bloed van de behandelde muizen juist minder cholesterol gemeten werd. Dit kwam doordat er meer cholesterol werd opgenomen door de lever, maar ook doordat de opname van cholesterol door de darm lager was. Om het effect op aderverkalking te meten, bestudeerden we in de grootste lichaamsslagader vanaf het hart de grootte van de cholesterol- en immuuncelophopingen. Deze zogenaamde 'plaques' waren kleiner, waaruit we concludeerden dat BCG, ondanks de activerende effecten op het immuunsysteem, de ontwikkeling van aderverkalking in muizen vertraagt.

In **hoofdstuk 3** lag de nadruk van het onderzoek meer op de rol die immuuncellen in het vetweefsel hebben bij de ontwikkeling van insulineresistentie. Hierbij focusten we specifiek op een bepaald type immuuncellen, namelijk B cellen, waarvan eerder werd aangetoond dat de antilichamen die door deze cellen gemaakt worden (namelijk IgG) specifiek bijdragen aan de ontwikkeling van type 2 diabetes. IgG bindt en activeert zogenaamde Fc-receptoren en complement eiwitten, die onderdeel uitmaken van het immuunsysteem en betrokken zijn bij de afweer tegen indringers van buiten, zoals bacteriën. Om te bestuderen via welke mechanismen IgG precies bijdraagt aan de ontwikkeling van type 2 diabetes tijdens obesitas, voerden we muizen die géén Fc-receptoren hadden en het belangrijkste complementeiwit (C3) misten een vetrijk dieet. Vervolgens wogen we de dieren en maten we suikerniveaus in hun bloed. We vonden dat muizen zonder Fc-receptoren of complementeiwit C3 meer B cellen en antilichamen in hun witte vetweefsel hadden, maar geen andere bloedsuikerniveaus dan de controle muizen op een vetrijk dieet. Daarom

concludeerden we dat als obesitas-geïnduceerde IgG productie door B cellen in het witte vetweefsel bijdraagt aan de ontwikkeling van type 2 diabetes, dit niet via de activatie van Fc-receptoren of complementeiwitten verloopt.

Vervolgens hebben we het onderzoek naar het immuunsysteem in relatie tot diabetes voortgezet in mensen. Hindoestanen hebben een sterk verhoogd risico op diabetes, maar het immuunsysteem in deze bevolkingsgroep was nog nooit uitgebreid onderzocht. Daarom hebben we, zoals beschreven in **hoofdstuk 4**, de expressie van 144 genen die betrokken zijn bij de werking van het immuunsysteem vergeleken tussen Hindoestaanse en blanke Kaukasische mannen die allemaal overgewicht en verhoogde bloedsuikers hadden. We vonden in het witte vet en de spieren van Hindoestanen een lagere expressie van genen die betrokken zijn bij interferon-afgifte ten opzichte van blanke Kaukasiërs. Interferonen worden door immuuncellen uitgescheiden na contact met indringers, zoals virussen. We concludeerden dat Hindoestanen een verminderde interferon-werking hebben in hun witte vet en spieren. Recent onderzoek in muizen heeft laten zien dat verminderde interferon-werking in vet leidt tot insulineresistentie, wat erop duidt dat de lagere expressie van interferon-genen in Hindoestanen ten grondslag zou kunnen liggen aan hun verhoogde risico op het ontwikkelen van type 2 diabetes.

In het volgende deel van het proefschrift richtten we ons meer op de behandeling van metabole ontsteking. Zo was bekend dat de ontstekingsremmende stof salsalaat bloedsuikers en -vetten verlaagt in mensen met type 2 diabetes, maar het mechanisme achter deze effecten was nog onontdekt. Het doel van het onderzoek beschreven in **hoofdstuk 5** was om de werking achter deze positieve effecten van salsalaat te onderzoeken. Dit deden we door muizen een vetrijk dieet te voeren en te behandelen met salsalaat. We vonden dat salsalaat gewichtstoename kon voorkomen en zelfs kon verminderen. Daarnaast hadden de behandelde muizen inderdaad minder hoge suiker- en triglyceridenniveaus in hun bloed. Dit kwam doordat salsalaat bruin vet activeerde en daarmee de opname van vetten uit het bloed door het bruine vet stimuleerde. Als we bruine vetcellen in een kweekschaal behandelden met salsalaat, maten we dat de cellen meer zuurstof verbruikten en dat de genexpressie van bruin vet-specifieke genen hoger werd, wat erop duidt dat salsalaat een direct effect heeft op bruine vetcellen. Als resultaat van dit onderzoek ontdekten we daarom een nieuw mechanisme dat verklaart waarom salsalaat zulke gunstige metabole effecten heeft in mensen met type 2 diabetes.

Tot slot bestudeerden we de therapeutische mogelijkheden van activatie van het eiwit GPR120. GPR120 is een receptor voor vetten die in het witte en het bruine vet tot expressie komt. De expressie van deze receptor wordt verhoogd door kou; bekend is ook dat activatie van deze receptor ook remmende effecten heeft op ontsteking en insulinersistentie kan verminderen. Het was echter nog niet bekend of GPR120 ook een rol speelt in de vetstofwisseling. Daarom onderzochten we, zoals beschreven in **hoofdstuk 6**, wat de rol van GPR120 in vetstofwisseling is en of een specifieke activator van GPR120 het energieverbruik kan verhogen, om zo vetstofwisseling te verbeteren. Als we muizen die géén GPR120 hebben een vetrijk dieet voerden, hadden zij een hogere vetmassa, verminderde fysieke activiteit en een lager energieverbruik dan controle muizen. Ook

hadden GPR120-deficiënte muizen een lagere expressie van bruin vet-specifieke genen in hun bruine vet, wat suggereert dat ze minder actief bruin vet hebben. Omgekeerd verminderde behandeling van muizen met een GPR120 activator tijdens een vetrijk dieet hun vetmassa na enkele weken. Daarnaast zagen we dat een kortdurende behandeling van muizen gedurende 5 dagen met deze activator acuut de vetverbranding verhoogde, waarbij ze ook al een beetje afvielen. Hieruit concludeerden we dat een gebrek aan GPR120 een hogere vetmassa tot gevolg heeft, terwijl activatie van GPR120 vetverbranding verhoogt en vetmassa vermindert. Daarom zou activatie van GPR120 een mogelijk aangrijpingspunt kunnen zijn voor nieuwe therapieën tegen obesitas.

Om af te sluiten worden de resultaten van dit proefschrift bediscussieerd in **hoofdstuk 7**. Hierin wordt de veelbelovendheid besproken van therapieën die aangrijpen op vetweefsel en/of ontsteking om obesitas-gerelateerde ziekten zoals type 2 diabetes en hart- en vaatziekten te behandelen. Samen hebben de studies die beschreven zijn in dit proefschrift ons inzicht vergroot in de rol die het immuunsysteem heeft in vetweefsel en de vetstofwisseling tijdens de ontwikkeling van type 2 diabetes en hart- en vaatziekten (beoogde doelstellingen 1 en 2). Daarnaast hebben we mogelijke nieuwe strategieën geïdentificeerd die obesitas, metabole ontsteking en de gerelateerde stofwisselingsziekten kunnen bestrijden, zoals behandeling met interferonen, salsalaat of GPR120 activatoren (beoogde doelstelling 3).

DANKWOORD

Meten met maten is niet alleen leuker dan alleen; het was onmogelijk geweest om zonder de hulp van anderen dit proefschrift te voltooien. Daarom sluit ik graag af met een woord van dank aan alle mensen die hebben bijgedragen.

Prof. Rensen, beste Patrick, ik ben ontzettend dankbaar dat ik op de rijdende trein van jouw vet-onderzoek mocht meerijden. Ik bewonder je optimisme, en de toewijding en precisie waarmee jij onderzoek bedrijft en je groeiende team aanstuurt. Ik heb me de afgelopen vier jaar heel erg op mijn plek gevoeld in jouw groep, waarvoor veel dank. Dr. Boon, beste Mariëtte, jij zorgde ervoor dat ik een vliegende start maakte toen ik vier jaar geleden begon binnen de groep. Bedankt voor alles wat je me geleerd hebt en voor je onuitputtelijke enthousiasme en positiviteit, waarmee je mij vaak stimuleerde om met hernieuwde energie door te gaan.

Prof. Lutgens en Prof. De Winther, beste Esther en Menno, jullie wil ik bedanken voor alle immunologische steun die ik tijdens mijn promotietraject kreeg. Ik heb veel gehad aan de samenwerking met jullie Amsterdamse groep. Susan, ik had me geen betere Rembrandt-partner kunnen wensen. Je FACS-capaciteiten waren onmisbaar maar ik waardeer vooral je sereniteit tijdens onze experimenten. Ik herinner me het moment dat je voorstelde om 'alleen voor koffie' langs te komen in Leiden en ik vind het leuk dat de inhoud van onze gesprekken niet beperkt bleef tot project-gerelateerde zaken.

Mijn directe collega's wil ik bedanken voor de fijne samenwerking en vooral voor de leuke tijd die ik heb gehad. Rosa, Sander, Padmini en Geerte, tijdens de gezamenlijke experimenten en de verre congressen leerden we elkaar goed kennen, de momenten samen ga ik missen. Jimmy, bedankt voor je uitmuntende begeleiding tijdens ons verrassende BCG-project, al mijn athero-kennis heb ik aan jou te danken. Yanan en Edwin, jullie ben ik jullie zeer dankbaar voor alle experimentele vaardigheden en kennis die jullie me bijbrachten. Kimberly, Eline, Lisanne, Maaike, Lauren, Laura en Iris, ik kijk met een brede glimlach terug op alle kletspraat, onrust en chocola op C7. Ook wil ik Huub, Zhuang, Gustavo en Enchen voor de gezelligheid en samenwerking bedanken en de Meijer-groep, Onno, Lisa, José, Jan, Lisa, Jorge en Jinlan voor de hormonale input. Chris, Trea, Hetty en Lianne, jullie gaven zin en onzin aan mijn lableven en de koffiepauzes, en Isabel, onze gesprekken op E0 waren de beste. Zonder jullie praktische en mentale steun had ik het niet gered. Ben, Fred, Silvia, Diana, Norma, Martine en alle andere mensen van het PDC, bedankt voor jullie goede zorgen. Belangrijk waren ook de studenten die bij mij stage kwamen lopen, waaronder Anish, Takuya, Ellemiek, Annika, Jasmin, David, Erik en Robin. Van jullie begeleiden heb ik misschien nog wel het meeste geleerd. Jullie inzet was goud waard.

Ook wil ik alle collega's van andere afdelingen die bijgedragen hebben aan werkbesprekingen, experimenten, manuscripten en borrels bedanken. Ko, Vanessa, Jan, Amanda, Lianne, Mattijs, Sam, Lisa en Saeed van de Humane Genetica, jullie input en bereidheid om te helpen waren onmisbaar. Alle collega's van de Urologie en de Radiologie bedank ik voor de gezelligheid op het lab en de collega's van TNO voor de samenwerking en het vermaak op Havekes-weekenden. Bruno, thank you for the collaboration with

Parasitology and the immunometabolism meetings, those were my favorite. Ook wil ik mijn collega's in de kantoortuin bedanken waarmee ik misschien niet direct heb samengewerkt, maar die ik dagelijks zag in de wandelgangen en bij het koffiezetapparaat.

Buiten werk hebben ook veel mensen indirect bijgedragen aan mijn motivatie tijdens dit promotietraject. Ten eerste alle lieve mensen van Die Leythe en Leiden Atletiek, waarmee ik de laatste jaren fantastische uren op het water en de baan in Leiden heb beleefd. Ik kwam daar áltijd vrolijker vandaan. En dan de VLF-ers, ik vind het bijzonder dat we tien jaar geleden met een paar studiegenoten op vakantie gingen en dat we nu nog steeds zo veel lol hebben, samen op vakanties gaan en voor elkaar klaar staan. Ook mijn studie- en schoolvrienden, van de WB, BMW en Risico, wil ik bedanken voor alle leuke etentjes en activiteiten die we samen hebben gedaan de afgelopen jaren. Marin en Renée, we zien elkaar te weinig, maar elke keer dát het gebeurt is het zó leuk! Onze vriendschap duurt al erg lang en ik waardeer het enorm dat onze levens nog steeds zo veel overeenkomsten hebben.

Lieve Anne en mam, bedankt dat jullie me altijd de vrijheid hebben gegeven om zelf te kiezen en me hebben gestimuleerd om te doen wat ik leuk vind. Jullie hadden het de afgelopen jaren niet altijd makkelijk, maar ik heb toch onafgebroken en onvoorwaardelijke steun van jullie gevoeld. Ook wil ik oma en opa en oma bedanken voor alle steun en betrokkenheid. Ik voel me bevoorrecht dat ik jullie nog heb en omdat jullie altijd zo lief zijn. Alje en Tes, dank jullie wel voor de mooie reizen en gezellige bijeenkomsten de afgelopen jaren. Maarten en Annelies, leuk dat ik jullie inmiddels ook in dit rijtje kan noemen. Bedankt voor jullie onuitputtelijke interesse en alle geslaagde uitstapjes die we samen gemaakt hebben. Michiel, jij bent de beste reden om na een werkdag weer naar huis te gaan. Jou wil ik bedanken voor je eindeloze flexibiliteit en begrip tijdens dit traject. Zo was het nooit een probleem als ik in het weekend weer naar Leiden ging, of dat ik straks alvast naar Engeland ga. Ik word blij van hoe wij samen kunnen koken, fietsen, reizen, eten, klussen, dansen en lachen.

LIST OF PUBLICATIONS

Boon MR, Kooijman S, **Van Dam AD**, Pelgrom LR, Berbée JF, Visseren CA, Van Aggele RC, Van den Hoek AM, Sips HC, Lombès M, Havekes LM, Tamsma JT, Guigas B, Meijer OC, Jukema JW, Rensen PC. Peripheral cannabinoid 1 receptor blockade activates brown adipose tissue and diminishes dyslipidemia and obesity. **FASEB J** 2014; 28: 5361-75

Van Dam AD, Nahon KJ, Kooijman S, Van den Berg SM, Kanhai AA, Kikuchi T, Heemskerk MM, Van Harmelen V, Lombès M, Van den Hoek AM, De Winther MP, Lutgens E, Guigas B, Rensen PC, Boon MR. Salsalate activates brown adipose tissue in mice. **Diabetes** 2015; 64: 1544-54

Van Beek L, Van Klinken JB, Pronk AC, **Van Dam AD**, Dirven E, Rensen PC, Koning F, Willems van Dijk K, Van Harmelen V. The limited storage capacity of gonadal adipose tissue directs the development of metabolic disorders in male C57Bl/6J mice. **Diabetologia** 2015; 58: 1601-9

Rozema E, **Van Dam AD**, Sips H, Verpoorte R, Meijer OC, Kooijman S, Choi YH. Extending pharmacological dose-response curves for salsalate with natural deep eutectic solvents. **RSC Adv** 2015; 5: 61398-61401

Wang Y, van der Tuin S, Tjeerdema N, **Van Dam AD**, Rensen SS, Hendrikx T, Berbée JF, Atanasovska B, Fu J, Hoekstra M, Bekkering S, Riksen NP, Buurman WA, Greve JW, Hofker MH, Shiri-Sverdlov R, Meijer OC, Smit JW, Havekes LM, Willems van Dijk K, Rensen PC. Plasma cholesteryl ester transfer protein is predominantly derived from Kupffer cells. **Hepatology** 2015; 62: 1710-22

Van Dam AD, Kooijman S, Schilperoort M, Rensen PC, Boon MR. Regulation of brown fat by AMP-activated protein kinase. **Trends Mol Med** 2015; 21: 571-9

Liang W, Verschuren L, Mulder P, Van der Hoorn JW, Verheij J, **Van Dam AD**, Boon MR, Princen HM, Havekes LM, Kleemann R, van den Hoek AM. Salsalate attenuates diet induced non-alcoholic steatohepatitis in mice by decreasing lipogenic and inflammatory processes. **Br J Pharmacol** 2015; 172: 5293-305

Van Beek L, Vroegrijk IOCM, Katiraei S, Heemskerk MM, **Van Dam AD**, Kooijman S, Rensen PC, Koning F, Verbeek JS, Willems van Dijk K, Van Harmelen V. FcRγ-chain deficiency reduces the development of diet-induced obesity. **Obesity** 2015; 23: 2435-44

Van Dam AD, Bekkering S, Crasborn, Van Beek L, Van den Berg SM, Vrieling F, Joosten SA, Van Harmelen V, De Winther MPJ, Lütjohann D, Lutgens E, Boon MR, Riksen NP, Rensen PC, Berbée JF. BCG lowers plasma cholesterol levels and delays atherosclerotic lesion progression in mice. **Atherosclerosis** 2016; 251: 6-14

Van den Berg SM, **van Dam AD**, Rensen PC, de Winther MP, Lutgens E. Immune modulation of brown(ing) adipose tissue in obesity. **Endocr Rev** 2017; 38: 46-68

Van Dam AD, Boon MR, Berbée JF, Rensen, PC, Van Harmelen V. Targeting white, brown and perivascular adipose tissue in atherosclerosis development. **Eur J Pharmacol** 2017; *In press*

Van Dam AD, Van Beek L, Pronk AC, Van den Berg SM, Koning F, Van Kooten C, Rensen PC, Boon MR, Verbeek JS, Willems van Dijk K, Van Harmelen V. IgG is elevated in obese white adipose tissue but does not induce glucose intolerance via Fcγ-receptor or complement. *Submitted*

Van Dam AD, Hanssen MJ, Van Eenige R, Quinten E, Sips HC, Hülsman CJM, Jazet IM, Van Marken Lichtenbelt WD, Ottenhof THM, Haks MC, Rensen PC, Boon MR. South Asians have lower expression of interferon signaling genes in white adipose tissue and skeletal muscle compared to white Caucasians. *Submitted*

Van den Berg SM, **Van Dam AD**, Seijkens TTP, Kusters PJH, Beckers L, Den Toom M, Held NM, Van der Velden S, Van den Bossche J, Lombès M, Boon MR, Rensen PCN, Esther Lutgens E, De Winther MPJ. Diet-induced obesity induces rapid inflammatory changes in brown adipose tissue in mice. *Submitted*

Hoeke G, Wang Y, **Van Dam AD**, Mol IM, Van den Berg SM, Groen AK, Rensen PCN, Berbée JFP, Boon MR. Statins increase the lipid-lowering and anti-atherogenic potential of brown adipose tissue activation by accelerating lipoprotein remnant clearance. *Submitted*

Van den Berg SM, **Van Dam AD**, Kusters PJH, Beckers L, Den Toom M, Van der Velden S, Van den Bossche J, Van Die I, Boon MR, Rensen PCN, Lutgens E, De Winther MPJ. Helminth antigens counteract a rapid high-fat diet induced drop in eosinophils in a depot specific manner in mice. *Submitted*

Schilperoort M, **Van Dam AD**, Hoeke G, Okolo A, Hanyaloglu AC, Dib LH, Mol IM, Chan YW, Damak S, Reifel-Miller A, Coskun T, Shimpukade B, Ulven T, Kooijman S, Rensen PCN, Christian M. GPR120 agonism acutely increases lipid combustion by brown adipose tissue in a Ca^{2+}-dependent manner. *Submitted*

CURRICULUM VITAE

Andrea Dingena van Dam werd op 26 december 1988 geboren te Cabanatuan City (Filipijnen) en groeide op in Malawi, Costa Rica, Wageningen en Delft. In 2006 behaalde zij haar Gymnasium diploma aan het Haags Montessori Lyceum te 's Gravenhage. In dat zelfde jaar startte zij met de studie Scheikunde aan de Universiteit Utrecht, waarvan zij het eerste jaar afrondde. In 2007 werd zij toegelaten tot de bachelor Biomedische Wetenschappen, eveneens aan de Universiteit Utrecht. De scriptie voor deze bachelor schreef zij in 2010 aan het Rowett Institute of Nutrition and Health aan de Universiteit van Aberdeen (Schotland) in de groep van Dr. (nu Prof.) Baukje de Roos.

Na een periode van reizen en een opfriscursus Spaans in Costa Rica begon Andrea in 2011 aan haar master Biology of Disease aan de Universiteit Utrecht. In het kader van deze master deed zij twee onderzoeksstages: eerst onderzocht zij tropisme van HIV in het Universitair Medisch Centrum Utrecht onder begeleiding van Dr. Monique Nijhuis, en vervolgens werkte zij aan bruine en witte vetcellen onder leiding van Dr. Mark Christian aan het Institute of Reproductive and Developmental Biology aan Imperial College London (Engeland). Hier ontstond haar fascinatie voor het immuunsysteem en vetmetabolisme, waarna zij, onder supervisie van Dr. Rinke Stienstra aan de Wageningen Universiteit en het Radboud Universitair Medisch Centrum in Nijmegen, haar masterscriptie schreef over de wisselwerking tussen vetcellen en immuuncellen tijdens de ontwikkeling van insulineresistentie. Daarnaast schreef zij voor de Hersenstichting de folder "Hersenen en beweging", als onderdeel van een minor in de wetenschapscommunicatie.

In mei 2013 startte Andrea met haar promotieonderzoek bij de sectie Endocrinologie binnen de afdeling Interne Geneeskunde van het Leids Universitair Medisch Centrum, onder supervisie van Prof. Patrick Rensen en Dr. Mariëtte Boon. Het onderzoek werd uitgevoerd in nauwe samenwerking met Susan van den Berg uit de onderzoeksgroep van Prof. Esther Lutgens en Prof. Menno de Winther bij de afdeling Medische Biochemie in het Academisch Medisch Centrum in Amsterdam. Voor presentaties over haar werk won Andrea twee keer de poster award van het Rembrandt Institute of Cardiovascular Science (RICS) en een Young Investigator's Award van de Scandinavian Society for Atherosclerosis Research (SSAR). Het promotieonderzoek, waarvan de resultaten zijn beschreven in dit proefschrift, werd afgerond in mei 2017. Andrea zal na haar promotie als postdoc onderzoeker gaan werken aan de Universiteit van Oxford (Engeland), op een persoonsgebonden beurs toegekend in het kader van het Novo Nordisk Fellowship programme.

CURRICULUM VITAE

Andrea Dingena van Dam was born on 26 December 1988 in Cabanatuan City (Philippines) and grew up in Malawi, Costa Rica and The Netherlands. In 2006 she graduated from the secondary school Haags Montessori Lyceum in The Hague. That same year, she enrolled in a bachelor's programme in Chemistry at the University of Utrecht, of which she completed the first year. In 2007 she started with a bachelor's programme in Biomedical Sciences, also at the University of Utrecht. She wrote her bachelor's thesis in 2010 on a study at the Rowett Institute of Nutrition and Health at the University of Aberdeen (Scotland) within the group of Dr. (now Prof.) Baukje de Roos.

After a period of traveling and a refresher course in Spanish, Andrea started to work on a master's degree in Biology of Disease at the University of Utrecht in 2011. During her studies, she performed two research internships. First she investigated tropism of HIV under the supervision of Dr. Monique Nijhuis at the University Medical Centre in Utrecht, and then she examined brown and white adipocytes under the supervision of Dr. Mark Christian, at the Institute of Reproductive and Developmental Biology, Imperial College London (England). This provoked her fascination for immunology and lipid metabolism, upon which she wrote her master thesis – mentored by Dr. Rinke Stienstra at Wageningen University and Radboud University Medical Centre in Nijmegen – on the interaction between adipocytes and immune cells during the development of insulin resistance. She also wrote the brochure "Exercise and the brain" for the Netherlands Brain Foundation as part of a minor in scientific communication.

In May 2013, Andrea started her PhD at the division of Endocrinology at the Department of Medicine in the Leiden University Medical Centre, under the supervision of Prof. Patrick Rensen and Dr. Mariëtte Boon. Her research was conducted in close collaboration with Susan van den Berg in the group of Prof. Esther Lutgens and Prof. Menno de Winther at the department of Medical Biochemistry in the Academic Medical Centre in Amsterdam. For presentations on her research, Andrea won the poster award of the Rembrandt Institute of Cardiovascular Science (RICS) twice and a Young Investigator's Award from the Scandinavian Society for Atherosclerosis Research (SSAR). Her PhD research, the results of which are described in this thesis, was completed in May 2017. Andrea was awarded a Novo Nordisk Postdoctoral Research fellowship, which will fund her next research project as a postdoc at the University of Oxford (England).